PROCEEDINGS OF THE IRE®

SIEMENS & HALSKE
AKTIENGESELLSCHAFT
MÜNCHEN

Published Monthly by

The Institute of Radio Engineers, Inc.

VOLUME 44   *May, 1956*   NUMBER 5

CONTENTS

THE COVER—The waveform of broad-band thermal noise depicted on
the cover serves to call the attention of PROCEEDINGS readers to
two tutorial papers on noise which start on page 601 of this issue.
These outstanding papers inaugurate a program of presenting, from
time to time, recent developments in basic theory specially written
for the nonspecialist reader who wishes to catch up on the modern
fundamentals of radio engineering.

Scanning the Issue

Physical Sources of Noise (Pierce, p. 601)—This paper and its companion that follows are the opening guns of a program to bring before the practising engineer recent developments in the basic theories that form the foundation of radio engineering and to show him how these modern concepts and methods are being used to solve important practical problems. It is believed that this program, sponsored by the Tutorial Papers Subcommittee of the IRE Education Committee, will provide a good many engineers with a working knowledge of powerful new tools which will prove very valuable in their everyday work, and will give all readers an opportunity at least to cultivate a speaking acquaintance with important areas of knowledge which were hitherto unfamiliar to them. This first paper introduces the reader to a topic which is of great importance to every branch of the field—*i.e.*, noise. The author identifies the principal types of noise, discusses the physical mechanisms that give rise to it, and derives and explains in a lucid style the equations by which we describe this ever-present phenomenon.

Methods of Solving Noise Problems (Bennett, p. 609)— Having learned from the previous paper something of what noise is and where it comes from, we now turn our attention to the various methods of calculating the response of electrical systems to noise waves. True noise, in the purest sense, is the result of large number of random events which, individually, are unpredictable. Since it is not possible, under these circumstances, to calculate exactly what will happen at any given moment, the engineer has turned to the field of statistics in order to obtain an over-all picture of the probability that certain events will occur in some prescribed manner. The study of noise is, then, a study of statistics, and this paper leads the reader straight into the heart of this subject, pausing at such waystations as probability density, characteristic functions, Gaussian distribution, correlation, and power spectra. At each stop along the way, the author refreshes the traveler with practical examples to illustrate the concepts and techniques thus far covered. The reader will find in this and the preceding account a gold mine of instructive material. The author have provided a well-drawn chart of where the treasure lies, but the reader must come prepared to do his share of the digging.

Video Measurements Employing Transient Techniques (Samulon, p. 638)—Over the years several ingenious methods have been developed for determining the all-important amplitude- and phase-vs-frequency response curves of electrical networks. One of the most useful of these, especially in higher frequency applications such as television or radar, is the transient-response technique, in which an impulse of some specified shape is applied to the input of the network under study and the output waveform is carefully observed and measured. This test furnishes enough clues to the behavior of the network so that its over-all amplitude and phase response can then be calculated by various numerical and graphical methods. This paper was prepared at the suggestion of the Video Subcommittee of the IRE Committee on Measurements and Instrumentation, which felt that there is a substantial body of engineers who have to use transient techniques occasionally but who do not have an expert's knowledge of them. This discussion brings together a great deal of useful information on the proper methods of measuring and evaluating response curves, the types of waveforms to use. and the equipment required for transient tests.

The Design of High-Power Traveling-Wave Tubes (Chodorow and Nalos, p. 649)—In this paper the authors examine the problems involved in designing a traveling-wave tube to operate at power levels previously unachieved with this type of tube. They succeed in satisfactorily operating an experimental model at 300 kw pulsed power output. More important, they show that a one megawatt tube is entirely feasible and indicate what specific improvements should be made on their model to accomplish this feat. Most important of all, their work opens up a whole new range of power capabilities for the traveling-wave tube which will be of major interest to system designers as well as to microwave tube specialists.

Progress in the Development of Post-Acceleration and Electrostatic Deflection (Schlesinger, p. 659)—The extremely high sweep voltages that are required plus the defocussing and distortion that occurs, especially at wide deflection angles. have been serious handicaps in the development of electrostatic deflection systems for cathode-ray tubes. This paper describes two developments, namely, the Deflectron and the barrier mask, which together go a long way towards overcoming these major difficulties. The Deflectron consists of four deflection electrodes printed on the inside of the tube in such a way as to permit both vertical and horizontal deflection from a common center, instead of from the usual two separate centers placed one after the other along the beam path. This new arrangement results in much less distortion and wider deflection angles than were previously possible (50° instead of 25°). The barrier mask is a post-accelerator placed near the screen to boost, or intensify, the electron beam. thus permitting the use of much lower beam voltages at the gun end of the tube. This, in turn, has reduced the deflection voltage requirements to as little as 20 per cent of that previously needed. This work will have an important impact on the design of cathode-ray tubes, especially special purpose tubes.

IRE Standards on Audio System Measurements (p. 668)— The IRE Audio Techniques Committee and its appropriate subcommittee have set forth in this document the IRE-approved standard methods of measuring gain, amplification, loss, attenuation. and amplitude-frequency response of systems and components intended for application or operation at audio frequencies. Those readers wishing to go beyond the measuring techniques and to delve into the underlying theory will find a good bibliography included at the end.

Cascaded Feedthrough Capacitors (Schlicke, p. 686)—By physically stacking up a number of discoidal capacitors and placing ferrite washers between them. the author has developed a new and much improved type of ceramic filter capacitor for the vhf and uhf range. The unique high-frequency properties of this capacitor, coupled with the universal need for good filter capacitors at these frequencies, mark this as a clear-cut and important advance in the component art.

1955 Index to IRE Transactions (follows p. 732)—Immediately preceding the advertising section in the rear of this issue there appears the annual index to the 56 issues of TRANSACTIONS that were published by 21 IRE Professional Groups during 1955, listing the contents of each issue by Group and giving a single over-all index to authors and subjects.

Poles and Zeros

Math. Perhaps the most recurrent criticism voiced to Headquarters by readers of IRE publications is that the specialized symbolism of mathematics is used so much in so many papers. This complaint comes not only from members who have no formal training in higher mathematics, but also from an even larger number whose studies included advanced calculus but who, with the passing of busy years, find following a symbolic exposition far too costly of time and effort.

Said complainants, high brows and low, want to know the conclusions of the analysis in plain, or at least familiar, English. They are quite willing to take the details on faith—faith that expert editorial reviewers would not recommend for publication a paper whose details were in error.

This kind of IRE member is no doubt especially favored of the good Lord because He made so many of them. Mere weight of numbers, however, cannot be allowed to determine the editorial policy in favor of nonmathematical presentation. For in every field there is a minority of particularly well-trained and competent workers who need, and have a right to demand, the full analytical details. They are not merely interested generally in what is going on. They are the ones whose duty it is to *build* on the contributions of others, and they must know the precise nature and strength of the structure of the prior art. To leave out the analytic details in IRE papers would cut these important groups adrift, to the ultimate disadvantage of the profession as a whole.

So—all IRE publications must continue to publish the gory mathematical details whenever the editors and reviewers are satisfied that the contribution is a sound, original, logical link in the chain of technical development. But it is *not* necessary that mathematics, so essential to the inner circle, should completely obscure the view of the numerous interested onlookers. Math *can* be largely confined to appendices. Out of decent regard for the principles of fair play, in most cases it should be so confined. Every author, no matter how distinguished in his special field, should count it a duty and an honor to *explain* the meat of his findings in familiar terms, preferably in the first few paragraphs, for the benefit of those who occupy adjacent specialties in the IRE firmament.

It may once have been fashionable to disdain this courtesy, apparently on the score that such pandering would somehow dilute the fine heady flavor of a good, straight technical paper. But fashions change. Today, experienced workers recognize the virtues of lucidity in reporting their work. They accept two duties in writing a paper: (1) to prepare a sound base for future work by their specially knowledgeable colleagues and, (2) to be *understood*, without benefit of special words or symbols, by others who need to understand the significance of their work.

PROCEEDINGS VS TRANSACTIONS—III. The foregoing leads naturally to the third and last of our comparisons between PROC. IRE and TRANS. IRE. Papers in the Professional Groups TRANSACTIONS can, and should (and do, see next item), use the specialized language of the Group in question more freely than do papers intended for the more general audience of the PROCEEDINGS. Otherwise stated, a paper written in highly specialized language must weigh correspondingly heavy to merit exposure to 48,000 members, most of whom cannot readily follow the discourse. Moreover, the TRANSACTIONS can, and should, follow the expressed will of the Professional Group membership. They may be long-haired or short; they may have the resources to cover their fields completely, or (especially new groups or those in specially active fields) they may perforce limit themselves to occasional or limited coverage. The PROCEEDINGS, on the other hand, stands before the technical world for the whole membership and its professional standards must be above reproach.

In any event, neither PROCEEDINGS or TRANSACTIONS papers should be complex or complicated beyond the proper demands of the subject matter. Any other approach is sophistry at its worst. A short paper in simple, clear language takes longer to write than a long one in jargon. But the extra effort pays off. Most of the classic papers from the early history of electricity, and many of those on electronic subjects now emerging as classics, have the air of elegant simplicity. They deserve imitation.

Symposium. An excellent example of a Professional Group taking over an important extra publishing responsibility is the appearance within the month of a special 400-page issue of TRANSACTIONS prepared by the Professional Group on Antennas and Propagation. Subtitled the "Proceedings of the Symposium on Electromagnetic Wave Theory," it contains the full text of 44 invited papers and abstracts of 53 contributed papers presented at Ann Arbor last June under the sponsorship of URSI, the University of Michigan, the Armed Services, and eleven corporations. Plenty of math here, and well worth it at $8.50 per copy. Order from IRE Headquarters, New York City.—D.G.F.

E. Milton Boone

DIRECTOR, 1955–1956

E. Milton Boone was born on February 17, 1903, in Millersburg, Kentucky. In 1926 he received the B.A. degree in electrical engineering and physics and in 1932 the M.S. degree in physics, both from the University of Colorado. In 1937 he was awarded the M.S. degree in electrical engineering from the University of Michigan.

Professor Boone started his teaching career as an instructor at the University of Colorado, teaching engineering mathematics and physics. In 1930 he joined the General Electric Company as a research physicist at its Pittsfield, Massachusetts, laboratory. He joined the faculty of Amarillo College in Amarillo, Texas in 1932, remaining there for the next five years. In 1937 he became a member of the staff of the Electrical Engineering Department of the Ohio State University, where he has remained except for a year's leave of absence during World War II when he was a member of the Technical Staff of the Bell Telephone Laboratories.

Professor Boone became an Associate Member of the IRE in 1943, a Senior Member in 1946, and a Fellow in 1956. His Fellow citation reads "for contributions as an educator and research investigator in the field of electronics." He has been active in IRE technical committee work since 1945, particularly in the field of electron devices. In 1955 he was elected a Director. representing Region Four.

Two Tutorial Papers on Noise

Previous tutorial papers have been largely survey papers or papers reviewing progress in certain special fields. The Tutorial Papers Subcommittee of the Committee on Education has concluded that there is need for another type of paper which will help the engineer to keep abreast of developments in basic theory. Engineers some years out of college tend to lose the ability to read with profit even important papers in their own fields of interest, because new concepts have crept in with which they are only vaguely familiar and new methods have been adopted for handling basic problems. Such new concepts and methods usually first appear in the literature in scattered fragments, and a considerable time may elapse before a consecutive account is available which the nonspecialist engineer can study effectively. It is hoped that the new Tutorial Papers can shorten the gap between the evolution of new and useful ideas and their application to solving the everyday practical problems of the radio engineer.

The subject of noise is encountered in every branch of radio engineering and is of the highest importance. But is is an elusive subject and can be handled only by statistical methods with which the average engineer is unfamiliar. The subject is difficult to learn because new kinds of reasoning must be employed. The following two papers on noise, therefore, are not light, easy reading, but their study will make possible a real understanding of a large group of basic problems.

The project of writing a tutorial paper on noise as a part of the Tutorial Papers program was planned in detail at a meeting on January 26, 1954, attended by W. R. Bennett, F. K. Bowers, W. R. Davenport, B. McMillan, J. R. Pierce, S. O. Rice, C. E. Shannon, and D. Slepian. The original proposal was to obtain a number of individual contributions from different authors on selected topics. What has now emerged divides the subject into two main parts.

The first paper, by J. R. Pierce, deals primarily with descriptions of the various physical phenomena which lead to noise, and the second paper, by W. R. Bennett, explains mathematical techniques which have been developed for quantitative evaluations. The distinction is one of emphasis rather than complete separation, for it is necessary to include calculations in the physical description and to refer to physical models in the mathematical treatment.

The inclusion of topics within these main divisions is representative rather than exhaustive. A comprehensive coverage of the field appears to be inconsistent with a reasonable length of text. The second article in particular has grown bulkier than intended and still neglects a number of important analytic phases of the subject. Among the topics not even mentioned are Smoothing and Prediction of Noise, Likelihood Criteria for Detection of Signals in Noise, and Statistics in a Finite Time Interval. We do not claim that one who reads these articles will thereby be prepared to read the papers in the literature on the topics not included, but we think he will be helped. The topics treated are naturally the ones with which the authors are most familiar. An attempt is made to establish a background of fundamental concepts which are applied to progressively more difficult situations as the subject is developed. It is hoped that the readers who so wish will be able to apply these principles to similar problems on their own and that those who do not wish to derive formulas themselves will be aided toward a more effective use of results available in the more complete sources.

<div align="right">

W. N. TUTTLE, *Chairman*
W. R. BENNETT
Tutorial Papers Subcommittee

</div>

Physical Sources of Noise*

J. R. PIERCE†, FELLOW, IRE

Summary—Johnson noise is caused by the fluctuation of charges or polarizable molecules in lossy materials. Its magnitude can best be calculated by means of statistical mechanics, which tells us that each degree of freedom must have associated with it an energy of $\frac{1}{2}kT$. This leads to the usual expressions for Johnson noise, including the fact that the available thermal noise power, from a resistor, a lossy network, a lossy dielectric, or an antenna is always kTB. In the case of a resistor, network, or dielectric, T is the temperature of the lossy material. In the case of an antenna, T is the average temperature of the environment which the antenna "sees." Consistent with the power kTB available from an antenna, there is a particular density of radiation in space which is a function of temperature and frequency. Noise figure is defined in terms of Johnson noise.

Shot noise, due to the discrete nature of electron flow, is generally distinct from Johnson noise, although in some electron devices the expression for the noise in the electron flow has the same form as that for Johnson noise. When the noise in electron flow is greater or less than pure shot noise, the motions of the electrons must be in some degree correlated. In an electron stream of low noise, the random interception of a fraction of the electron flow can reduce the correlation and increase the noise. Johnson noise and shot noise have a flat frequency spectrum. Some active devices, such as vacuum tubes and transistors, have a 1/f frequency spectrum at low frequencies.

INTRODUCTION

MANY SORTS of electric signals are called noise. In the early days of radio we were most familiar with the crash and crackle of static. Later, we encountered the rasp of ignition noise and the hiss of the thermal and shot noise generated in radio circuits themselves. In the end, many engineers have come to regard any interfering signal of a more or less unpredictable nature as noise. An interfering sine wave of absolutely constant frequency is predictable, and it can be filtered out with negligible loss of channel capacity. Crosstalk from one telephone channel to another is not predictable, at least, not in the same way as a sine wave is, and it cannot be eliminated, at least not by practical means. The engineer is apt to consider it as so much noise.

The study of noise began with the consideration of certain physical sources of noise and the sorts of noise that they generate. At first, only very simple properties of the noise signals so generated were understood and described. As the art has progressed, a mathematical theory of noise has grown up. This theory is a part of the general field of statistics, and it deals with signals which have an unpredictable, a statistical, a random element. Some understanding of this theory is essential in dealing with engineering problems involving noise.

The theory of noise as it is usually presented is not valid for all signals or phenomena which the engineer may identify as noise, though it may be adequate in a practical sense in dealing with signals (multichannel crosstalk, for instance) which do not meet the mathematician's strict requirements of randomness. The theory of noise is best adapted to handling signals which originate in truly random processes, such as the emission of electrons from a photo-surface or a hot cathode, or the thermal agitation of charges in a resistor. When a cathode emits electrons at so slow a rate that we observe their effects in a circuit as separate pulses, we have *impulse noise*, and the theory of noise has something to say about this. When electrons are randomly emitted so rapidly that the pulses they produce in the circuit overlap, the statistics of large numbers applies, and the theory of noise tells us a great deal that must be true of a large class of noise signals, despite differences in the exact nature of their sources.

The statistical theory of noise will be treated in a paper by W. R. Bennett.[1] In this paper, as an introduction to noise, we consider important physical sources which produce noise of just the type to which the statistical theory applies exactly.

JOHNSON NOISE

The first source of noise which we consider is Johnson noise, the thermal noise from a resistor. The engineering fact is that a resistor of resistance R acts as a noise generator. The resistor as a noise generator can be described as a zero-impedance voltage generator in series with the resistance of the resistor. The mean square voltage $\overline{V^2}$ (V is the open-circuit voltage of the generator) is given by

$$\overline{V^2} = 4kTRB \qquad (1)$$

This generator is shown in Fig. 1.
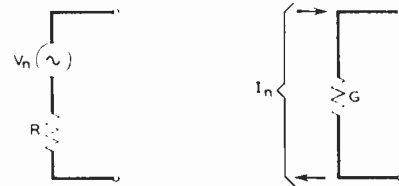
Fig. 1—The thermal power source associated with a resistance or conductance can be represented as a series voltage source or a shunt current source.

Also, as shown in Fig. 1, we can as easily describe the resistor as a noise generator as a mean square impressed current from an infinite-impedance source, $\overline{I^2}$, (I is the short-circuit current), in shunt with the conductance G of the resistor.

$$\overline{I^2} = 4kTGB \qquad (2)$$

In (1) and (2) B is the bandwidth in which the noise voltage or current lies, k is Boltzmann's constant, and T is the absolute temperature in degrees Kelvin, which is the temperature in degrees centigrade plus 273°.

Expressions (1) and (2) also apply to the noise from any complex passive circuit which is all at one temperature. A passive circuit is one to which no power is supplied except by heating it; that is, no dc current is supplied, or no regular mechanical motion. In case of such circuits, R is the resistive component of the impedance, or G is the conductive component of the admittance. Because R and G vary with frequency f, B is taken as a small incremental bandwidth df and $\overline{V^2}$ or $\overline{I^2}$ must be evaluated by integration.

What is the source of Johnson noise? In an ordinary resistor, it is a summation of the effects of the very short current pulses of many electrons as they travel between collisions, each pulse individually having a flat spectrum. In this case the noise is a manifestation of the Brownian movement of the electrons in the resistor. In a resistor consisting of two opposed, close-spaced, hot, electron-emitting cathodes, it is a result of the current pulses of randomly-emitted electrons passing from one cathode to the other. In a lossy dielectric it is the result of random thermal excitations of polarizable molecules, forming little fluctuating dipoles. The case of noise in the radiation resistance of an antenna, which will be discussed later, is quite involved.

For any particular sort of resistor, it should be possible to trace out the source and calculate the magnitude of the Johnson noise, and indeed, this approach has been used. However, there is something very general about

---

[1] "Methods of solving noise problems," PROC. IRE, pp. 609–637; this issue.

an expression which applies to so wide a variety of physical systems. It turns out that there is a very general way of deriving the expression for Johnson noise; this is afforded by thermodynamics and statistical mechanics.

Consider a network containing many resistors. If we heat one hotter than the rest, energy tends to flow from the hot resistor to the cooler resistors. Johnson noise is such energy flowing as electric power. Even when the resistors are all at the same temperature, power will flow back and forth between them through the connecting network, always so that on the average a resistor receives just as much power as it sends out. We may note that if we know the resistance of one portion of the network, its internal impedance, and the impedance of the rest of the network acting as a load, by using (1) we can calculate the power flow. But really, it is from a knowledge of the general behavior of systems in equilibrium, that is, all at the same temperature, that we can derive (1) and (2).

Statistical mechanics tells us how much energy must on the average be associated with each *degree of freedom* of a system when the system is in thermal equilibrium. In an electrical network of inductors, capacitors, and resistors in which there are no inductors connected directly in series nor capacitors connected directly in shunt, the number of degrees of freedom is the number of inductors plus the number of capacitors. In setting up a signal on the network, we are free to specify arbitrary currents in all the inductors and arbitrary voltages across all capacitors. If we know these currents and voltages at any instant, we can (disregarding Johnson noise, which acts as a power source) calculate all future voltages and currents.

Classical statistical mechanics says that in a system (in our case, such an electrical network) which is in equilibrium (all at the same temperature) there is on the average an energy

$$\tfrac{1}{2}kT \text{ joules}$$

associated with each degree of freedom:

$$k = 1.380 \times 10^{-23} \text{ joule/degree.}$$

According to quantum mechanics, the energy is less than this at high frequencies; Nyquist and others have used the quantum-mechanical expression to get the correct result. However, even up to tens of thousands of megacycles the classical expression is accurate.

Let us consider two simple circuits as particular examples, to see how things work out. In these circuits an inductance L is in series with a resistance R at temperature T, and a capacitance C is in shunt with a conductance G at a temperature T, as shown in Fig. 2.

Let $\overline{I^2}$ be the total mean square noise current in the inductor. We can write

$$\tfrac{1}{2}L\overline{I^2} = \tfrac{1}{2}kT.$$

On the left we have the average power in the inductance. On the right we have the average value this must have according to statistical mechanics. Accordingly,

$$\overline{I^2} = \frac{kT}{L}. \qquad (3)$$

$$I^2 = \frac{kT}{L} \qquad\qquad V^2 = \frac{kT}{C}$$
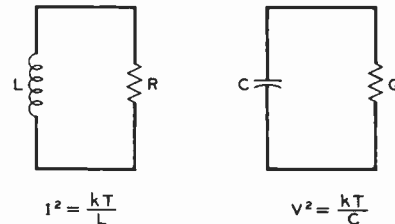
Fig. 2—The total Johnson noise current squared in an inductance in series with a resistance, and the total Johnson noise voltage squared across a capacitance in shunt with a conductance, are independent of the resistance or the conductance.

This must be true regardless of the value of R. If R is low we have a narrow-band circuit; if R is high we have a broad-band circuit. As the noise current is made up of various frequency components, more low-frequency current must flow in the narrow-band case when R is small than in the broad-band case when R is large, if the total mean squared current is to be the same in both cases.

In a similar way, in the case of the capacitance C and the conductance G in shunt we easily find that

$$\tfrac{1}{2}C\overline{V^2} = \tfrac{1}{2}kT$$

$$\overline{V^2} = \frac{kT}{C}. \qquad (4)$$

If the conductance is small, we have a narrow-band circuit with high low-frequency noise components. If the conductance is large we have less low-frequency noise but more bandwidth.

Relations (3) and (4) of course apply to capacitors and inductors not merely in the simple circuits we have considered, but to capacitors and inductors anywhere in all circuits, no matter how complicated they may be. In any case, we see that the noise voltage or current squared is proportional to the temperature T.

Among the circuits to which (3) and (4) apply is the resonant circuit shown in Fig. 3, which consists of an inductance L, a capacitance C and a conductance G in shunt. This circuit is characterized by a resonant frequency f_0, a Q, and an impedance the square of whose magnitude is $|Z|^2$, given by

$$f_0 = \frac{1}{2\pi\sqrt{LC}}$$

$$Q = \sqrt{C/L}/G$$

$$|Z|^2 = \frac{(L/C)Q^2}{Q^2\left(\dfrac{f}{f_0} - \dfrac{f_0}{f}\right)^2 + 1}.$$

We can regard this circuit as excited by the impressed shunt Johnson noise current I. If we make the Q very high, so that the bandwidth of the circuit is very narrow, we can find out something about the spectral distribution of the impressed noise current.

Because the mean square value of a number of voltages or currents of different frequencies is the sum of the mean square values of the different frequency components, we will assume that

$$d\overline{I^2} = F(f)df. \tag{5}$$
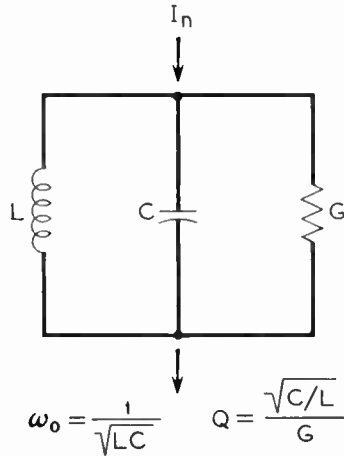
Fig. 3—We can use a tuned circuit to explore the frequency spectrum of Johnson noise.

That is, each frequency range df contributes some part $d\overline{I^2}$ of the total mean square current. In (3), $F(f)$ is a function of frequency.

Let us now calculate the total mean square noise voltage across the capacitance and set it equal to the value given by (2). This gives

$$\frac{kT}{C} = \frac{L}{C} Q^2 \int_0^\infty \frac{F(f)df}{Q^2\left(\frac{f}{f_0} - \frac{f_0}{f}\right)^2 + 1}.$$

Now suppose we make Q very large, so that the band is very narrow. Then $F(f)$ will not vary much over the band, and we can take it outside the integral and give f the value f_0. With some rearrangement and substitutions we obtain

$$kT = \frac{F(f_0)}{2\pi G} \int_0^\infty \frac{Qd(f/f_0)}{Q^2(f/f_0 - f_0/f)^2 + 1}.$$

The value of the integral is found to be independent of Q and f_0, so that $F(f_0)$ is a constant, independent of frequency. Let us call the integral I. The substitution

$$\frac{f}{f_0} = e^x$$

leads to

$$I = \int_{-\infty}^\infty \frac{Qe^x dx}{4Q^2 \sinh^2 x + 1}.$$

The value is unchanged if we replace e^x by e^{-x}, so that

$$I = \int_{-\infty}^\infty \frac{Q \cosh x dx}{4(Q \sinh x)^2 + 1}$$

$$= \frac{1}{2} \int_{-\infty}^\infty \frac{\frac{1}{2}du}{u^2 + (\frac{1}{2})^2}.$$

By Pierce 480

$$I = \frac{\pi}{2}$$

$$F(f_0) = 4kTG$$

$$d\overline{I^2} = 4kTGdf.$$

This is often written in the form (2), where

$$\overline{I^2} = 4kTGB. \tag{2}$$

Here B is bandwidth and $\overline{I^2}$ is understood to be the part of the mean square impressed noise current lying in the bandwidth B.

The spectrum of Johnson noise is flat; it is called *white* noise.

We can evaluate the series noise voltage much as we evaluated the shunt noise current, and we obtain (1):

$$\overline{V^2} = 4kTRB \tag{1}$$

We can of course obtain (1) directly from (2) by asking what current flows when the resistance is shorted; this is

$$\overline{I^2} = \frac{\overline{V^2}}{R^2} = \frac{4kTB}{R} = 4kTGB.$$

What happens if we connect two resistances in series or two conductances in parallel? In a given frequency range, the voltages or currents produced by different resistances are uncorrelated; they have random phases, and the mean square of the sum of the separate voltages or currents is equal to the sum of the mean square voltages or currents of the separate resistors. This is in accord with (1) and (2), taking R and G as total resistance and conductance.

As we have noted, for a complex impedance the series noise voltage generator at any frequency can be calculated from the resistive component R of the impedance, and the shunt noise current generator from the conductive component G of the admittance.

Relations (3) and (4) tell us something which is sometimes useful in connection with networks. From (1) or (2) we can calculate the mean square thermal noise current or voltage lying in a narrow frequency range for any network, simply by associating with the resistance or conductance series voltage generators or impressed currents according to these relations.

There is another way of expressing the information in (1) or (2). We may ask, what is the thermal noise power P available from a resistor? We will draw off the maximum power if we supply a matched load of the same resistance. Thus, the available noise power in the bandwidth B can be obtained by calculating the noise

power flowing into a resistance R from a source with an internal resistance R and an open-circuited voltage given by (1). This power is

$$P = \frac{1}{2}\frac{\overline{V^2}}{(2R)^2}.$$

$$P = kTB. \tag{6}$$

Thus, the Johnson noise power available from a resistor is independent of the resistance.

Let us assume that a resistance R is matched to a waveguide W, and the waveguide is terminated in an antenna, perhaps a horn antenna, as shown in Fig. 4. A power P given by (6) is radiated from the antenna in a beam; to the beam we assign some nominal solid angle ψ steradians. Suppose that the antenna is surrounded by a perfectly absorbing box D (a "black box") at the same temperature as the resistance R. Since there can be no average power flow between two objects at the same temperature, a power P given by (6) will flow back from the box D to the resistance R. This power must be independent of the size and the directivity of the antenna.
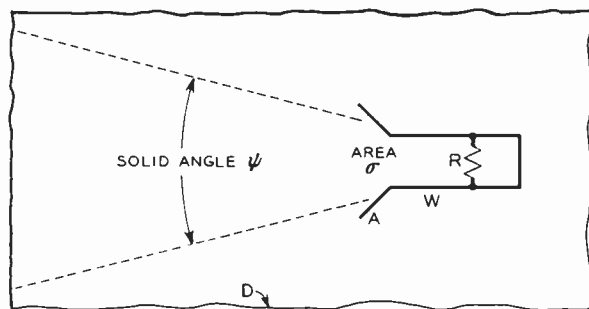
Fig. 4—An antenna A in a black box D.

No matter what direction we point the antenna in the box, the power received will be the same. The box is full of electromagnetic power flow in all directions. The antenna receives power over a solid angle ψ, and over the area σ of the antenna. At a given wavelength, ψ is inversely proportional to σ; that is, the bigger the antenna the narrower the beam, so the product of $\psi\sigma$ remains constant as the antenna size is varied.

We know, however, that for an antenna of given size, the shorter the wavelength, or the higher the frequency, the narrower the beam. If the antenna is to receive a power P per unit bandwidth, the radiation flux for unit solid angle and unit area must be proportional to the square of the frequency.

Consider a little area $d\sigma$ receiving radiation from a direction θ with respect to the normal to the area, over a solid angle $d\psi$. (See Fig. 5.) The area of $d\sigma$ seen from the direction of radiation is

$$\cos \theta d\sigma.$$

From this and the previous argument, we see that the power dP received must be

$$dP = Af^2 \cos \theta d\psi d\sigma,$$

where A is a constant. When the constant is evaluated, we find

$$dP = \frac{f^2 df}{c^2} kT \cos \theta d\psi d\sigma. \tag{7}$$

Here c is the velocity of light. This is the power in one polarization; there is an equal power in the other polarization which is not accepted by the antenna. It is also the power radiated by an absorbing surface in one polarization in a direction θ to the normal, over a solid angle $d\psi$ and over an area $d\sigma$.
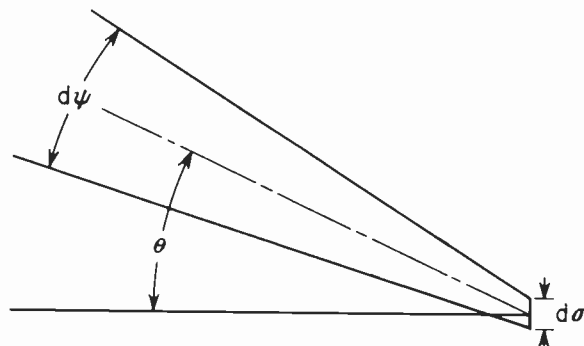
$$dP = \frac{f^2}{c^2} kT B \cos\theta \, d\psi \, d\sigma$$

Fig. 5—The power radiated or absorbed in one polarization at a frequency f in a direction making an angle θ with the normal, in a bandwidth B, a solid angle d_4, over an area $d\sigma$.

Why cannot one get the total power radiated per unit area from a solid body by integrating twice dP as given by (7) with respect to $d\psi$ and df? The answer is, because (7) is incorrect at high frequencies, and gives an infinite answer; this is the "ultra-violet catastrophe" of pre-quantum physics.

We can, however, use (7) to calculate the power received in a given bandwidth by an antenna from some hot body of narrow extent, such as the sun.

Relation (7) is accurate at microwave frequencies, and it is consistent with the fact that the total noise power received from the walls of a nonreflecting enclosure held at temperature T must be kTB. Ordinarily, however, what surrounds an antenna is neither perfectly absorbing nor at a uniform temperature. In this case we may use an average temperature T_A in order to calculate how much Johnson noise an antenna will receive.

If we used the antenna in question as a transmitting antenna, part of the power might be absorbed directly by trees in the beam, part might be reflected from the ground into the sky, to be absorbed ultimately by cosmic matter, and some might go directly to the sky. Suppose a fraction p_n of the total radiated power is either directly, or after reflection, or due to imperfect reflection, ultimately absorbed by matter of temperature T_n. Then, the Johnson noise power received when the antenna is used for receiving instead of transmitting will be correctly given by (6), where as T we use an average temperature T_A given by

$$T_A = \sum_n p_n T_n. \tag{8}$$

Johnson noise serves as a reference for the noisiness of radio receivers and amplifiers. Suppose, for instance, that the input of an amplifier is connected to an antenna pointed at an absorbing body of temperature T, or, simply to a transmission line terminated at the other end in a resistance of temperature T. Let the ratio of the power output to the available power at the antenna or resistive source be N at some reference frequency f. Then, if the amplifier introduced no noise but merely amplified Johnson noise, the power output P_j over a narrow bandwidth B would be

$$P_j = NkTB.$$

Actually, the amplifier will generate noise. Let the total output noise power be P_t. Then the noise factor or noise figure NF of the amplifier is defined as

$$NF = \frac{P_t}{P_j} = \frac{P_t}{NkTB} . \tag{9}$$

This defines noise figure for some narrow band B at a specific frequency. Under such circumstances, P_t is found to be proportional to B, and the noise figure is independent of B and varies somewhat with frequency, as P_t/B and N vary with frequency.

SHOT NOISE AND OTHER NOISE IN ELECTRON TUBES

Electricity is not a smooth fluid; it comes in little pellets, that is, electrons. The flow of electrons in a vacuum tube is accompanied by a noise of the same nature as the patter of rain on a roof. Schottky, who first investigated this phenomenon, called it the *Schroteffekt* (from shot); it is now usually called simply *shot noise*.
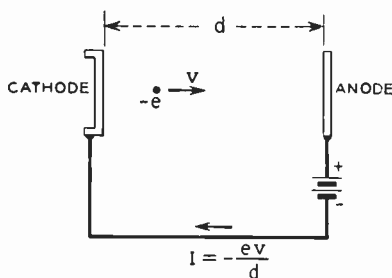
Fig. 6—An electron leaves the cathode at time t_1 and travels with increasing speed between cathode and anode and strikes the anode at time t_2.

Consider an electron of charge $-e$ moving with a velocity v between parallel plane conductors a distance d apart, for instance, a cathode and an anode, as shown in Fig. 6. If the cathode and anode are connected by a wire of zero impedance, a current I flows to the wire, and I is given by

$$I = - \frac{ev}{d} .$$

The current starts when the electron leaves the cathode at time t_1 and ends when the electron reaches the anode at time t_2. If the electron leaves the cathode with zero velocity and is accelerated by a dc field between the cathode and the anode, the current pulse, that is, I plotted against time, will look something as shown in Fig. 7. The total charge Q flowing as a result of the passage of the electron is

$$Q = \int_{t_1}^{t_2} I dt = \int_{t_1}^{t_2} - \frac{ev}{d} dt = \int_0^d - \frac{edx}{d}$$

$$Q = - e.$$
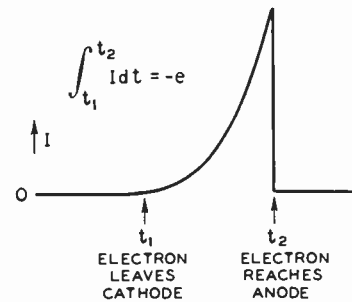
Fig. 7—The current flow in the case of Fig. 6 starts at time t_1, increases as the electron is accelerated between cathode and anode, and stops when the electron strikes the anode. The total transfer of charge between cathode and anode is the electronic charge, $-e$.

That is, a charge equal to the charge of the electron flows into the circuit in the form of a short pulse during the transit of the electron between cathode and anode.

Suppose that the cathode and anode form part of a shunt resonant circuit of inductance L, capacitance C and conductance G, as shown in Fig. 3. If the current pulse due to the passage of the electron is short compared with the period of the circuit, we can regard the transfer of charge as instantaneous and say that the passage of the electron from cathode to anode is equivalent to putting a charge $-e$ on the capacitance C. If we do this we give to the circuit an energy W:

$$W = \frac{1}{2} \frac{e^2}{C} .$$

We see that the energy given to the circuit is dependent only on C, and is not dependent on the resonant frequency. The energy is gradually dissipated in the conductance G as the circuit oscillates with exponentially decaying amplitude following the pulse.

If we put N charges on a circuit at random times, over an interval T, the waves initiated have random phases, and the powers add, so the total energy is NW:

$$NW = \frac{1}{2} N \frac{e^2}{C} .$$

The rate P at which power is dissipated in the circuit is thus

$$P = \frac{NW}{T} = \frac{1}{2} \frac{N}{t} \frac{e^2}{C} .$$

The number N of electrons which flow in a time T is related to the average electron current I_0:

$$N = \frac{IT}{e},$$

so that

$$P = \frac{1}{2}\frac{eI_0}{C}. \tag{10}$$

Thus, the power in the circuit is dependent on C only and is independent of the resonant frequency.

As before, we will assume that the impressed noise current I is such that

$$\overline{I^2} = F(f)df. \tag{11}$$

This current flows into an impedance Z:

$$Z = \frac{1}{G}\frac{(1 - jQ)\left(\dfrac{f}{f_0} - \dfrac{f_0}{f}\right)}{1 + Q^2\left(\dfrac{f}{f_0} - \dfrac{f_0}{f}\right)^2}. \tag{12}$$

By equating the power calculated from (11) and (12) with the power as given by (10) we obtain

$$\frac{1}{2}\frac{eI_0}{C} = \frac{1}{G}\int_0^\infty \frac{F(f)df}{1 + Q^2\left(\dfrac{f}{f_0} - \dfrac{f_0}{f}\right)^2}.$$

As before, we can assume that Q is very high, so that the circuit impedance is appreciable over a very narrow frequency range only, and take $F(f)$ outside of the integral. This gives, with some rearrangement and substitutions

$$eI_0 = \frac{F(f_0)}{\pi}\int_0^\infty \frac{Qd(f/f_0)}{1 + Q^2\left(\dfrac{f}{f_0} - \dfrac{f_0}{f}\right)^2}.$$

This is the same integral we encountered before. Its value is independent of Q and f_0. Thus, we find that $F(f_0)$ is a constant, so that the noise current per unit bandwidth is independent of frequency.

$$F(f_0) = 2eI_0$$
$$\overline{I^2} = 2eI_0B. \tag{13}$$

Like Johnson noise, shot noise has a flat spectrum.[2] This is really what we should expect of a random collection of very short pulses, each of which has a flat spectrum.

In a given frequency range, a current of electrons can have either more or less noise than pure shot noise as given by (13). For the noise to be either greater or less than shot noise, the times of emission of various electrons must be correlated in some degree.

Suppose, for instance, that the I_0/e electrons which leave the cathode each second were emitted at evenly spaced times e/I_0 seconds apart. The flow would have no ac component at all at frequencies below I_0/e. The only frequencies present would be I_0/e and its harmonics.

On the other hand, suppose that the electrons left n at a time but that the bunches of n electrons left at uncorrelated times. This is equivalent to saying that the current is carried by randomly emitted charges of charge ne, and from (13) the noise current would be

$$\overline{I^2} = 2(ne)I_0B.$$

Random processes other than the random emission of electrons can give rise to noise. Suppose, for instance, that electrons enter an electron multiplier periodically, so that there is no noise in the electron stream at ordinary frequencies. If the electron multiplier gave out exactly the same number N of electrons each time one went in, there would be no noise in the output. It doesn't, however, for sometimes an electron produces more electrons and sometimes fewer. This randomness gives rise to noise in the output current of the multiplier.

Similarly, noise can be introduced into an initially noiseless electron flow if the electrons randomly hit or miss the wires of a grid, with a certain average interception of current. Such noise is called *partition noise* or *interception noise*. If a small fraction only of the current is intercepted, the added noise is roughly equal to shot noise for the intercepted current.

At high frequencies and long transit times the excitation of a circuit may depend on the velocity of the entering electrons. In such a case the random variation of velocity of emission from one electron to another, associated with the Maxwellian velocity distribution of electrons leaving a cathode, can give rise to noise. This fluctuation in velocity is also responsible for what is commonly called the *modified* or *reduced* shot noise in space-charge-limited flow of electrons from a cathode.

A very simple theory of noise in space-charge-limited diodes and triodes at frequencies low enough so that transit time is not important predicts that the noise can be represented by an impressed noise current in the plate circuit I^2, given by

$$\overline{I^2} = (.644)4kT_cgB. \tag{14}$$

Here T_c is the temperature of the cathode and g is the conductance of the diode or the transconductance of the triode. More elaborate theories lead to a factor which, in various circumstances, may be a little greater or a little less than .644.

Expression (14) is of the same form as that for Johnson noise, but the expression cannot be derived in a manner analogous to that which we have used in treating Johnson noise, for a conducting diode or triode

---

[2] At frequencies for which the transit time from cathode to plate is comparable with the period, the noise induced in the plate circuit is a function of frequency.

cannot be in thermal equilibrium. It is interesting to note that when the plate of a diode is very negative, so that there is no potential minimum between cathode and plate, the impressed noise current is given by

$$\overline{I^2} = (.5)4kT_cgB$$
$$= 2eI_0B.$$

That is, the noise is shot noise, but it can also be expressed in a form analogous to that for Johnson noise, and like expression (14).

At moderate frequencies, noise in triodes and diodes agrees fairly well with (14), being perhaps a little higher. At frequencies high enough so that transit time is important, noise associated with the electronic loading of the grid circuit becomes important. At low audio frequencies and below, *flicker noise* appears. This typically but not always has a $1/f$ spectrum (discussed in the following section). Flicker noise is very variable from tube to tube. It has been ascribed to fluctuations in the work function of the cathode surface.

A detailed treatment of the generation of noise through random processes in active devices is very complicated and would be out of place here.

NOISE WITH A $1/f$ SPECTRUM

It is clear that different Johnson noise spectra are associated with circuits for which the impedance varies in different manners with frequency. However, Johnson noise is in a sense inherently white noise in that the fundamental relation between the noise source—the resistance or conductance—and the amount of noise per unit bandwidth is independent of frequency. Shot noise is in the same sense inherently white noise too, although it can give rise to different spectra in circuits in different transfer admittances or in tubes of different transit times. Presumably it must be, because in a close-spaced diode formed of opposed cathodes at the same temperature and with no average current, shot noise and Johnson noise are two names for the same thing.

Some important sorts of noise are generated *only* in nonequilibrium systems, for instance, in systems in which dc current flows. Among these are *contact noise*, such as is produced in a carbon microphone, and the noise produced in carbon resistors and in silicon and germanium diodes and transistors. Both contact noise and transistor noise have a spectrum such that the noise power per unit bandwidth varies nearly as $1/f$ over a large frequency range, though it may be constant at high frequencies and at very low frequencies.

A noise made up of a random sequence of short pulses, or impulses, as are Johnson noise and shot noise, has a flat spectrum. A noise made up of a random sequence of step functions would have a $1/f^2$ spectrum. This is because a step is the integral of an impulse, and the amplitude of any frequency component of the step is $1/2\pi f$ times that for the impulse. If the amplitude varies as $1/f$, the power will vary as $1/f^2$.

One could obtain a $1/f$ spectrum down to any given frequency by a proper mixture of pulses of various lengths. The longer pulses might actually be a result of a correlation between short pulses, so that pulses tended to occur in groups or bursts over a period longer than that of one pulse; this could give, in effect, a "long" pulse.

Transistor noise has been attributed to the trapping of the holes or electrons (*carriers*) which form the current flow. The trapping and subsequent release of a charge carrier is equivalent to a rectangular pulse in the current. The effect may be strengthened by the charge of the trapped carrier modulating the flow of other charges. By assuming a particular distribution of trapping times, or pulse lengths, a $1/f$ spectrum can be obtained. The matter of noise in semiconductors is by no means thoroughly understood, and somewhat different mechanisms have been suggested.

Actually, the power spectrum cannot vary as $1/f$ right down to $f=0$, for this would imply an infinite noise power. Measurements do show a $1/f$ spectrum down to frequencies as low as 10^{-4} cycles per second.

BIBLIOGRAPHY

This is not a comprehensive bibliography. It is intended to direct the reader to some important early papers and to later papers or books in which more detailed treatments and some further references are given.

Johnson Noise

Johnson, J. B., "Thermal Agitation of Electricity in Conductors." *Physical Review*, Vol. 32 (July 1928), pp. 97–109.
Nyquist, H., "Thermal Agitation of Electric Charge in Conductors." *Physical Review*, Vol. 32 (July 1928), pp. 110–113.
Spenke, E., "Zur korpuskularen Behandlungsweise des Thermischen Rauschens elektrischer Widerstände." *Wissenschaftliche Veröffentlichungen aus den Siemens-Werken*, Vol. 18 No. 2 (February 16, 1939), pp. 54–72.

Shot Noise

Schottky, W., "Spontaneous Current Fluctuations in Various Conductors." *Annalen der Physik*, Vol. 57 No. 23 (1918), pp. 541–567.

Noise in Tubes and Multipliers

Pierce, J. R., "Noise in Resistances and Electron Streams." *Bell System Technical Journal*, Vol. 27 (January, 1948), pp. 158–174.
Beck, A. H. W., *Thermionic Valves*. Cambridge, Cambridge University Press, 1953.

Transistor Noise

Shockley, W., *Electrons and Holes in Semiconductors*. New York, D. Van Nostrand Co., 1950.
MacFarlane, G. G., "A Theory of Contact Noise in Semiconductors." *Proceedings of the Physical Society*, Vol. 63 (October 1, 1950), pp. 807–813.
Bess, Leon, "A Possible Mechanism for 1/f Noise Generation in Semiconductor Filaments." *Physical Review*, Vol. 91 (September 15, 1953), p. 1569.

General

van der Ziel, A., *Noise*. New York Prentice-Hall, 1954.
MacDonald, D. K. C., "Brownian Movement and Spontaneous Fluctuations of Electricity." *Research* (London), Vol. 1 (February, 1948), pp. 194–203.

Methods of Solving Noise Problems[*]

W. R. BENNETT[†], SENIOR MEMBER, IRE

Summary—A tutorial exposition is given of various analytical concepts and techniques of proved value in calculating the response of electrical systems to noise waves. The relevant probability theory is reviewed with illustrative examples. Topics from statistics discussed include probability density, moments, stationary and ergodic processes, characteristic functions, semi-invariants, the central limit theorem, the Gaussian process, correlation, and power spectra. It is shown how the theory can be applied to cases of noise and signal subjected to such operations as filtering, rectification, periodic sampling, envelope detection, phase detection, and frequency detection.

SIGNIFICANCE OF PROBABILITY DENSITY

NOISE-LIKE phenomena have the common property that we do not specify precisely what magnitudes are observed at what times. The reasons for our failure to give such complete descriptive data are various—we may not know enough, we may consider the system to be so complicated that complete use of all possible knowledge is not practical, or we may decide that all we really need to know is furnished by a smoothed-out picture of the true state of affairs. Whatever our motives, by refraining from precise specification, we resign ourselves to a statistical description and we must get used to the appropriate mathematical tools.

The first concept we introduce is that of the probability density function. Even though the numerical outcome of a noise measurement may vary widely when what we choose to call the same experiment is repeated many times, we can distinguish relative likelihood of obtaining various values. Suppose a single property of the noise, as for instance the instantaneous voltage or current, is under measurement. Let x represent a typical measured value. Imagine each x to define a point at the corresponding distance from a fixed reference point on a straight line. Then if we divide this line into small equal intervals of length Δx, and count the number of points in each interval, we approximate a density function of x, which we shall call $p(x)$. We proceed as if there existed such a function defined by

Symbolically

$$\text{Prob } (x_1 < x < x_2) = \int_{x_1}^{x_2} p(x)dx. \tag{2}$$

A second important function called the distribution function $P(x)$ is defined as the probability that the value is less than some specified x. It is given by

$$P(x) = \int_{-\infty}^{x} p(x)dx. \tag{3}$$

It follows that

$$p(x) = \frac{d}{dx} P(x) = P'(x) \tag{4}$$

for such values of x for which $P(x)$ has a derivative.

Note that not all functions are suitable for probability density or distribution functions. To be meaningful, $p(x)$ cannot be negative or imaginary. Also if it is certain that every measurement must yield some real value, we must have

$$\int_{-\infty}^{\infty} p(x)dx = 1 \tag{5}$$

signifying a certainty that the value of x lies somewhere between $-\infty$ and ∞. From the non-negative character of $p(x)$, the value of $P(x)$ cannot decrease with increasing x, and from (5)

$$P(-\infty) = 0. \qquad P(\infty) = 1. \tag{6}$$

An instructive use of the probability density function occurs in the calculation of averages. Suppose we wish to know what average value of some specified function of the quantity x would be obtained from a large number of measurements. The function might for example be the value of x raised to some power, it might be the exponential or sine of x, and of course it might in the simplest nontrivial case be proportional to x itself. In

$$p(x) = \lim_{\substack{\Delta x = 0 \\ N = \infty}} \frac{(\text{Number of Values in Range } \Delta x \text{ at } x)/\Delta x}{\text{Total Number of Values} = N}. \tag{1}$$

We call $p(x)$ the probability density function. As with other densities with which we are familiar, we obtain the probability that a particular measured value lies in an interval of infinitesimal length dx centered at x by multiplication of $p(x)$ by dx. Then if we wish to find the probability that the value is in a specified larger range, say x_1 to x_2, we integrate $p(x)$ through this range.

general let $F(x)$ represent the function of x which is to be averaged and suppose data from many measurements are available. Assume that we calculate the average of $F(x)$ in the usual way by dividing the sum of the values obtained for $F(x)$ by the number of observations. By considering fine divisions of width dx on the x scale, and noting that for a large number of trials a fraction $p(x)dx$ of the total observations belong to an interval of length dx containing the value of x and hence give the obser-

vation $F(x)$, we reason that in the limit as the number of measured values becomes very large

$$\text{av } F(x) = \int_{-\infty}^{\infty} F(x)p(x)dx. \tag{7}$$

Here we have used the abbreviation "av $F(x)$" to mean the average value of $F(x)$ approached by a very large number of trials. Other designations in use include "$<F(x)>$" and "mathematical expectation of $F(x)$," abbreviated as $E[F(x)]$.

The positive integer powers constitute a particular set of functions with averages of outstanding interest. We define the average of x^n as the nth moment of the distribution, and write

$$m_n = \text{av } x^n = \int_{-\infty}^{\infty} x^n p(x)dx. \tag{8}$$

We note that $m_0 = 1$. Of the others, our attention is most often concentrated on m_1, which is the ordinary arithmetical mean, and m_2, which is the mean square. To the electrical engineer dealing with the case in which x is a voltage or current, m_1 represents the constant or dc component of the process and m_2 multiplied by the conductance or resistance respectively gives the mean power. Frequently it is found convenient to study the data with the average subtracted from all values. This concentrates attention on the ac component of the phenomenon. The corresponding power averages are called central moments and are defined by

$$\mu_n = \text{av } (x - m_1)^n = \int_{-\infty}^{\infty} (x - m_1)^n p(x)dx. \tag{9}$$

Evidently $\mu_1 = 0$. The most important central moment is μ_2, which is defined as the variance of the distribution. From the definitions,

$$\mu_2 = \int_{-\infty}^{\infty} (x^2 - 2m_1 x + m_1{}^2)p(x)dx$$
$$= \int_{-\infty}^{\infty} x^2 p(x)dx - 2m_1 \int_{-\infty}^{\infty} xp(x)dx + m_1{}^2 \int_{-\infty}^{\infty} p(x)$$
$$= m_2 - 2m_1{}^2 + m_1{}^2 = m_2 - m_1{}^2$$
$$= \text{av } x^2 - (\text{av } x)^2. \tag{10}$$

The square root of the variance is called the standard deviation, σ, that is

$$\sigma = (\mu_2)^{1/2}, \quad \text{and} \quad \sigma^2 + m_1{}^2 = m_2. \tag{11}$$

In electrical language, the standard deviation is the root-mean-square or rms value of the ac component. The variance is the mean square and when multiplied by the conductance or resistance as appropriate gives the mean power represented by the ac component. In noise theory, it is usually convenient to express results in terms of the variance directly rather than complicate the formulas by introducing conductance or resistance to convert to power values. The variance is sometimes referred to as ac power in a one-ohm circuit.

Up to this point we have spoken somewhat blithely about dc and ac components in a process without revealing our plan of relating actual measurements to the statistical quantities we have been discussing. There are two basic physical programs for doing this which we should now explain. One is based on a series of measurements on one system throughout a very long time and the other calls for a simultaneous set of measurements on a large number of similar systems. In the first case, which we might call the extension-in-time program, we evaluate probability density and distribution functions by observations over a considerable period of time. For example, we could install a set of level recorders at the output of the system and note the fractions of time in which output values are found in sufficiently fine subintervals of the range of variation. To measure average values we use integrating meters, such as may be approximated by voltmeters, ammeters, or wattmeters with long time constants, to measure average voltage, current, or power. The averaging time is prescribed roughly as long enough so that if it were made longer the result would not be changed. Since we must conclude our experiment some time in order to use the data, we cannot extend our measurements throughout all time. A question then arises as to whether we would get the same statistical results if we repeated the entire experiment an hour, a day, or a week later. Such processes as would give the same probability density function and consequently all the other statistical parameters derived therefrom no matter where we localize our observation interval in time are called stationary. A truly stationary process for all future and past time is difficult to imagine, but over the elapsed time in which we retain interest in our apparatus the concept of stationarity is often an appropriate one.

The other program which we might call an extension in space but which is more often called the ensemble method furnishes a more elegant basis for mathematical analysis than the first mentioned. We suppose that a large number of systems are available which differ only in ways of which we are ignorant or which we choose to ignore. Identical measuring instruments are inserted in each system and a set of instantaneous values are read on all meters at the same time. From these data all the statistical functions and parameters are determined by arithmetic calculation. The question of how long a time over which to continue our observations in the first method is replaced by the question of how many systems should we measure in the second. Here again we use enough so that if we added more the results would not be significantly changed.

A stationary process from the ensemble point of view is now defined as one in which the statistics measured at any two distinct instants of time are the same. We thereby avoid one difficulty of the extension-in-time program in that an infinite time is required there to complete the measurements, and no time is left to take a new run. However it could be argued that we are

likewise in difficulty when we call for an infinite number of measurements on distinct systems at one time. In any practical case we must be able to get our data from a finite number of observations. A more important difference from the theoretical viewpoint is that in some cases of importance the limits exist over the ensemble whereas no limit may be approached for the corresponding averages over a long time.

A matter of considerable theoretical interest now arises in that we can not say in general that the two methods we have described for obtaining statistics of noise processes will yield the same results even when the process is stationary in accordance with both definitions. We therefore introduce a new term by defining an *ergodic* process as one in which the statistics over a long time interval for any one system are the same as the statistics over the ensemble of systems at any one instant of time. An ergodic process is always stationary, but a stationary process can be nonergodic. Examples of the latter tend to be somewhat artificial. To illustrate assume that a certain model of amplifier is placed in quantity production. The tubes for the amplifier are obtained from two different manufacturing lots and the tubes of one lot are definitely noisier than the others. The two lots of tubes are thoroughly mixed. Then the average noise power from any one amplifier tends to be either high or low depending on whether it is equipped with tubes from the noisy or quiet lot. The noise power averaged over the ensemble of amplifiers however is intermediate between the noisy and quiet species.

Illustrative Examples of Probability Density

The Uniform or Rectangular Distribution

In Fig. 1(a), the variable has no preference with respect to any part of the range α to $\alpha+\beta$, but it is never outside this range. Then

$$p(x) = \begin{cases} 0, & x < \alpha \text{ and } x > \alpha + \beta \\ k, & \alpha < x < \alpha + \beta. \end{cases} \qquad (12)$$

The constant k is determined from the condition

$$\int_{\alpha}^{\alpha+\beta} k\,dx = 1, \text{ whence } k = 1/\beta. \qquad (13)$$

The average value is given by

$$m_1 = \int_{\alpha}^{\alpha+\beta} \frac{x\,dx}{\beta} = \frac{1}{2\beta}\left[x^2\right]_{\alpha}^{\alpha+\beta} = \alpha + \frac{\beta}{2} \qquad (14)$$

as could have been determined by inspection. The mean square is

$$m_2 = \int_{\alpha}^{\alpha+\beta} \frac{x^2\,dx}{\beta} = \frac{1}{3\beta}\left[x^3\right]_{\alpha}^{\alpha+\beta} = \alpha^2 + \alpha\beta + \beta^2/3. \qquad (15)$$

The variance is

$$\mu_2 = m_2 - m_1^2 = \beta^2/12. \qquad (16)$$

The standard deviation is

$$\sigma = \frac{\beta}{2\sqrt{3}}. \qquad (17)$$

The distribution function [Fig. 1(b)] is

$$P(x) = \begin{cases} 0, & x < \alpha \\ (x - \alpha)/\beta, & \alpha < x < \alpha + \beta \\ 1, & x > \alpha + \beta \end{cases}. \qquad (18)$$

These results are immediately applicable to the problem of "quantizing noise" arising from the errors in conversion of a signal in analog form to a digital approximation. Suppose the range of signal magnitudes is divided into uniform intervals of width Δ. All magnitudes falling within each interval are equated to a single value at midinterval. If the intervals are made small, the magnitudes falling within any particular one are uniformly distributed within the interval and the errors, which are the differences between the original value and the midinterval approximation, are uniformly distributed between $-\Delta/2$ and $\Delta/2$. Therefore the errors have a uniform distribution in which $\alpha = -\Delta/2$ and $\beta = \Delta$. From the above results, then the dc component of the error is zero and the rms error is $\Delta/2\sqrt{3}$. These are fundamental relations for digital-to-analog conversion in which the quantizing steps are all the same size. It is also applicable in straight numerical computation as a means of estimating the error from rounding off at a certain number of decimal places.

A rectangular distribution is often assumed for the phase of a sine wave with respect to a particular origin of time or with respect to the phase of some other sine wave. What we mean by such an assumption is that no information is available to make any particular phase angle more likely than any other. If, as is often the case, angles differing by multiples of 2π can not be distinguished, it is convenient to take a fixed interval of 2π radians as defining the complete range of possible angles. In Fig. 1(a) this would mean $\beta = 2\pi$ and α arbitrary. We may then wish to calculate the statistics of some function of the angle.

In general, if we are given the probability density function $q(\theta)$ of a variable θ, and we wish to calculate the probability density function $p(x)$ for $x = F(\theta)$, it is convenient to invert the functional relationship and write $\theta = f(x)$. Then by direct substitution,

$$q(\theta)d\theta = q[f(x)]f'(x)dx \qquad (19)$$

where $f'(x) = df(x)/dx$. Hence if $f(x)$ is a single valued function of x,

$$p(x) = q[f(x)]f'(x). \qquad (20)$$

If $f(x)$ is multiple valued, the expression on the right is summed over all the values. We shall apply these relations in the next example.
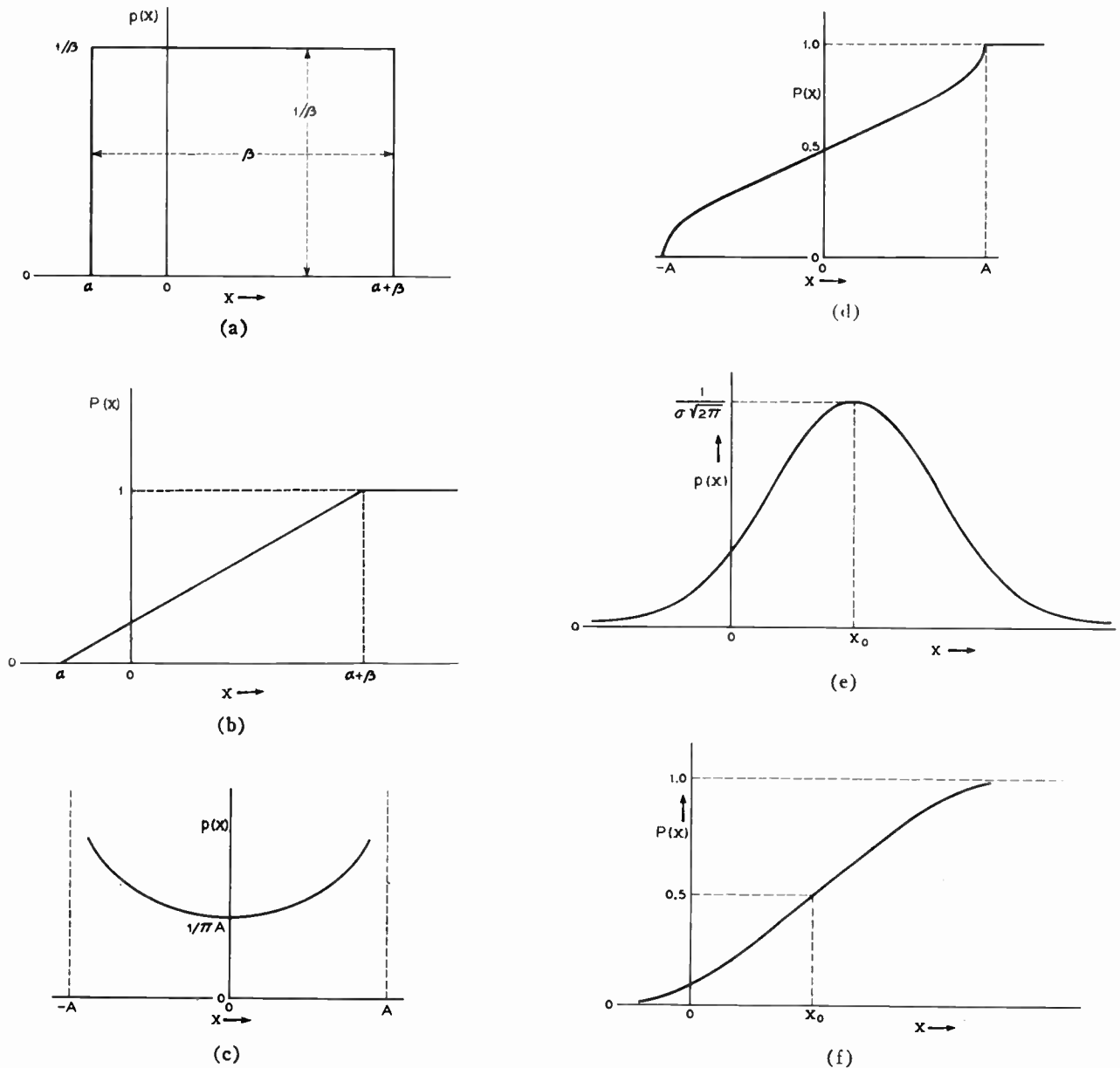
Fig. 1—(a) Probability density function for rectangular distribution, (b) Distribution function for rectangular case. (c) Probability density function for sinusoidal distribution. (d) Distribution function for sinusoidal case. (e) Probability density function for Gaussian distribution. (f) Distribution function for Gaussian case.

The Sinusoidal Distribution

Let

$$x = A \sin \theta \tag{21}$$

where θ has a uniform distribution in range $-\pi/2$ to $3\pi/2$. Then the values of x are distributed like those of the ordinates of a sine wave with amplitude A. To find the probability density function for x, we write $\alpha = -\pi/2, \beta = 2\pi$, and

$$q(\theta) = \begin{cases} 0, & \theta < -\pi/2 \text{ and } \theta > 3\pi/2 \\ \dfrac{1}{2\pi}, & -\pi/2 < \theta < 3\pi/2. \end{cases} \tag{22}$$

Then solving (21) for θ as a function of x, we find

$$\theta = f(x) = \arcsin \frac{x}{A} \tag{23}$$

$$f'(x) = (A^2 - x^2)^{-1/2}. \tag{24}$$

We note that each value of x in the range $-A$ to A corresponds to two values of θ and hence that we must multiply the right hand side of (20) by two to obtain $p(x)$. Then

$$p(x) = \begin{pmatrix} 0, & x < -A \text{ and } x > A \\ (A^2 - x^2)^{-1/2}/\pi, & -A < x < A \end{pmatrix}. \tag{25}$$

Fig. 1(c) shows the graph of this function.

The average value over the ensemble is given by

$$m_1 = \int_{-A}^{A} \frac{x\,dx}{\pi(A^2 - x^2)^{1/2}} = 0. \tag{26}$$

Likewise the mean square is

$$m_2 = \int_{-A}^{A} \frac{x^2\,dx}{\pi(A^2 - x^2)^{1/2}} = \frac{A^2}{2}. \tag{27}$$

Since $m_1 = 0$, m_2 is also the variance. The distribution function, Fig. 1(d), is

$$P(x) = \int_{-A}^{x} \frac{dx}{\pi(A^2 - x^2)^{1/2}} = \frac{1}{\pi}\left(\frac{\pi}{2} + \arcsin\frac{x}{A}\right). \tag{28}$$

This example shows that it is possible for the probability density to become infinite provided the integral over a finite interval including the singularity exists.

The sinusoidal distribution is appropriate for the noise produced by cw interference of constant amplitude and random phase. What we have illustrated above is the ensemble approach which assumes an infinite number of possible sources of form $A \sin(\omega t + \theta)$ with A fixed and θ distributed uniformly throughout the range α to $\alpha + 2\pi$. We averaged over the ensemble with t fixed, noting that adding the constant ωt to θ does not change the distribution except for a trivial shift in α. We can also work out time averages over a single function of time belonging to the ensemble. Let

$$E(t) = A \sin(\omega t + \theta) \tag{29}$$

with A, ω, and θ fixed. To evaluate the mean square over a long time we write

$$\begin{aligned}
\overline{E^2} &= \operatorname*{Lim}_{T \to \infty} \frac{1}{T} \int_{t_1}^{t_1+T} E^2(t)\,dt \\
&= \operatorname*{Lim}_{T \to \infty} \frac{1}{T} \int_{t_1}^{t_1+T} \frac{A^2}{2}[1 + \cos 2(\omega t + \theta)]\,dt \\
&= \frac{A^2 T}{2T} = \frac{A^2}{2}.
\end{aligned} \tag{30}$$

Since the process is stationary the result does not depend on t_1. The fact that we obtained the same result as by the ensemble method is illustrative of the ergodicity of the process.

The Gaussian Distribution

One of the most important distributions in noise theory is that in which the probability density is proportional to the exponential of a negative quadratic function of the values of the variable. The general form for one variable is

$$p(x) = \frac{1}{\sigma\sqrt{2\pi}} e^{-(x-x_0)^2/2\sigma^2}. \tag{31}$$

The parameters have been adjusted here to give the required condition

$$\int_{-\infty}^{\infty} p(x)\,dx = 1, \tag{32}$$

and also

$$m_1 = \int_{-\infty}^{\infty} x p(x)\,dx = x_0 \tag{33}$$

$$m_2 = \int_{-\infty}^{\infty} x^2 p(x)\,dx = x_0^2 + \sigma^2 \tag{34}$$

$$\mu_2 = m_2 - m_1^2 = \sigma^2. \tag{35}$$

That is x_0 is the mean, σ^2 is the variance, and σ is the standard deviation. This distribution is called normal or Gaussian. An important theorem in statistics called the central limit theorem shows under very general assumptions that the distribution of the sum of an indefinitely large number of other independently distributed quantities must approach the Gaussian distribution, no matter what the individual distributions may be. We shall not prove this theorem here, but shall indicate later by examples the sort of mechanism by which it operates. The phenomenon called Johnson noise, resistance noise, or thermal noise associated with thermal agitation of electrons in conductors gives rise to voltages and currents with Gaussian distribution. It may be thought of as the sum of a very large number of practically independent pulses. When the receiver is linear, there is no preference between positive and negative values, and the mean value x_0, which represents the dc component, is zero. The parameter σ is then the rms value.

Figs. 1(e) and 1(f) show the nature of the Gaussian functions for $p(x)$ and $P(x)$. The latter may be expressed by

$$P(x) = \frac{1}{2}\left[1 + \operatorname{erf}\frac{(x - x_0)}{(\sqrt{2}\sigma)}\right],$$

where

$$\operatorname{erf} z = \frac{2}{\sqrt{\pi}} \int_0^z e^{-\lambda^2}\,d\lambda. \tag{36}$$

The theory we have given so far is sufficient to solve a number of interesting noise problems. Suppose we are asked to calculate the dc component in the output of a half-wave linear rectifier when the input is resistance noise. The probability density function of the input wave with the negative lobes cut off is given by

$$p(x) = \frac{1}{\sigma\sqrt{2\pi}} e^{-x^2/2\sigma^2} + \frac{1}{2}\delta(x), \qquad x \geqq 0 \tag{37}$$

where $\delta(x)$ is defined by

$$\delta(x) = 0 \qquad x \neq 0 \tag{38}$$

$$\int_{0-\epsilon}^{0+\epsilon} \delta(x)\,dx = 1, \qquad \epsilon > 0. \tag{39}$$

The δ function is introduced as a convenient symbol for the fact that the suppressed negative lobes transfer all their accumulated probability to the value $x = 0$.

Then if a_1 is the conductance of the rectifier during the conducting phase, the dc component is

$$\text{av } (a_1 x) = a_1 \int_{-\infty}^{\infty} x p(x) dx$$

$$= a_1 \int_{0}^{\infty} \frac{x}{\sigma \sqrt{2\pi}} e^{-x^2/2\sigma^2} dx + a_1 \int_{-\infty}^{\infty} x \delta(x) dx$$

$$= \frac{a_1}{\sigma \sqrt{2\pi}} \left[-\sigma^2 e^{-x^2/2\sigma^2} \right]_{0}^{\infty} = \frac{a_1 \sigma}{\sqrt{2\pi}} \cdot \quad (40)$$

Rectification with other functional laws can be treated in a similar manner.

A curious property of the Gaussian distribution is that no matter how large a value we may consider there is a finite probability of it being exceeded in an observation. The probability diminishes so rapidly at very large values however that for practical purposes peaks exceeding some reasonable value can be regarded as impossible.

DISTRIBUTION OF SUMS—THE CHARACTERISTIC FUNCTION

There are many physical situations in which we wish to relate the statistics of the measured sum of a number of components to the statistics of the individual contributions. We have already mentioned one example—the representation of thermal noise as the sum of a large number of practically independent pulses. Another case is that of atomic radiation considered as the sum of a large number of independent sine waves of limited duration. An important case to which we shall devote much attention in this paper is that of the sum of a wanted signal and an undesired noise component. The fundamental relation, given $p_1(x)$ and $p_2(y)$ as the probability density function of two *independent* quantities x and y, and that $z = x + y$, is

$$p(z) = \int_{-\infty}^{\infty} p_1(x) p_2(z - x) dx. \quad (41)$$

That is, in order to obtain the value z for a given x, we must have y in the range $(z - x)dx$. This is a compound event in which the individual events are independent and hence the probability is found by multiplying the separate probabilities. The total probability is found by integrating over all x.

Integrals of the form (41) are commonly known as convolution integrals. The communication engineer has become familiar with them in relation to Fourier analysis. As an example, suppose that $g_1(\lambda)$ is the amplitude of a wave at the time λ, and $g_2(t - \lambda)$ is the response of a linear network at time $t - \lambda$ after it has been excited by a unit impulse. Then the response of the network to $g_1(t)$ is given as a function of time t by

$$g(t) = \int_{-\infty}^{\infty} g_1(\lambda) g_2(t - \lambda) d\lambda. \quad (42)$$

A basic theorem on Fourier transforms states that if $g_1(t)$, $g_2(t)$ have the Fourier transforms $S_1(\omega)$, $S_2(\omega)$ respectively; that is, if

$$S_1(\omega) = \int_{-\infty}^{\infty} g_1(t) e^{-i\omega t} dt \quad (43)$$

and

$$S_2(\omega) = \int_{-\infty}^{\infty} g_2(t) e^{-i\omega t} dt \quad (44)$$

then the Fourier transform of $g(t)$ is $S_1(\omega) S_2(\omega)$. That is

$$S_1(\omega) S_2(\omega) = \int_{-\infty}^{\infty} g(t) e^{-i\omega t} dt \quad (45)$$

and by inversion

$$g(t) = \frac{1}{2\pi} \int_{-\infty}^{\infty} S_1(\omega) S_2(\omega) e^{i\omega t} d\omega. \quad (46)$$

This means that we can calculate $g(t)$ by calculating the inverse Fourier transform of the product of the Fourier transforms of $g_1(t)$ and $g_2(t)$. (Note that the sign of i may be changed throughout without changing the validity.)

We can apply these same results of Fourier analysis to (41). We must then conclude that the probability density function for the sum of two independent variables is the inverse Fourier transform of the product of the Fourier transforms of the individual probability density functions. It therefore appears that an important function to be defined is the Fourier transform of a probability density. In statistics this function is called the *characteristic function* (ch.f.). It is a function of a dummy variable ξ, and is in fact seen to be the average value of $e^{i\xi x}$. That is, the ch.f. corresponding to the variable x is defined by

$$C_x(\xi) = \text{av } e^{i\xi x} = \int_{-\infty}^{\infty} e^{i\xi x} p(x) dx. \quad (47)$$

If we write $C_x(\xi)$ for the ch.f. of x, $C_y(\xi)$ for the ch.f. of y, and $C_z(\xi)$ for the ch.f. of $z = x + y$, then

$$C_z(\xi) = C_x(\xi) C_y(\xi) \quad (48)$$

and $p_2(z)$, the probability density function of the sum $z = x + y$ is

$$p_z(z) = \frac{1}{2\pi} \int_{-\infty}^{\infty} C_x(\xi) C_y(\xi) e^{-i\xi z} d\xi. \quad (49)$$

Extending the process now to the sum of n variables, let $z_n = x_1 + x_2 + \cdots + x_n$. Then

$$C_{z_n}(\xi) = C_{x1}(\xi) C_{x2}(\xi) \cdots C_{x_n}(\xi) \quad (50)$$

$$p(z_n) = \frac{1}{2\pi} \int_{-\infty}^{\infty} C_{x1}(\xi) C_{x2}(\xi) \cdots C_{x_n}(\xi) e^{-i\xi z} d\xi. \quad (51)$$

It will be noted that as n is made very large the integrand shrinks rapidly as we move away from the origin and that only the values very near $\xi = 0$ contribute much. When $\xi = 0$, the integrand becomes unity. In the neighborhood of $\xi = 0$, the integrand is of form

$$\frac{\left[\dfrac{\beta\xi}{2} - \dfrac{(\beta\xi)^3}{48} + \cdots\right]^n e^{-ix\xi}}{(\beta\xi/2)^n}$$

$$= \left[1 - \frac{(\beta\xi)^2}{24} + \cdots\right]^n e^{-ix\xi}$$

$$= \left[1 - \frac{n}{24}(\beta\xi)^2 + \cdots\right] e^{-ix\xi}. \quad (54)$$

We may approximate the integral by replacement with a function which has the same initial terms in its power series expansion and drops rapidly to zero away from the origin. Such a function is

$$e^{-n(\beta\xi)^2/24 - ix\xi}.$$

Then for large n,

$$p_n(x) = \frac{1}{2\pi}\int_{-\infty}^{\infty} e^{-n\beta^2\xi^2/24} \cos x\xi \, d\xi \quad (55)$$

or

$$p_n(x) = \frac{1}{\pi}\sqrt{\frac{6\pi}{n\beta^2}}\, e^{-6x^2/n\beta^2}$$

$$= \frac{1}{\sigma_n\sqrt{2\pi}}\, e^{-x^2/2\sigma_n^2} \quad (56)$$

where

$$\sigma_n = \beta\sqrt{\frac{n}{12}} = \sigma_1\sqrt{n}. \quad (57)$$

Thus we tend toward a Gaussian distribution with $\sqrt{n}$ times the standard deviation of the original or n times the variance. That is, the mean power values in independent uniform noise sources add directly, and if enough are added a Gaussian distribution is approached. Since each component represents an independent occurrence, the Gaussian limit could have been deduced from the central limit theorem previously mentioned. Our calculation may be regarded as a verification for this particular case. Since the range of each component is $-\beta/2$ to $\beta/2$, the range of the sum cannot exceed $-n\beta/2$ to $n\beta/2$. The Gaussian approximation, which gives nonzero probability for all finite ordinates, should only be applied to values well within the range of possible sums. As n becomes indefinitely large, the excluded range recedes away from any values of physical interest.

An engineering application of the above result may be made to the case of resultant quantizing noise when a number of alternate analog-to-digital and digital-to-analog conversions are made on a signal. We can also identify the sum as noise caused by superimposing inde-

Fig. 2—(a) Symmetrical uniform probability density function. (b) Characteristic function of symmetrical uniform case. (c) Characteristic function of sinusoidal case.

We illustrate by calculating the characteristic functions for the previous examples and show how they may be used to calculate distributions of corresponding sums.

Consider first the symmetrical uniform distribution with $\alpha = -\beta/2$, Fig. 2(a).

Then

$$C_x(\xi) = \int_{-\beta/2}^{\beta/2} e^{i\xi x}\, \frac{dx}{\beta} = \frac{2\sin\beta\xi/2}{\beta\xi}. \quad (52)$$

This function is plotted in Fig. 2(b). The probability density function of the sum of n uniformly distributed variables in the same range is

$$p_n(x) = \frac{1}{2\pi}\int_{-\infty}^{\infty} \frac{\sin^n\beta\xi/2}{(\beta\xi/2)^n}\, e^{-ix\xi} d\xi. \quad (53)$$

pendently occurring triangular pulses of equal height $\beta/2$, random sign, and random times of occurrence.

As a second example, consider the sum of a number of independent sinusoidal distributions such as might be obtained by combining the outputs of nonsynchronous oscillators. From (25), a component of peak amplitude A has the ch.f.

$$C_x(\xi) = \frac{1}{\pi} \int_{-A}^{A} \frac{e^{i\xi x} dx}{(A^2 - x^2)^{1/2}}$$
$$= J_0(A\xi). \qquad (58)$$

where J_0 is the zero order Bessel function of the first kind. The graph of $C_x(\xi)$ is shown in Fig. 2(c). Hence the probability density function for the sum of n independent sinusoidal sources with peak values $A_1, A_2, \cdots, A_n$ is

$$p_n(x) = \frac{1}{2\pi} \int_{-\infty}^{\infty} J_0(A_1\xi) J_0(A_2\xi) \cdots J_1(A_n\xi) e^{-i x\xi} d\xi. \quad (59)$$

The limiting case when n is large may be studied by the same method as used for the sum of n uniform distributions. We substitute the first two terms of the power series for each Bessel function, namely

$$J_0(x) = 1 - \frac{x^2}{4} \text{ for } x \text{ small}, \qquad (60)$$

and note that for ξ small,

$$J_0(A_1\xi) J_0(A_2\xi) \cdots J_0(A_n\xi),$$
$$= 1 - \frac{A_1^2 + A_2^2 + \cdots + A_n^2}{4} \xi^2. \qquad (61)$$

Replacing this expression by $\exp\left[-(A_1^2+A_2^2+\cdots+A_n^2)\xi^2/4\right]$ which has the same first two terms in its power series expansion, we then deduce that for n large

$$p_n(x) \sim \frac{1}{2\pi} \int_{-\infty}^{\infty} e^{-i x\xi - (A_1^2+A_2^2+\cdots+A_n^2)\xi^2/4} d\xi$$
$$= \frac{1}{\sigma\sqrt{2\pi}} e^{-x^2/2\sigma^2} \qquad (62)$$

where

$$\sigma^2 = \tfrac{1}{2}(A_1^2 + A_2^2 + \cdots + A_n^2). \qquad (63)$$

This shows that the resultant distribution approaches the Gaussian form with standard deviation equal to the square root of the sum of the mean squares of each individual distribution. This is another example of the central limit theorem. By taking the A's unequal we have illustrated that the component distributions do not have to be the same to produce the Gaussian limit.

In the case of the Gaussian distribution, the ch.f. is

$$C_x(\xi) = \frac{1}{\sigma\sqrt{2\pi}} \int_{-\infty}^{\infty} e^{-(x-x_0)^2/2\sigma^2 + ix\xi} dx$$
$$= \frac{1}{\sigma\sqrt{2\pi}} \int_{-\infty}^{\infty} e^{-u^2/2 + i\xi(\sigma u + x_0)} \sigma du$$
$$= e^{i\xi x_0 - \sigma^2\xi^2/2}. \qquad (64)$$

This is an example of the self-reciprocal property of the Gaussian function with respect to Fourier transformation. Since the product of Gaussian functions is also Gaussian, the distribution of the sum of Gaussian variables must remain Gaussian. This is certainly to be expected from the central limit theorem, for if the addition of other distributions tends toward the Gaussian, the Gaussian form must represent an equilibrium-case preserving its form when more like itself are added.

We calculate for the probability density function of the sum of n Gaussian variables having mean values $a_1, a_2, \cdots, a_n$ and standard deviation $\sigma_1, \sigma_2, \cdots, \sigma_n$

$$p_n(t) = \frac{1}{2\pi} \int_{-\infty}^{\infty} e^{-\xi^2/2(\sigma_1^2+\sigma_2^2+\cdots\sigma_n^2)+i\xi(a_1+a_2+\cdots+a_n)-ix\xi} d\xi$$
$$= \frac{1}{\sigma\sqrt{2\pi}} e^{-(x-x_0)^2/2\sigma} \qquad (65)$$

where

$$x_0 = a_1 + a_2 + \cdots + a_n \qquad (66)$$
$$\sigma^2 = \sigma_1^2 + \sigma_2^2 + \cdots + \sigma_n^2. \qquad (67)$$

That is, the mean values add, and the squares of the variances add. Any number of Gaussian distributions may be combined in this way.

In many practical problems our ultimate goal is the determination of the moments, particularly the first and second, which give the dc voltage or current and the ac power. The probability density function is in these cases merely a means to an end, and we should be on the alert for the possibility of simpler methods of getting the moments. The characteristic function furnishes one such possibility, for we observe that

$$C_x(\xi) = \text{av } e^{i\xi x} = \text{av} \sum_{r=0}^{\infty} \frac{(i\xi x)^r}{r!}$$
$$= \sum_{r=0}^{\infty} \frac{(i\xi)^r}{r!} \text{av } x^r = \sum_{r=0}^{\infty} \frac{(i\xi)^r}{r!} m_r. \qquad (68)$$

This equation shows that m_r, which is the rth moment or average rth power, may also be defined as

$$m_r = \begin{array}{l} r!/i^r \text{ times coefficient of } \xi^r \text{ in the expansion of} \\ C_x(\xi) \text{ in powers of } \xi. \end{array} \qquad (69)$$

We thus see that we can compute moments from the characteristic function directly. For example, to obtain the moments of the sum of n variables, we may calculate the ch.f. of each, multiply the ch.f.'s together, and expand the product in a power series in ξ. The moments are then given by (69). Calculation of the Fourier transform of the resultant ch.f. with a subsequent integration for the typical moment is thereby avoided.

If we combine (68) with (48), letting the moments of x, y, and z be represented respectively by m_{xr}, m_{yr}, m_{zr}, we note that

$$\sum_{r=0}^{\infty} \frac{(i\xi)^r}{r!} m_{zr} = \sum_{r=0}^{\infty} \sum_{s=0}^{\infty} \frac{(i\xi)^{r+s}}{r!s!} m_{xr} m_{ys}. \qquad (70)$$

Now if we equate coefficients of the first and second powers of ξ on the two sides of the equation, we verify that

$$m_{z1} = m_{x1} + m_{y1} \tag{71}$$

$$m_{z2} - m_{z1}^2 = m_{x2} - m_{x1}^2 + m_{y2} - m_{y1}^2. \tag{72}$$

Eq. (71) states that the mean value of the sum is equal to the sum of the means. This is elementary and is in fact true of dependent as well as independent processes. In electrical engineering terminology, the equivalent statement is that dc components may be added algebraically. Eq. (72) says that the variance of the sum of *independent* components is equal to the sum of the variances of the individual components. It is important to observe that independence was assumed in our derivation, for this law does not hold for dependent processes. In electrical engineering language, the equivalent statement is that the total power from independent components is the sum of the power in the individual components. The statement does not hold for example when two sine waves of the same frequency and fixed phase are added. In the latter case if the two amplitudes are equal, the power in the sum may have any value from zero when the waves are oppositely phased to four times the power of each component when phases coincide.

It is sometimes convenient to make use of a complete set of parameters which like the mean and variance are additive when distributions of sums of independent quantities are calculated. Such a set is furnished by the semi-invariants. The rth semi-invariant s_r is defined as the coefficient of $(i\xi)^r/r!$ in the power series expansion of $\ln C_x(\xi)$. That is, noting from (47) that $C_x(0) = 1$ and hence $\ln C_x(0) = s_0 = 0$, we write

$$\ln C_x(\xi) = \sum_{r=1}^{\infty} \frac{(i\xi)^r}{r!} s_r \tag{73}$$

Taking exponentials of both sides and recalling (68), we find

$$C_x(\xi) = e^{\sum_{r=1}^{\infty}(i\xi)^r s_r/r!} = \sum_{r=0}^{\infty} \frac{(i\xi)^r}{r!} m_r. \tag{74}$$

This equation may be used to obtain either the semi-invariants in terms of the moments, or vice versa. The results are

$$\left.\begin{aligned} s_1 &= m_1 \\ s_2 &= m_2 - m_1^2 \\ s_3 &= m_3 - 3m_1m_2 + 2m_1^3, \text{ etc.} \end{aligned}\right\} \tag{75}$$

and

$$\left.\begin{aligned} m_1 &= s_1 \\ m_2 &= s_2 + s_1^2 \\ m_3 &= s_3 + 3s_1s_2 + s_1^3, \text{ etc.} \end{aligned}\right\}. \tag{76}$$

Now since the ch.f. $C_n(\xi)$ for the distribution of $x_1 + x_2 + \cdots + x_n$ is

$$C_n(\xi) = C_{x_1}(\xi)C_{x_2}(\xi) \cdots C_{x_n}(\xi), \tag{77}$$

it follows that

$$\ln C_n(\xi) = \ln C_{x_1}(\xi) + \ln C_{x_2}(\xi) + \cdots + \ln C_{x_n}(\xi) \tag{78}$$

so from (73) if we let $s_r^{(k)}$ represent the rth semi-invariant of the kth distribution, and s_{nr} represent the rth semi-invariant of the sum,

$$\begin{aligned} \sum_{r=1}^{\infty} \frac{(i\xi)^r}{r!} s_{nr} &= \sum_{r=1}^{\infty} \frac{(i\xi)^r}{r!} s_r^{(1)} + \sum_{r=1}^{\infty} \frac{(i\xi)^r}{r!} s_r^{(2)} + \cdots \\ &\quad + \sum_{r=1}^{\infty} \frac{(i\xi)^r}{r!} s_r^{(n)} \\ &= \sum_{r=1}^{\infty} \frac{(i\xi)^r}{r!} [s_r^{(1)} + s_r^{(2)} + \cdots + s_r^{(n)}]. \end{aligned} \tag{79}$$

Therefore

$$s_{nr} = s_r^{(1)} + s_r^{(2)} + \cdots + s_r^{(n)}. \tag{80}$$

In other words as previously implied, the rth semi-invariant of the distribution of the sum of any number of independent variables is equal to the sum of the rth semi-invariants of the individual distributions. The first and second semi-invariants are identical with the mean and variance respectively.

A practical calculating procedure to determine the moments for the sum is then:

1) Calculate individual moments.
2) Calculate individual semi-invariants from moments by (75).
3) Add semi-invariants to obtain semi-invariants of sum.
4) Calculate moments of sum by (76).

An interesting example of the use of semi-invariants to determine the moments of the sum of n quantities whose logarithms have Gaussian distributions has been given by Holbrook and Dixon [2].

Two-Dimensional Probability Theory

Up to now we have dealt with probability density functions of a single variable. We are able to obtain statistical information as to relative numbers of occurrence of different magnitudes in this way, but we cannot deduce anything about the time scale over which we would expect to observe such a representative set of values. This defect must be remedied because all our engineering data are obtained with the circuits which are frequency selective—that is, they do not respond equally to all impressed waves, but are sensitive also to the rapidity with which changes are made. The communication engineers' statement of this is that circuits respond appreciably only to those disturbances which fall within their transmission bands.

Our one-variable theory dealing with values isolated from each other in time was demonstrated to be capable of solving one problem in frequency selectivity—that of distinguishing between dc and ac. That is, by taking averages over a long time we can resolve a noise wave into one component which is constant and therefore contains only the frequency zero and a second com-

ponent which is variable with zero mean and hence can be said to contain only frequencies greater than zero. This resolution is entirely too crude to be adequate for any but the simplest situations.

The next step is to study the statistics of pairs of values of voltage or current separated by specified instants of time. It turns out that these additional statistics are sufficient for practically all the problems of engineering importance. We accordingly digress to state some needed facts about probability relations concerning two coordinates x and y which may be dependent on each other—that is, specifying the value of one affects the statistics of the other. Such distributions are called bivariate. It is convenient to consider first two generalized variables x and y. Later we shall specialize to the case in which x and y represent values of the same voltage or current wave at two different instants of time.

The necessary techniques are an easy generalization of what has gone before. We define $p(x, y)$, the probability density function of two coordinates, as to be that function which when multiplied by the infinitesimal area $dxdy$ gives the probability that the value of the first coordinate is in the range x to $x+dx$ and the value of the second coordinate is simultaneously within the range y to $y+dy$. Then as before the probability that the first coordinate falls somewhere in the finite range x_1 to x_2 while the second falls somewhere in the range y_1 to y_2 is expressed by

$$\text{Prob } (x_1 < x < x_2, y_1 < y < y_2)$$
$$= \int_{x_1}^{x_2} \int_{y_1}^{y_2} p(x, y)dxdy. \quad (81)$$

As before we may express the probability that the values are less than specified ones in terms of the probability density function. The complete distribution function $P(x, y)$ is now

$$P(x, y) = \int_{-\infty}^{x} \int_{-\infty}^{y} p(x, y)dxdy. \quad (82)$$

What are called marginal distribution functions define probabilities of x without regard to y and vice versa. There are two of these

$$P_y(x) = \int_{-\infty}^{x} dx \int_{-\infty}^{\infty} p(x, y)dy = \int_{-\infty}^{x} p_y(x)dx \quad (83)$$

$$P_x(y) = \int_{-\infty}^{y} dy \int_{-\infty}^{\infty} p(x, y)dx = \int_{-\infty}^{y} p_x(y)dy. \quad (84)$$

The functions $p_y(x)$, $p_x(y)$ defined by

$$p_y(x) = \int_{-\infty}^{\infty} p(x, y)dy \quad (85)$$

$$p_x(y) = \int_{-\infty}^{\infty} p(x, y)dx \quad (86)$$

may be called marginal probability density functions.

Evidently when the indicated derivatives exist

$$p(x, y) = \frac{\partial^2 P(x, y)}{\partial_x \partial_y} \quad (87)$$

$$p_y(x) = dP_y(x)/dx \quad (88)$$

$$p_x(y) = dP_x(y)/dy. \quad (89)$$

We must likewise have

$$P(\infty, \infty) = \int_{-\infty}^{\infty} \int_{-\infty}^{\infty} p(x, y)dxdy = 1 \quad (90)$$

$$P_y(\infty) = \int_{-\infty}^{\infty} p_y(x)dx = 1 \quad (91)$$

$$P_x(\infty) = \int_{-\infty}^{\infty} p_x(y)dy = 1. \quad (92)$$

Averages are computed in the same way as before except that we now have two integrations to perform

$$\text{av } F(x, y) = \int_{-\infty}^{\infty} \int_{-\infty}^{\infty} F(x, y)p(x, y)dxdy. \quad (93)$$

For functions of one of the coordinates only, we may use

$$\text{av } F(x) = \int_{-\infty}^{\infty} F(x)p_y(x)dx \quad (94)$$

$$\text{av } F(y) = \int_{-\infty}^{\infty} F(y)p_x(y)dy. \quad (95)$$

In the special case in which the values of x and y are independent, $p(x, y)$ can be written as $p_y(x)p_x(y)$; *i.e.*, as the product of a function of x only and one of y only.

The moments now become doubly infinite in number and require a double subscript. We write

$$m_{jk} = \text{av } x^j x^k = \int_{-\infty}^{\infty} \int_{-\infty}^{\infty} x^j y^k p(x, y)dxdy. \quad (96)$$

We see that $m_{00} = 1$ and that the means of x and y separately are

$$m_{10} = x_0 = \text{av } x = \int_{-\infty}^{\infty} \int_{-\infty}^{\infty} xp(x, y)dxdy$$
$$= \int_{-\infty}^{\infty} xp_y(x)dx \quad (97)$$

$$m_{01} = y_0 = \text{av } y = \int_{-\infty}^{\infty} \int_{-\infty}^{\infty} yp(x, y)dxdy$$
$$= \int_{-\infty}^{\infty} yp_x(y)dy. \quad (98)$$

As in the one-variable case, we often wish to subtract out the mean values, and correspondingly we define the central moments as

$$\mu_{jk} = \text{av } \left[(x - x_0)^j(y - y_0)^k \right]$$
$$= \int_{-\infty}^{\infty} \int_{-\infty}^{\infty} (x - x_0)^j(y - y_0)^k p(x, y)dxdy. \quad (99)$$

The most important central moments are the second order ones μ_{20}, μ_{11}, and μ_{02}. Since

$$\mu_{20} = \text{av} \, (x - x_0)^2 = \int_{-\infty}^{\infty} x^2 p_y(x) dx$$

$$= \text{av} \, x^2 - (\text{av} \, x)^2 \qquad (100)$$

$$\mu_{02} = \text{av} \, (y - y_0)^2 = \int_{-\infty}^{\infty} y^2 p_x(y) dy$$

$$= \text{av} \, y^2 - (\text{av} \, y)^2 \qquad (101)$$

we see that they are simply the variances of x and y separately. The quantity

$$\mu_{11} = \text{av} \, [(x - x_0)(y - y_0)]$$

$$= \int_{-\infty}^{\infty} \int_{-\infty}^{\infty} (xy - x_0 y - y_0 x + x_0 y_0) p(x, y) dx dy$$

$$= \text{av} \, (xy) - x_0 y_0 - y_0 x_0 + x_0 y_0$$

$$= \text{av} \, (xy) - (\text{av} \, x)(\text{av} \, y) \qquad (102)$$

is defined as the covariance of the two quantities. It is the most significant contribution of two-dimensional theory over the one-dimensional case and will enable us to define the power spectra, or density of mean power along the frequency scale, for our random processes. We remark that when two quantities are independent, their covariance vanishes and their average product is equal to the product of their individual averages. The converse is not true in general but is true for jointly Gaussian processes, which we shall discuss next.

In the two-dimensional jointly Gaussian distribution, the probability density function is proportional to the exponential of a negative quadratic function in x and y. By assuming the most general function of this type and determining the constants by evaluating x_0, y_0, μ_{20}, μ_{02}, μ_{11} and also equating the integral to unity, we find

$$p(x, y) = \frac{1}{2\pi A} e^{[-\mu_{02}(x-x_0)^2 + \mu_{20}(y-y_0)^2 - 2\mu_{11}(x-x_0)(y-y_0)]/2A^2} \quad (103)$$

where

$$A^2 = \mu_{20}\mu_{02} - \mu_{11}^2. \qquad (104)$$

Fig. 3 shows the surface defined by (103). It is symmetrical about an axis which is displaced and rotated with respect to the coordinate axes. By the central limit theorem, this is the form of probability density function approached for the values of x and y when x is the sum of the independent values $x_1, x_2, \cdots x_n$, y is the sum of the independent values $y_1, y_2, \cdots y_n$, the probability density function $p_k(x_k, y_k)$ holds for the values x_k, y_k, and n is large.

The characteristic function of a bivariate distribution is a double Fourier transform which we write as

$$C_{xy}(\xi_1, \xi_2) = \text{av} \, e^{i(\xi_1 x + \xi_2 y)}$$

$$= \int_{-\infty}^{\infty} \int_{-\infty}^{\infty} e^{i(\xi_1 x + \xi_2 y)} p(x, y) dx dy. \quad (105)$$

The distribution function of the sum of bivariates may be calculated from the ch.f. as in the single variable case. That is, if

$$\begin{pmatrix} X = x_1 + x_2 \\ Y = y_1 + y_2 \end{pmatrix} \qquad (106)$$

and the ch.f.'s of (x_1, y_1) and x_2, y_2 are given, then

$$C_{XY}(\xi_1, \xi_2) = C_{x_1 y_1}(\xi_1, \xi_2) C_{x_2 y_2}(\xi_1, \xi_2) \qquad (107)$$

and

$$p(X, Y) = \frac{1}{(2\pi)^2} \int_{-\infty}^{\infty} \int_{-\infty}^{\infty} e^{-i(\xi_1 X + \xi_2 Y)} C_{XY}(\xi_1, \xi_2) d\xi_1 d\xi_2. \quad (108)$$
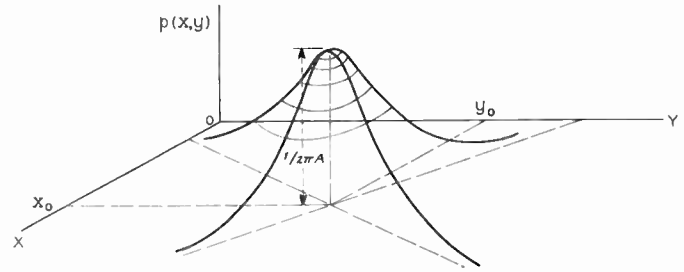
Fig. 3—Two-dimensional Gaussian probability density function.

The bivariate moments can be calculated by expanding the ch.f. in a power series in x and y by analogy with the single variable case. From (105) we obtain

$$C_{xy}(\xi_1, \xi_2) = \text{av} \, (e^{i\xi_1 x} e^{i\xi_2 y})$$

$$= \text{av} \, \sum_{j=0}^{\infty} \sum_{k=0}^{\infty} \frac{(i\xi_1 x)^j (i\xi_2 y)^k}{j! k!}$$

$$= \sum_{j=0}^{\infty} \sum_{k=0}^{\infty} \frac{i^{j+k} \xi_1^j \xi_2^k}{j! k!} \, \text{av} \, x^j y^k$$

$$= \sum_{j=0}^{\infty} \sum_{k=0}^{\infty} \frac{i^{j+k} \xi_1^j \xi_2^k}{j! k!} \, m_{jk} \qquad (109)$$

Therefore m_{jk} is $j! \, k!/i^{j+k}$ times the coefficient of $\xi_1^j \xi_2^k$ in the power series expansion of $C_{xy}(\xi_1, \xi_2)$.

As in the one-dimensional case, the ch.f. of the bivariate Gaussian distribution is a bivariate Gaussian function of the transformation variables ξ_1 and ξ_2. To simplify the results we set x_0 and $y_0 = 0$ which can always be accomplished by a change of variable. Then the Gaussian ch.f. may be written

$$C_{xy}(\xi_1, \xi_2) = \frac{1}{2\pi A} \int_{-\infty}^{\infty} \int_{-\infty}^{\infty} e^{i\xi_1 x + i\xi_2 y - (\mu_{02} x^2 + \mu_{20} y^2 - 2\mu_{11} xy)/2A^2} dx dy$$

$$= e^{-(\mu_{20}\xi_1^2 + \mu_{02}\xi_2^2 + 2\mu_{11}\xi_1\xi_2)/2}. \quad (110)$$

We may expand this in a power series in ξ_1 and ξ_2 by using the exponential series

$$C_{xy}(\xi_1, \xi_2) = 1 - \frac{\mu_{20}\xi_1^2 + \mu_{02}\xi_2^2 + 2\mu_{11}\xi_1\xi_2}{2}$$

$$+ \frac{(\mu_{20}\xi_1^2 + \mu_{20}\xi_2^2 + 2\mu_{11}\xi_1\xi_2)^2}{2! 2^2} - \cdots . \quad (111)$$

Now invoking the rule derived in (109), we note, for example, that the coefficient of ξ_1^2 is $-\mu_{20}/2$ and multiplying this value by $2!\ 0!/i^{2+0} = -2$ gives μ_{20}. In a similar manner it may be checked that μ_{02} and μ_{11} are actually the specific moments stated.

The characteristic function of a multivariate Gaussian distribution of n dependent quantities is the natural generalization of (110). It may be written for the case in which the average of each variable is zero as

$$C_{x_1 x_2 \cdots x_n} = \text{av}\ (e^{i(\xi_1 x_1 + \xi_2 x_2 + \cdots + \xi_n x_n)})$$
$$= \exp\left[-\frac{1}{2} \sum_{j=1}^{n} \sum_{k=1}^{n} \lambda_{jk} \xi_j \xi_k \right]. \qquad (112)$$

Here λ_{jk} is the covariance of x_j and x_k. The generalized central moments for this multivariate case are given by

$$\mu_{j_1 j_2 \cdots j_n} = \text{av}\ (x_1{}^{j_1} x_2{}^{j_2} \cdots x_n{}^{j_n})$$
$$= \frac{j_1! j_2! \cdots j_n!}{i^{j_1 + j_2 + \cdots + j_n}} \text{Coeff. of } \xi_1{}^{j_1} \xi_2{}^{j_2} \cdots \xi_n{}^{j_n} \text{ in } C_{x_1 x_2 \cdots x_n}. \ (113)$$

The multivariate probability density function is not so simply expressed in terms of second order moments because the Fourier transform of (112) introduces a quadratic form reciprocal to that having the coefficients λ_{jk}. The result may be expressed as

$$p(x_1, x_2, \cdots x_n) = \frac{\exp\left[-\frac{1}{2\lambda} \sum_{j=1}^{n} \sum_{k=1}^{n} \Lambda_{ik} x_j x_k \right]}{(2\pi)^{n/2} \lambda^{1/2}} \qquad (114)$$

where λ is the nth order determinant with typical element λ_{jk} and Λ_{jk} is the cofactor of λ_{jk} in λ. Note that $\lambda_{jk} = \lambda_{kj}$ and $\Lambda_{jk} = \Lambda_{kj}$ throughout.

The central limit theorem for a multivariate distribution states under very general conditions that if each $x_1, x_2 \cdots x_n$ is itself the sum of a large number of independent quantities with arbitrary distributions the probability density function $p(x_1, x_2, \cdots x_n)$ approaches the n-dimensional Gaussian form.

AUTOCORRELATION AND POWER SPECTRA

An immediate application of bivariate statistics may be made to the case in which the two values represent measurements made on a single noise source at two specified instants of time. In the case of the extension-in-time program, we consider a single noise wave $v(t)$ and let $x = v(t_1)$, $y = v(t_1 + \tau)$. If the noise wave represents a stationary process, the statistics of x and y do not depend on t_1 but only on the time difference τ. In the case of the ensemble representation we make observations at the instants t_1 and $t_1 + \tau$ on a large number of similar noise sources. We thereby obtain an ensemble of paired values, which we may write

$$(x, y) = (v(t_1), v(t_1 + \tau)). \qquad (115)$$

If the ensemble $[v(t)]$ is stationary, the statistics of the ensemble (x, y) do not depend on t_1 but only on the time shift τ. Finally if the noise process is ergodic, the ensemble statistics and time statistics coincide.

In the extension-in-time program for stationary processes it is customary to define the average product of $v(t)$ and $v(t + \tau)$ as the autocorrelation function, which we shall designate here as $R_v(\tau)$. Then

$$R_v(\tau) = \lim_{T \to \infty} \frac{1}{T} \int_0^T v(t) v(t + \tau) dt. \qquad (116)$$

If the process is ergodic, the autocorrelation can also be computed by averaging over the ensemble, thus

$$R_v(\tau) = \text{av}\ (xy) = \int_{-\infty}^{\infty} \int_{-\infty}^{\infty} xy p(x, y) dx dy. \qquad (117)$$

We recall that the covariance of the jointly distributed quantities x and y has been previously defined by (102) as av $[x - \text{av } x)\ (y - \text{av } y)]$. The autocovariance of $v(t)$ may accordingly be defined as the covariance of x and y when $x = v(t)$ and $y = v(t + \tau)$. It is equal to the autocorrelation in the case of ac ergodic noise sources. For ergodic sources in general, we have the relation that the autocovariance is equal to the autocorrelation minus the square of the average. The autocovariance of the sum of two independent processes is the sum of the autocovariances of the individual processes as may be seen by writing out the expression for the required average and setting the covariances of one process with the other equal to zero.

It is possible to proceed further by defining the third order probability density function $p(x, y, z)$ where $x = v(t)$, $y = x(t + \tau_1)$, $z = v(t + \tau_1 + \tau_2)$ and the third order autocorrelation function

$$\psi(\tau_1, \tau_2) = \text{av}\ (xyz) \qquad (118)$$

Similar generalization can be extended to any order. Second order statistics are however sufficient for most engineering problems and in one important case, that of the Gaussian process, the higher order statistics are completely determined when the second order is known.

THE POWER SPECTRUM

It has proved to be of inestimably great value in communication engineering to resolve waves into sinusoidal components of specified frequencies. The central application may be summarized thus: if a wave $v(t)$, which to be definite we shall say is a voltage, can be represented in the form

$$v(t) = \int_{-\infty}^{\infty} F(\omega) e^{it\omega} \frac{d\omega}{2\pi} \qquad (119)$$

and if a linear system has the steady state transmission function $Y(\omega)$, which for definiteness, we shall say means that a voltage $V_0 e^{i\omega t}$ produces current $I_0 e^{i\omega t}$, with $I_0 = Y(\omega) V_0$, then the current $I(t)$ in response to $v(t)$ is

$$I(t) = \int_{-\infty}^{\infty} Y(\omega) F(\omega) e^{it\omega} \frac{d\omega}{2\pi} \qquad (120)$$

The formal rule for calculating $F(\omega)$ from $v(t)$ is

$$F(\omega) = \int_{-\infty}^{\infty} v(t)e^{-i\omega t}dt \qquad (121)$$

$F(\omega)d\omega/2\pi$ is interpreted physically as the amplitude (in complex form) of an infinitesimal component of $v(t)$, containing frequencies in the range $d\omega$ at ω.

This is the conventional Fourier integral theory as applied to linear systems and it is highly satisfactory when the operations indicated can be given numerical meaning. In case of a noise wave it is inadequate because the integral (121) does not converge for a typical $v(t)$ from a noise ensemble. The difficulty can be remedied by basing our calculations on mean square voltages in infinitesimal frequency intervals instead of first powers.

Suppose we consider a finite interval of time from $t=0$ to $t=T$. If we replace the values of $v(t)$ outside this interval by zero, we can write

$$F(\omega) = \int_{0}^{T} v(t)e^{-i\omega t}dt \qquad (122)$$

which can be calculated even for a noise wave because the limits are finite.

Then for $0<t<T$,

$$v(t) = \int_{-\infty}^{\infty} F(\omega)e^{i\omega t}\frac{d\omega}{2\pi}. \qquad (123)$$

The total energy represented by $v(t)$ in the interval 0 to T is proportional to

$$\int_{0}^{T} v^2(t)dt = \int_{0}^{T} v(t)dt \int_{-\infty}^{\infty} F(\omega)e^{i\omega t}\frac{d\omega}{2\pi}$$

$$= \int_{-\infty}^{\infty} F(\omega)\frac{d\omega}{2\pi}\int_{0}^{T} v(t)e^{i\omega t}dt$$

$$= \int_{-\infty}^{\infty} F(\omega)F(-\omega)\frac{d\omega}{2\pi} = \int_{-\infty}^{\infty} \frac{|F(\omega)|^2}{2\pi}d\omega. \qquad (124)$$

The average power S_T in the voltage wave in the time interval from 0 to T is obtained (again for unit resistance) by dividing by T. Hence

$$S_T = \frac{1}{T}\int_{0}^{T} v^2(t)dt = \int_{-\infty}^{\infty} \frac{|F(\omega)|^2}{2\pi T}d\omega. \qquad (125)$$

Let us define the function $W_v(\omega, T)$ by

$$W_v(\omega, T) = \frac{|F(\omega)|^2}{2\pi T}. \qquad (126)$$

We may then write (125) in the form

$$S_T = \int_{-\infty}^{\infty} W_v(\omega, T)d\omega. \qquad (127)$$

This expression for average power over a finite but arbitrarily long time interval T is in the form of an integral of a density function of frequency. We can interpret this as meaning that an infinitesimal frequency interval $d\omega$ at ω contributes average power $W_v(\omega, T)d\omega$ to the total. It is tempting to assume now that T approaches infinity and define the corresponding limit of $W_v(\omega, T)$ as the spectral density of $v(t)$. This has in effect been implied in much of the literature, and for most problems the results thereby obtained are correct. The procedure is not without its hazards, however, and we must caution the reader that a straightforward limiting process applied to (126) in specific cases will almost always fail to converge.

There are two ways of escaping from this seeming mathematical quandary. First, if we prefer to continue with a single function of time, we examine a finite segment of frequency interval by defining the function

$$\Omega(\omega, T, \Delta\omega) = \int_{\omega-\Delta\omega/2}^{\omega+\Delta\omega/2} W_v(\omega, T)d\omega. \qquad (128)$$

Now if $\Delta\omega$ is held fixed and T made indefinitely large a limit is actually approached, defining the function

$$\Omega(\omega, \Delta\omega) = \lim_{T\to\infty} \Omega(\omega, T, \Delta\omega). \qquad (129)$$

We may now take the limit of the ratio of this quantity to $\Delta\omega$ as $\Delta\omega$ approaches zero and thereby define the spectral density by

$$W_v(\omega) = \lim_{\Delta\omega\to 0} \frac{\Omega(\omega, \Delta\omega)}{\Delta\omega}. \qquad (130)$$

The subscript v is inserted to designate the power spectrum of $v(t)$.

The second procedure is based on the ensemble approach. We first average $W_v(\omega, T)$ over the ensemble of possible noise functions and then take the limit as T approaches infinity. In symbols, we define the spectral density as

$$W_v(\omega) = \lim_{T\to\infty}\left[\text{av }\frac{|F(\omega)|^2}{2\pi T}\right]. \qquad (131)$$

When the calculation is made in this way, the mathematical difficulties disappear, except when the ensemble contains periodic components, as will be discussed below. If the process is ergodic, this definition suffices for the spectral density of a single function from the ensemble as well. Note that we have defined the spectral density in terms of ω expressed in radians per second. We shall adopt the convention here that $w_v(f) = 2\pi W_v(\omega)$ is the density when the frequency is expressed in cps.

The ensemble approach is the preferred one in modern analytical work. Experimental work in spectral analysis on the other hand with its long tradition going back to the earliest work in optics, has been almost entirely based on the first procedure outlined above. The bandwidth $\Delta\omega$ is the width of the resolving filter and in practice it must always be finite. The averaging interval T is not infinite, but is sufficiently large to make

the effect of any further increment negligible. In general, the smaller $\Delta\omega$ the longer T should be. In practice there is very little difficulty in fitting $\Delta\omega$ and T to the scale of the experiment. Fig. 4 indicates the type of apparatus suitable for the experimental determination of $W_v(\omega)$ from the definition (130). We note that for mathematical convenience we have defined a spectral density function for both positive and negative frequencies. It is clear from (126) that the function so defined must be an even function of frequency since $F(\omega)$ and $F(-\omega)$ are conjugate. In physical apparatus the mean power contributions from intervals $d\omega$ at $-\omega$ and ω add to give a single contribution equal to their sum at ω. Hence the measured outputs correspond to $2W_v(\omega)\Delta\omega$.
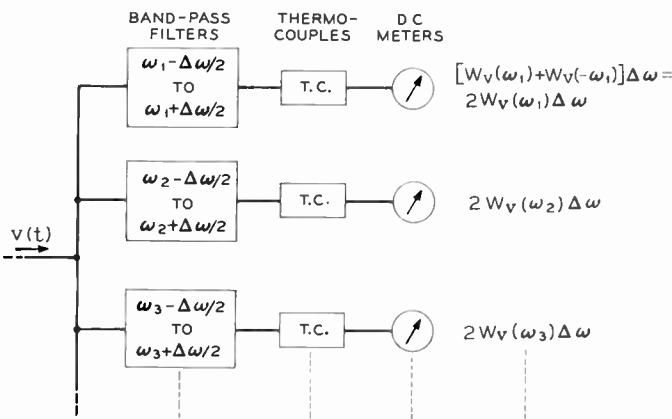

Fig. 4—Schematic circuit for measuring power spectrum.

If $v(t)$ contains one or more purely sinusoidal components, we tend to approach indefinitely large spectral densities at the corresponding frequencies. There is no analytical difficulty here if we deal with the integral of the spectral density up to frequency w, for the value of this integral can change abruptly as we pass the frequency of the sinuosidal component. A convenient symbolic representation is obtained by writing $P_0\delta(f-f_0)$ for the spectral density of a component having mean power P_0 and frequency f_0. The usual rules for calculating with δ functions are then applied.

A great convenience obtained by introduction of the power spectrum is the associated application of steady state network theory to evaluate effects of transmission through linear systems. Thus going back to (119) and (120) we note that if $v(t)$ has the power spectrum $w_v(f)$, the power spectrum of $I(t)$ is

$$w_I(f) = |Y(\omega)|^2 w_v(f). \tag{132}$$

The analytical simplifications thereby achieved are indispensable to orderly progress.

The power spectrum has been defined in terms of squaring and averaging operations on the time function. It is accordingly a second-order statistic and can be related to the other second-order statistic we have

defined as the autocorrelation. We develop this relation in the next section.

RELATION BETWEEN AUTOCORRELATION AND THE POWER SPECTRUM

Let us write $R_v(\tau, T)$ for the approximate autocorrelation evaluated by averaging over a finite interval T. Then

$$R_v(\tau, T) = \frac{1}{T}\int_0^T v(t)v(t+\tau)dt. \tag{133}$$

Substituting the expression (123) for $v(t+\tau)$, we then find

$$R_v(\tau, T) = \frac{1}{2\pi T}\int_0^T v(t)dt \int_{-\infty}^{\infty} F(\omega)e^{i\omega(t+\tau)}d\omega$$

$$= \frac{1}{2\pi T}\int_{-\infty}^{\infty} F(\omega)e^{i\omega\tau}d\omega \int_0^T v(t)e^{i\omega t}dt. \tag{134}$$

The last integral may be evaluated from (122) giving

$$R_v(\tau, T) = \frac{1}{2\pi T}\int_{-\infty}^{\infty} F(\omega)e^{i\omega\tau}F(-\omega)d\omega$$

$$= \int_{-\infty}^{\infty} \frac{|F(\omega)|^2}{2\pi T} e^{i\omega\tau}d\omega$$

$$= \int_{-\infty}^{\infty} W_v(\omega, T)e^{i\omega\tau}d\omega. \tag{135}$$

This is seen to be a generalization of (127). The difficulties with the limits are similar to those previously described in defining the spectral density and need not be discussed again. With similar reservations, we pass to the limit for T large and write

$$R_v(\tau) = \int_{-\infty}^{\infty} W_v(\omega)e^{i\omega\tau}d\omega. \tag{136}$$

We note that

$$R_v(0) = \int_{-\infty}^{\infty} W_v(\omega)d\omega = \lim_{T\to\infty} S_T. \tag{137}$$

That is, the autocorrelation for zero time shift is equal to the average power over all time. This is the maximum value which $R_v(\tau)$ can have since $W_v(\omega)$ is always positive and the term $e^{i\omega\tau}$ with absolute value unity can not increase the integrand of (136) over that of (137) at any value of ω. Thus the autocorrelation function is the Fourier transform of the power spectrum. Also by the inverse Fourier transform theorem

$$W_v(\omega) = \frac{1}{2\pi}\int_{-\infty}^{\infty} R_v(\tau)e^{-i\omega\tau}d\tau. \tag{138}$$

Hence we may compute the power spectrum from the autocorrelation function and when the noise source is ergodic from the autocovariance of the ensemble. It is

in fact convenient from the mathematical point of view to define the ac power spectrum of a stationary ensemble of functions as the Fourier transform of the autocovariance. It is desirable from the computational standpoint to deal with the dc term separately.

The power spectrum, like the autocorrelation from which it can be linearly calculated, is an additive property for independent noises. This is consistent with our familiar procedure of adding average power from incoherent sources to obtain the average total power in their sum.

We shall now give some illustrations. Consider an ergodic Gaussian noise source, $v(t)$, with mean value zero. The probability density function $p(x, y)$ with $x = v(t)$, $y = v(t+\tau)$ is obtained by setting $x_0 = y_0 = 0$ in (103), giving

$$p(x, y) = \frac{1}{2\pi\sqrt{\mu_{20}^2 - \mu_{11}^2}}$$
$$\cdot \exp\left[- \frac{p_{20}^2(x^2 + y^2) - 2\mu_{11}xy}{2(\mu_{20}^2 - \mu_{11}^2)} \right]. \quad (139)$$

Here $\mu_{20} = \mu_{02}$ is the variance σ^2 or in this case, the mean square value of $v(t)$, and μ_{11} is the autocovariance or autocorrelation $R_v(\tau)$. The power spectrum $W_v(\omega)$ is given by (137). Similarly, if we are given an ac Gaussian noise source with power spectrum $W_v(\omega)$, we obtain the probability density function $p(x, y)$ by inserting in (139)

$$\mu_{11} = \int_{-\infty}^{\infty} W_v(\omega)e^{-i\omega\tau}df = R_v(\tau) \quad (140)$$

$$\mu_{20} = [\mu_{11}]_{\tau=0} = R_v(0) = \sigma^2. \quad (141)$$

Let us complete a problem started in the second section—the half-wave rectification of a given band of Gaussian noise. Before we were able to calculate only the average ac power in the rectifier output. Now we can calculate the complete power spectrum. To do so, let the output voltage of the rectifier be $u(t)$ and let

$$\left.\begin{array}{l} \xi = u(t) \\ \eta = u(t + \tau) \end{array}\right\}. \quad (142)$$

Then ξ is equal to x when x is positive, but is zero when x is negative. Likewise η is equal to y when y is positive and is zero when y is negative. The probability density function $q(\xi, \eta)$ can then be expressed in terms of $p(x, y)$ by

$$\left.\begin{array}{l} q(\xi, \eta) = p(\xi, \eta) \text{ when } \xi > 0 \text{ and } \eta > 0 \\ q(\xi, \eta) = 0 \text{ when } \xi < 0 \text{ or when } \eta < 0 \end{array}\right\}. \quad (143)$$

These expressions do not include the origin at which all the probability associated with negative values of either x or y is condensed. Since ξ and η are both zero here there is no contribution to the autocorrelation ensemble average and we write for the autocorrelation function $R_u(\tau)$ of the half-wave rectifier output

$$R_u(\tau) = \int_0^\infty \int_0^\infty \xi\eta p(\xi, \eta) d\xi d\eta$$

$$= \frac{1}{2\pi(\mu_{20}^2 - \mu_{11}^2)} \int_0^\infty \int_0^\infty \xi\eta$$

$$\cdot \exp\left[- \frac{\mu_{20}^2(\xi^2 + \eta^2) - 2\mu_{11}\xi\eta}{2(\mu_{20}^2 - \mu_{11}^2)} \right] d\xi d\eta$$

$$= \frac{1}{2\pi}\left[(\mu_{20}^2 - \mu_{11}^2)^{1/2} + \mu_{11} \arccos \frac{-\mu_{11}}{\mu_{20}} \right]$$

$$= \frac{1}{2\pi}\left\{ [R_v^2(0) - R_v^2(\tau)]^{1/2} \right.$$
$$\left. + R_v(\tau) \arccos \frac{-R_v(\tau)}{R_v(0)} \right\}. \quad (144)$$

The autocorrelation of the rectified output is thus expressed in terms of the autocorrelation of the Gaussian noise input. The power spectrum $W_u(\omega)$ of the rectified output follows immediately by use of the Fourier transform relationship (138) replacing the subscript v by u throughout. There is however a computational difficulty in that the $R_u(\tau)$ defined by (144) gives a divergent integral when substituted in (138). This can be seen from the fact that $R_v(\tau)$ approaches zero as τ goes to $\pm \infty$, and hence $R_u(\tau)$ approaches the constant $R_v^2(0)/2\pi$. To resolve this difficulty, we observe that the autocorrelation function of a constant voltage E is by (116).

$$R_E(\tau) = \lim_{T\to\infty} \frac{1}{T} \int_{t+T}^{T} E^2 dt = E^2 \quad (145)$$

and hence that the presence of an additive constant R_0 in an autocorrelation means that there is a dc component E_0 in the wave satisfying

$$E_0 = R_0^{1/2} \quad (146)$$

and hence having mean power $E_0^2 = R_0$. We therefore subtract a dc component of power R_0 to obtain the ac component of the wave. The autocorrelation of the ac component of $u(t)$ is therefore

$$R_{uac}(\tau) = R_u(\tau) - \frac{R_v^2(0)}{2\pi}. \quad (147)$$

Since we have already calculated the dc component for half-wave rectified Gaussian noise by a more elementary procedure, we can check this part of our more sophisticated calculation. Our earlier result was given by (40) in the form $\sigma/(2\pi)^{1/2}$ when we set the rectifier constant a_1 equal to unity. In the present solution we substitute

$$R_0 = \frac{R_v^2(0)}{2\pi} = \frac{\sigma^2}{2\pi} \quad (148)$$

and hence

$$E_0 = R_0^{1/2} = \sigma/(2\pi)^{1/2} \tag{149}$$

as before.

But we now may go on and calculate the remainder of the spectrum of the rectified output. The result depends of course on the power spectrum of the input. Some interesting facts can be deduced from (144) by a power series expansion without specifying the spectrum. The following result is obtained

$$R_u(\tau) = \frac{\mu_{20}}{2\pi} + \frac{\mu_{11}}{4} + \frac{\mu_{11}^2}{4\pi\mu_{20}} + \frac{\mu_{11}^4}{24\pi\mu_{20}^3}\left[\frac{1}{2} + \frac{3^2}{5\cdot 2\cdot 3!}\frac{(\mu_{11})^2}{(\mu_{20})}\right.$$
$$\left. + \frac{3^2\cdot 5^2}{5\cdot 7\cdot 2^2\cdot 4!}\frac{(\mu_{11})^4}{(\mu_{20})} + \frac{3^2\cdot 5^2\cdot 7^2}{5\cdot 7\cdot 9\cdot 2^3 5!}\frac{(\mu_{11})^6}{(\mu_{20})} + \cdots \right]$$
$$= \frac{R_v^2(0)}{2\pi} + \frac{R_v(\tau)}{4} + \frac{R_v^2(\tau)}{4\pi R_v(0)} + \frac{R_v^4(\tau)}{24\pi R_v^3(0)}$$
$$\cdot \left\{\frac{1}{2} + \frac{3^2}{5\cdot 2\cdot 3!}\left[\frac{R_v(\tau)}{R_v(0)}\right]^2 + \cdots \right\}. \tag{150}$$

The first term of the series after the constant is one-fourth the autocorrelation function of $v(t)$, the input wave. The Fourier transform of this term in accordance with (138) is therefore one-fourth of the original power spectrum. This verifies a familiar fact that a half-wave linear rectifier with a multifrequency sine wave input delivers among other things a set of fundamental components of half amplitude and hence one quarter power. The next term is proportional to the square of $R_v(\tau)$. This is the kind of behavior found in autocorrelation when the output voltage is proportional to the square of the input. It is well-known that in such cases we may resolve the output into components with frequencies which are sums and differences of the frequencies present in the original wave. The Fourier transform of this term therefore leads to a sum and difference spectrum. Similarly the higher power terms represent contributions from correspondingly higher orders of modulation. It should be noted that we have taken the linear rectifier merely as a typical example and that the procedure is applicable to the response of nonlinear devices in general. For further applications see [3].

We have shown earlier in (62) how a Gaussian process could be approached as the limiting form of the sum of a large number of sinusoidal distributions. This suggests a method of constructing Gaussian ensembles with specified spectral density functions. First, divide the frequency range into small intervals of width $\Delta\omega$. Then assume sinusoidal components of random phase, frequencies equal to each midinterval value, and amplitudes proportional to the square root of the spectral density function. The ensemble of sums of these sinusoidal components approaches the required Gaussian ensemble as the division points are taken infinitesimally close together. Specifically, the ensemble

$$v(t) = 2\sum_{n=1}^{N}\sqrt{W_v(\omega_1+n\Delta\omega)\Delta\omega}\cos\left[(\omega+n\Delta\omega)t+\theta_n\right] \tag{151}$$

with $N = (\omega_2-\omega_1)/\Delta\omega$ and the θ_n's uniformly and independently distributed approaches a Gaussian ensemble with spectral density $W_v(\omega)$ in the range $\omega_1 < |\omega| < \omega_2$. The mean square of the typical component is one-half the square of its amplitude, or $2W_v(\omega_1+n\Delta\omega)\Delta\omega$, which represents a contribution of $W_v(\omega_1+n\Delta\omega)\Delta\omega$ centered around the frequency $\omega_1+n\Delta\omega$ and a like contribution centered around the frequency $-\omega_1-n\Delta\omega$.

We may use this model to solve a wide variety of noise problems by first evaluating the response of the system under study to the wave (151) with N finite and then taking the limit of our solution as N goes to infinity. It is to be noted that the solution thus obtained is for a Gaussian noise source. Compared to modern techniques, the approximation of a noise source by a sum of sine waves is crude, but it is nevertheless effective in situations where the algebra can be kept under control. It forms a transition between the kinds of waves transmitted in multichannel frequency division systems and the waves produced by Gaussian noise. When the number of channels in such systems is large, it has been found helpful to use noise waves in both experiment and analysis as a simulation of average loading conditions [4, 18].

A disadvantage of the sine-wave series as a model of noise is the cumbersomeness of the calculations in complicated situations. For an example of moderate complexity see the author's paper [5] on linear rectification of a sine wave superimposed on noise. For an analysis of some considerably more intricate situations, we cite a paper by Lewin [6], in which the question of coherence between various terms obtained in the computing process becomes an issue. It seems that it is very hard to insure analytical rigor in such calculations. We shall return later however to the use of the sine-wave series as a very valuable adjunct in explaining the properties of narrow band noise.

We next illustrate some typical spectral density functions and their associated autocorrelations.

Band Limited White

In this case, the input spectrum is spread uniformly over a specified range of frequencies and vanishes outside. In theory, it is obtained by passing white noise through an ideal filter. Since neither white noise nor ideal filters exist it is only an approximation to reality. We shall continue for computational simplicity the model containing both positive and negative frequencies and write for this case,

$$W(\omega) = \begin{cases} W_0, & \omega_1 < |\omega| < \omega_2 \\ 0, & |\omega| < \omega_1 \text{ and } |\omega| > \omega_2. \end{cases} \tag{152}$$

The plot of this spectrum is shown in Fig. 5(a). The mean total power is equal to the area of the two rectangles, giving

$$P = 2W_0(\omega_2 - \omega_1). \tag{153}$$

The autocorrelation function $R(\tau)$ is found to be
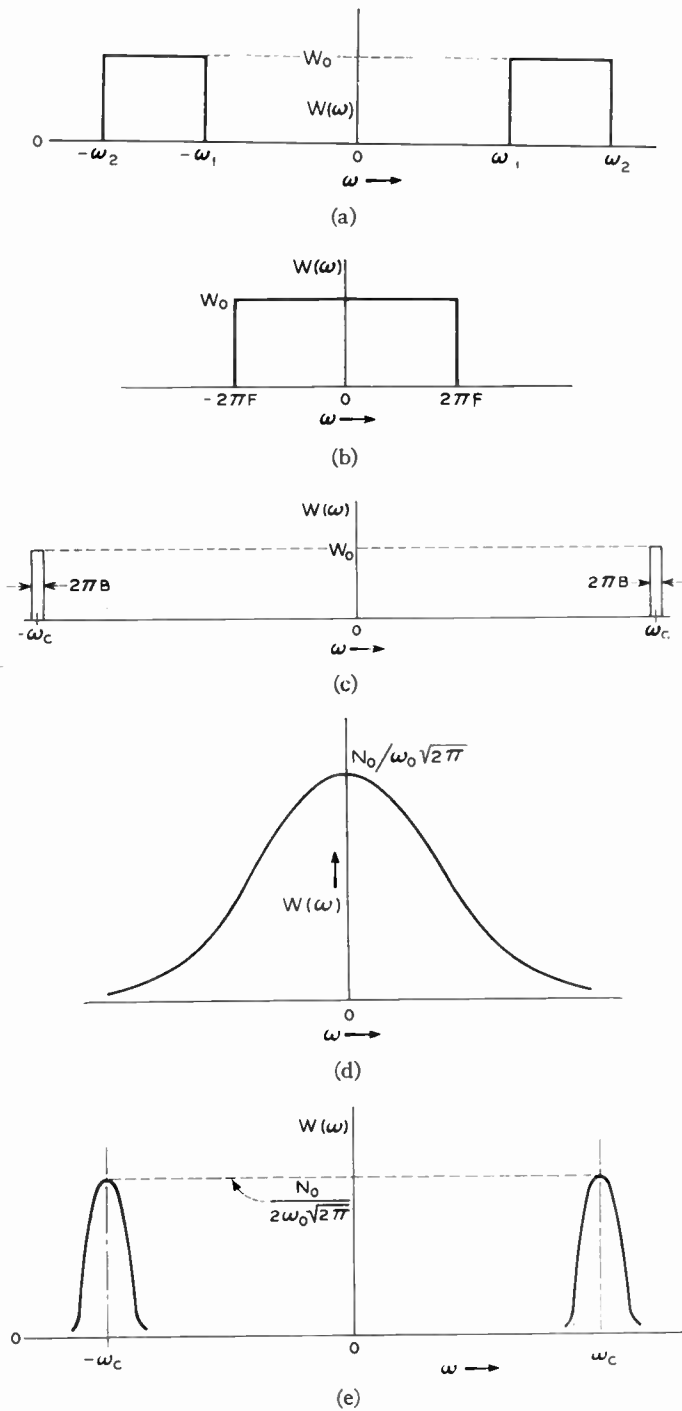
Fig. 5—(a) Power spectrum of band-limited white noise. (b) Power spectrum of low pass white noise. (c) Power spectrum of narrow band white noise. (d) Gaussian low pass power spectrum. (e) Gaussian band pass power spectrum.

$$R(\tau) = \left[\int_{-\omega_2}^{-\omega_1} + \int_{\omega_1}^{\omega_2} \right] W_0 e^{i\omega\tau} d\omega$$

$$= \frac{4W_0}{\tau} \sin \frac{(\omega_2 - \omega_1)}{2} \tau \cos \frac{(\omega_2 + \omega_1)}{2} \tau. \quad (154)$$

Substitution of this term in (144) leads to rather involved integrations, but evaluation has at least been reduced to an explicit computational procedure. From here on it is a matter of ingenuity in evaluating integrals or effective employment of machine techniques.

Special cases of the band-limited white noise of considerable importance are

The Low Pass Case:

$$\omega_1 = 0, \quad \omega_2 = 2\pi F, \quad R(\tau) = \frac{2W_0 \sin 2\pi F\tau}{\tau}, \quad (155)$$

[See Fig. 5(b).]
and

The Narrow Band Case:

$$\omega_1 \gg \omega_2 - \omega_1.$$

Here we would write for convenience,

$$\frac{\omega_1 + \omega_2}{2} = \omega_c, \qquad \omega_2 - \omega_1 = 2\pi B$$

$$R(\tau) = \frac{4W_0}{\tau} \sin \pi B\tau \cos \omega_c\tau. \quad (156)$$

[See Fig. 5(c).]

In many problems, the exact shape of the spectrum within the narrow range to which it is confined is not critical. We shall devote a later section to an intensive treatment of the narrow band case with arbitrary spectral shape.

The Gaussian Spectrum

A Gaussian low pass spectrum has spectral density [Fig. 5(d)]

$$W(\omega) = \frac{N_0}{\omega_0(2\pi)^{1/2}} e^{-\omega^2/2\omega_0^2}. \quad (157)$$

N_0 is the mean total power. At $\omega = \omega_0$, the power per unit bandwidth is down one-quarter neper or 2.17 db relative to the density at zero frequency. The spectrum is of considerable importance because it simulates the gradual kind of cutoff which is more realistic in physical networks than the abrupt transition of the ideal filter. Specifically a Gaussian frequency selectivity is approached by an RC-coupled amplifier of many stages. We must not confuse the Gaussian frequency spectrum with the Gaussian probability density function previously discussed. Both are Gaussian functions, but the variables are different. A computational advantage of the Gaussian spectrum is that its Fourier transform is also Gaussian and hence the autocorrelation is Gaussian. Furthermore a Gaussian function raised to a power remains Gaussian so that a series expansion such as (150) in power of the autocorrelation can be Fourier-transformed term by term to yield a corresponding series of Gaussian spectral densities.

The autocorrelation function for the Gaussian low pass spectrum is

$$R(\tau) = \frac{N_0}{\omega_0(2\pi)^{1/2}} \int_{-\infty}^{\infty} e^{-\omega^2/2\omega_0^2} e^{i\omega\tau} d\omega$$

$$= N_0 e^{-(\omega_0\tau)^2/2}. \quad (158)$$

The Gaussian band pass spectrum is also important.

It is

$$W(\omega) = \frac{N_0}{2\omega_0(2\pi)^{1/2}} \left[e^{-(\omega-\omega_c)^2/2\omega_0^2} + e^{-(\omega+\omega_c)^2/2\omega_0^2} \right] \quad (159)$$

$$R(\tau) = N_0 e^{-(\omega_0\tau)^2/2} \cos \omega_1\tau. \quad (160)$$

[See Fig. 5(e).]

The narrow band case in which $\omega_0 \ll \omega_c$ is the one most frequently of interest. Here the effect of the tails crossing over from positive to negative and negative to positive frequencies is negligible, and we obtain a good approximation for a sharply-tuned multi-stage amplifier response to white noise. This is the network-theory analog of the central limit theorem on probability density functions. The Gaussian band pass case will be treated along with other narrow band distributions in a later section.

In general, the power spectrum, like the autocorrelation function, is representative of second order statistics and does not give a complete statistical description of the process. An important exception is the Gaussian process (referring now to Gaussian probability function), which yields statistics of all orders in terms of second order only. We assume here and later that the average value of the ensemble has been subtracted out, so that when we refer to Gaussian noise we mean "ac Gaussian Noise." For this case the autocorrelation $R_v(\tau)$ is sufficient to determine all orders of statistics. Since the autocorrelation is calculated from the spectral density $W(\omega)$ and vice versa, we can equally well relate all orders of statistics to $W(\omega)$.

SIGNAL AND NOISE

The study of noise itself is interesting and important, but a still more useful analysis deals with combinations of noise and signal waves. By "signal" we mean some information-bearing component of a wave which we desire to isolate. We regard the undesirable remainder as noise. The separation may be of varying degrees ranging all the way from freeing a high fidelity musical program from any trace of a noise background to answering with yes or no the question: is there or is there not a signal present in this wave? As we approach the latter type of problem the use of statistics rather than an exact description becomes more and more the proper approach.

The signal may take on many forms, but whatever it is, we usually fall back on Fourier analysis to resolve it into sinusoidal components, and to simplify the problem we usually begin the analysis in terms of one sinusoidal wave accompanied by noise. An important ensemble for study is that of the sine wave plus Gaussian noise. We may write this ensemble as

$$[y(t)] = [x(t) + A \cos (\omega_0 t + \theta)] \quad (161)$$

where $[x(t)]$ is a Gaussian ensemble and $[A \cos (\omega_0 t + \theta)]$ $= [s(t)]$ is an independent sinusoidal ensemble defined with A and ω_0 constant and θ uniformly distributed in

the range 0 to 2π. The probability density function of $[y(t)]$ may be obtained by the use of the characteristic functions. The characteristic function of $[x(t)]$ is given by (64). We shall assume that the average value of the ensemble is zero and hence

$$C_x(\xi) = e^{-\sigma^2\xi^2/2}. \quad (162)$$

The characteristic function of the sinusoidal ensemble has been found in (58). We write it in our present notation as

$$C_s(\xi) = J_0(A\xi). \quad (163)$$

It follows that the ch.f. of $[y(t)]$ is

$$C_y(\xi) = C_x(\xi)C_s(\xi) = J_0(A\xi)e^{-\sigma^2\xi^2/2}. \quad (164)$$

Hence the probability density function for $[y(t)]$ is

$$p_y(z) = \frac{1}{2\pi} \int_{-\infty}^{\infty} J_0(A\xi)e^{iz\xi-\sigma^2\xi^2/2}d\xi$$

$$= \frac{1}{\pi} \int_0^{\infty} J_0(A\xi)e^{-\sigma^2\xi^2/2} \cos z\xi d\xi. \quad (165)$$

It seems we are forced to leave this function in integral form. It is sometimes convenient to replace $J_0(A\xi)$ by an integral representation

$$J_0(A\xi) = \frac{1}{\pi} \int_{-\pi/2}^{\pi/2} e^{-iA\xi \sin \theta}d\theta \quad (166)$$

and perform the integration with respect to ξ. The equivalent form for $P_y(z)$ thereby obtained is

$$p_y(z) = \frac{1}{\pi(2\pi)^{1/2}} \int_{-\pi/2}^{\pi/2} e^{-(z-A \sin \theta)^2/2\sigma^2}d\theta. \quad (167)$$

The probability density function is sufficient to solve the problem of calculating the dc output when a sine wave plus Gaussian noise is applied to a rectifier. If the rectifier is linear half wave with forward conductance α, the dc component y_0 is

$$y_0 = \alpha \int_0^{\infty} z p_y(z)dz. \quad (168)$$

The resulting integral can be evaluated in closed form to give

$$y_0 = \alpha(\sigma/2\pi)^{1/2}e^{-A^2/4\sigma}$$

$$\cdot \left\{ I_0(A^2/4\sigma) + \frac{A^2}{2\sigma} \left[I_0(A^2/4\sigma) + I_1(A^2/4\sigma) \right] \right\}. \quad (169)$$

We may calculate the spectrum of the rectified output if we first determine the autocorrelation function of $y(t)$. The latter can be computed from the two-dimensional probability density function of $y(t)y(t+\tau)$, and this in turn can be found by combining bivariate characteristic functions of the component ensembles. The two-dimensional ch.f. of the Gaussian ensemble has previously been given by (110). The ch.f. of the two-dimensional sinusoidal ensemble is

$C_s(\xi_1, \xi_2)$

$= \text{av } (e^{i\xi_{1s}(t)}e^{i\xi_{2s}(t+\tau)})$

$= \text{av exp } (i\xi_1 A \cos (\omega_0 t + \theta) + i\xi_2 A \cos [\omega_0(t + \tau) + \theta])$

$= \dfrac{1}{2\pi} \displaystyle\int_{-\pi+\alpha}^{\pi+\alpha} e^{iA(\xi_1 \cos (\omega_0 t+\theta)+\xi_2 \cos [\omega_0(t+\tau)+\theta])} d\theta$

$= \dfrac{1}{2\pi} \displaystyle\int_{-\pi+\alpha}^{\pi+\alpha} d\theta e^{iA \sqrt{(\xi_1+\xi_2 \cos \omega_0\tau)^2+\xi_2^2 \sin^2 \omega_0\tau} \cos (\omega_0 t+\theta+\beta)}$ (170)

where α is arbitrary and

$$\tan \beta = \frac{\xi_2 \sin \omega_0\tau}{\xi_1 + \xi_2 \cos \omega_0\tau}. \quad (171)$$

By changing variable to $\phi = \theta + \beta + \omega_0 t$, we observe that

$$C_s(\xi_1, \xi_2) = J_0(A\sqrt{\xi_1^2 + \xi_2^2 + 2\xi_1\xi_2 \cos \omega_0\tau}). \quad (172)$$

Writing $C_x(\xi_1, \xi_2)$ for the two-dimensional ch.f. of the Gaussian ensemble, we have from (110)

$$C_x(\xi_1, \xi_2) = e^{[-\sigma^2(\xi_1^2+\xi_2^2)+2R_x(\tau)]/2} \quad (173)$$

and thence from (107), the two-dimensional ch.f. of the $y(t)$ ensemble is

$$C_y(\xi_1, \xi_2) = C_s(\xi_1, \xi_2)C_x(\xi_1, \xi_2). \quad (174)$$

If $y_1 = y(t)$ and $y_2 = y(t+\tau)$, the required two-dimensional probability density function is

$$p(y_1, y_2) = \frac{1}{4\pi^2} \int_{-\infty}^{\infty} \int_{-\infty}^{\infty} C_y(\xi_1, \xi_2)e^{-i(y_1\xi_1+y_2\xi_2)} dy_1 dy_2. \quad (175)$$

The autocorrelation function of a rectifier output when sine wave and noise form the input can now be computed by the method used in (144). The spectral density follows from the Fourier transform of the auto-correlation. The results are not simple, but this is not a simple problem—the remarkable thing is that a solution can be computed at all. Variations in the procedure are possible and the complications may be changed if not actually reduced by employing some of them. For example, we can compute the autocorrelation function of the rectified output directly from the characteristic function of the input in the important case in which the rectifying characteristic is itself expressible by a Fourier integral. The latter representation may not be possible when the path of integration is along the real axis, but becomes so when a properly chosen path in the complex plane is used. It is also useful to note that if we are interested only in the discrete components of the output spectrum, we may take the limit of the autocorrelation function as the shift time τ approaches infinity. This removes the contribution of the continuous part of the spectrum. For further treatment of these problems see papers by Rice and Middleton, [3] and [7].

DISCRETE SAMPLING OF A NOISE SOURCE—
INTRODUCTION TO TIME SERIES

In many cases the measured noise data consist of observations made at discrete instants of time. This is a familiar situation in statistical work of all kinds. The instants of observation usually have a uniform spacing. The name "time series" is commonly given to such a collection of measured values at specified instants. In our treatment so far we have tacitly assumed that the functions of time we are studying could be observed continuously. The question then arises as to how we might apply our results to cases wherein only regularly spaced samples are available. The "sampling theorem" gives us an important leverage on those cases in which the power spectrum of the noise source vanishes outside a finite range. Physically we can only approximate such a condition, but the approximation is often sufficiently good to make the mathematical model useful. The theorem states that if a noise wave contains no frequencies of absolute value equal to or greater than W cps it can be completely reconstructed from its samples taken at instants $1/2W$ apart [8]. Specifically if $x(t)$ represents the noise wave, we may write the identity

$$x(t) = \sum_{n=-\infty}^{\infty} x\left(\frac{n}{2W}\right) \frac{\sin \pi(2Wt - n)}{\pi(2Wt - n)}. \quad (176)$$

The right-hand side is the response of an ideal low pass filter cutting off at $f = \pm W$ to impulses proportional to the sampled values. The samples and the continuous functions $x(t)$ thus give completely equivalent data, since we can either by experiment or calculation recover the complete $x(t)$ by passing the samples through an ideal low pass filter.

Now consider what would happen if we sample a wave for which the spectral density does not vanish for frequencies exceeding W. Assume

$$x(t) = \sum_{n=-\infty}^{\infty} y\left(\frac{n}{2W}\right) \frac{\sin \pi(2Wt - n)}{\pi(2Wt - n)} \quad (177)$$

where $y(t)$ is not band-limited. This is the ensemble of functions produced by passing the y-samples through an ideal filter cutting off at W. The function $x(t)$, is, of course, band-limited because it is a sum of ideal filter responses. Also by setting $t = n/2w$, we see that

$$y\left(\frac{n}{2W}\right) = x\left(\frac{n}{2W}\right). \quad (178)$$

That is, the values of $y(n/2W)$ are actually samples of the band-limited function $x(t)$, as well as of the un-limited function $y(t)$. A difference is that $x(t)$ can be generated from these samples, while $y(t)$ in general cannot. We ask the question as to what relation there is between the statistics of $x(t)$ and $y(t)$.

We may compute autocorrelation of ensemble $x(t)$ by averaging $x(t) x(t+\tau)$ over the y-ensemble with t fixed.

$R_x(\tau) = \text{av } x(t)x(t + \tau)$

$= \displaystyle\sum_{m=-\infty}^{\infty} \sum_{n=-\infty}^{\infty} \text{av } y\left(\frac{m}{2W}\right) y\left(\frac{n}{2W}\right) \frac{\sin \pi(2Wt - m)}{\pi(2Wt - m)}$

$\cdot \dfrac{\sin \pi[2W(t + \tau) - n]}{\pi[2W(t + \tau) - n]}. \quad (179)$

We may write

$$\text{av } y\left(\frac{m}{2W}\right) y\left(\frac{n}{2W}\right) = R_y\left(\frac{n-m}{2W}\right) \quad (180)$$

where $R_y(\tau)$ is the autocorrelation function of the y-ensemble, or if y is ergodic, the autocorrelation function of any $y(t)$. The summation in (179) appears to depend on the value of t but this is an illusion which can be dispelled by means of the following useful identity

$$\sum_{m=-\infty}^{\infty} \sum_{n=-\infty}^{\infty} \phi(n-m)\frac{\sin \pi(x-m)\sin \pi(x-n+a)}{\pi^2(x-m)(x-n+a)}$$
$$= \sum_{j=-\infty}^{\infty} \phi(j)\frac{\sin (j-a)\pi}{(j-a)\pi}. \quad (181)$$

The following derivation of this formula due to D. Slepian is much simpler than the process by which I obtained it. Let $g(x)$ be any function of x band-limited to the range $-1/2 < f < 1/2$. Then

$$g(x) = \sum_{m=-\infty}^{\infty} g(m)\frac{\sin \pi(x-m)}{\pi(x-m)}. \quad (182)$$

An example of such a band-limited function is

$$g_1(x) = \frac{\sin \pi(x-y)}{\pi(x-y)} = \frac{\sin \pi(y-x)}{\pi(y-x)} \quad (183)$$

where y is a constant. The Fourier transform of $g_1(x)$ is equal to exp $(-iyf)$ in the range $-1/2 < f < 1/2$ and is zero outside this range. Substituting (183) in (182) gives the identity

$$\frac{\sin \pi(x-y)}{\pi(x-y)} = \sum_{m=-\infty}^{\infty} \frac{\sin \pi(y-m)}{\pi(y-m)}\frac{\sin \pi(x-m)}{\pi(x-m)}. \quad (184)$$

Assign to y the value

$$y = x - j + a$$

where j is zero or any positive or negative integer and a is a constant. Then

$$\frac{\sin \pi(j-a)}{\pi(j-a)} = \sum_{m=-\infty}^{\infty} \frac{\sin \pi(x-j+a-m)}{\pi(x-j+a-m)}$$
$$\cdot \frac{\sin \pi(x-m)}{\pi(x-m)}. \quad (185)$$

Multiply both sides by $\phi(j)$ and sum over all values of j

$$\sum_{j=-\infty}^{\infty} \phi(j)\frac{\sin \pi(j-a)}{\pi(j-a)}$$
$$= \sum_{j=-\infty}^{\infty} \sum_{m=-\infty}^{\infty} \phi(j)\frac{\sin \pi(x-j+a-m)}{\pi(x-j+a-m)}\frac{\sin \pi(x-m)}{\pi(x-m)}.$$

Substitution of $j = n - m$ in the double summation now gives (181).

Applying (181) to (179) and (180), we obtain

$$R_x(\tau) = \sum_{n=-\infty}^{\infty} R_y\left(\frac{n}{2W}\right)\frac{\sin \pi(n+2W\tau)}{\pi(n+2W\tau)}. \quad (186)$$

The results of this section are expressed in cps instead of radians as used hitherto. We shall use a lower case w to represent spectral density as a function of f in cps; $w(f) = 2\pi W(\omega)$. The power spectrum $w_x(f)$ of the band-limited ensemble is then, by (138),

$$w_x(f) = \int_{-\infty}^{\infty} e^{-i2\pi f\tau}R_x(\tau)d\tau$$
$$= \begin{cases} 0, & |f| > W \\ \dfrac{1}{2W} \displaystyle\sum_{n=-\infty}^{\infty} R_y\left(\dfrac{n}{2W}\right)e^{in\pi f/W}, & |f| < W. \end{cases} \quad (187)$$

We next replace R_y by its expression in terms of the power spectrum of y with the result that for $|f| < W$,

$$w_x(f) = \frac{1}{2W}\sum_{n=-\infty}^{\infty} e^{in\pi f/W}\int_{-\infty}^{\infty} w_y(\lambda)e^{in\pi\lambda/W}d\lambda. \quad (188)$$

Further simplification requires in effect an inversion of the order of summation and integration, but as the expression stands a divergent series would block progress. The difficulty could be avoided by judicious manipulation of δ functions, but fortunately we have available an impeccable theorem from analysis to produce the desired form of result immediately. This is Poisson's Summation Formula [9]:

$$\sum_{n=-\infty}^{\infty} \int_{-\infty}^{\infty} \phi(z)e^{inz}dz = 2\pi\sum_{n=-\infty}^{\infty} \phi(2n\pi). \quad (189)$$

In this case we set $\pi(f+\lambda)/W = z$ and find that

$$2\pi\phi(z) = w_y\left(\frac{zW}{\pi} - f\right). \quad (190)$$

Therefore for $|f| < W$,

$$w_x(f) = \sum_{n=-\infty}^{\infty} w_y(f + 2nW). \quad (191)$$

The interpretation of this result is clear. The contribution to the spectrum at the typical frequency f within the filter band is the sum of spectral densities occurring f cps above and below each harmonic of the sampling frequency $2W$. In Fig. 6 all the small full line
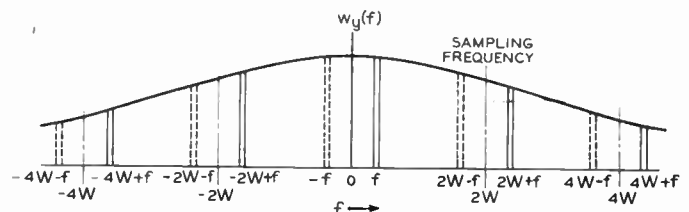

Fig. 6—Power spectrum obtained by low sampling rate.

rectangular slices shown contribute to the spectrum at f. The dashed rectangles give an equal contribution to $-f$. In the language of the communication engineer, the sampling process is equivalent to modulating the height of periodic short pulses by the noise. This may also be expressed as modulating the amplitude of all harmonics

(including the zeroth) of the sampling frequency, since a very sharp pulse contains all harmonics with nearly the same amplitude. The result is that each harmonic beats down into the low pass filter band all the noise in the range W cps above and below it. There is no way of telling from the output which part of the original spectrum of $y(t)$ produces the individual contributions to the spectrum of $x(t)$. This phenomenon has been called "sideband overlap" in telephony. J. W. Tukey has contributed the name "aliasing." We remark that the result (191) can be obtained far more easily [10] by the sine-wave composition treatment of noise based on (141) than by the method used here; in fact a practical communication engineer would probably regard the result as intuitively obvious. However, as pointed out before, the sine-wave model must lead to Gaussian noise and is hence less general than our treatment here.

In communication engineering it is possible to limit the input band by filtering before sampling and thereby avoid multiple contributions to the desired output band. In statistical data such as obtained on prices, crops, weather, and the like, the input circuit is not accessible for filtering, and it may be difficult to separate the aliased from the original spectrum.

The total power represented by the band-limited noise is

$$\sigma_x{}^2 = \psi_x(0) = \sum_{n=-\infty}^{\infty} \psi_y\left(\frac{n}{2W}\right)\frac{\sin n\pi}{n\pi} = \psi_y(0) = \sigma_y{}^2. \quad (192)$$

Hence the mean total power of the limited and unlimited ensembles is the same. If the samples of the $y(t)$-ensemble are mutually independent

and

$$\left.\begin{aligned}
\psi_y\left(\frac{n}{2W}\right) &= 0 \text{ when } n \neq 0 \\[2mm]
\psi_x(\tau) &= \psi_y(0)\frac{\sin 2\pi W\tau}{2\pi W\tau} \\[2mm]
w_x(f) &= \begin{cases} 0, & |f| > W \\ \sigma_y{}^2/2W, & |f| < W \end{cases}
\end{aligned}\right\}. \quad (193)$$

This case thus gives a constant spectral density over the range $-W$ to W and zero spectral density outside. This is what we previously called band-limited white noise, (152).

In the important case in which the ensemble $y(t)$ is Gaussian, the values $y(n/2W)$ are Gaussian variates. If we then consider values of $x(t)$ at times other than the sampling instants we obtain values related to Gaussian variates by a linear transformation. It follows that values of $x(t)$ for any t, or set of t values, are also Gaussian variates and that their statistics are completely determined by either the autocovariance or power spectrum of the ensemble $x(t)$ as determined by (186) and (191). This convenient property may be summarized in the statement that the noise produced by filtered samples of Gaussian noise is also Gaussian. We can not make a corresponding statement about most other kinds of noise. The response of a low pass filter to samples having uniform or sinusoidal distribution, for example, does not have uniform or sinusoidal distribution respectively when the complete wave form of the filter output is considered.

CROSSCORRELATION AND CROSS-POWER SPECTRA

We next consider the statistics of two or more dependent noise sources. These might, for example, be one noise wave applied as input to a network and the resulting noise wave received as output from the network. Another important example consists of the amplitude and phase variations of a narrow band noise source.

As in the single noise source case, second order statistics are sufficient for most purposes. Corresponding to the autocorrelation function $R_x(\tau)$ for the ensemble of single functions $[x(t)]$, we define the crosscorrelation functions $R_{xy}(\tau)$ and $R_{yx}(\tau)$ for the ensemble of paired functions $[x(t), y(t)]$ by

$$R_{xy}(\tau) = \text{av } [x(t)y(t+\tau)]$$
$$= \int_{-\infty}^{\infty}\int_{-\infty}^{\infty} x_1 y_2 p(x_1, y_2)dx_1 dy_2 \quad (194)$$

where $x_1 = x(t)$, $y_2 = y(t+\tau)$.

$$R_{yx}(\tau) = \text{av } [y(t)x(t+\tau)] = R_{xy}(-\tau). \quad (195)$$

Corresponding to the power spectrum $W_x(\omega)$, we define the cross-power spectra

$$W_{xy}(\omega) = \frac{1}{2\pi}\int_{\infty}^{\infty} R_{xy}(\tau)e^{-i\omega\tau}d\tau$$
$$= \lim_{T=\infty} \frac{F_x(-\omega)F_y(\omega)}{2\pi T} \quad (196)$$

$$W_{yx}(\omega) = \frac{2}{2\pi}\int_{-\infty}^{\infty} R_{yx}(\tau)e^{-i\omega\tau}d\tau$$
$$= \lim_{T\to\infty} \frac{F_y(-\omega)F_x(\omega)}{2\pi T} = W_{xy}{}^*(\omega). \quad (197)$$

In the above, $F_x(\omega)$ and $F_y(\omega)$ are defined by

$$F_x(\omega) = \int_0^T x(t)e^{-i\omega t}dt \quad (198)$$

$$F_y(\omega) = \int_0^T y(t)e^{-i\omega t}dt. \quad (199)$$

The asterisk means "conjugate of." We shall not enter into another discussion of the limiting processes indicated above as the arguments are entirely similar to those discussed in the definition of the spectral density of a single source. The measurement of cross spectra has been discussed by Barnes and Krendel [11, 12].

The cross-power spectra are seen to be conjugate complex numbers. The real parts are even functions of frequency and the imaginary parts are odd functions of frequency. The crosscorrelations can be calculated from the cross-power spectra by inverting the Fourier transforms, thus

$$R_{xy}(\tau) = \int_{-\infty}^{\infty} W_{xy}(\omega) e^{i\tau\omega} d\omega \qquad (200)$$

$$R_{yx}(\tau) = \int_{-\infty}^{\infty} W_{yx}(\omega) e^{i\tau\omega} d\omega. \qquad (201)$$

If we write

$$W_{xy}(\omega) = U_{xy}(\omega) + iV_{xy}(\omega) \qquad (202)$$

where U_{xy} and V_{xy} are real, then

$$U_{xy}(-\omega) = U_{xy}(\omega) = U_{yx}(\omega) \qquad (203)$$

$$V_{xy}(-\omega) = -V_{xy}(\omega) = V_{yx}(\omega) \qquad (204)$$

and

$$R_{xy}(\tau) = 2\int_{0}^{\infty} U_{xy}(\omega) \cos \tau\omega d\omega$$

$$- 2\int_{0}^{\infty} V_{xy}(\omega) \sin \tau\omega d\omega. \qquad (205)$$

Given any two noise ensembles $[x(t)]$ and $[y(t)]$ with specified power spectra $W_x(\omega)$, $W_y(\omega)$ respectively and cross-power spectrum $W_{xy}(\omega) = U_{xy}(\omega) + iV_{xy}(\omega)$, it is possible to resolve either ensemble into the sum of three components which have cross spectra purely real, purely imaginary, and zero respectively relative to the other. Specifically, if we take $x(t)$ as the reference, we may write

$$[y(t)] = [\alpha(t)] + [\beta(t)] + [\gamma(t)] \qquad (206)$$

where

$$W_{x\alpha} = U_{xy}, \quad W_{x\beta} = iV_{xy}, \quad W_{xy} = 0. \qquad (207)$$

The resolution is easily affected from the limiting definition (196). We first note that if $W_x = 0$, then $W_\alpha = W_\beta = W_\gamma = 0$. When W_x is not zero then

$$\left. \begin{array}{ll} W_\alpha = U_{xy}^2/W_x, & W_{\alpha\beta} = iU_{xy}V_{xy}/W_x \\ W_\beta = V_{xy}^2/W_x, & W_{\alpha\gamma} = 0 \\ W_\gamma = W_y - |W_{xy}|^2/W_x, & W_{\beta\gamma} = 0. \end{array} \right\} \qquad (208)$$

In accordance with the above resolution, we may define some particular types of paired noise sources with interesting properties. *Incoherent* noise ensembles $[x(t)]$ and $[y(t)]$ have the property that $W_{xy} = 0$ for all frequencies. The converse is not necessarily true, for in general there might be higher order cross spectra and corresponding higher order crosscorrelations which do not vanish. For the important case of jointly Gaussian noise pairs however, the vanishing of W_{xy} is sufficient to insure that all orders of cross spectra vanish and hence that $W_{xy} = 0$ is a necessary and sufficient condition for incoherence. For other sources, we might define $W_{xy} = 0$ as equivalent to "second order incoherence." The word "incoherence" as used here is equivalent to "independence" as used in general statistical terminology, and is introduced here because of the similarity to the generally accepted usage of the term in optics.

If W_{xy} does not vanish at some ω, the sources are *partially coherent*. If furthermore $|W_{xy}|^2 = W_x W_y$, the coherence is total in the second order sense for non-Gaussian sources and totally coherent without further qualification in the case of jointly Gaussian pairs. If in addition to this condition, we also have W_{xy} equal to a purely real quantity U_{xy} at all frequencies, the noise sources will be said to be colinear. Here two conditions can be distinguished. When $U_{xy}(\omega)$ is positive the phases are additive, and if $U_{xy}(\omega)$ is negative the phases are subtractive. A null spectrum can be obtained from the sum of two colinear noise sources at any frequency by relative amplitude adjustment and choice of sign. Eq. (205) shows that the crosscorrelation of colinear noise ensembles is an even function of τ.

If in the case of total coherence, the value of $W_{xy}(\omega)$ has a pure imaginary value iV_{xy} at all frequencies, the sources will be said to be in *quadrature*, indicating that a ninety-degree phase shift exists between components at the same frequencies. A positive value of V_{xy} indicates that the x-component lags the corresponding y-component by ninety degrees, while a negative sign indicates a corresponding leading phase angle. From (205) we see that the cross-correlation function of quadrature noise sources is an odd function of τ and vanishes for $\tau = 0$. Simultaneous samples of Gaussian quadrature noise pairs are therefore independent.

A particular virtue of the cross spectrum in analysis is the aid it furnishes in calculating the effect of linear operations on the noise. From the definition, we see that passing the wave $x(t)$ through the transfer admittance $Y_1(\omega)$ and the wave $y(t)$ through the transfer admittance $Y_2(\omega)$ gives two resulting waves, $\xi(t)$, $\eta(t)$, with cross spectra

$$\left. \begin{array}{l} W_{\xi\eta} = Y_1(-\omega)Y_2(\omega)W_{xy}(\omega) \\ W_{\eta\xi} = Y_1(\omega)Y_2(-\omega)W_{yx}(\omega) \end{array} \right\}. \qquad (209)$$

The cross correlations of ξ and η are then calculable by Fourier transforming the cross spectra.

If $\xi(t)$ represents the input and $\eta(t)$ the output of a network with transfer admittance $Y(\omega)$, when a single noise source $x(t)$ is applied, $Y_1(\omega) = 1$, $Y_2(\omega) = Y(\omega)$, $W_{xy}(\omega) = W_x(\omega)$ and

$$W_{\eta\xi} = Y(\omega)W_x(\omega). \qquad (210)$$

If $[x(t)]$ is a white noise source, $W_x(\omega)$ is a constant, and it follows that the cross spectrum is in fact proportional to the complex transfer admittance of the network.

Cross spectra of derivatives and integrals of noise waves are readily obtained from the original cross spectra since they are linear operations describable in terms of admittance functions. Thus if we represent differentiations with respect to time by a dot above the symbol,

$$W_{\dot{x}y}(\omega) = -i\omega W_{xy}(\omega) \qquad (211)$$

$$W_{x\dot{y}}(\omega) = i\omega W_{xy}(\omega). \qquad (212)$$

Then from (200),

$$R_{\dot{x}y}(\tau) = \frac{1}{2\pi} \int_{-\infty}^{\infty} W_{\dot{x}y}(\omega) e^{i\tau\omega} d\omega$$

$$= -\frac{1}{2\pi} \int_{-\infty}^{\infty} i\omega W_{xy}(\omega) e^{i\tau\omega} d\omega = -R_{xy}'(\tau) \quad (213)$$

where the prime represents differentiation with respect to τ. Similarly,

$$R_{x\dot{y}}(\tau) = R_{xy}'(\tau) = -R_{\dot{x}y}(\tau). \quad (214)$$

Cross correlations of higher derivatives can be evaluated from these; *e.g.*,

$$R_{xy}''(\tau) = -\frac{d}{d\tau}[R_{\dot{x}y}(\tau)] = R_{xy}''(\tau), \text{ etc.} \quad (215)$$

We also note that

$$W_{x\dot{x}}(\omega) = i\omega W_x(\omega),$$

and

$$|W_{x\dot{x}}{}^2| = W_x W_{\dot{x}}. \quad (216)$$

Since $W_x(\omega)$ is real, we see that a noise wave and its derivative form a pair of quadrature noise sources. Also,

$$R_{x\dot{x}}(\tau) = R_x'(\tau). \quad (217)$$

Likewise a noise source and its second derivative are colinear since

$$W_{x\ddot{x}}'' = \omega^2 W_x(\omega) \quad (218)$$

and

$$W_{x\ddot{x}}''{}^2 = W_x W_x''. \quad (219)$$

Relations between a noise source and its integral may be evaluated in a similar way dividing by $i\omega$ instead of multiplying. If the integral is taken over a fine time, say from $-T$ to 0, the transfer factor becomes

$$Y(\omega) = \frac{1 - e^{-iT\omega}}{i\omega}. \quad (220)$$

When the integration is taken over all time we may justify discarding the term in $e^{-iT\omega}$, particularly if the integral is subject to further linear operations.

It is interesting and useful to extend the model based on randomly phased sine waves, (151), to include cross-correlated Gaussian ensembles. Given the jointly Gaussian ensemble $[x(t), y(t)]$ with self-power spectra $W_x(\omega)$, $W_y(\omega)$ and cross-power spectrum $W_{xy}(\omega) = U_{xy}(\omega) + iV_{xy}(\omega)$ we can approximate $x(t)$ say by

$$x_N(t) = 2\sum_{n=1}^{N} \sqrt{W_x(\omega_n)\Delta\omega} \cos(\omega_n t + \theta_n) \quad (221)$$

as in (151), when N is large, $\Delta\omega$ is small but not zero, $\omega_n = \omega_1 + n\Delta\omega$, and θ_n is random. Then $y(t)$ may be approximated by

$$y_N(t) = 2\sum_{n=1}^{N} \left[U_{xy}(\omega_n) \sqrt{W_x{}^{-1}(\omega_n)\Delta\omega} \cos(\omega_n t + \theta_n) \right.$$

$$- V_{xy}(\omega_n) \sqrt{W_x{}^{-1}(\omega_n)\Delta\omega} \sin(\omega_n t + \theta_n)$$

$$+ \sqrt{[W_y(\omega_n) - |W_{xy}(\omega_n)|^2/W_x(\omega_n)]\Delta\omega}$$

$$\left. \cdot \cos(\omega_n t + \psi_n) \right]. \quad (222)$$

where the angles ψ_n are random with respect to each other and with respect to θ_n.

ENVELOPE, PHASE, AND INSTANTANEOUS FREQUENCY—EVALUATION OF NOISE IN AM, PM, AND FM SYSTEMS

The case in which the width of the frequency interval occupied by the noise is small compared with the mid-frequency of the interval is the next important communication problem we shall consider. The systems commonly designated as radio frequency (rf) and intermediate frequency (if) generally have this narrow band property. The waves passed by such systems consist of oscillations in the high frequency range. The amplitude and frequency of these oscillations can change with time only at rates comparable with the bandwidth.

If $v(t)$ is a representative wave of a narrow band noise ensemble with spectrum centered at frequency ω_e radians per second, it is convenient to seek a resolution of form

$$v(t) = x(t) \cos \omega_c t - y(t) \sin \omega_c t \quad (223)$$

where $x(t)$ and $y(t)$ are slowly varying functions of time relative to oscillations of frequency ω_e.

Such resolution could be performed physically by multiplying the wave by $2\cos\omega_c t$ to determine $x(t)$ and by $-2\sin\omega_c t$ to determine $y(t)$. The results of such multiplications are

$$\left. \begin{aligned} 2v(t)\cos\omega_c t &= x(t) + x(t)\cos 2\omega_c t - y(t)\sin 2\omega_c t \\ -2v(t)\sin\omega_c t &= y(t) - y(t)\cos 2\omega_c t - x(t)\sin 2\omega_c t \end{aligned} \right\}. \quad (224)$$

The only low frequency terms in the two cases are contained in $x(t)$ and $y(t)$ respectively and they are separable from the high prequency terms by a low pass filter. This is the principle of homodyne or local carrier detection of rf waves. It is to be noted that (224) can be used to give added precision to the requirement on relative magnitudes of the frequencies involved. It follows by expressing products of sine and cosine terms by sines and cosines of sums and differences that if $x(t)$ and $y(t)$ have zero spectral density at frequencies equal to or greater than ω_e then the highest frequency in $x(t)$ and $y(t)$ will be less than the lowest frequency in the other terms and separation is possible. The resolution is thus physically significant when the original noise bandwidth of $v(t)$ is less than $2\omega_e$.

In the above representation we note that the frequency ω_e can be chosen arbitrarily to a considerable extent since to make the resolution physically significant

we require only that the spectral density be negligibly small at frequencies exceeding $2\omega_c$. In the important case in which a signal is present in a narrow band of noise, it becomes convenient to use the signal as a reference to make the resolution unique. Specifically if the signal is a sine wave, we designate the signal as

$$s(t) = A \cos \omega_c t \qquad (225)$$

and study the ensemble

$$u(t) = v(t) + s(t)$$
$$= [x(t) + A] \cos \omega_c t - y(t) \sin \omega_c t. \qquad (226)$$

A further important significance now appears when we rewrite the equation in the equivalent form

$$u(t) = \rho(t) \cos [\omega_c t + \phi(t)] \qquad (227)$$

where

$$\rho^2(t) = [x(t) + A]^2 + y^2(t) \qquad (228)$$

$$\tan \phi(t) = \frac{y(t)}{x(t) + A} . \qquad (229)$$

The function $\rho(t)$ with positive sign is commonly called the envelope of the rf wave and gives the low frequency response of an amplitude detector. The function $\phi(t)$ determined as to quadrant by (229) but ambiguous to within any multiple of 2π is called the phase of the wave and gives the low frequency response to a phase detector. Still another important function is the time rate of change of phase

$$\dot{\phi}(t) = \frac{d}{dt} \phi(t) = \frac{[x(t) + A]\dot{y}(t) - \dot{y}(t)\dot{x}(t)}{[x(t) + A]^2 + y^2(t)} \qquad (230)$$

which is the *instantaneous frequency displacement* from ω_c. $\dot{\phi}(t)$ is by accepted convention the ac component of the response of an ideal frequency detector to the wave. It is uniquely determined by (230).

A model leading to an appropriate mathematical description of a narrow band Gaussian ensemble is obtained as in (151) by a finite approximation to $v(t)$ of form

$$v_N(t) = 2 \sum_{n=1}^{N} \sqrt{W_v(\omega_1 + n\Delta\omega)\Delta\omega} \cos [(\omega_1 + n\Delta\omega)t + \theta_n] \quad (231)$$

where the narrow band is assumed to extend from ω_1 to $\omega_1 + \Omega$ and $\Omega = N\Delta\omega$. The θ_n's are uniformly and independently distributed. By adopting this model our discussion will be confined in this section to Gaussian narrow noise sources. Let

$$\omega_c = \omega_1 + \Omega/2 \qquad (232)$$

and replace $\omega_1 + n\Delta\omega$ in the argument of the cosine by $(\omega_1 + n\Delta\omega + \omega_c) - \omega_c$. We then find that we can write

$$v_N(t) = x_N(t) \cos \omega_c t - y_N(t) \sin \omega_c t \qquad (233)$$

where, for large N

$$x_N(t) = 2 \sum_{n=0}^{N} \sqrt{W_v(\omega_1 + n\Delta\omega)\Delta\omega}$$
$$\cdot \cos [(\omega_1 - \omega_c + n\Delta\omega)t + \theta_n]$$
$$y_N(t) = 2 \sum_{n=0}^{N} \sqrt{W_v(\omega_1 + n\Delta\omega)\Delta\omega}$$
$$\cdot \sin [(\omega_1 - \omega_c + n\Delta\omega)t + \theta_n]$$
$$\qquad (234)$$

The substitution $n = m + N/2$ results in the equations

$$x_N(t) = 2 \sum_{m=-N/2}^{N/2} \sqrt{W_v(\omega_1 + n\Delta\omega)\Delta\omega}$$
$$\cdot \cos (m\Delta\omega t + \theta_{m+N/2})$$
$$y_N(t) = 2 \sum_{m=-N/2}^{N/2} \sqrt{W_v(\omega_1 + n\Delta\omega)\Delta\omega}$$
$$\cdot \sin (m\Delta\omega t + \theta_{m+N/2})$$
$$\qquad (235)$$

Now by letting $\Delta\omega$ become small and N large with the θ's independent, we deduce from the central limit theorem that the ensemble $[x_N(t), y_N(t)]$ approaches the jointly Gaussian ensemble $[x(t), y(t)]$. Furthermore the power spectra of $x(t)$ and $y(t)$ are equal and are given by

$$W_x(\omega) = W_y(\omega) = W_v(\omega_c + \omega) + W_v(\omega_c - \omega). \quad (236)$$

The two terms of (236) come from combining the power contributions of the corresponding positive and negative values of n in (235). Physically they are the upper and lower sideband contributions to the low frequency spectrum. We remark that the computational procedure can be carried out without regard to any limitation on bandwidth of the original noise but that the physical significance of the resolution is lost when the low frequency spectra cannot be separately observed.

It is seen by comparison with (222) that in the limit $x(t)$ and $y(t)$ constitute noise sources in quadrature with

$$W_{xy}(\omega) = iV_{xy}(\omega), \qquad (237)$$

$$V_{xy}(\omega) = W_v(\omega_c - \omega) - W_v(\omega_c + \omega). \qquad (238)$$

The cross-correlation $R_{xy}(\tau)$ is accordingly found from (205), and is

$$R_{xy}(\tau) = -\frac{1}{\pi} \int_0^\infty [W_v(\omega_c - \omega) - W_v(\omega_c + \omega)] \sin \tau\omega d\omega. (239)$$

If the spectral density of $v(t)$ is symmetrical about ω_c, $W_v(\omega_c - \omega) = W_v(\omega_c + \omega)$ and $V_{xy}(\omega) = 0$. For this case then, the cross correlation vanishes, and since we are dealing with jointly Gaussian sources, $x(t)$ and $y(t+\tau)$ constitute independent ensembles. The auto-correlations of x and y are equal and are given by

$$R_x(\tau) = R_y(\tau)$$
$$= \frac{1}{\pi} \int_0^\infty [W_v(\omega_c - \omega) + W_v(\omega_c + \omega)] \cos \tau\omega d\omega. \quad (240)$$

We note that even in the unsymmetrical case the cross correlation vanishes when $\tau = 0$. Since the ensemble is jointly Gaussian, this means that $x(t)$ and $y(t)$ are independent. The probability density function of x and y evaluated at the same instant of time is therefore the product of single-variable Gaussian functions in x and y, that is,

$$p(x, y) = \frac{1}{2\pi\sigma^2} e^{-(x^2+y^2)/2\sigma} \qquad (241)$$

where

$$\sigma^2 = R_x(0) = R_y(0) = R_v(0) \qquad (242)$$

is the variance of $x(t)$, $y(t)$, and $v(t)$. We note that in the absence of signal (228) and (229) may be also written

$$\left.\begin{array}{l} x(t) = \rho(t) \cos \phi(t) \\ y(t) = \rho(t) \sin \phi(t) \end{array}\right\} \qquad (243)$$

and hence transforming from noise components in quadrature to envelope and phase noise is like transforming from rectangular to polar coordinates. Hence if $q(\rho, \phi)$ is the probability density function with respect to envelope and phase of the noise wave,

$$p(x, y)dxdy = p(\rho \cos \phi), (\rho \sin \phi)\rho d\rho d\phi$$
$$= q(\rho, \phi)d\rho d\phi \qquad (244)$$

and

$$q(\rho, \phi) = \frac{\rho}{2\pi\sigma^2} e^{-\rho^2/2\sigma^2}. \qquad (245)$$

The probability density function of the noise envelope alone is obtained by averaging over all phases and is

$$q_1(\rho) = \int_0^{2\pi} q(\rho, \phi)d\phi = \frac{\rho}{\sigma^2} e^{-\rho^2/2\sigma^2}. \qquad (246)$$

This is known as the Rayleigh distribution. Much confusion has been caused in discussions when one participant had in mind this distribution which is appropriate to the envelope of narrow band Gaussian noise while the other was thinking of the previously introduced distribution of wide band Gaussian noise. The probability density function of ϕ is

$$q_\phi(\phi) = \int_0^\infty q(\rho, \phi)d\rho = \frac{1}{2\pi}. \qquad (247)$$

The values of $\phi(t)$ are thus found to have a rectangular distribution.

We may obtain the probability density function for the combination of the sine wave signal and noise by substituting

$$\xi(t) = x(t) + A \qquad (248)$$

in (241). The resulting probability density function in ξ and y is

$$p(x, y) = r(\xi, y) = \frac{1}{2\pi\sigma^2} e^{-[(\xi-A)^2+y^2]/2\sigma}. \qquad (249)$$

Now transform to polar coordinates by

$$\left.\begin{array}{l} \xi = \rho \cos \phi \\ y = \rho \sin \phi \end{array}\right\} \qquad (250)$$

where ρ now represents the envelope and ϕ the phase of the signal plus noise. Then the joint probability density function $q(\rho, \phi)$ is calculated to be

$$q(\rho \cdot \phi) = \frac{\rho}{2\pi\sigma^2} e^{-(\rho^2+A^2-2A\rho \cos \phi)/2\sigma}. \qquad (251)$$

The probability density function of the envelope itself is

$$q_\rho(\rho) = \int_0^{2\pi} q(\rho, \phi)d\phi = \frac{\rho}{\sigma^2} I_0\left(\frac{A\rho}{\sigma^2}\right) e^{-(\rho^2+A^2)/2\sigma^2} \qquad (252)$$

while the probability density function of the phase is

$$q_\phi(\phi) = \int_0^\infty q(\rho, \phi)d\rho = \frac{e^{-A^2/2\sigma^2}}{2\pi} + \frac{A \cos \phi}{2\sigma\sqrt{2\pi}}$$
$$\cdot \left[1 + \mathrm{erf}\left(\frac{A \cos \phi}{\sqrt{2\sigma}}\right)\right] e^{-A^2 \sin \phi^2 1/2\sigma^2}. \qquad (253)$$

Eqs. (252) and (253) reduce to (246) and (247) respectively when $A = 0$.

Application of (252)—Probability of Error in Carrier Telegraph Signal Received Through Gaussian Noise

Suppose a telegraph message is sent by on-off bursts of a sine wave and is received by an envelope detector. Also suppose that Gaussian noise is picked up at the receiver input. We wish to calculate the probability of error in the received signal. The result will depend on how the decisions are made at the detector output. We consider the simple case in which a threshold indicator operates at the midpoint of each signaling interval. If the envelope is greater than some fixed threshold value ρ_0, the signal is judged to be a mark; otherwise it is called a space. We note that we have two kinds of envelope ensembles to choose between—1) the mark ensemble which has the probability density function $q_\rho(\rho)$ of (252) for sine wave plus noise and 2) the space ensemble which has the probability density function $q_\rho(\rho)$ of (246) for envelope of noise alone. We designate the latter function here as $q_{\rho 0}(\rho)$.

There are two kinds of error which can occur:

Type I) send "SPACE" receive "MARK"
Type II) send "MARK" receive "SPACE."

Let p_s represent the probability of sending a space and p_M the probability of sending a mark. Then the probability p_I of an error of Type I is p_s multiplied by the probability that the envelope value from noise alone exceeds ρ_0. Therefore

$$P_I = p_s \int_{\rho_0}^{\infty} q_{\rho_0}(\rho) d\rho = p_s \int_{\rho_0}^{\infty} \frac{\rho e^{-\rho^2/2\sigma^2}}{\sigma^2} d\sigma \quad (254)$$
$$= p_s e^{-\rho_0^2/2\sigma^2}.$$

The probability p_{II} of a Type II error is p_M multiplied by the probability that noise superimposed on the sine wave depresses the envelope below ρ_0. Therefore

$$p_{II} = p_M \int_0^{\rho_0} q_\rho(\rho) d\rho$$
$$= p_M \int_0^{\rho_0} \frac{I_0(A\rho/\sigma^2)}{\sigma^2} \rho e^{-(\rho^2+A^2)/2\sigma^2} d\rho$$
$$= p_M e^{-(A^2+\rho_0^2)/2\sigma^2} \sum_{n=1}^{\infty} \left(\frac{\rho_0}{A}\right)^n I_n(A^2/\sigma^2). \quad (255)$$

The evaluation of the integral in terms of a sum is accomplished by successive integration by parts making use of the indefinite integral

$$\int z^n I_{n-1}(az) dz = z^n I_n(az)/a. \quad (256)$$

The two types of error are not equally probable in general, but can be made so for a specific signal-to-noise ratio by a proper choice of the threshold level ρ_0. Determination of the proper value requires the solution of a transcendental equation. If $p_M = p_s$ and $\rho_0 = A/2$ the probability of Type II errors is smaller than Type I. The two types of errors can be made equally probable here by setting the threshold level at more than half the peak carrier amplitude. We reproduce the results of such a computation in Fig. 7 opposite. The corresponding curve for baseband pulse transmission is shown for comparison. In the latter case the two kinds of error are equally probable for threshold at half the pulse peak. The total probability of error is given by (36) with $x_0 = 0$ and $x = $ half the pulse peak. The power scale of the abscissa applies to a rectangular baseband pulse. The curve would be shifted 3 db to the left for a sinusoidal baseband pulse.

A more potent probability density function from which the spectra of envelope and phase can be obtained is the four-dimensional one in $x(t)$, $y(t)$, $x(t+\tau)$, $y(t+\tau)$. Here the fundamental simplifying property is that in a jointly Gaussian process all multivariate distributions obtained by linear operations on the functions are also jointly Gaussian. Hence if we write

$$\begin{aligned} x_1 &= x(t) & x_2 &= x(t+\tau) \\ x_3 &= y(t) = y_1 & x_4 &= y(t+\tau) = y_2 \end{aligned} \quad (257)$$

we refer back to (112)–(114) and note that the probability density function can be entirely constructed from

$$C_{x_1 x_2 x_3 x_4} = \exp\left[-\frac{1}{2} \sum_{j=1}^{4} \sum_{k=1}^{4} \lambda_{jk} \xi_j \xi_k\right] \quad (258)$$

where λ_{jk} is the typical crosscorrelation or average of $x_j x_k$. In our case

$$\left.\begin{aligned} \lambda_{11} &= \lambda_{22} = \lambda_{33} = \lambda_{44} = R_x(0) = R_y(0) = R_v(0) = \sigma^2 \\ \lambda_{12} &= \lambda_{34} = R_x(\tau) = R_y(\tau) = R_I \\ \lambda_{13} &= \lambda_{24} = R_{xy}(0) = 0 \\ \lambda_{14} &= -\lambda_{23} = R_{xy}(\tau) = R_Q \end{aligned}\right\} \quad (259)$$

$$\lambda = \begin{vmatrix} \sigma^2 & R_I & 0 & R_Q \\ R_I & \sigma^2 & -R_Q & 0 \\ 0 & -R_Q & \sigma^2 & R_I \\ R_Q & 0 & R_I & \sigma^2 \end{vmatrix} = (\sigma^4 - R_I^2 - R_Q^2).^2 \quad (260)$$

Let

$$A_0 = \sigma^4 - R_I^2 - R_Q^2. \quad (261)$$

Then

$$A_0^2 = \lambda \quad (262)$$
$$\Lambda_{11} = \Lambda_{22} = \Lambda_{33} = \Lambda_{44} = -\sigma^2 A_0$$
$$\Lambda_{12} = \Lambda_{34} = -R_I A_0$$
$$\Lambda_{14} = -\Lambda_{23} = -R_Q A_0$$
$$\Lambda_{13} = \Lambda_{24} = 0 \quad (263)$$

$$p(x_1, x_2, y_1, y_2)$$
$$= \frac{1}{4\pi^2 A_0} \exp\left(-\frac{1}{2A_0}\left[\sigma^2(x_1^2 + x_2^2 + y_1^2 + y_2^2)\right.\right.$$
$$\left.\left. - 2R_I(x_1 x_2 + y_1 y_2) - 2R_Q(x_1 y_2 - x_2 y_1)\right]\right). \quad (264)$$

This probability density function is sufficient to calculate the autocorrelation and hence the power spectrum of the envelope and phase of the noise ensemble. It is also adequate to obtain the same quantities when a sine wave signal is added to the noise. The latter includes the former as a special case. To calculate the autocorrelation of the envelope of signal and noise, we compute the ensemble average of $\rho(t)\rho(t+\tau)$, with $\rho(t)$ defined by (239) and (240). The above formulas are sufficient for this. We have

$$R_\rho(\tau) = \text{av} \left[(x_1+A)^2+y_1^2\right]^{1/2}\left[(x_2+A)^2+y_2^2\right]^{1/2}$$
$$= \int_{-\infty}^{\infty}\int_{-\infty}^{\infty}\int_{-\infty}^{\infty}\int_{-\infty}^{\infty}\left[(x_1+A)^2+y_1^2\right]^{1/2}$$
$$\cdot\left[(x_2+A)^2+y_2^2\right]^{1/2} p(x_1, x_2, y_1, y_2) dx_1 dx_2 dy_1 dy_2. \quad (265)$$

A double transformation to polar coordinates is indicated to evaluate this integral.

The autocorrelation of the phase is likewise

$$R_\phi(\tau) = \text{av} \left(\arctan \frac{y_1}{x_1 + A}\right)\left(\arctan \frac{y_2}{x_2 + A}\right)$$
$$= \int_{-\infty}^{\infty}\int_{-\infty}^{\infty}\int_{-\infty}^{\infty}\int_{-\infty}^{\infty} \arctan \frac{y_1}{x_1 + A}$$
$$\cdot \arctan \frac{y_2}{x_2 + A} p(x_1, x_2, y_1, y_2) dx_1 dx_2 dy_1 dy_2. \quad (266)$$

Here again we would introduce polar coordinates.
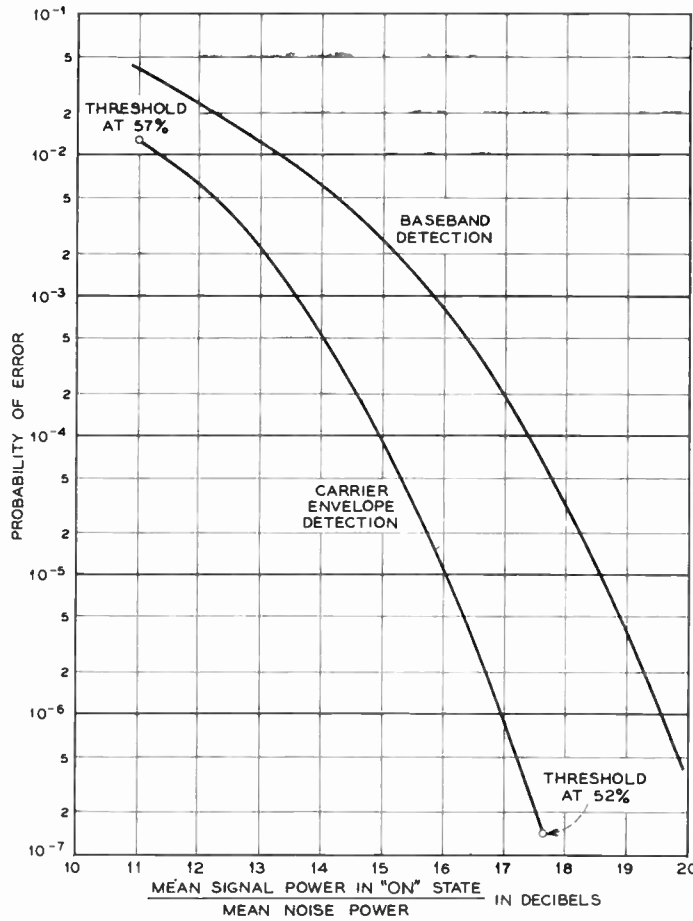
Fig. 7(a)—Probability of error from Gaussian noise in detection of random on-off pulses.

Fig. 7(b)—Power spectrum of instantaneous frequency of sine wave plus noise.

Fig. 7(c)—Power spectrum of instantaneous frequency of sine wave plus noise.

The formula for $R_\phi(\tau)$ should be accompanied by a reminder that by our definition the phase has been confined to a single interval of width 2π. This is all right for a static case in which angles are ambiguous by any additive multiple of 2π, but it may not be good for a phase which varies continuously with time. In the latter case when we reach the edge of our basic 2π interval and the slope does not change sign, continuity requires us to cross the boundary into the next interval rather than shift abruptly by 2π to stay within one interval. For this reason, we would use (266) only for the case in which the phase excursion can be wholly confined to a single range of width 2π. In such cases which might be approximated by low index phase or frequency modulation with no dc signal component, and with signal large compared to noise, we could use (266) not only for the phase, but for the instantaneous frequency as well, since

$$W_{\dot\phi}(\omega) = | i\omega |^2 W_\phi(\omega) = \omega^2 W_\phi(\omega) \qquad (267)$$

Signal-to-Noise Ratio in FM with Strong Carrier

Before proceeding to a more comprehensive look at the fm case, let us test the theory developed so far by working through the familiar case in which the amplitude of the sine wave is large compared to the rms value of the noise. The principal term in the numerator of
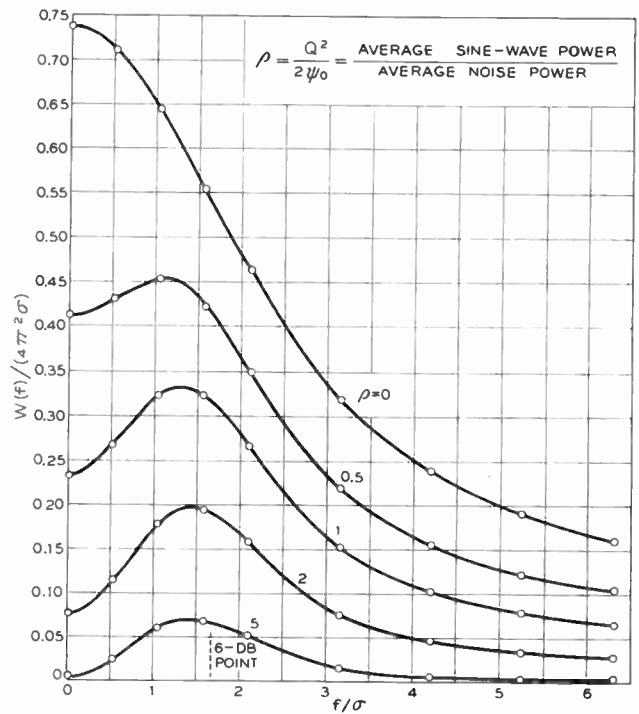
(230) for the instantaneous frequency is then $A\dot{y}(t)$ and in the denominator, A^2. Hence we have approximation

$$\dot\phi(t) = \frac{\dot{y}(t)}{A}. \qquad (268)$$

The spectral density of the instantaneous frequency is then

$$W_{\dot\phi}(\omega) = \frac{|i\omega|^2}{A^2} W_{y}(\omega) = \frac{\omega^2[W_v(\omega_c+\omega)+W_v(\omega_c-\omega)]}{2W_c} \quad (269)$$

where

$$W_c = \frac{A^2}{2}. \quad (270)$$

W_c is the mean square of the carrier wave. This is the familiar formula for the mean square frequency error spectrum caused by perturb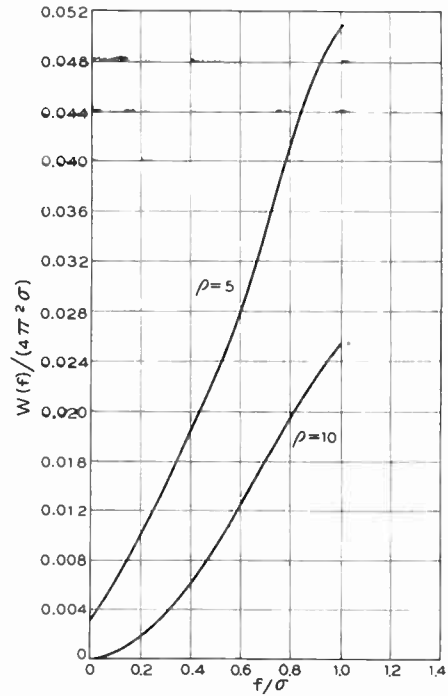ing a sine wave with narrow band noise of relatively small mean power. If the power spectrum of the noise is flat throughout the range of interest, we obtain the type of error spectrum often referred to as triangular since the rms value in a narrow band is proportional to ω. In general, for the case of small noise, the rms of $\dot\phi$ in a narrow band $\Delta\omega$ at ω is

$$\dot\phi_{rms} = \omega\sqrt{\frac{W_v(\omega_c+\omega)+W_v(\omega_c-\omega)}{2W_c}}\,\Delta\omega. \quad (271)$$

The signal-to-noise ratio S^2/N^2 in the output of an fm receiver is commonly expressed as the ratio of the mean square frequency deviation caused by modulating the carrier frequency with a full load sine wave test signal to the mean square frequency deviation produced by noise when the carrier frequency is constant. The denominator is therefore given by

$$N^2 = \left[\int_{-\omega_2}^{-\omega_1} + \int_{\omega_1}^{\omega_2}\right] W_{\dot\phi}(\omega)d\omega = 2\int_{\omega_1}^{\omega_2} W_{\dot\phi}(\omega)d\omega \quad (272)$$

where f_1 and f_2 are the lower and upper cutoff frequencies of the filter following the frequency detector. The numerator is

$$S^2 = \frac{\omega_s^2}{2} \quad (273)$$

where ω_s is the peak frequency deviation caused by the test fm signal. If the output filter is essentially low pass with cutoff at ω_a, and the noise band is flat,

$$W_r(\omega_c + \omega) = W_r(\omega_c - \omega) = W_v \quad (274)$$

$$N^2 = \int_0^{\omega_a} \frac{4\omega^2 W_v}{2W_c}\,d\omega = \frac{2W_v\omega_a^3}{3W_c} \quad (275)$$

$$\frac{S^2}{N^2} = \frac{3W_c}{4W_v\omega_a}\left(\frac{\omega_s}{\omega_a}\right)^2 = \frac{3}{2}\,\kappa^2\,\frac{W_c}{W_a} \quad (276)$$

where $\kappa = \omega_s/\omega_a$ is the ratio of test signal peak frequency deviation to width of accepted signal output band, and $W_a = 2W_v\omega_a$ is the equivalent noise power accepted by the receiver input in a band of width equal to the accepted output band. This formula is well-known in the fm art and its derivation is given here only as a warm-up exercise for a really tough problem—fm with no restriction on the noise power relative to signal power.

FM with Signal and Noise Comparable in Strength

The instantaneous frequency in the general case is defined uniquely by the nonlinear relationship (257). It seems best to calculate first the autocorrelation and then the spectrum. We note that in addition to $x(t)$ and $y(t)$ the relation includes $\dot x(t)$ and $\dot y(t)$. To obtain the autocorrelation, we must also make use of each of these functions evaluated at $t+\tau$, so we require an eight-dimensional probability density function, in which we now shall set

$$x_1 = x(t), \qquad x_2 = x(t+\tau) \qquad x_3 = \dot x_1 = \dot x(t),$$
$$x_4 = \dot x_2 = \dot x(t+\tau) \quad x_5 = y_1 = y(t), \quad x_2 = y_2 = y(t+\tau),$$
$$x_7 = \dot y_1 = \dot y(t), \qquad x_8 = \dot y_2 = \dot y(t+\tau). \quad (277)$$

These eight variables are jointly Gaussian since the various operations are linear. The covariances λ_{jk} can be evaluated from our previous observation on the effect of linear operation on cross spectra. Thus for instance,

$$\lambda_{18} = \text{av}\,[x(t)\dot y(t+\tau)] = R_{x\dot x}(\tau) = R_x'(\tau). \quad (278)$$

This representative example should make it clear how all the λ's can be found. The evaluation of the Λ's then proceeds in a manner exactly as in the previous illustration and the eight-fold probability density function thus obtained. If the noise spectrum is symmetrical about ω_c a considerable number of zero values in the determinant appear. The autocorrelation of the instantaneous frequency is then

$$R_{\dot\phi}(\tau) = \text{av}\,[\dot\phi(t)\dot\phi(t+\tau)]$$
$$= \int_{-\infty}^{\infty} \cdots \int_{-\infty}^{\infty} \frac{[(x_1+A)\dot y_1 - y_1\dot x_1][(x_2+A)\dot y_2 - y_2\dot x_2]}{[(x_1+A)^2+y_1][(x_2+A)^2+y_2]}$$
$$\cdot p(x_1,\,x_2,\,\dot x_1,\,\dot x_2,\,y_1,\,y_2,\,\dot y_1,\,\dot y_2)$$
$$\cdot dx_1 d\dot x_2 d\dot x_1 d\dot x_2 dy_1 dy_2 d\dot y_1 d\dot y_2. \quad (279)$$

A prescription for the calculation is thereby achieved. The spectrum of the instantaneous frequency is

$$W_{\dot\phi}(\omega) = \frac{1}{2\pi}\int_{-\infty}^{\infty} R_{\dot\phi}(\tau)e^{-i\omega\tau}d\tau. \quad (280)$$

The spectrum of the phase is obtained by noting that the admittance function needed to produce it from the frequency is $1/i\omega$ corresponding to integration in the time domain and hence

$$W_\phi(\omega) = W_{\dot\phi}(\omega)/\omega^2. \quad (281)$$

Fortunately for the engineer it should not often be necessary to work through calculations of this type. Altruistic investigators have done the work for representative problems and their results are available in tabular and graphical form. We should at this point then merely cite the appropriate references and give helpful explanatory hints on how to use them effectively. It is possible to understand how the results were obtained and to use them intelligently without checking through the details of the evaluations.

S. O. Rice [13] has computed the power spectrum of $\dot{\phi}$ for various ratios of sine wave power to noise power for the case in which the sine wave frequency is at the center of a narrow Gaussian band of noise. This is the noise spectrum illustrated in Fig. 5(e). The dc component is not shown and is not usually of interest. Rice uses the symbol ρ for the ratio of mean sine wave power to mean total noise power. In our notation, $\rho = A^2/2 N_0$, since the mean square of $A \cos \omega_c t$ is $A^2/2$ and N_0 in (159) is the total power represented by the noise spectrum. The frequency abscissa is f/σ where σ is the frequency displacement from the center of the band at which the spectral density is down one-quarter neper or 2.17 db. In our notation, $\sigma = \omega_0/2\pi = f_0$. The ordinate is labeled $W(f)/4\pi^2\sigma$ and includes the contributions at f and $-f$. In our notation, this is $W_{\dot{\phi}}(f)/2\pi^2 f_0 = 2W_{\dot{\phi}}(\omega)/\omega_0$. We reproduce Rice's published curves here plus a supplementary curve computed by him since the publication of his paper.

We shall illustrate the use of these curves starting with typical data available to the engineer. In the case of an fm receiver, the ratio ρ can be calculated from the signal power at the input and the noise figure of the rf- and if-part of the receiver. The noise figure is defined as the ratio [16] of the signal-to-noise ratio at the input to the available signal-to-noise ratio at the output. If the receiver itself did not contribute any noise the noise figure would be unity. In the case in which the noise accompanying the input signal is thermal noise only, we have in effect a noise source with flat spectrum of density 204 db below one watt in a band of width one cps at room temperature. A noise figure of F in effect increases the spectral density of the equivalent source to $204-10 \log F$ below one watt per cps. If the mean carrier input power is $W_c = A^2/2$, the appropriate value of ρ to calculate the spectral density of the mean square frequency of signal and noise when the carrier wave is at constant frequency is W_c/N_0, where N_0 is the mean power of that part of the input which the selective circuits of rf- and if-branches accept. If we assume the rf- and if-branches are adequately described by a Gaussian band pass curve, the input spectrum of interest is that of Fig. 5(e). We add the contributions at corresponding positive and negative frequencies and write

$$2\left(\frac{N_0}{2f_0\sqrt{2\pi}}\right) = 10^{-20.4}F \text{ watts/cps} \qquad (282)$$

which corresponds to a mean total of N_0 watts of noise power with a band pass spectrum down 2.17 db at $f_0 = \omega_0/2\pi$ cps away from midband and with maximum density at midband equal to thermal noise density multiplied by the noise figure. Then

$$N_0 = f_0 F 10^{-20.4}\sqrt{2\pi}. \qquad (283)$$

If we wish to base our calculations on any other loss point—say f_k cps from midband (or ω_k radians per second) with transmission k db down, we may use the Gaussian relations,

$$2.17 f_k^2/f_0^2 = k \text{ db} \qquad (284)$$

from which

$$f_0 = f_k\sqrt{\frac{2.17}{k}} = \frac{1.473 f_k}{\sqrt{k}} \qquad (285)$$

$$N_0 = 10^{-20.4}F f_k\sqrt{\frac{4.34\pi}{k}}. \qquad (286)$$

The ρ curve we select then is given by

$$\rho = \frac{W_c}{N_0} = \frac{10^{20.4}W_c}{F f_k}\sqrt{\frac{k}{4.34\pi}}. \qquad (287)$$

If we represent the abscissa of the typical curve as x_ρ and the ordinate by y_ρ, then

$$x_\rho = \frac{f}{f_0} = \frac{\omega}{\omega_0}, \qquad y_\rho = 2W_{\dot{\phi}}(\omega)/\omega_0. \qquad (288)$$

The mean square frequency error in the detector output at frequency $\omega = \omega_0 x_\rho$ is $2W_{\dot{\phi}}(\omega) = \omega_0 y_\rho$. The total noise output from the receiver is expressed as in (272) by

$$N^2 = 2\int_{\omega_1}^{\omega_2} W_{\dot{\phi}}(\omega)d\omega = 2\int_{\omega_1/\omega_0}^{\omega_2/\omega_0} \frac{\omega_0 y_\rho}{2} \cdot \omega_0 dx_\rho$$

$$= \frac{2.17\omega_k^2}{k} \int_{\omega_1/\omega_0}^{\omega_2/\omega_0} y_\rho dx_{\rho_0} \qquad (289)$$

Finally from (273),

$$\frac{S^2}{N^2} = \frac{k}{4.34}\left(\frac{\omega_s}{\omega_k}\right)^2\left[\int_{\omega_1/\omega_0}^{\omega_2/\omega_0} y_\rho dx_\rho\right]^{-1}. \qquad (290)$$

Corresponding results for a flat band of input noise have been given by F. L. H. M. Stumpers. Stumpers uses an entirely different analytical approach from that given here. The more general problem in which the signal wave is frequency modulated has been treated by D. Middleton [15] by an extension of the methods here described. A discussion of various aspects of the problem is also given in Chapter 13 of vol. 24 of the Radiation Lab. Series [17].

When the signal wave is frequency modulated by a band of noise, the autocorrelation of the signal becomes the two-dimensional characteristic function of the noise. This helpful computing aid has been applied by Bennett, Curtis, and Rice to the problem of evaluating interchannel interference in FM transmission of carrier groups [18].

BIBLIOGRAPHY

[1] Cramer, H., *Mathematical Methods of Statistics.* Princeton, New Jersey, Princeton University Press, 1951.

[2] Holbrook, B. D., and Dixon, J. T., "Load Rating Theory for Multi-Channel Amplifier," *Bell System Technical Journal*, Vol. 18 (October, 1939), pp. 624–644.

[3] Rice, S. O., "Mathematical Analysis of Random Noise," *Bell System Technical Journal*, Vol. 23 (July, 1944), pp. 282–332; Vol. 24 (January, 1945), pp. 46–156.

[4] Bennett, W. R., "Cross-Modulation in Multichannel Amplifiers," *Bell System Technical Journal*, Vol. 19 (October, 1940), pp. 587–610.

[5] Bennett, W. R., "Response of a Linear Rectifier to Signal and Noise," *Journal of the Acoustical Society of America*, Vol. 15 (January, 1944), pp. 164–172.

[6] Lewin, L., "Interference in Multi-Channel Circuits," *Wireless Engineer*, Vol. 27 (December, 1950), pp. 294–304.

[7] Middleton, D., "Some General Results in the Theory of Noise Through Non-Linear Devices," *Quarterly of Applied Mathematics*, Vol. 5 (January, 1948), pp. 445–498.

[8] Whittaker, J. M., *Interpolatory Function Theory*, No. 33, *Cambridge Tracts in Mathematics and Mathematical Physics*. Cambridge, England, Cambridge University Press, 1935.

[9] Courant, R., and Hilbert, D., *Methoden der Mathematischen Physik*. Berlin, Germany, Springer, Vol. 1, p. 65, 1924.

[10] Bennett, W. R., "Time Division Multiplex Systems," *Bell System Technical Journal*, Vol. 20 (April, 1941), pp. 119–221.

[11] Barnes, G. H., *Data Reduction Equipment for the Analysis of Human Tracking*. Franklin Institute Laboratories for Research and Development, Final Report No. F-2333, September 5, 1952–May 15, 1953.

[12] Krendel, E. S., and Barnes, G. H., *Interim Report on Human Frequency Response Studies*. WADC Technical Report 54-370, June, 1954.

[13] Rice, S. O., "Properties of a Sine Wave Plus Random Noise," *Bell System Technical Journal*, Vol. 27 (January, 1948), pp. 109–157.

[14] Stumpers, F. L. H. M., "Theory of Frequency Modulation Noise," PROCEEDINGS OF THE IRE, Vol. 36 (September, 1948), pp. 1081–1092.

[15] Middleton, D., "The Spectrum of Frequency-Modulated Waves After Reception in Random Noise—Part I," *Quarterly of Applied Mathematics*, Vol. 7 (July, 1949), pp. 129–173; Part II, Vol. 8 (April, 1950), pp. 59–80.

[16] Friis, H. T., "Noise Figures of Radio Receivers," PROCEEDINGS OF THE IRE, Vol. 32 (July, 1944), pp. 419–422.

[17] Lawson, J. L., and Uhlenbeck, G. E., *Threshold Signals*. New York, New York, McGraw-Hill Book Company, Inc., Chapter 13, 1950.

[18] Bennett, W. R., Curtis, H. E., and Rice, S. O., "Interchannel Interference in FM and PM Systems Under Noise Loading Conditions," *Bell System Technical Journal*, Vol. 34 (May, 1955), pp. 601–636.

Video Measurements Employing Transient Techniques*

H. A. SAMULON†, SENIOR MEMBER, IRE

Summary—After some general remarks regarding the proper place of transient techniques in the field of video measurements, suitable waveforms and equipment are described. Methods of measurement and evaluation of response curves are discussed. An attempt is made to estimate the effect of small variations in the transfer function on the transient response. A tentative list of criteria is prepared which, though not fully defining the transient response, may often serve as a useful and satisfactory description.

I. INTRODUCTION

THIS PAPER is intended as a compilation of those facts which are pertinent to the performance of transient tests at video frequencies. Many points which this report stresses are well known to the experts in the field but not sufficiently disseminated among those people who must use transient techniques only occasionally. Some remarks are fairly obvious but have been added for the sake of completeness. Wherever statements are made which are neither obvious nor believed to be in the literature the author has added the proof in the Appendix. For the sake of brevity, it was necessary to omit some interesting facts from the manuscript.

The work was suggested by the IRE Subcommittee 25.5[1] which, under Dr. G. L. Fredendall's chairmanship, frequently reviewed the paper and added greatly by suggestions and criticism. This help is warmly acknowledged.

II. GENERAL REMARKS

The main part of this paper will be restricted to those cases for which the transient response completely and uniquely describes the transfer function of the active or passive network to be tested. This condition is fulfilled for all linear and nearly linear systems. It does not necessarily exclude networks containing nonlinear elements, since a system performing modulation and demodulation might well satisfy the condition mentioned above. This restriction has been made for the sake of generality in the treatment of transient measurements. In many nonlinear cases, transient techniques may be used to great advantage; however, it would be difficult if not impossible to give general rules of procedure. In such cases the transient techniques must be adapted to the particular situation. Since the transient response uniquely determines the complete transfer function for a linear network—not just the angle or the magnitude

[1] Video Subcommittee of the Committee on Measurements and Instrumentation (25).
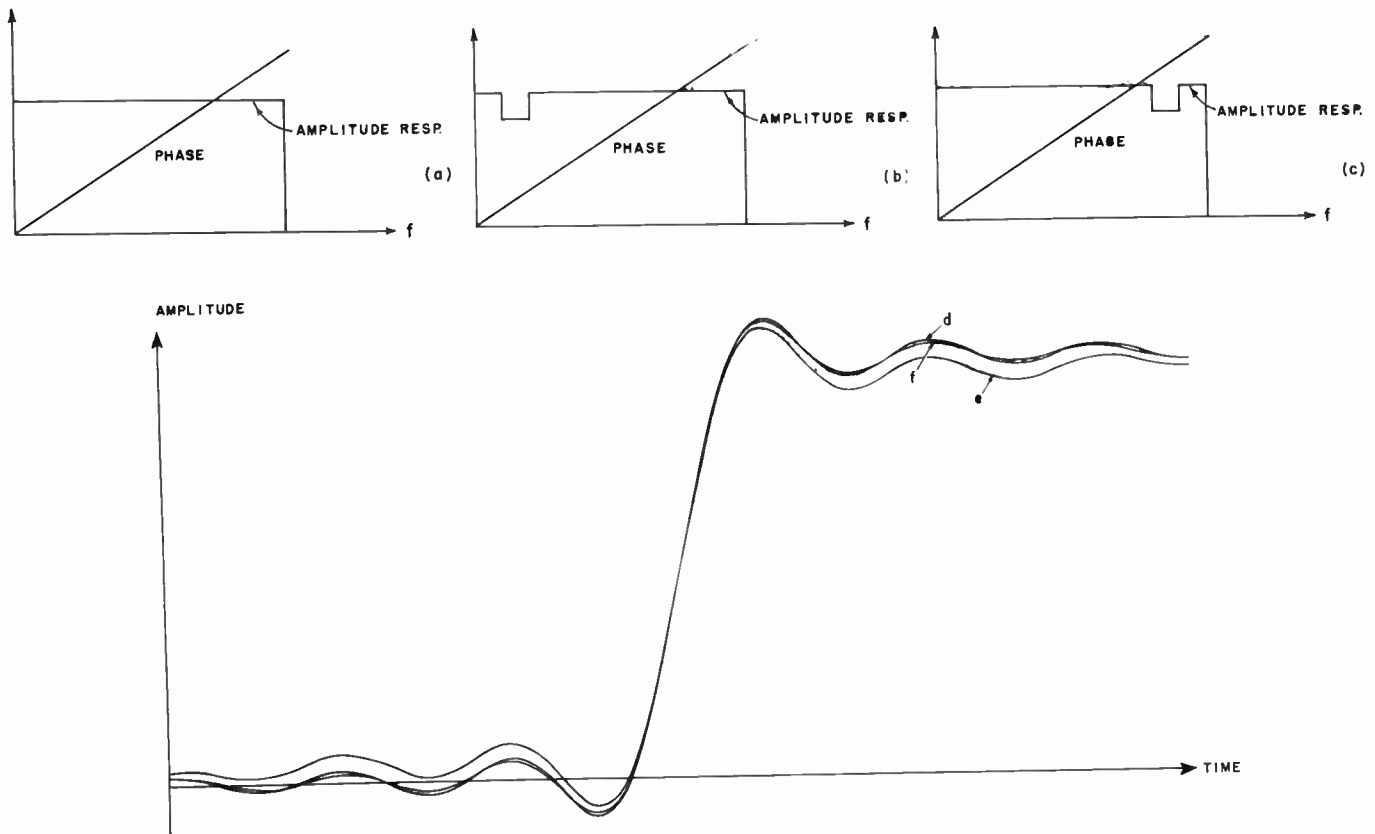
Fig. 1—Amplitude and phase response of "ideal lowpass" without (a) and with (b) and (c) indentations in the amplitude response. Effect of indentation in the amplitude response on the step response: (d) no indentation, (e) indentation at low frequencies, and (f) indentation at high frequencies.

alone—the greatest usefulness of transient techniques will be found in those fields in which the complete transfer function is of importance, as in television and radar. Since in audio work, for instance, the primary interest is in many cases in only the amplitude response of a system, transient techniques will in general be less often employed here than steady state methods.

It should also be mentioned that transient methods are not recommended for the measurement of selectivity properties, since they are considerably less accurate in measuring the transfer function in regions of high attenuation than the well-known steady state methods.

It should be realized that, in these two methods, measurement errors may have quite different effects on the accuracy with which the transfer function is determined. In the steady state method, where the transfer function is determined directly, measurement errors appear directly in the final result. In the transient method, however, where the transfer function is computed from the measured time response, the parts of the transfer function having an important effect in shaping the time response are determined with the best accuracy, and those parts of the transfer function which do less appreciably affect the time response are less precisely determined. A given error in measuring the time response will produce little error, then, in that part of the transfer function which is important in determining

the time response, but it may produce considerably more error in the determination of the less important parts of the transfer function.

An example may serve to illustrate these statements. Let us consider the transient responses of networks having the transfer functions shown in Figs. 1(a)–1(c). The corresponding response curves are shown in Figs. 1(d)–1(f). It is easy to see that a "dent" in the transfer function at low frequencies has a considerably greater effect on the transient than the same "dent" at higher frequencies. If instead of a step function, an impulse function were to have been used in this example, the maximum effect of the dent in the transfer function on the transient response would have been largely independent of the dent position. If we take the maximum change of ordinates of the transient response curve due to such a dent as a measure of the effect of the dent, then we can state:

The effect of a narrow dent in the amplitude response on a bandlimited impulse is the same as on a bandlimited step if the dent occurs at about $\frac{1}{3}$ of the common cutoff frequency f_c; the maximum amplitudes of the bandlimited step and impulse are assumed to be unity. If the dent occurs at high frequencies the effect will be greater for the impulse, if it occurs at lower frequencies it will be greater for the step. A more detailed discussion of this subject will be found in section V, (B-2).

III. Appropriate Test Waveforms

A. General Remarks; Step Function; Square Wave

Though transient techniques in the strict sense of the word assume a nonrepetitive waveform at the input terminals, the use of a periodic function with a very low repetition rate approaches this condition very closely and offers considerable advantage such as high brightness if displayed on an oscilloscope, and continuous observation.

In the case where a square wave or a repetitive impulse is used as the test waveform, limits for the repetition frequency should be stated. It can be shown by the sampling theorem in the frequency domain [1, 2] that in order to define a given transfer function completely, only discretely spaced samples of the transfer function are required if the time response does not change outside a finite region. If the time during which the transient response differs significantly from a stationary condition is T_0, the requirement is that the samples of the transfer function should be spaced not more than $1/T_0$ apart. This means that with a number of discrete frequencies at $f = 1/T_0, 2/T_0, 3/T_0, \cdots$ the transfer function and/or the transient response of the network is completely determined. In other words, a repetitive time function containing the frequency $1/T_0, 2/T_0, 3/T_0, 4/T_0, \cdots$ will be sufficient to define uniquely the transient response of the network. If T_0 is known or can be easily determined, the upper limit of the repetition frequency is thus given to be $1/T_0$.

These considerations establish the highest possible repetition rate. It is, however, advantageous in the case of the square wave (with 50 per cent duty cycle) to use a repetition frequency of less than one half of $(1/T_0)$ in order to be able to discriminate completely the transient response due to the leading edge and the one due to the trailing edge. Only if the repetition frequency is kept below $1/2T_0$ will the response of a system to the leading (or trailing) edge of a square wave be the same as the response to the nonrepetitive step-function during interval T_0. In practice it is generally inadvisable to make the period of the square wave long enough so that a perfectly stationary condition is reached after the main transition. It is considered better to measure the very low frequency region separately[2] and place the repetition frequency at a somewhat higher region where the transfer function has a flat amplitude and linear phase response. If this condition is not fulfilled the response will not give any indication of a stationary condition and the value of the tests will be greatly reduced.

An experimental check on whether the repetition rate is low enough, can be made easily. If changing the repetition rate—say—20 per cent does not affect the response noticeably, the repetition rate is low enough.

In Fig. 2(a) a case is shown where the repetition frequency is too high, which is demonstrated by a response

---

change when the repetition rate is somewhat changed. Fig. 2(b) shows a sufficiently low repetition rate.

B. Impulse, Pulse Train

Instead of using step functions, single or repetitive, a single or repetitive impulse is sometimes used in transient testing. The statements made about repetition frequency under (A) hold here too.

Since the response to an impulse wave is the time derivative of the response to a step wave, it is possible to obtain one response from the other with some loss of accuracy. Which waveform to use in a specific test depends on the purpose of the test, the normal operation of the equipment to be tested and the availability of test equipment. Refer also to section V, (B-2a).

$f_r = 40$ KC $f_r = 24$ KC

$f_r = 50$ KC $f_r = 30$ KC

TOO HIGH   SATISFACTORY
REPETITION FREQUENCY   REPETITION FREQUENCY
(a)   (b)
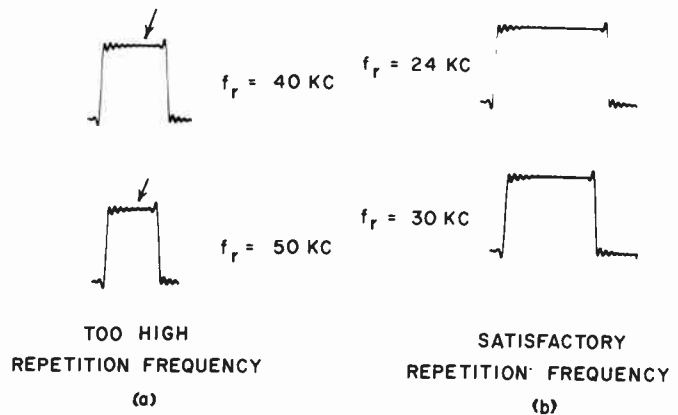
Fig. 2—Square-wave response for different repetition frequencies.

C. Other Waveforms

Besides impulse and step functions other waveforms have been proposed as test signals [3, 4]. The reason often given is that the particular waveform approaches more nearly a typical signal than the impulse or step—or that it does not have frequency components in a region where the actual signal would not have any.

Though in some cases it may be advantageous, this report refrains from recommending special waveforms for various reasons, some of which are listed below. There are only a few systems which have one single typical waveform. Any standardization of a typical transient might require changes if the equipment is altered (e.g. in the case of television, improved camera resolution might result in steeper typical transients).

By decreasing the energy content of the waveform near the cutoff, the results will tend to be less accurate in that region; this is not always desirable. Also, it may be harder to judge the effect of cascading units of which the individual response to a special waveform is known than it would be if their tests would have been performed with impulse or step inputs.

Equipment-wise, the special waveform is generally produced by the addition of a shaping network to the equipment as described in section IV, (E). This shaping network has to be frequently checked and if necessary realigned.

The vast amount of knowledge about step and impulse responses which is available to the student of modern network theory today would be of little value without recalculations or at least reinterpretations if other waveforms are used.

Most important, the hope for standardization of transient testing (using step functions or the closely related impulse functions) would be considerably decreased by any widespread use of special waveforms.

It should be added, that, though impulse and step response carry all the information required for the testing of linear networks, special waveforms will be required for most nonlinear systems—as discussed in section VI (Appendix I).

IV. Suitable Equipment

A. General

Basically, the equipment necessary for transient tests consists of a generator to produce the input waveform and a device to observe the output waveform of the apparatus to be transient tested.

The most commonly used test apparatus consists of a square wave generator (or, in the case of impulse testing, a pulse generator with low duty cycle) and an oscilloscope, Fig. 3.

Fig. 3—Block diagram of test set-up.

B. Impedance Requirements

Though it is in general desirable to have a low impedance generator and a high impedance oscilloscope, the impedance requirements actually depend on the object to be transient tested and will be discussed in more detail under section V, (A).

C. Amplitude Linearity

Slight amplitude nonlinearities of the oscilloscope which would not appreciably change the measurements of an amplitude response, might quite substantially change the transient and the transfer function computed from it. Since it is difficult to give numbers for the tolerable nonlinearity, it is recommended that nonlinearities be kept to an order of magnitude comparable to the error of observation.

D. Time Calibration

In order to evaluate the transient response, an accurate time calibration of the response curve has to be obtained [5-7]. This can be done by modulating the intensity of the beam ("blanking") of the cathode ray tube of the oscilloscope by means of a calibrated periodic signal; or, such a signal can be added to the transient itself and, if relatively small in amplitude, will not impair significantly the measurement of the transient response amplitudes. Its frequency should be of the same order of magnitude as the highest component contained in the transient response. If the test signal is repetitive, the calibrating signal must be synchronized with it. In cases where the transient is sampled for computation of the transfer function [see section V, (B-2)] it will be convenient to make the frequency of the calibrating wave equal to the sampling frequency.

E. Bandwidth or Transient Response Requirements

In general, it will not be necessary to specify the frequency response or transient response of generator and indicator separately. Instead, it is sufficient to specify the over-all response of the test set-up *without* the apparatus to be tested.[3] The measurements will be further discussed under section V, (A).

The ideal condition would be to make the amplitude response of the test set-up constant and its phase response linear over the frequency range in which the object to be tested has any appreciable response.[4] The tolerances on the constancy of the amplitude response and the linearity of the phase response depend upon the type of apparatus to be tested. It is possible to use test equipment with a sharp cutoff only slightly above the cutoff region of the apparatus to be tested; since, however, in general appreciable deviation from the linear phase response will result inside the pass band of the equipment, an elaborate phase compensation might be required. If however, the cutoff (3 db point) of the equipment is placed at, say, twice the cutoff frequency of the test object, the results will be quite acceptable for a great number of purposes. An amplitude response with a very gradual cutoff beginning past or near the cutoff region of the apparatus under test will also in general result in an approximately linear phase response of the test equipment inside the frequency range of interest.

Summarizing, one can say that the transfer function of the test set-up is prescribed to have a reasonably constant amplitude and linear phase only within the frequency range in which the object to be tested has an appreciable response. Of course, this statement holds for step as well as for impulse testing.

Since the transfer function of the test equipment is determined over only a limited frequency range (*i.e.,*

---

[3] Whereas the term "bandwidth" with regard to an oscilloscope is self-explanatory, the same term needs clarification if used for generators. Here we assume that the actual generator consists of an ideal generator (*i.e.*, a generator producing an ideal step or impulse function) in cascade with a network which changes the ideal waveform into the actual observed waveform. The "equivalent bandwidth" is the bandwidth of this hypothetical network.

[4] Neglecting the frequency region at which the amplitude response of the network under test is small (but not zero) will result in an error: the relative error (*i.e.* the ratio of error to maximum ordinate of the transient) will generally be of the same order of magnitude as the ratio of the area under the amplitude response curve which was neglected to the area under the non-truncated curve. If this error is less than the error of the transient measurement (which is, say, 2 per cent) the approximation is well justified.
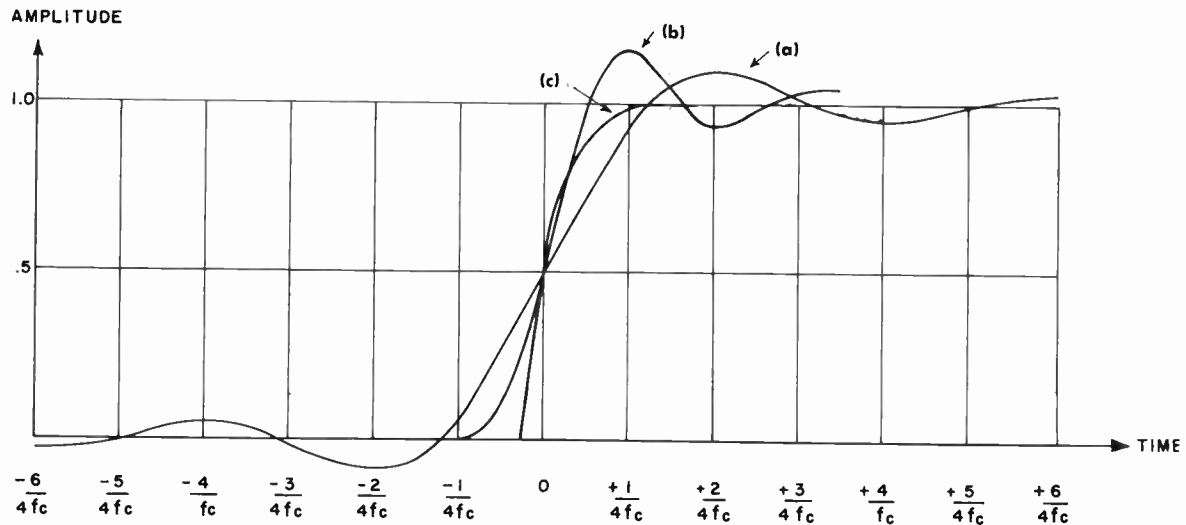
over the pass band of the test object[5]), the transient response of the test equipment will not be fully determined either; a great variety of different transient shapes will be equally satisfactory for test purposes. It is quite beyond the scope of this paper to give a comprehensive list of acceptable transient shapes. We will, however, try to give a small number of differently shaped typical transient responses representing test equipment which would give very nearly correct results provided that the network under test has no appreciable response beyond f_c. Response of Fig. 4(a) corresponds to a transfer-function with extremely sharp cutoff at f_c and linear phase; a network [see Fig. 4(d)] having this type of response is sometimes called an "ideal lowpass" and is physically not exactly realizable. Response of Fig. 4(b) corresponds to a minimum phase, Butterworth-type network with $n = 7$ [see Fig. 4(e)] and response of Fig. 4(c) to a simple RC network [see Fig. 4(f)].

Under the earlier assumption that the network under test has no appreciable response beyond f_c the equipment with response of Fig. 4(a) does not introduce any error. The equipment in Fig. 4(b) introduces a small error, mainly due to a rather small deviation from linear phase (at f_c this deviation is less than 4.3°). Equipment in Fig. 4(c) likewise introduces a small error, due mainly to deviation of equivalent amplitude response from flatness (approximately 12.5 per cent at f_c).

It is important to note that the transient response of the equipment may have considerable over-shoot (like the response in Fig. 4(b)) without causing errors in the measurements, a fact not always fully recognized. A "most desirable transient" for the test equipment cannot be defined without a full knowledge of the properties and use of the circuits to be tested. The same holds true for the specification of tolerances for the equipment.[6]

Fig. 4—Examples of step response for different transient test equipments: (a) for "ideal lowpass," (b) for Butterworth-type network ($n = 7$), and (c) for RC type network. Examples of amplitude and phase response for different transient test equipments: (d) for "ideal lowpass," (e) for Butterworth-type network ($n = 7$), and (f) for RC type network.

[5] By pass band of the network we mean here the frequency range for which the network has an appreciable amplitude response; *e.g.*, for many applications in television a 5 per cent figure might be considered as a reasonable limit.

[6] If, for instance a circuit under test is specified to within ±2 db and ±10° the test equipment should not deviate if possible by, say, more than 0.5 db from the ideal amplitude response and by more than 2.5° from the ideal phase response within the region of interest.

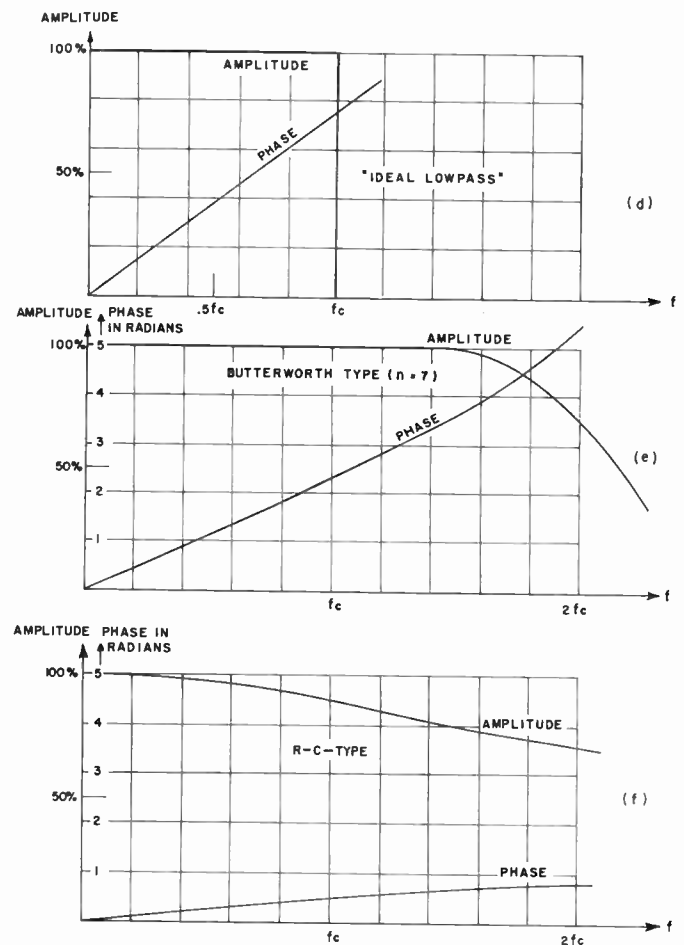If there is any doubt whether the test equipment is satisfactory from the standpoint of bandwidth, an analysis of the test equipment should be made as described in section V, (B-2).

The recommendation of making the bandwidth of the test equipment exceed the bandwidth of the ap-

paratus under test becomes problematic if the latter has a very gradual cutoff. In such a case, it might be necessary to use test equipment, the bandwidth of which is comparable to the one of the object under test. If this is done, however, the resulting transient will require certain corrections which are discussed in more detail under section V, (B-1).

V. Measurements and Analysis

A. Measurements

1) *Impedance Levels:* It is of great importance that the input as well as the output terminals of the network to be tested are, impedance-wise, correctly terminated, *i.e.*, terminated in the same way in which they actually are used. Failure to do this can result in a very considerable error in the transient response.

If the transient response of the test equipment alone is to be measured, the generator has to be correctly terminated, *i.e.*, with an impedance with which it will be terminated in the transient measurement of the test object.

2) *Input Signal Level:* In strictly linear networks, the actual level is not critical at all. In "almost linear" circuits (*e.g.*, circuits containing tubes) a signal level has to be chosen which, without producing too much nonlinear distortion, will result in an output signal which is sufficiently above the noise level to be useful for measurements. A specification of input level should generally accompany the results of transient measurements.

3) *Recording of Transient Response Curves or Sampling Points:* In tracing or photographing transient response curves, special care must be taken to prevent errors due to parallax. When photographic techniques are used, the picture plane and the plane in which the response curve lies must be sufficiently parallel if a serious error should be avoided.

It is also essential to provide an accurate time calibration of the measured curves.

For the purpose of analyzing transient response curves by methods described in section V, (B-2), only a finite number of sample points of the response curves need to be recorded. The maximum permissible spacing of the sampling points depends upon cutoff frequency of the test object and the method chosen for the analysis.

B. Evaluation and Analysis of Transient Response Curves

1) *Characteristics of Transients:* An accurated description of a transient will require, in general, a large number of characteristics. In fact the "Sampling Theorem" shows that for a transient of finite duration T with a frequency spectrum not exceeding f_c, a total number of $2Tf_c$ values are required [2]. Fortunately there are a small number of simple characteristics which, though not completely defining the transient, will in many cases describe the transient quite satisfactorily from a practical standpoint. If it is borne in mind that such characteristics will be of value only as

long as the shape of the transient does not differ too much from the well-known "textbook transients" of lowpass filters [8–11], such a description will be quite worthwhile. A list of such characteristics for step responses is given below.[7]

(a) Rise time (the time required for the ordinate of the transient to increase from 10 per cent above the original steady state value to 90 per cent of the final steady state value of the transition) [see Figs. 5(a) and 5(d)]. For some transients, like the one in Fig. 5(c), such a characteristic would be rather meaningless. In such a case the rise time measurement would be replaced by that given under (b).

(b) Steepest slope of the transition and the time duration of this part of the transient.

(c) Axis of oscillation (if an oscillatory transient precedes or follows the main transition it is often possible to sketch an "axis of oscillation" and specify its slope) [Figs. 5(a)–5(d).]

(d) Heights of first overshoots and undershoots preceding and following the transition. "Overshoots" will be defined as deviations away from the signal average, undershoots as deviations towards the signal average. The height is measured from the "axis of oscillation" [Figs. 5(a)–5(d).]

(e) Secondary transitions. In cases where the main transition is not preceded or followed by oscillatory transients it is frequently preceded or followed by a transition of considerably smaller slope than that of the main transition. The duration and slope of this part (or these parts) of the response curve are often of great interest. (If the slope has the same sign as the main transition it is sometimes referred to as "smear," an expression originating in television engineering.)

It should be noted that for all slope specifications the height of the response (between stationary values) should be assumed to be unity.

Figs. 5(a)–5(d) show different transients with these characteristics indicated.

In section IV, (E) it was mentioned that it might not always be possible to make the bandwidth of the test equipment exceed the bandwidth of the object under test. In such a case the characteristics mentioned above are of much less value. Certain rules are given in the literature which take the imperfection of the test equipment into account. The most important rule is: if neither the test equipment transient nor the transient of the object under test have any overshoots and if the measured rise time (the combination of the object under test and the test equipment) is τ_T, the rise time of the equipment transient τ_E and the unknown rise time of the object under test τ_0,

$$\tau_0 = (\tau_T^2 - \tau_E^2)^{1/2}.$$

The reader will find discussions in the literature of the case of nonzero overshoot which, however, are only of a rough qualitative nature. [12]

---

[7] No standard definitions exist for some of the expressions used here to characterize transient response curves.

(a)
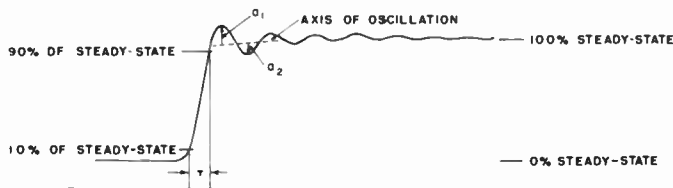
τ = time of rise
a_1 = first overshoot following transition
a_2 = first undershoot following transition
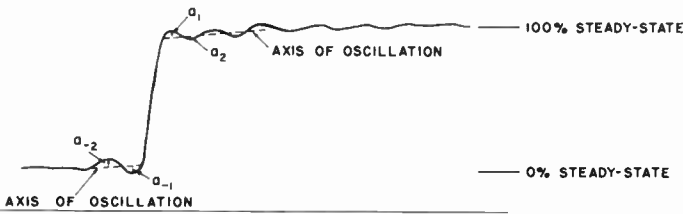
(b)

a_1 = first overshoot ⎫
a_2 = first undershoot ⎬ following transition
a_{-1} = first overshoot ⎫
a_{-2} = first undershoot ⎬ preceding transition
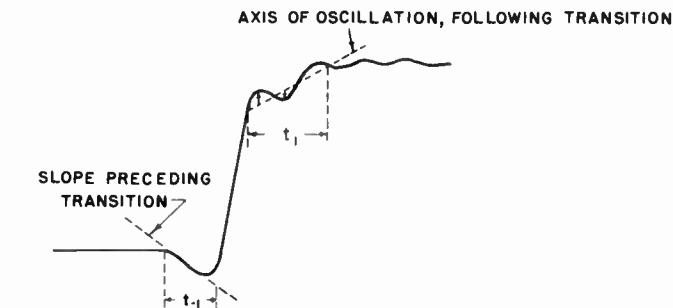
(c)

t_1 = duration of slope following transition
t_{-1} = duration of slope preceding transition
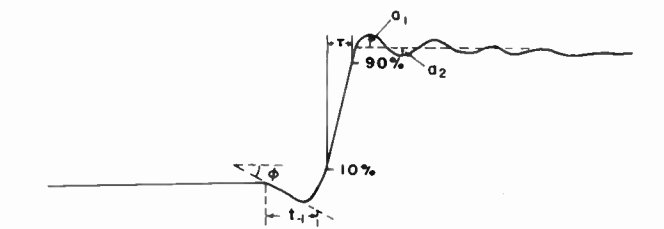
(d)

a_1 = first overshoot
a_2 = first undershoot
τ = time of rise
t_{-1} = duration of slope preceding transition

Fig. 5—Typical, measured, transients illustrating certain characteristics of step responses.

2) Accurate Analysis: "Analysis of a transient response" generally refers to the determination of the transfer function from the measured transient response.

Since measurements as well as calculations are of limited accuracy it is important to consider the effects of small errors of the measured transient response on the calculated transfer function. It seems, however, simpler to consider slight changes in the transfer func-

tion and to ask how they affect the ordinates of the transient response. If the resulting ordinate changes are below the measurement accuracy, it is then obvious that the corresponding transfer function changes cannot be determined by transient analysis:

(a) We assume a transfer function with a narrow dent in the amplitude response at f_0, but linear phase within the whole pass band. The dent dimensions as shown (in Fig. 6) are δf_0 and a. A bandlimited impulse
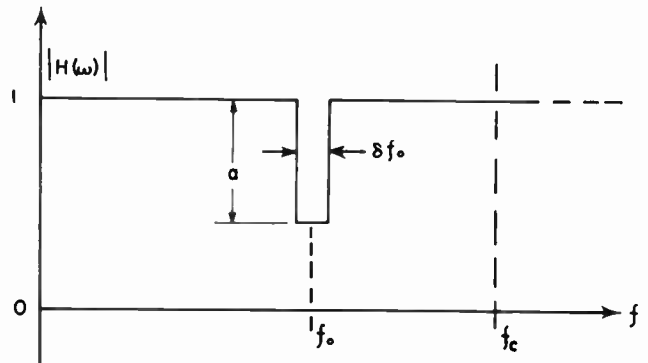
Fig. 6—Dimensions of indentation in the amplitude response.

whose maximum amplitude is unity and whose cutoff frequency is f_c is passed through a network with such a transfer function. Then the maximum change in ordinates caused by the dent is

$$E_1 = \frac{a\delta f_0}{f_c} .$$

We can say that the maximum change of ordinates of the impulse response produced by the dent is equal to the ratio of the dent to the area under the total amplitude response curve as shown in Fig. 6, regardless of the location of the dent (f_0).

If we pass a bandlimited step-function whose steady state amplitude is unity through the same network with the dent, the maximum change in ordinates caused by the dent is:

$$E_2 = \frac{a\delta f_0}{\pi \cdot f_0} .$$

The ratio of the two effects, E_1/E_2 is

$$\frac{E_1}{E_2} = \frac{\pi f_0}{f_c} .$$

At about $f_0 = (1/\pi)f_c$ the effects will be equal; if the dent occurs at the cutoff frequency, the effect of the dent will be roughly three times greater on the impulse than on the step. For frequencies below f_c/π the effect of the dent on the step becomes increasingly greater.

As an example let us consider a "dent" which is 6 db deep and with a width of 5 per cent of the cutoff frequency. Such a dent causes a maximum change in the ordinates of the impulse response of less than 2.5 per

cent of the maximum amplitude of the impulse response. The accuracy required for such a measurement (*i.e.* considerably better than 2.5 per cent) can hardly be expected from conventional transient testing.

By combining several "dents" the results shown above can be made more general. Certain details of the transfer function might be considered as a sum of such elementary dents. A first approximation to the effect of several "dents" will be equal to the sum of the effects of the individual "dents."

(b) Since under (2a) above the idealized case of a linear phase was treated it remains to be shown that the results for an actual network with minimum phase shift characteristic do not greatly deviate from the results obtained above. Here we will assume that the narrow dent is caused by a circuit as shown in Fig. 7(a).
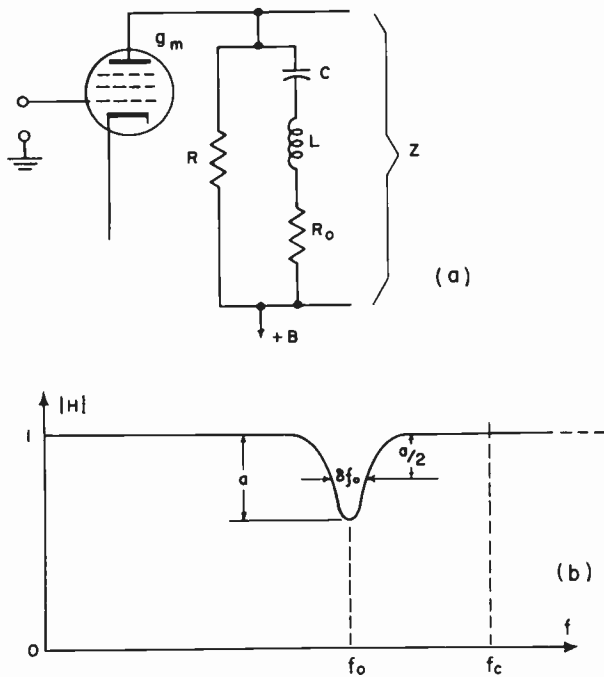
Fig. 7—Trap circuit and its amplitude response.

If the maximum height of the dent is a and the width of the dent (measured between the points for which the dent height is $a/2$) is δf_0 then the maximum change in ordinate of response curve to a bandlimited impulse is

$$E_0 = \frac{\delta f_0}{f_c} \cdot a\sigma$$

where

$$\sigma < \sqrt{\frac{1 - a/4}{1 - 3a/4}}\, \pi$$

and lies between π and $\pi\sqrt{3}$. This result is of the same order of magnitude as the one for the dent with linear phase.

The same is true for the step function response.

The mathematical proofs for the statements in paragraphs (2a, b) may be found in section VI (Appendix II).

For the numerical analysis, *i.e.* the calculation of the transfer function from the transient response, several methods exist.

α) A theoretically straightforward but actually fairly cumbersome method is the graphical evaluation of the Fourier integral for various values of frequency.

β) It is sometimes possible to approximate the transient response piecewise by different simple functions of which the Fourier transform can be easily found. This method will sometimes lead to very short numerical evaluations but the process of approximation is generally lengthy and can not be treated as a mere routine job.

γ) A method which has been widely used in television applications is the one introduced by Bedford and Fredendall. This method approximates the measured transient response by a sum of equally spaced step functions and gives the transfer function as a sum of complex numbers. The summing is performed graphically by simple vector additions [13].

δ) Another method is the one introduced by the author. This method replaces the transient response by a sum of $(\sin x)/x$ functions. Again the result is given as a sum of complex numbers. The summing is performed with the help of tables published in the literature [14]. For a transient with a limited frequency spectrum this method requires the least number of sample points since it makes use of the well-known Sampling Theorem. A comparison between methods γ and δ is contained in [14].

Of course all of these methods can be used to analyze not only the transient response of the network under test, but also the transient response of the test equipment. If the bandwidth of the test equipment does not exceed the bandwidth of the network under test, two transients have to be analyzed, *i.e.* the over-all transient response of the test equipment together with the network under test and the transient response of the test equipment alone.

If the following symbols are used:

$H_0(\omega) = \left| H_0(\omega) \right| e^{j\phi_0(\omega)}$ Transfer function of object under test.

$H_T(\omega) = \left| H_T(\omega) \right| e^{j\phi_T(\omega)}$ Over-all transfer function of test equipment plus object under test.

$H_E(\omega) = \left| H_E(\omega) \right| e^{j\phi_E(\omega)}$ Transfer function of test equipment alone.

then the true transfer function of the object under test is given by:

$$\left| H_0(\omega) \right| = \frac{\left| H_T(\omega) \right|}{\left| H_E(\omega) \right|}$$

and

$$\phi_0 = \phi_T - \phi_E.$$

VI. Appendix I

Nonlinear Systems

A. General

In section II it was pointed out that the use of transient techniques becomes rather involved for nonlinear systems. However, a system which contains nonlinear elements (*e.g.* expanders, compressers, modulators and demodulators, etc.) does not necessarily fall into this category. If the over-all system behaves linearly, *i.e.* if the superposition principle holds, the rules laid down in previous chapters might well apply. Also, it might be said that linear circuits are generally only idealizations of practical circuits with some nonlinearity. How far a system may deviate from the ideal linearity and still be tested by methods of the previous chapters is a matter of engineering judgment. For a truly nonlinear system, the transient response does not constitute a unique measure of its performance. As an example let us consider a network consisting of a conventional lowpass followed by an ideal limiter. For certain input levels (below limiting) the transient response will be completely determined by the lowpass, while for other input levels it will be almost independent of it. The dependence of the output shape on the input level is but another way of stating that the response of a nonlinear system to an arbitrary input shape can no longer be found by proper superposition of step or impulse responses (nonapplicability of the superposition principle).

This, however, should not imply that transient tests for nonlinear systems are useless; it only should justify the restrictions to linear or almost linear systems imposed on the main part of this paper. In many nonlinear cases in which the signal has step or impulse character, transient tests might in fact be the only simple way of checking the system performance.

In the testing of nonlinear systems a single transient test will rarely suffice. Instead, tests have to be made for different, typical wave forms and for different, typical levels. This might sometimes mean 10 or even 100 tests instead of one. Also, an analysis of the type described in section V (*B*) is of little value. Any specific suggestions for the case of general nonlinear circuits are hardly practical.

Among the large class of nonlinear systems is one type which deserves special attention because of its wide use: Transmission systems using vestigial sideband (vsb) techniques [15–21].

Transient measurements have become an indispensable tool of the video engineer in testing TV receivers and transmitters employing vsb techniques.

B. Transient Testing of VSB Systems

A system containing an ideal amplitude modulation and an ideal envelope detection can be transient tested according to the rules of the preceding sections only if the over-all transfer function between modulation and detection fulfills the condition of even symmetry for the magnitude (amplitude response) and odd symmetry for the angle (phase response)—symmetry here is understood with regard to the carrier frequency. If these conditions are not fulfilled, the total system will in general not behave like a linear system and can be classified as a vestigial sideband system. Such systems have been extensively analyzed in the literature. Let us denote the input to the modulator by $f_1(t)$ and the output of the detector by $f_2(t)$; then

$$f_2(t) = (f_I{}^2(t) + f_Q{}^2(t)]^{1/2},$$

where f_I and f_Q can be considered as responses of linear networks to $f_1(t)$.

Though $f_I(t)$ as well as $f_Q(t)$ can be derived from $f_1(t)$ by linear networks, this is obviously not true for $f_2(t)$, except if the symmetry conditions discussed above hold, in which case $f_Q(t)$ goes to zero and

$$f_2(t) \rightarrow f_1(t).$$

There is an important difference between f_I and f_Q which increases the value of transient tests of vsb systems considerably: the dc content of f_I depends on the depth of modulation, whereas f_Q never has any dc component. Hence, if the depth of modulation is low, $f_Q{}^2 \ll f_I{}^2$ and

$$f_2(t) \approx f_1(t).$$

In words, we may say that for low modulation depths the vsb transmission system approaches a linear system.
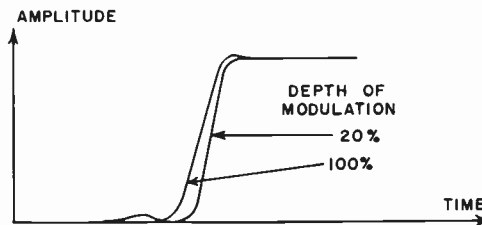
Fig. 8—Step response of a vsb system for 60 per cent and 20 per cent modulation depths.

Fig. 8 shows an example of the difference in resulting waveforms for two different degrees of depth of modulation.

It is of course not possible to say where a vsb system ceases to be nonlinear though it is generally considered sufficient for TV test purposes to keep the modulation depth below 30 per cent. This, of course, does not exclude tests with higher modulations, though the rules of linear systems will be less and less applicable.

Appendix II

Mathematical Proofs

A. Bandlimited Step (of Bandwidth f_c and a Steady-State Height of Unity) Passed Through a Network with Linear Phase and a Flat Amplitude Response with an Indentation at f_0

The amplitude response (Fig. 6) is given as:

$$|H(\omega)| = 1 \quad \text{for} \quad \begin{cases} 0 < \omega < \left(\omega_0 - \dfrac{\delta\omega_0}{2} \right) \\ \omega > \left(\omega_0 + \dfrac{\delta\omega_0}{2} \right) \end{cases} \tag{1a}$$

$$|H(\omega)| = (1 - a) \text{ for}$$

$$\left(\omega_0 - \frac{\delta\omega_0}{2}\right) < \omega < \left(\omega_0 + \frac{\delta\omega_0}{2}\right) \tag{1b}$$

Since the transform of the input function is $1/j\omega$ for $\omega < \omega_c$ and zero for $\omega > \omega_c$ the transient response can be written as

$$f(t) = \frac{1}{2\pi} \int_{-\omega_c}^{+\omega_c} \frac{H(\omega)}{j\omega} e^{+j\omega t} d\omega \tag{2}$$

or since $H(\omega)/j\omega$ is an odd function of ω

$$f(t) = \frac{1}{\pi} \int_0^{\omega_c} \frac{H(\omega)}{\omega} \sin \omega t d\omega \tag{3}$$

$$= \frac{1}{\pi} \int_0^{\omega_c} \frac{\sin \omega t}{\omega} d\omega - \frac{a}{\pi} \int_{\omega_0-(\delta\omega_0/2)}^{\omega_0+(\delta\omega_0/2)} \frac{\sin \omega t}{\omega} d\omega. \tag{4}$$

The first term is the unchanged input function, *i.e.* a bandlimited step function of the steady state value of unity. The second term is the change E_2 caused by the dip in the amplitude response. We may write:

$$E_2 = \frac{a}{\pi} \int_{\delta\omega=-(\delta\omega_0/2)}^{\delta\omega=+(\delta\omega_0/2)} \frac{\sin (\omega_0 + \delta\omega)t}{\omega_0 + \delta\omega} d(\delta\omega). \tag{5}$$

Since we have assumed that the dip is narrow, *i.e.* that $\delta\omega_0 \ll \omega_0$, we may write:

$$E_2 \approx \frac{-a}{\pi\omega_0 t} \cos (\omega_0 + \delta\omega)t \Big|_{\delta\omega=-(\delta\omega_0/2)}^{\delta\omega=+(\delta\omega_0/2)} \tag{6}$$

$$\approx \frac{a}{\pi\omega_0 t} 2 \sin \omega_0 t \sin \frac{\delta\omega_0 t}{2} \tag{7}$$

or differently written:

$$E_2 \approx \frac{a}{\pi} \frac{\delta\omega_0}{\omega_0} \frac{\sin \frac{\delta\omega_0}{2} t}{\frac{\delta\omega_0}{2} t} \sin \omega_0 t. \tag{8}$$

An inspection of this expression shows that the time dependent parts of it correspond to a sine-carrier modulated by a $(\sin x)/x$-type function. If $\delta\omega_0 \ll \omega_0$, the maximum will be near the first maximum of $\sin \omega_0 t$, *i.e.* near $t = \pi/2\omega_0$; thus $(E_2)_{max}$ will be approximated by:

$$(E_2)_{max} \approx \frac{a}{\pi} \cdot \frac{\delta\omega_0}{\omega_0} \tag{9}$$

B. Bandlimited Impulse (of Bandwidth f_c and a Maximum Height of Unity) Passed Through a Network with Linear Phase and a Flat Amplitude Response with an Indentation at f_c

Since the transform of such an impulse is $1/2f_c$ for $|\omega| < \omega_0$ and zero for $|\omega| > \omega_0$ the transient response can be written as:

$$f(t) = \frac{1}{2\pi} \int_{-\omega_0}^{+\omega_0} \frac{H(\omega)}{2f_c} e^{+j\omega t} d\omega, \tag{10}$$

where $|H(\omega)|$ is given by (1).

Since $H(\omega)$ is an even function of ω:

$$f(t) = \frac{1}{2\pi f_c} \int_0^{\omega_c} H(\omega) \cos \omega t d\omega \tag{11}$$

$$= \frac{1}{2\pi f_c} \int_0^{\omega_c} \cos \omega t d\omega - \frac{a}{2\pi f_c} \int_{\omega_0-(\delta\omega_0/2)}^{\omega_0+(\delta\omega_0/2)} \cos \omega t d\omega. \tag{12}$$

The first term is the unchanged input function, *i.e.* the bandlimited impulse function of unity maximum amplitude. The second term is the change E_1 caused by the dip in the amplitude response. We may perform the integration and write:

$$E_1 = \frac{a}{2\pi t f_c} \sin \omega t \Big|_{\omega=\omega_0-(\delta\omega_0/2)}^{\omega=\omega_0+(\delta\omega_0/2)} \tag{13}$$

or

$$E_1 = \frac{a}{2\pi t f_c} \left[\sin \left(\omega_0 + \frac{\delta\omega_0}{2}\right)t - \sin \left(\omega_0 - \frac{\delta\omega_0}{2}\right)t \right] \tag{14}$$

$$= \frac{a\delta\omega_0}{\omega_c} \frac{\sin \frac{\delta\omega_0}{2} t}{\frac{\delta\omega_0}{2} t} \cos \omega_0 t. \tag{15}$$

This expression corresponds to a cos-carrier modulated by a $(\sin x)/x$-type function. It has its maximum value at $t = 0$, namely

$$(E_1)_{max} = \frac{a\delta\omega_0}{\omega_c}. \tag{16}$$

C. Effect of a Minimum Phase Shift Type Network with a Narrow Notch in the Amplitude Response on Bandlimited Impulse Whose Maximum Amplitude is Unity

One of the simplest networks which gives a flat amplitude response with a narrow notch consists of two resistors, a capacitance and an inductance. Such a network is shown in Fig. 7(a).

The amplitude response is shown in Fig. 7(b). The maximum depth of the notch is a and the width (between points of $[1-(a/2)]$ response) is $\delta\omega_0$. Without losing generality, we may assume that the g_m of the tube is equal to $1/R$. Then the transfer function becomes:

$$H(\omega) = g_m Z = \frac{Z}{R}; \quad \text{and since} \tag{17}$$

$$Z = \frac{R \left\{ j\omega L + \frac{1}{j\omega C} + R_0 \right\}}{(R + R_0) + j\omega L + \frac{1}{j\omega C}} \tag{18}$$

$$H(\omega) = \frac{(1 - \omega^2 LC) + j\omega C R_0}{(1 - \omega^2 LC) + j\omega C(R + R_0)}$$

$$= 1 - \frac{j\omega CR}{(1 - \omega^2 LC) + j\omega C(R + R_0)}. \tag{19}$$

The impulse response of a network is given by the inverse Laplace transform of its transfer function, hence

$$h(t) = \mathcal{L}^{-1}\{H(\omega)\}$$

$$= \mathcal{L}^{-1}\left\{1 - \frac{pCR}{1 + p^2LC + pC(R + R_0)}\right\} \quad (20)$$

$$= h_I(t) - \frac{R}{L}\mathcal{L}^{-1}\left\{\frac{p}{(\omega_0{}^2 + p^2) + p\left(\frac{R + R_0}{L}\right)}\right\} \quad (21)$$

$$= h_I(t) + h_{II}(t). \quad (22)$$

The first term of the right side is the impulse function, the second term is the effect of the trap in the passband. By conventional methods we obtain for the second term $h_{II}(t)$:

$$h_{II} = -\frac{R}{L}\cdot\frac{e^{-(R+R_0)t/2L}}{\sqrt{1 - \left(\frac{R+R_0}{\omega_0 2L}\right)^2}}\sin\left\{\omega_0 t\sqrt{1 - \left(\frac{R+R_0}{2\omega_0 L}\right)^2}\right.$$

$$\left. - \text{arctg}\sqrt{\left(\frac{2L\omega_0}{R+R_0}\right)^2 - 1}\right\}. \quad (23)$$

Our assumption of a narrow dip (*i.e.* $\delta\omega_0 \ll \omega_0$) means that $(R_0 + R) \ll \omega_0 L$ and therefore we might approximate:

$$h_{II}(t) = -\frac{R}{L}e^{-(R+R_0)t/2L}\sin\left\{\omega_0 t + \frac{\pi}{2}\right\} \quad (24)$$

$$= -\frac{R}{L}e^{-(R+R_0)t/2L}\cdot\cos\omega_0 t \text{ for } t > 0 \quad (25)$$

$h_{II}(t)$ is zero for $t < 0$

In order to obtain the response of the network to a bandlimited (f_c) impulse of unit maximum amplitude we now have to convolve the impulse response $h(t)$ with the bandlimited impulse $f_1(t)$. Since:

$$f_1(t) = \frac{\sin\omega_c t}{\omega_c t} \quad (26)$$

the total response of the network to a bandlimited impulse becomes:

$$f(t) = \int_{\tau=-\infty}^{t}\left[h_I(t-\tau) + h_{II}(t-\tau)\right]\frac{\sin\omega_c\tau}{\omega_c\tau}d\tau. \quad (27)$$

Since $h_I(t)$ is the unit impulse function:

$$f(t) = \frac{\sin\omega_c t}{\omega_c t}$$

$$- \frac{R}{L}\int_{\tau=-\infty}^{t}\left[e^{-\alpha(t-\tau)}\cos\omega_0(t-\tau)\cdot\frac{\sin\omega_c t}{\omega_c\tau}\right]d\tau \quad (28)$$

where

$$\alpha = \frac{R + R_0}{2L}.$$

The first term is the result which would be obtained without the dip in the passband, the second term is the effect (E) of the dip.

E can be written as

$$E = \frac{R}{2L}\left\{\int_{-\infty}^{t}\frac{\sin\left[(\omega_c - \omega_0)\tau + \omega_0 t\right]}{\omega_c\tau}e^{+\alpha(\tau-t)}d\tau\right.$$

$$\left. + \int_{-\infty}^{t}\frac{\sin\left[(\omega_c + \omega_0)\tau - \omega_0 t\right]}{\omega_c\tau}e^{+\alpha(\tau-t)}d\tau\right\} \quad (29)$$

$$(\tau - t) \leq 0$$

$$\alpha \ll (\omega_c - \omega_0).$$

In the region in which the integrand is significantly different from zero, *i.e.*, for small τ, the exponential factor $e^{+\alpha(t-t)}$ approaches $e^{-\alpha t}$ and therefore

$$E \approx \frac{R}{2L}e^{-\alpha t}\left[\int_{-\infty}^{t}\frac{\sin\left[(\omega_c - \omega_0)\tau + \omega_0 t\right]}{\omega_c\tau}d\tau\right.$$

$$\left. + \int_{-\infty}^{t}\frac{\sin\left[(\omega_c + \omega_0)\tau - \omega_0 t\right]}{\omega_c\tau}d\tau\right]. \quad (30)$$

If we write

$$\omega_c - \omega_0 = \omega_D$$

$$\omega_c + \omega_0 = \omega_S$$

we obtain

$$E \approx \frac{R}{2\omega_c L}e^{-\alpha t}\left\{\cos\omega_0 t\left[\pi + Si(\omega_S t) + Si(\omega_D t)\right]\right.$$

$$\left. + \sin\omega_0 t\left[Ci(\omega_S t) - Ci(\omega_D t)\right]\right\}. \quad (31)$$

The expression

$$\left[\pi + Si(\omega_S t) + Si(\omega_D t)\right]$$

has a maximum value near 2π (actually it can under certain conditions exceed this value by 9 per cent). The expression $\left[Ci(\omega_S t) - Ci(\omega_D t)\right]$ has its maximum at $t = 0$ where its value is $\ln\omega_S/\omega_D$. If $\omega_c/\omega_0 \geqq 1.02$, *i.e.* if the notch in the amplitude response is not too close to the cutoff of the impulse function, the contribution of the Ci terms to the maximum value are small and we can say that

$$E_{max} \approx \pi\frac{R}{\omega_c L}. \quad (32)$$

It now remains to be shown how the circuit constants, R and L, are related to the properties of the transfer function, a and δf_0 [see Fig. 7(b)]. It is

$$(1 - a) = \frac{R_0}{R + R_0} \quad (33)$$

or

$$R_0 = \frac{1 - a}{a} \quad (34)$$

and

$$|H_{(\omega)}|_{f=f_0\pm(\delta f_0/2)} = \left(1 - \frac{a}{2}\right). \quad (35)$$

This can be written as

$$\frac{(1 - \omega^2 LC)^2 + \omega^2 C^2 R_0{}^2}{(1 - \omega^2 LC)^2 + \omega^2 C^2(R + R_0)^2} = \left(1 - \frac{a}{2}\right)^2 \quad (36)$$

From this we obtain:

$$\omega_{1,2} = \omega_0 \sqrt{\left[1 + \left(\frac{K}{\omega_0 a}\right)^2 \frac{4-3a}{8-2a}\right] \pm \frac{K}{\omega_0 a}\sqrt{\frac{4-3a}{4-a}}\sqrt{1 + \left(\frac{K}{\omega_0 a}\right)^2 \cdot \frac{4-3a}{2a-8}\frac{1}{2}}} \tag{37a}$$

where

$$K = \frac{R}{L}$$

Assuming

$$\frac{R}{a\omega_0 L} \ll 1$$

we obtain:

$$\omega_{1,2} = \omega_0 \left\{1 \pm \frac{1}{2}\frac{R}{L}\frac{1}{\omega_0 a}\sqrt{\frac{4-3a}{4-a}}\right\} \tag{37b}$$

or

$$\delta\omega_0 = \frac{R}{La}\sqrt{\frac{4-3a}{4-a}} \tag{38}$$

and therefore

$$E_{\max} \approx \pi \frac{\delta\omega_0 a}{\omega_c}\sqrt{\frac{4-a}{4-3a}}. \tag{39}$$

BIBLIOGRAPHY

[1] Goldman, S., *Information Theory*. New York, Prentice-Hall, Inc., 1953, p. 73.
[2] Shannon, C., "Communications in the Presence of Noise." PROCEEDINGS OF THE IRE, vol. 37, no. 1 (January, 1949).
[3] Macdairmid, I. F., "A Testing Pulse for Television Links." PROCEEDINGS OF THE IEE, Part III A (1952).
[4] Kennedy, R. C., "Sine-Squared Pulse Test Color TV Systems." *Electronics*, vol. 27 (December, 1954).
[5] Kell, R. D., Bedford, A. V., and Kozanowski, H. N., "A Portable High-Frequency Square-Wave Oscillograph for Television." PROCEEDINGS OF THE IRE, Vol. 30, No. 10 (October, 1942).
[6] Fisher, J. F., "TV Receiver Transient Analysis," *Electronics*, Vol. 23 (September, 1950).
[7] Standards on Television, "Methods of Measurement of Time of Rise, Pulse Width and Pulse Timing of Video Pulses in Television." PROCEEDINGS OF THE IRE, Vol. 38 (November, 1950).
[8] DiToro, M. J., "Phase and Amplitude Distortion in Linear Networks." PROCEEDINGS OF THE IRE, Vol. 36'(January, 1948).
[9] Valley and Wallman, *Vacuum Tube Amplifiers*, Radiation Laboratory Series No. 18, New York, McGraw-Hill, 1948, pp. 66, 74, 76, 82, 91, 275, 280, 281, 283.
[10] Chance, Hughes, MacNichol, Sayer, Williams, *Waveforms*, Radiation Laboratory Series No. 19, New York, McGraw-Hill, 1949, pp. 734-741.
[11] Kell, R. D., and Fredendall, G. L., "Standardization of the Transient Response of Television Transmitters." *RCA Review*, Vol. 10, No. 1 (March, 1949).
[12] Valley and Wallman, *Vacuum Tube Amplifiers*, Radiation Laboratory Series No. 18, New York, McGraw-Hill, 1948, pp. 77, 78.
[13] Bedford A. V., and Fredendall, G. L., "Analysis, Synthesis and Evaluation of the Transient Response of Television Apparatus," PROCEEDINGS OF THE IRE, Vol. 30, No. 10 (October, 1942).
[14] Samulon, H. A., "Spectrum Analysis of Transient Response Curves." PROCEEDINGS OF THE IRE, Vol. 39, No. 2 (February, 1951).
[15] Nyquist, H., "Telegraph Transmission Theory." *Transactions of the AIEE*, Vol. 47 (April, 1928).
[16] Hollywood, J. M., "Single-Sideband Filter Theory with Television Applications." PROCEEDINGS OF THE IRE, Vol. 27 (July, 1939).
[17] Goldman, S., "Television Detail and Selective-Sideband Transmission," PROCEEDINGS OF THE IRE, Vol. 27 (November, 1939).
[18] Nyquist, H., and Pfleger, K. W., "Effect of the Quadrature Component in Single Sideband Transmission." *Bell System Technical Journal*, Vol. 19 (January, 1940).
[19] Kell, R. D., and Fredendall, G. L., "Selective Side-Band Transmission in Television." *RCA Review*, Vol. 4 (April, 1940).
[20] Kallmann, H. E., and Spencer, R. E., "Transient Response of Single-Sideband Systems." PROCEEDINGS OF THE IRE, Vol. 28 (December, 1940).
[21] Kerr, J. S. S., "Transient Response in a Color Carrier Channel with Vestigial Side Band Transmission," CONVENTION RECORD IRE, Part 4, 1953 National Convention.

The Design of High-Power Traveling-Wave Tubes*

M. CHODOROW† AND E. J. NALOS‡

Summary—This paper discusses the problems involved in designing traveling-wave tubes in the range of pulsed powers of the order of a megawatt. Suitable circuits are described, together with their advantages and limitations. In general, the all-metal structures described are capable of dissipating high average powers, have good impedances at the required voltages (100-kv range), but at a sacrifice in bandwidth. Nevertheless, this class of traveling-wave tube is useful where bandwidths of 10 to 20 per cent, not obtainable from klystrons of equivalent power outputs, are of interest. The problems of tube construction and tube design are discussed. Results of tests on an experimental model tube are described, showing good agreement with available theory. A gain uniformity of 3 db over a 9 per cent bandwidth, with power outputs of 300 kw pulsed have been obtained using attenuators of nonoptimum design. Better performance should be obtainable with further improvements in beam focusing and coupler design. Higher power levels with same efficiency should be possible, by designing the tube to operate at higher potentials.

INTRODUCTION

THE MAIN objective of this program was to investigate some of the fundamental problems involved in the design and operation of pulsed traveling-wave tubes, operating at power levels of the order of a megawatt. Assuming reasonable perveances and efficiencies, the voltage range corresponding to this power level falls in the vicinity of 50 to 100 kv. In this range of operating voltages and powers, a whole new set of problems arise as compared to conventional low-voltage tubes. First, there is the problem as to a suitable slow-wave circuit for such powers. Secondly, it is necessary to evolve techniques for measuring the impedance and propagation properties of such circuits, and to design couplers to match these circuits to conventional transmission lines over a broad-band. There is also the matter of attenuation for non-helix circuits. This involves the problem of suitable location as well as distribution of the attenuator inside the tube to get optimum behavior, and also the choice of suitable attenuating materials for the high power levels of interest. In this paper, we shall describe our attempts to solve these various problems and give some experimental results. The tube upon which these experiments were done was designed to operate in the 3,000-mc range.

CHOICE OF CIRCUIT

For conventional traveling-wave tubes for low voltages, say, up to about 5 to 10 kv, the helix is an excellent circuit having both good impedance and bandwidth. As the voltage is increased, however, the required helix becomes a more open structure and a large fraction of the energy is stored in space harmonics not useful for amplifier interaction.[1] This results in a reduced impedance and increased tendency to oscillate as a backward-wave oscillator. More complex circuits, such as crosswound helices or multifilar helices, offer possibilities of avoiding these difficulties at higher voltages, but these, as well as the single helix, are subject to severe power-handling limitations which make any of these structures unsuitable for high-power application. For this reason, circuits having all-metal envelopes with short metallic paths from the interaction region to the exterior are desirable for powers in the megawatt range.

One class of such structures which has been successfully used as slow-wave circuits for linear accelerators consists of periodically-loaded waveguides. These structures can have impedances much higher than the helix at high voltage, although at a sacrifice in bandwidth.[2] However, bandwidths much less than those obtainable with the helix are still of interest, and for a range of bandwidths of 10 to 20 per cent, loaded waveguides are

feasible. Two basic types of periodic structures were investigated. These are shown in Fig. 1. In Fig. 1(a) is shown the structure which we shall call the fundamental structure. Adjacent sections are coupled capacitatively (electrostatically) through the hole in the axis and analysis indicates that the phase shift per section is positive as shown in Fig. 2. In Fig. 1(b), the space-harmonic structure is shown, in which adjacent sections are coupled inductively (magnetically) through the side slots. For this circuit the phase shift per section is negative, as shown in Fig. 2. In both cases the direction of energy propagation, or the group velocity, is assumed from left to right and then positive or negative refers to a phase velocity which is in the same or opposite direction to the group velocity. For the structure shown in Fig. 1(a) it is possible to pick an electron velocity such that the electrons will synchronize with the fundamental component of the wave, whereas for the structure shown in Fig. 1(b) the fundamental component has a negative phase velocity and therefore it is necessary to synchronize with one of the space harmonics.
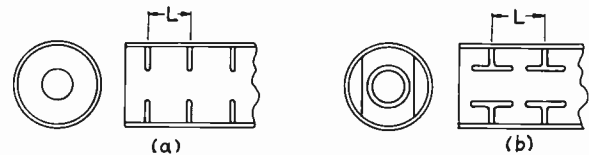
Fig. 1(a)—Periodically-loaded structures: fundamental. (b) Periodically-loaded structures: space-harmonic.
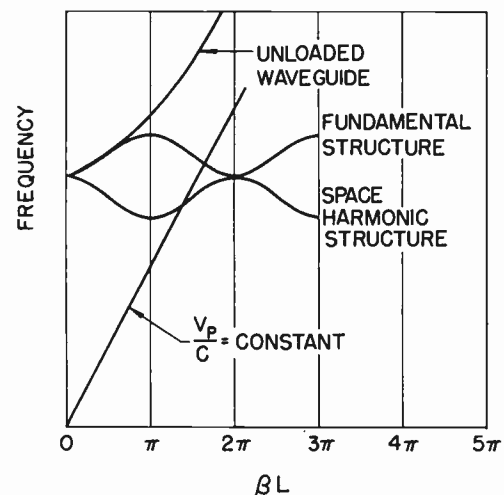
Fig. 2—Brillouin diagram.

CIRCUIT PARAMETERS

For both structures [Figs. 1(a) and 1(b)] the values of all the relevant parameters can best be obtained by a series of cold measurements which we shall describe later in this section. However, a great deal of qualitative understanding of these circuits can be obtained by the use of suitable equivalent circuit representations. Thus, for the fundamental structure we can represent

[1] P. K. Tien, "Traveling-wave tube helix impedance," PROC. IRE, vol. 41, p. 1917; November, 1953.
[2] J. R. Pierce, "Traveling-Wave Tubes," D. Van Nostrand Co., New York, N. Y., p. 92; 1950.

the separate cavities as resonant lumped constant circuits, such as shown in Fig. 3(a) with capacitive coupling between them. By a series of ordinary circuit transformations it can be converted into Fig. 3(c). It is to be noted that in making this conversion, every other LC circuit has to be inverted so that the frequency at which one would get zero phase shift in the original propagating structure; *i.e.*, fields in each cavity pointing in the same direction, would correspond to π-phase shift in the final equivalent circuit because of the inversion.
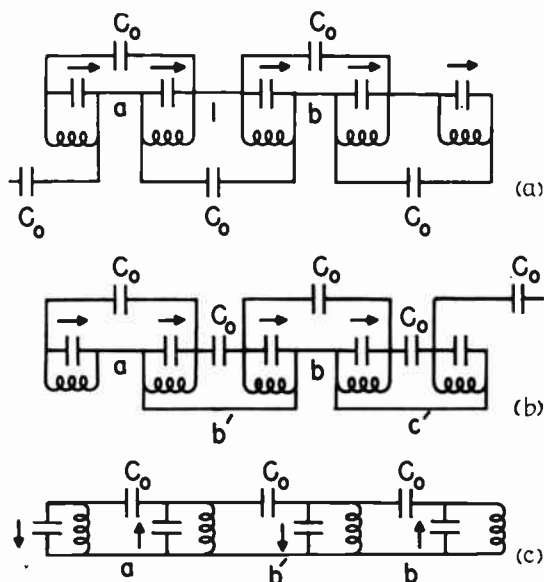
Fig. 3—Equivalent circuit of fundamental structure.
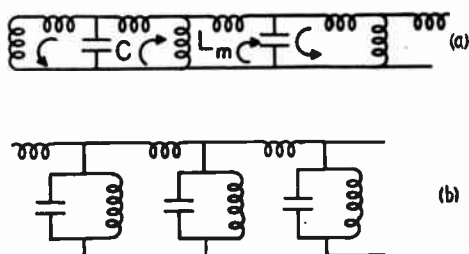
Fig. 4—Equivalent circuit of space-harmonic structure.

Similarly, the frequency at which the voltage pattern corresponds to π-phase shift per section in the original structure will correspond to zero-phase shift in the final circuit. Therefore, whatever the dispersion characteristic of the filter network shown in Fig. 3(c), it must be remembered that one must add π to this to get the appropriate characteristic for the original structure. An analysis by conventional filter theory of this final equivalent circuit gives us the dispersion characteristic for the original structure shown in Fig. 2. Similarly, for the structure in Fig. 1(b), separate cavities can also be represented as resonant LC circuits, which are now coupled inductively (Fig. 4). Resulting propagation char-

acteristic for structure in Fig. 1(b) is shown in Fig. 2. In both cases the bandwidth is determined by the magnitude of the coupling impedance; in Fig. 1(a), the coupling capacity and in Fig. 1(b), the coupling inductance. In both cases, this coupling impedance (and the corresponding bandwidths) will be larger, the larger the size of the coupling aperture. It is possible to arrive at the same pass-band characteristics starting from other descriptions of the structures. For example, one can obtain the properties of the structures in Figs. 1(a) and 1(b) by considering an unloaded cylindrical waveguide in the TM_{01} mode which is then loaded periodically by suitable susceptances. The susceptances will have the opposite sign for the two types of structures shown. This alternative approach gives additional insight into the properties of the structure, but does not necessarily lend itself to calculations of quantitative values particularly for large or odd-shaped apertures, or slightly re-entrant perturbations such as actually used in the tube we will describe.

Both structures in Figs. 1(a) and 1(b) have the common property that they are periodic and satisfy Floquet's theorem; *i.e.*, the field can be written as

$$E_s = \sum_n A_n F_n(x, y) e^{i\beta_n z}$$

$$\beta_n = \beta_0 + \frac{2\pi n}{L} \tag{1}$$

where L is the periodic spacing and β_0 is propagating constant of the fundamental component. The various terms in this summation are the various space harmonics of a given mode and the electron beam can synchronize with any one space harmonic, which of course requires that the space harmonic have a positive-phase velocity. In addition, for a traveling-wave tube the group velocity must be in the same direction as the electron velocity. The existence of these space harmonics are indicated by the multiple branches of ω-β curve for both structures in Figs. 1(a) and 1(b). For the structure in Fig. 1(a), of course, one can synchronize with the fundamental component, and for the structure in Fig. 1(b) one must synchronize with the first space harmonic since the fundamental has a negative-phase velocity. The relevant parameters that one must evaluate in order to calculate the performance for any of these structures are: the dispersion; *i.e.*, the variation of phase velocity with frequency (and, of course, the cold pass band, since this will determine the possible operating pass band of the tube); and the rf impedance of the circuit, defined by Pierce as

$$K = \frac{E_n^2}{2\beta_n^2 P} = \frac{E_n^2}{2\beta_n^2 W \nu_g} \tag{2}$$

where W is the energy stored per unit length of the structure, ν_g the group velocity, and E_n the amplitude of the particular space harmonic with which synchronism occurs.

To determine the values of these numbers by cold measurements one proceeds as follows. One converts a portion of a propagating circuit, such as shown in Figs. 1(a) and 1(b), into a resonant circuit of length NL by putting shorting surfaces across the symmetry planes of the end cavities. This resonator then will contain $(N-1)$ full sections and a half-section at each end. Under these conditions, with the shorts in the symmetry planes of cavities, one obtains $(N+1)$ resonances[3] corresponding to phase shifts per section, given by

$$\beta_0 L = \frac{M}{N} \qquad (\pi M = 0, \quad 1, \cdots N.) \quad (3)$$

The corresponding field configurations are given by

$$E_z = \sum_n A_n F_n \cos \left(\beta_0 + \frac{2\pi n}{L} \right) z$$

$$= \sum_n A_n F_n \cos \frac{\pi}{NL} (M + 2nN)z. \quad (4)$$

The cosine function is a consequence of the fact that the transverse E field must be zero at the end planes, and since div $E = 0, \partial E_z/\partial z$ is also zero over the end plane. To fulfill this requirement, E_z must be a sum of cosines. Taking into account the allowed values of β_0, this equation for E_z is seen to be an even Fourier series of period NL.

If one measures the resonant frequencies of this composite cavity one gets $(N+1)$ points on the dispersion curve; *i.e.*, one gets the values of ω corresponding to the allowed values of β_0. The number of sections thus determines the number of points on the curve. This provides one piece of information, namely, the phase velocity. The slope of the curve; *i.e.*, $d\omega/d\beta$ provides the group velocity. The remaining quantity to be determined is E^2/W. To determine this, one must resort to perturbation techniques. These can be applied in various ways.[4] In general, one uses a metallic or dielectric bead which is moved through the resonator. The frequency perturbation produced by the bead of volume ΔV will be given by an expression of the form

$$\Delta f = \frac{P_1 E_z^2 + P_2 E_r^2 + \cdots M_1 H_z^2 + \cdots}{W NL} \Delta V$$

where the coefficients will depend on size and shape of the bead, as well as the orientation relative to the fields. In particular, for the case of interest to us, the bead is moved along the axis where the only field is E_z and

the frequency change is thus proportional to E_z^2. If one knows the theoretical value for the proportionality constant or has calibrated the bead in some other way, one can determine the value of E_z^2/W along the axis. Of course, this does not give us the answer which we are looking for, namely, E_n^2/W; *i.e.*, the amplitude of a particular space harmonic. However, as stated previously, the total field is really a Fourier sum of the various space harmonics; therefore, having determined the field variation along the axis, one can, by a graphical Fourier analysis, determine the amplitude of any particular space harmonic. By these measurements one can get all the desired parameters of the structures. Actually, one can get a reasonably accurate idea as to the *relative* value of the space harmonics from an analysis which is given in Pierce,[5] which can also be used to determine the optimum gap dimensions. Nevertheless, the bead measurements are still necessary to obtain the absolute value of E_n^2/W.

Tube Design

As a rough objective, the aim was to design a tube with about 30-db gain and about 10 per cent bandwidth, between 3-db points. The frequency of 3,000 mc was picked as a convenient range in which to work, and with these objectives a series of cold tests were made on the two types of structures previously described to see if they were satisfactory.

Fundamental Structure

It is obvious that if one wishes to get something like a 10 per cent bandwidth between 3-db points, this will require synchronization or approximate synchronization over at least this range of frequencies. For the fundamental structure, the phase velocity varies from infinity at the low-frequency cutoff to some finite value at the high-frequency cutoff. Even though space-charge effects and large C effects will permit one to get a fairly constant gain over a region somewhat greater than that determined purely by synchronism, it is quite obvious that one must aim at a cold pass-band of the order of 20 per cent, since a considerable portion of the pass-band near the low-frequency cutoff is not usable. With this objective we explored a series of cold structures of the type shown in Fig. 1(a). For thin disks, the low-frequency cutoff is determined by the cutoff of the waveguide for the TM$_{01}$ mode, given by $\lambda = 2.61a$. The high-frequency cutoff is determined by the amount of coupling; *i.e.*, the capacitative coupling between adjacent cavities. To get some idea as to how this coupling will depend upon the size of the aperture, one can use the small coupling iris theory due to Bethe.[6] If one

[3] For certain symmetries, including those circuits in which the periodicity involves a translation as well as a rotation by π, as for example an interdigital line, the symmetry planes for the shorting surfaces must be so located that one gets only N resonances for a length NL corresponding to $M = 0, 1, N-1$.

[4] W. W. Hansen and R. F. Post, "On the measurement of cavity impedance," *Jour. Appl. Phys.*, vol. 10, p. 1059; 1948.
   E. J. Nalos, "Measurement of circuit impedance of periodically loaded structures by frequency perturbations," *Proc. IRE*, vol. 42, p. 1508; October, 1954.

[5] J. R. Pierce, "Traveling-Wave Tubes," D. Van Nostrand Co., New York, N. Y., p. 72; 1950.

[6] H. A. Bethe, "Theory of diffraction by small holes," *Phys. Rev.*, vol. 66, p. 163; 1944.

makes a resonator consisting of two half-sections ($N=1$), the resonant frequencies correspond to zero and π-phase shifts of the propagating circuit. The Bethe theory predicts that if the coupling aperture is in the region of strong electric field, then one frequency (zero-phase shift) will be at the resonant frequency of the cavity, and the π-phase shift (the perturbed frequency) will be at a higher frequency, the difference being proportional to the cube of the hole radius for a circular aperture. The experiments verified the Bethe theory quite well [see Fig. 5(a)]. Figs. 5(b) and 5(c) show the effect

Fig. 5—Bandwidth as a function of geometry: (a) hole size; disk thickness = 3/32 inch, disk spacing = 0.323 inch; (b) disk spacing; disk thickness = 3/32 inch; hole diameter = 1.18 inches; (c) disk thickness; hole diameter = 1.18 inches; disk spacing = 0.323 inch.

of disk spacing and disk thickness on the bandwidth. Unfortunately, numerical values were such that to get the desired 20 per cent total pass-band bandwidth, a coupling hole diameter of about 3.5 cm was required. Since the electron beam also must pass through this hole, certain criteria having to do with the interaction of the electrons and the field must also be fulfilled. There is evidence from various sources[7] that for opti-

mum efficiency, the normalized beam radius (γa) should not be greater than unity. With the numbers we have quoted, assuming 100-kv operation, the above hole size would correspond to (γb) of about 2–3. Since the interaction with the field component varies across the cross section of the hole as $I_0(\gamma r)$, this would mean that the field at the beam would be much smaller than at the edge of the hole and that the impedance correspondingly would be lowered. In addition to this, as one varies the frequency through the pass-band, γb and γa would vary greatly as would the effective value of the gain parameter C. These lead to the conclusion that a hole of the size quoted would not be desirable.

Some structures were tested to try to overcome this defect. All aimed at providing a large coupling aperture and still having the beam coupled to the strong part of the field (see Fig. 6). Another alternative, of course,

Fig. 6—Methods of overcoming beam-coupling problems: (a) off-center holes, centers staggered by variable angle θ; (b) "grid-type" structure.

would be to use a hollow beam which grazes the edge of the hole and therefore has strong and uniform interaction with the field. It should be pointed out that for a smaller bandwidth than we have quoted, it is possible to have a smaller coupling aperture and avoid the disadvantages just quoted. Under these circumstances (for a narrow bandwidth) the impedance of the simple disk-loaded circuit is very good, giving values of C of the order of 0.25 for typical operation.[8] Calculated performance characteristics of the fundamental structure shown in Fig. 6(b) is given in Fig. 7. These structures also offer interesting possibilities as high-power backward-wave oscillators operating on a space harmonic.

[7] P. K. Tien, L. R. Walker, and V. M. Wolontis, "A large signal theory of traveling-wave amplifiers," PROC. IRE, vol. 43, p. 260; March, 1955.

[8] Since this work was completed, M. Chodorow and R. A. Craig (IRE Tube Conference, Maine, June, 1954) have devised a wide-band fundamental circuit with a small central aperture by using negative-mutual inductive coupling.
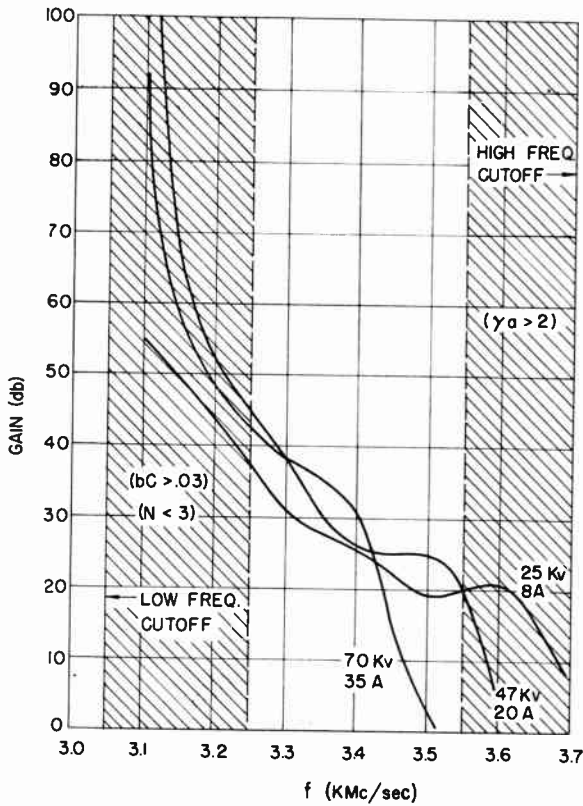
Fig. 7—Calculated performance of fundamental structure: perveance $=2\times10^{-6}$; beam diameter$=2$ ccm; Hole diameter$=3$ cm; tube length$=18$ cm.

values of bandwidth refer to the case of the bars lined up parallel or at right angles to one another. The structure shown in Fig. 8(c) was adopted because of the best compromise between bandwidth and impedance. For this structure one uses the space harmonic such that the center of the pass-band corresponds to $\beta_n L = 3\pi/2$ or an electron transit time from cavity to cavity of about $\frac{3}{4}$ of a cycle. If one used very thin disks, this would also correspond to about $\frac{3}{4}$ of a cycle transit time across the gap and the interaction with the field would not be good since the phase of the field would change while the electron was in transit across the gap. Otherwise stated, one should apportion the total distance from cavity to cavity between drift tube and gap in such a way as to optimize E_n^2/W. In terms of gap-coupling theory, making the gaps very small gives better interaction with the field; but for any given voltage across the gap, there would be an increase in energy stored as compared to a wider gap. This problem has been treated by Pierce[4] with the result that the optimum transit angle across the gap is about $3\pi/4$. His calculation is based on the assumption that the energy stored per cavity can be calculated by treating the gap as a simple planar capacity. Presumably, one should optimize the gap spacing by actually going through a series of measurements for different ratios of gap spacing to total periodic spacing, since the nonplanar gaps may give somewhat different energy storage than that used by Pierce.

% BANDWIDTH 0°	23%
% BANDWIDTH 90°	30%
MIDBAND $E^2/\beta^2 P$	11.4
REL. GAIN BANDWIDTH	5.1

(a)

% BANDWIDTH 0°	33%
% BANDWIDTH 90°	37%
MIDBAND $E^2/\beta^2 P$	4.5
REL. GAIN BANDWIDTH	5.4

(b)

% BANDWIDTH 0°	16.5%
% BANDWIDTH 90°	19%
MIDBAND $E^2/\beta^2 P$	24.2
REL. GAIN BANDWIDTH	4.8

(c)
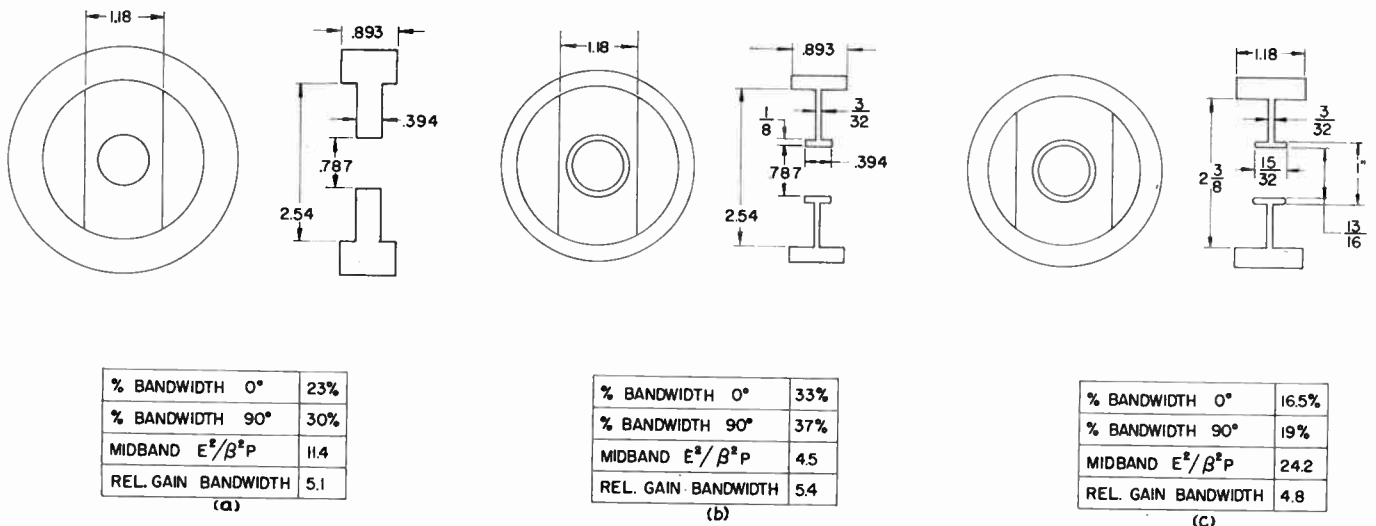
Fig. 8—Some possible space-harmonic structures: (a) thick disks; (b) thin disks; (c) adopted structure.

Space-Harmonic Structure

In order to avoid the disadvantage of having the coupling aperture and the beam aperture satisfy two conflicting requirements, attention was directed to the space-harmonic structure such as shown in Fig. 1(b). In this structure, the beam aperture and the coupling aperture are separate and the bandwidth can be adjusted by picking a suitable length of the coupling slot. In Fig. 8 are shown three geometries which were considered with their respective bandwidths. The two

However, since both E_n^2 and W vary in the same direction with gap spacing, it is probable that their ratio has a broad maximum in the neighborhood of the optimum value and it is probably not of great value to try to find this optimum precisely. For this reason we chose the value determined by Pierce's calculation.

It might be pointed out that there are various possible modifications of the circuit we used, including one in which the drift tubes are mounted at the ends of posts which go alternately to the top and bottom of a rec-

tangular or circular waveguide. In this case one can consider the propagating mode as a perturbation of a TE waveguide mode with the transverse E field being concentrated and distorted into an axial E field in the region between the drift tubes. However, for the beam voltages of interest, the drift tube diameters were of the order of $\frac{3}{4}$ wavelength ($\gamma a = 1$ at $v/c = 0.5$ corresponds to a diameter of about 0.2λ). Under these circumstances, using drift tubes at the ends of posts would require the post to be quite short resulting in having a nonuniform field across the diameter of the gap, due to the fact that one edge of the gap would be much closer to the waveguide wall than the other. In the structure shown in Fig. 8(b), the drift tubes are at the center of the bars which have a symmetrical radial field distribution (corresponding to a distorted half sine wave or Bessel function) and the distribution of fields around the drift tube is thus symmetrical.
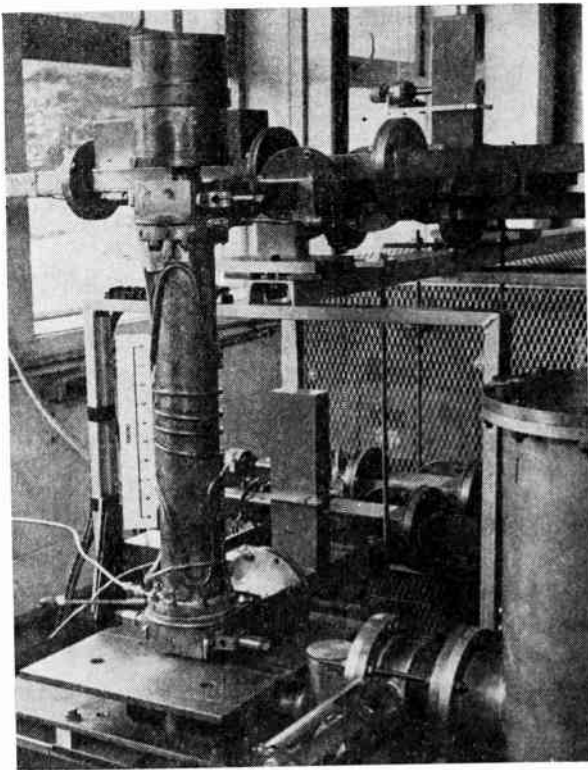
Fig. 9—Experimental model tube.

TUBE CONSTRUCTION

General

The dimensions of the structure were chosen for operation between 2.7 and 3.1 kmc and the disk spacing was selected for a midband synchronous voltage of about 60 kv. A photograph of the tube is shown in Fig. 9. This particular model was assembled by stacking the disks (separately machined and slightly oversize) on a mandrel, immersing them in liquid air, inserting the mandrel into an accurately machined cylinder while cold, and allowing the disks to expand into the cylinder wall. This shrinking technique has been successfully used on the assembly of linear accelerator sections. To ensure good rf contacts, the OD of the disks and ID of the cylinder were silver-plated, and the entire assembly heated to silver-melting temperature in a hydrogen furnace. This worked successfully, but an easier technique, that of electroforming the cylinder on top of the disks (which are spaced by aluminum spacers and etched out later), avoids the difficult problem of making a long uniform pipe. This technique has been successfully used on the Stanford Medical Accelerator and worked well on a later model of the space-harmonic tube. The cathode assembly is shown in Fig. 10. This cathode was designed for a 1-megw klystron amplifier and proved satisfactory for the traveling-wave tube.
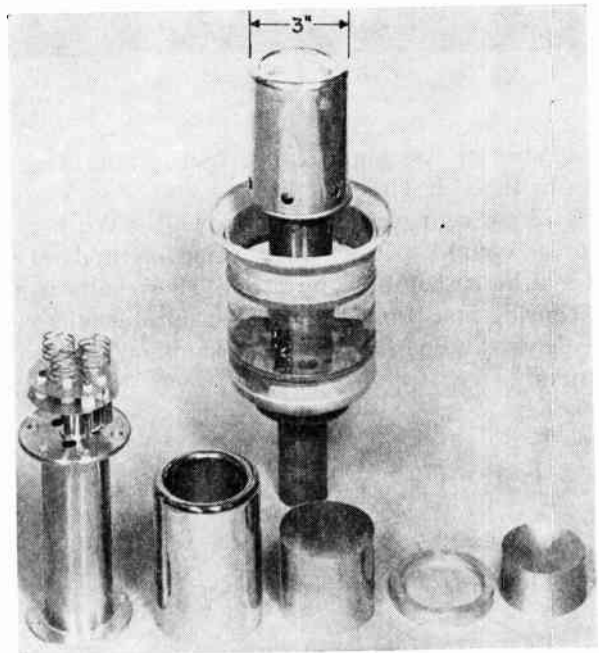
Fig. 10—Cathode assembly.

The perveance was made variable by means of bellows between the high-voltage seal and anode. Changing the perveance in this manner also changes the beam radius. An insulated beam collector was provided. Typical beam transmission of 80 per cent was obtained but frequently the best rf performance occurred at a lower beam transmission of about 65 to 70 per cent. It is possible though, that a large fraction of the loss occurred in a region between the output coupler and the collector. The magnetic field required to obtain best transmission was of the order of 1.5 times the Brillouin flow field using the beam diameter as obtained from other measurements. The complete setup, including the modulator, is shown in Fig. 11.

Coupler Design

The problem of coupling into the periodic structure over a broad band is not easily susceptible to an analytic approach and only qualitative guides were used in the design. The detailed geometry has to be deter-
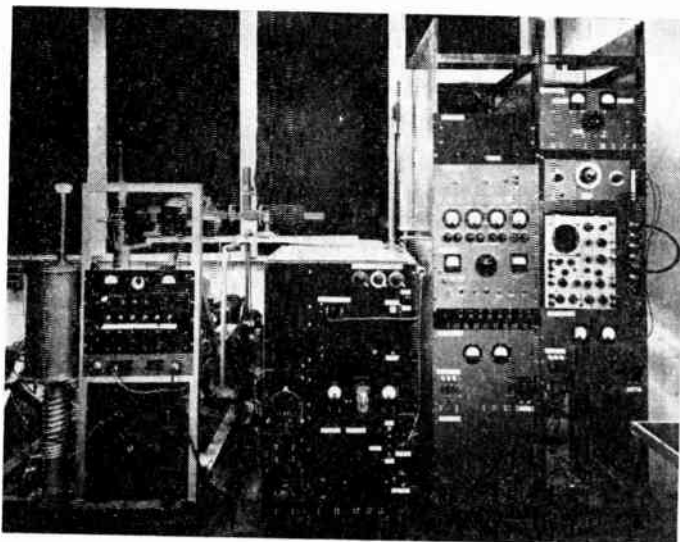
Fig. 11—Setup for tube testing.

mined more or less empirically. A workable design is shown in Fig. 12. This coupler has a vswr of less than 2 over 75 per cent of the cold bandwidth. Work to improve the coupler performance, using methods of network synthesis, has been initiated. The results to date show considerable promise, provided suitable microwave equivalents can be found for some simple compensating networks.
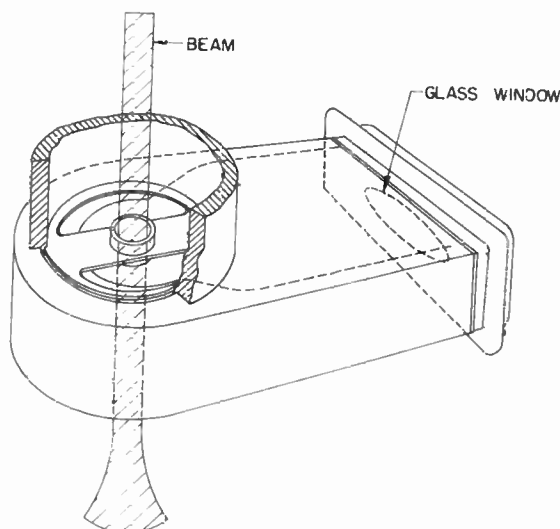
Fig. 12—Broadband coupler.

Attenuation

The general effects of attenuators on TW tube performance are extremely complex and in general not too well understood. We have followed the general outlines given by Cutler and Brangaccio[9] by locating the

[9] C. C. Cutler and D. J. Brangaccio, "Factors affecting traveling-wave tube power capacity," TRANS. IRE, vol. ED-3, pp. 9–24; June, 1953.

attenuator in approximately the middle third of the tube. This allows the exponential wave to build up adequately ($CN = 0.3$ before attenuation is introduced) and for part of the frequency range allows adequate gain in the lossless output section of the tube. At the high-frequency end of the range this condition was not fulfilled. The amount of attenuation chosen is adequate to ensure stable operation into a matched load (including mismatches in couplers) but not stable for an arbitrary load. It is possible that this could be taken care of by ferrite isolators in the output line.

The physical location of the attenuation is shown in Fig. 13. A separate vacuum channel is provided for the attenuator, making it possible to vary its position as well as explore various types of attenuating materials.
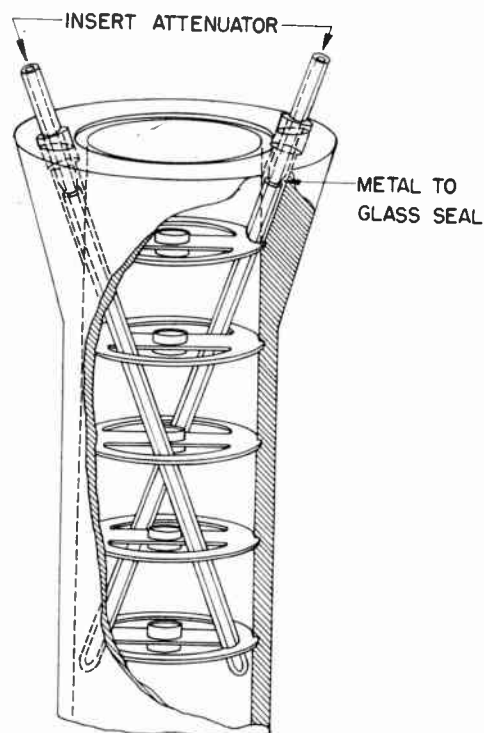
Fig. 13—Method of inserting attenuation into traveling-wave tube.

Water, aquadag-coated rods, and carbonized ceramics were some of the materials which were found successful. The channel is purposely introduced at an angle to ensure that the attenuator would enter the fringing E field of the gap in a tapered fashion and thus be reasonably well matched. An alternative approach offering promise for high power dissipation is that of depositing high-loss metals in sufficient thickness (several skin depths) on the wall of the tube and on the disks. Iron plating has been tried but does not provide sufficient loss. Other materials are currently being tried. The fact that the material may be magnetic need not interfere with the dc focusing if the deposit is sufficiently thin.

1	2	3	4	5	6	7	8	9	10	11	12	13	14	15	16	17	18	19
Frequency kmc/s	Phase velocity v_1/C	N wavelengths (note 1)	$I_0^{2/3}(0.7\gamma b)$	V_0 at opt. gain kv experimental	I_0 (perveance 2×10^{-6}) amps	$(I_0/8V_0)^{1/3}$	C_{av} (note 2)	Plasma frequency f_p (note 3)	Reduction factor	$\dfrac{\omega_q}{\omega}$	QC (see note 4)	d (see note 5)	b_{opt} (QC, $d=0.125$, C)	b from exper. value of V_0 (see note 6)	$\left(\dfrac{x_1}{1+bC}\right)_{max}$	$A(QC, d, b, C)db$	Gain db theoretical (see note 7) db	Observed gain db
2.8	0.41	10.8	1.1	69	28	0.037	0.15	Approx. constant 640 mc	$\omega_q/\omega_p=0.55$ ($b/a=0.5$)	0.15	0.25	0.37	0.8	1.0	0.65	−12	45	33
2.9	0.37	12.6	1.1	60	27	0.038	0.11			0.20	0.82	0.36	2.1	1.8	0.47	−10	26	27
3.0	0.35	13.7	1.2	53	24	0.038	0.10			0.20	1.0	0.21	2.4	2.0	0.43	− 8	24	23
3.1	0.34	14.6	1.2	49	20	0.037	0.08			0.20	1.5	0.17	3.0	2.5	0.40	− 7	19	18.5
3.2	0.34	15	1.2	48	13	0.032	0.07			0.19	1.8	0.12	3.3	2.7	0.39	− 7	15	14
3.3	0.33	16	1.3	48	13	0.033	0.07			0.23	2.7	0.13	4.0	3.3	0.32	− 6	13	11

Notes:

1. Tube length = 48 cm.
2. $C_{av} = C_{axis} I_0^{2/3}(0.7\gamma b)$
   where b = beam radius
   C_{axis} from perturbation measurements.
3. Assume $b/a = 0.5$, $a = 1$ cm.
4. $QC = (\omega_q/2C\omega)^2$.
5. Cold loss of 10 db at hf end and 20 db lf end. (Aquadag Attenuator 1.75 thick coating, 5 inches long.)
6. $u_0 = v_1(1+bC)$, u_0 known from v_0; v_1 from cold tests; *i.e.*, can get b experimental.
7. $G = .1 + \dfrac{54.5x_1CN}{1+bC}$.

Fig. 14—Calculated performance of 60-kv space-harmonic structure.

Performance of Space-Harmonic Tube

Performance at Optimum Low-Level Gain

The low-level gain, calculated on the basis of small-signal finite-C theory[10] and based on impedance measurements previously described, is given in Figs. 14 and 15 (dotted) at optimum voltage. In this calculation, the beam size is an important parameter and calculations are shown for various values of the beam radius. Experimental curves are shown for comparison (in solid) indicating good agreement. For these the beam radius was varied by adjusting the cathode bellows and the value of the radius was determined from data described below. As can be seen, the gain, especially at the high-frequency end, can be much improved if the beam diameter is but slightly increased.

The beam radius is determined experimentally by comparing, at each frequency, the difference between synchronous voltage, and voltage at optimum gain. Defining the velocity parameter b from $u_0 = v_p(1+bC)$ where u_0 = beam velocity; v_p = phase velocity of cold circuit, C = gain parameter, it has been shown[10] that at *optimum gain*, bC is given over a wide range of parameters by ω_q/ω where ω_q is the effective plasma frequency of the beam. Assuming a given beam radius, one can calculate this plasma frequency, and using the previously measured value of C, one can obtain a value of the parameter b. For a *particular* beam radius one can obtain good agreement between theory and experiment for the difference between synchronous and maximum

gain voltage over the entire passband. This radius can be taken as the correct one and was used to label the corresponding experimental gain curve. The good over-
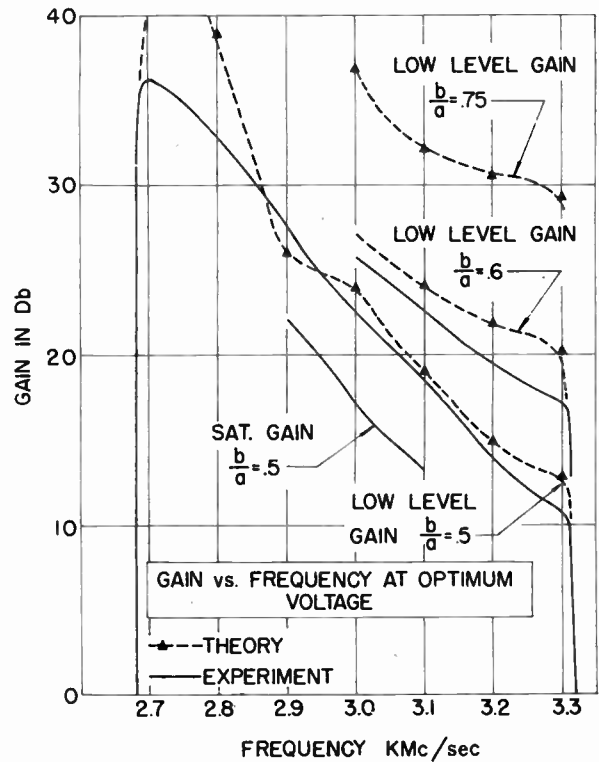
Fig. 15—Gain vs frequency at optimum voltage.

all agreement seems to indicate that small-signal assumptions have nowhere been violated, thus making the performance predictable from existing theories.

[10] C. K. Birdsall and G. R. Brewer, "Traveling-wave tube characteristics for finite values of C," Trans. IRE, vol. ED-1, pp. 1–11; August, 1954.

Performance at Constant Voltage

The performance of interest in most applications is at a constant beam voltage. Typical experimental data for this condition are shown in Fig. 16. Taking into account the reduction in gain near saturation, this data can also be reconciled with calculated performance. The results indicate that a 9 per cent bandwidth between 3-db gain points is obtainable at 65 kv, with pulsed power outputs of 300 ± 100 kw. By operating at higher voltages, a larger power output can be traded for bandwidth and vice versa. It should be added that in the design, the parameters (such as perveance, and particularly beam diameter) are not optimized to obtain the greatest uniformity of gain with frequency. It seems entirely reasonable that with a different choice of parameters, a 15 per cent bandwidth ought to be realizable.
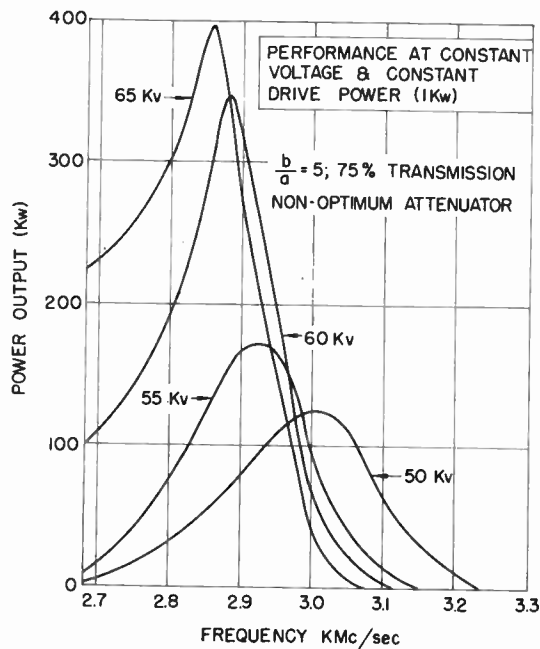
Fig. 16—Performance at constant voltage (perveance $= 2 \times 10^{-6}$).

Saturation Power and Efficiency

The saturation power and efficiency are shown in Fig. 17 for two different attenuators. The observed efficiencies are reasonably high and in agreement with predictions of Cutler.[11] Better performance at selected frequencies has been observed at higher voltages with improved attenuators. (At 2.7 kmc, saturation power of 700 kw was observed with 25 per cent efficiency.) Continuing studies on attenuator materials should result in somewhat better performance. In general, saturation gains are about 5 db below low-level optimum-gain voltages. This is in agreement with results of other

[11] Efficiency increases with C until space charge takes over, the maximum observed efficiency being about 3.5 C.

workers. The present saturation levels are limited by the amount of power available in the beam at the proper interaction voltage. If the disk spacings were increased, increasing the phase velocity and optimum voltage, there is no reason why the efficiency should decrease. Under these conditions, much higher saturation powers should be available. There is no fundamental reason to set any limit to which one can go, any more so than in klystrons, which have been made to operate successfully at 30 megw.
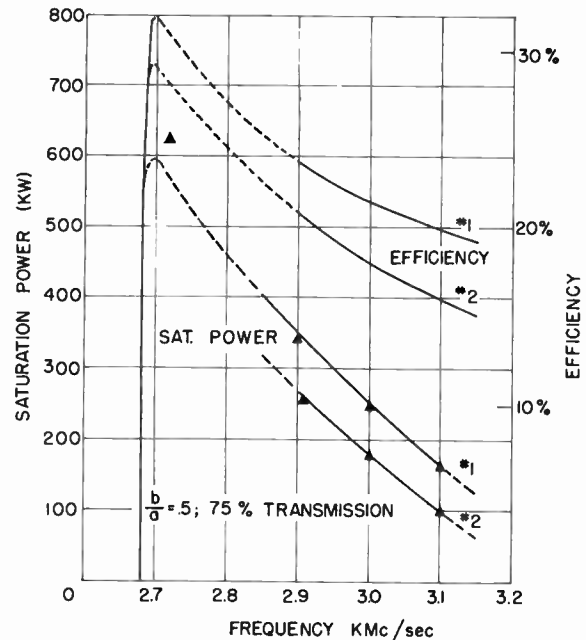
Fig. 17—Saturation power and efficiency for two attenuators: (1) uniform aquadag coating 0.002 in. thick; (2) uniform aquadag coating 0.003 in. thick.

Effect of Attenuator Characteristics

Much work remains to be done to determine the optimum attenuator configuration. In the limited tests which were made, the effect of attenuator resistivity and length on the saturation gain, power and efficiency were observed. (See Figs. 18 and 19 opposite.) As expected, the best performance is obtained with the smallest amount of attenuation required to suppress oscillation. Also larger saturation powers were observed, if the attenuator was placed somewhat closer to the input section of the tube.

Backward-Wave Oscillations

No difficulty was experienced with backward-wave oscillations. A calculation of the starting value of CN in the region from $\beta L = 2\pi$ to 3π (about 20 kv) shows that the backward-wave impedance is just barely too low for oscillations. The tube did show a slight amount of backward-wave amplification in this range. In the fundamental branch, from $\beta L = 0$ to π, voltages of about

300 kv or more are required to initiate backward-wave oscillations according to theory. These were not available and also nowhere near the operating voltages, hence no troubles were encountered in this region. Since the nature of the Brillouin diagram is such that a constant voltage line from the origin to the propagation curve only crosses the lowest pass band once, no simultaneous forward and backward-wave interaction is expected. No oscillations in higher pass bands of any type were detected, indicating that the impedance in this region is sufficiently low not to cause troubles.

Fig. 19—Effect of attenuator resistivity on performance (frequency =3 kmc, uniform aquadag attenuator). Measurements were made with constant length attenuator; resistance controlled by coating thickness.

Conclusion

Results on an experimental model of an S-band disk-loaded traveling-wave tube indicate that pulsed-power outputs in the megawatt range are entirely feasible with this class of structure, for bandwidths of 10 to 20 per cent, with reasonably good efficiency. In addition, the performance is found to agree well with existing small-signal theory. For high average power applications, more work on attenuating materials needs to be done. A better job of beam-focusing and coupler design is also needed to make tubes of this type really useful

Fig. 18—Effect of attenuator length on performance (frequency =3 kmc, attenuator: 0.001-inch thick aquadag).

Progress in the Development of Post-Acceleration and Electrostatic Deflection*

KURT SCHLESINGER†, FELLOW, IRE

Summary—Electrostatic deflection from a common center is possible by the use of electrostatic yokes, or Deflectrons. These consist of a 4-terminal pattern, printed on the inside of glass cylinders or cones. An analysis of the pattern geometry is presented which gives simple expressions for deflection factor of electrostatic yokes.

The theory also accounts for a small residual noncircularity of scan, and gives clues as to its correction.

Equipment to test tube performance is described, including ultra-violet mapping and electronic detection of the axis.

The most suitable type of post-accelerator for use with Deflectrons employs a long drift space, bounded by a metallic mask, and confines the high gradient to a narrow region close to the screen.

It is shown that this mask intensifier suffers from secondary emission. This effect can be effectively suppressed by an insulating coating of the first surface of the mask, while connecting the support metal to a lower potential than the drift space. The resulting double layer of charges prevents the escape of secondaries towards the screen. This *barrier-mask* intensifier permits post-acceleration ratios of 10 to 1 without loss of deflection.

INTRODUCTION

CONSIDERING the continued improvement of our technique of magnetic deflection, progress in the development of electrostatic deflection appears slow by comparison. It appears that the electrostatic approach is up against two major difficulties:

1) High deflection voltage demand.
2) Relatively high deflection aberrations.

The voltage demand is in direct proportion to beam voltage, and increases with the square of the tangent of the sweep half-angle. It equals anode potential at a design-angle of 54°, doubles it at 72°. This fact, plus severe problems of insulation, have precluded the use of electrostatic deflection for "stiff" beams at the high ultor voltages now in use (15–30 kv).

Deflection defects, such as defocussing, spot and pattern distortion, are worse than with magnetic deflection
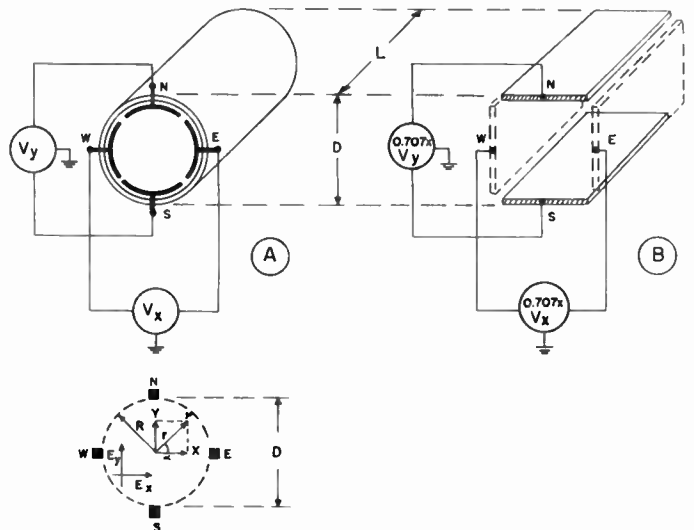
Fig. 1— Principle of the electrostatic yoke.
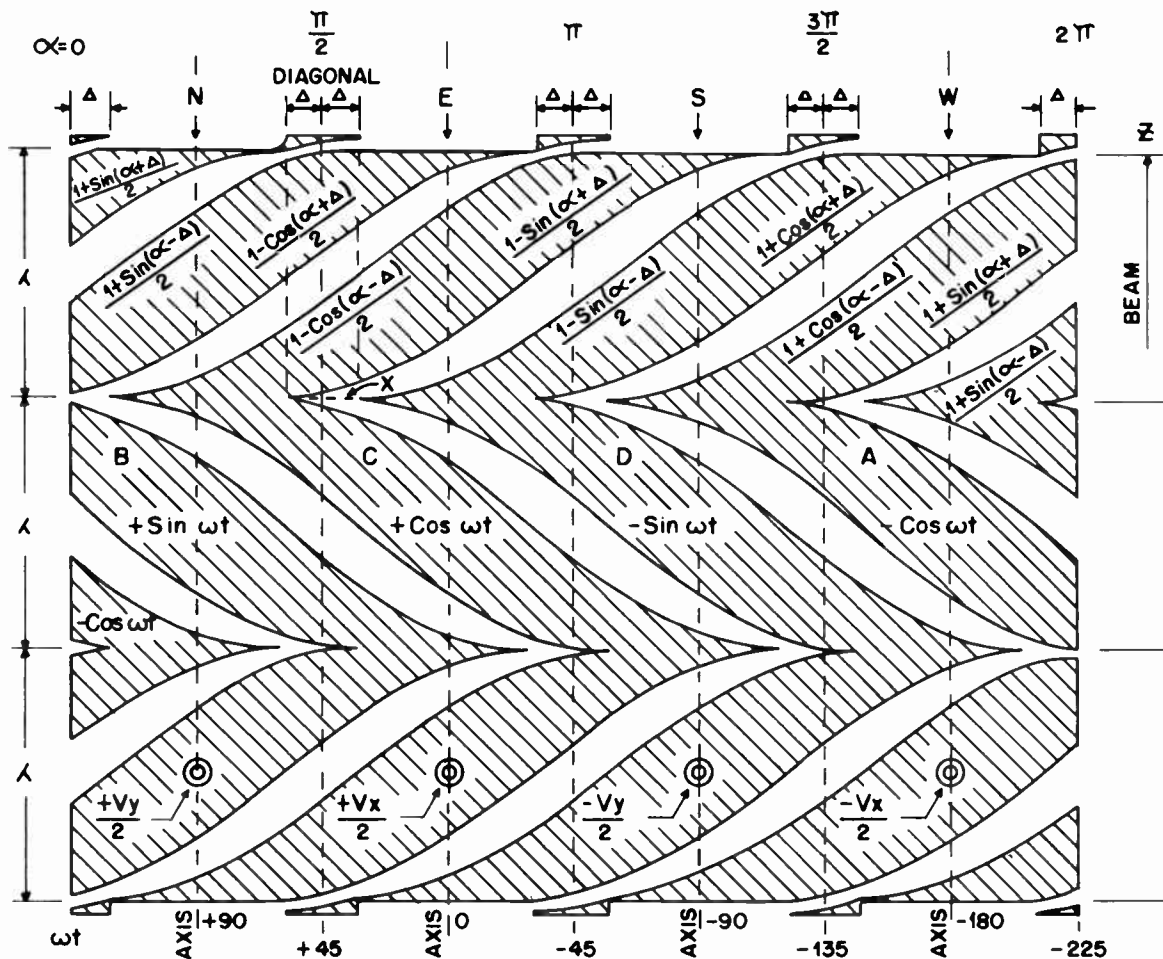
Fig. 2—Deflection printed circuit with correcting tabs.

and increase rapidly with angle, at least in conventional deflection units. This has limited electrostatic sweep to narrow angle applications, such as oscilloscopes ($\beta \leq 25°$).

Recently, two developments have taken place, which in combination may make further progress possible. One is the development of electrostatic yokes which permit

bi-axial deflection from a common center with much less scan distortion, and at wider angles than previously possible. The other is the advent of the mask-type intensifiers which permit a high order of post-acceleration without loss of deflection. Both developments will be discussed in the following paper.

THE ELECTROSTATIC YOKE

Early work on the electrostatic yoke, or "Deflectron," has been reported previously.[1] The basic principle is briefly reviewed with aid of Fig. 1 on the preceding page. Two voltages V_x and V_y, both balanced to ground, are applied to four separate electrodes, printed on the inside of a cylinder as symbolized in Fig. 1(a). The actual pattern geometry is of a special design (see Fig. 2, preceding page), such that the effective wall potential seems to vary sinusoidally with angle:

$$\Phi_{R_1\alpha} = K\left[\tfrac{1}{2}V_y \sin\alpha + \tfrac{1}{2}V_x \cos\alpha\right] \qquad K < 1. \qquad (1)$$

The potential on the inside then becomes[2]

$$\phi_{r_1\alpha} = \Phi_{R_1.\alpha}\cdot r/R = \frac{K}{2R}\left[V_y\cdot y + V_x\cdot x\right]. \qquad (2)$$

The fields in x and y direction are the respective gradients of (2):

$$E_x = \frac{\partial\phi}{\partial x} = K\cdot\frac{V_x}{2R}$$

$$E_y = \frac{\partial\phi}{\partial y} = K\cdot\frac{V_y}{2R}. \qquad (3)$$

This is the same field as would be produced for each axis by a parallel pair of plates bounding the cylinder, each pair being connected to a voltage of KV_x and KV_y respectively, as shown in Fig. 1(b). It will be shown below [see (7)] that K has the value 0.707. This is the relative sensitivity of the Deflectron as compared to the plate capacitor. However, the equivalent pairs of plates cannot be arranged along the sides of a box, as shown in Fig. 1(b), since each pair would distort the field produced by the other. The crossed capacitor approach can thus be realized only by mounting the two units sequentially along the tube axis. This results in two separate centers of deflection. By contrast, the electrostatic yoke can perform bi-axial deflection simultaneously; *i.e.*, with a common center for both coordinates. This saves two-to-one in over-all length for the same system aperture. It will be shown in the following section that an electrode configuration has been found the mean potential of which along the generatrix of the cylinder approaches very closely the form of (1).

PRINTED CIRCUIT GEOMETRY FOR ELECTROSTATIC YOKES

Fig. 2 shows the pattern geometry of an electrostatic yoke, evolved into a plane. The pattern has double periodicity, namely four cycles to the perimeter and three or four cycles (λ) along the length of the cylinder. All boundaries shown are halfwaves of sin α offset by a

[1] K. Schlesinger, "Internal electrostatic deflection yokes," *Electronics*, vol. 25, pp. 105–109; July, 1952.
[2] V. K. Zworykin, G. A. Morton, E. G. Ramberg, J. Hillier, and A. W. Vance, "Electronic Optics and the Electron Microscope," John Wiley and Sons, New York, N. Y., ch. XI; 1945.

small "dead-angle" $\pm\Delta$ at the starting point, to provide insulation. Various boundaries are thus formulated by

$$\lambda\cdot\frac{1\pm\sin(\alpha\pm\Delta)}{2} \quad \text{and} \quad \lambda\cdot\frac{1\pm\cos(\alpha\pm\Delta)}{2}, \qquad (4)$$

in a sequence as indicated on Fig. 2.

To predict the performance of this device, we assume two equal and balanced deflection voltages:

$$V_x = \cos\omega t \quad \text{and} \quad V_y = \sin\omega t, \qquad (5)$$

to be connected to the four metal stripes as shown in Fig. 2. Across the insulating interfaces we assume the potential to vary linearly from one boundary to the other. Limiting ourselves to one wavelength λ as unit length, the effective potential is found in the interval: $+\Delta \leq \alpha \leq (\pi/2)-\Delta$ surrounding the N axis, by summing up the terms in Table 1 below.

TABLE I

Area	Effective length	Potential
Metal strip A	$1 - \dfrac{1+\sin(\alpha+\Delta)}{2}$	$-\cos\omega t$
Metal strip B	$\dfrac{1+\sin(\alpha-\Delta)}{2} - \dfrac{1-\cos(\alpha+\Delta)}{2}$	$+\sin\omega t$
Metal strip C	$\dfrac{1-\cos(\alpha-\Delta)}{2}$	$+\cos\omega t$
Interface AB	$\dfrac{1+\sin(\alpha+\Delta)}{2} - \dfrac{1+\sin(\alpha-\Delta)}{2}$	$\dfrac{\cos\omega t + \sin\omega t}{2}$
Interface BC	$\dfrac{1-\cos(\alpha+\Delta)}{2} - \dfrac{1-\cos(\alpha-\Delta)}{2}$	$\dfrac{\sin\omega t + \cos\omega t}{2}$

The end result of this calculation is as follows:

Zone	Effective Potential	
Metallized areas	$\phi_m = 0.707\,(\cos\Delta - \sin\Delta)\cdot\sin\left(\alpha + \omega t - \dfrac{\pi}{4}\right)$	(6a)
Glass interfaces	$\phi_g = 0.707\cdot\sin\Delta\cdot\sin\left(\alpha + \omega t - \dfrac{\pi}{4}\right)$	(6b)
Resulting total effective potential	$\phi_a = 0.707\cdot\cos\Delta\cdot\sin\left(\alpha + \omega t - \dfrac{\pi}{4}\right)$	(6c)

This result is interesting in several respects:

1) It indicates the establishment of a uniform rotating field, moving counter-clockwise at constant angular velocity.
2) It informs that the electrical axis lies at multiples of 45° off the axis of pattern symmetry, as shown in Fig. 2.

3) It indicates that the sensitivity of a cylindrical yoke of this type is, for each axis, K times down from the equivalent pair of plates, where

$$K = 0.707 \cdot \cos \Delta. \qquad (7)$$

Since the deflection factor of parallel plates can be written as follows[3]

$$F_p = 35 \cdot \frac{d}{l} \, x \quad \text{(volts per kilovolt-degree)}, \qquad (8)$$

the corresponding figure for the Deflectron is

$$F_d = 50 \cdot \frac{d}{l} \quad \text{(volts per kilovolt-degree)}. \qquad (9)$$

Each terminal gets one half of this voltage in push-pull operation.

The dead-angle Δ in Fig. 2 is usually smaller than 18 degrees (cos $18° = 0.95$). Hence it is safe to say that the sensitivity of a practical Deflectron unit, taken per axis, is two-thirds of a pair of deflection plates of the same length, tangent to it. The same statement holds for conical units as well (see the section following).

Fig. 3 shows equipment to detect the electrical axis on a finished Deflectron unit. The unit is energized by a balanced 3-mc signal at two opposite terminals.
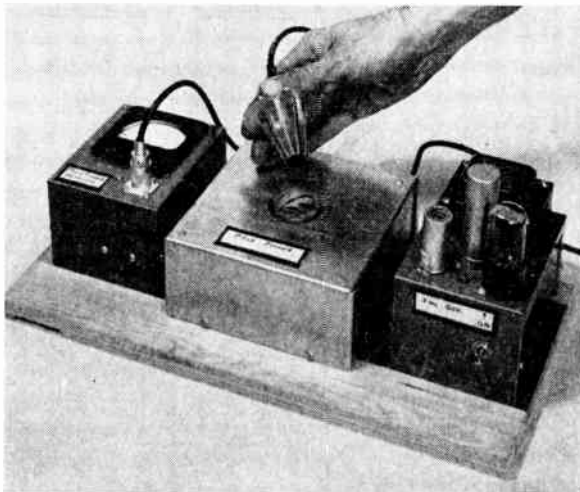
Fig. 3—Equipment to detect the axis of deflection in an electrostatic yoke.

The other two segments are grounded. If the probe-quadrant is bisected by the neutral axis of the Deflectron, the charges induced on both blades are equal and opposite. As a result, a null detector indicates the position of the axis of deflection within less than one degree. Similar accuracy has been achieved with probes using a balanced dipole configuration. This approach has the further advantage of being less susceptible to parallax between probe and yoke.

[3] For derivation see Appendix.

(a)

(b)
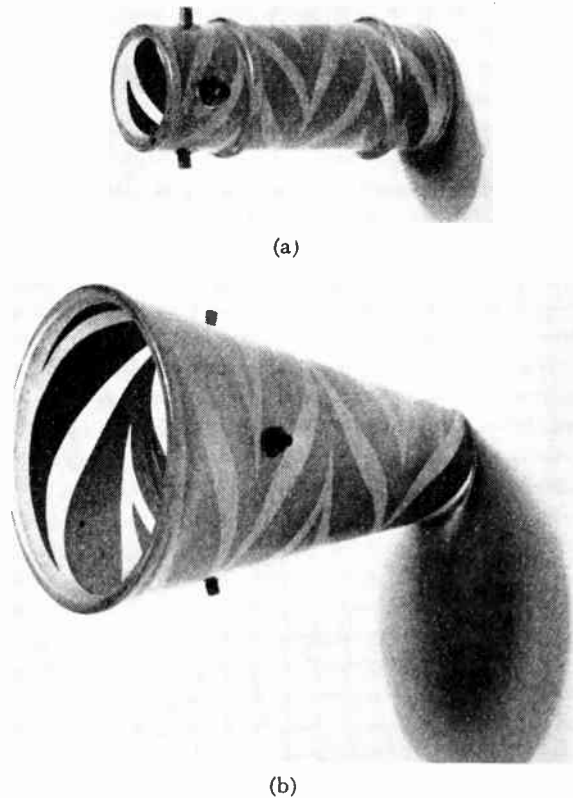
Fig. 4—(a) Narrow-angle pencil Deflectron type CY1-33, (b) wide-angle Deflectron type CO4-66.

DEFLECTRON SENSITIVITY

Figs. 4(a) and 4(b) show two types of electrostatic yokes produced by photo-engraving methods on the inside of glass cylinders and cones. The large unit has a diameter ratio $m = 4:1$ (taper-ratio). The structural and

TABLE II

Fig.	Unit	Length	Exit Diameter	Aperture		Deflection Factor in volt/kv. deg. (each terminal)
				Physical	Usable	
4(a)	Pencil Deflection	$1\frac{1}{2}''$	$\frac{1}{2}''$	33°	27°	9.2
4(b)	Cone Deflection	2''	$1-\frac{3}{8}''$	66°	50°	9.8

electrical characteristics are given in Table II. The measured deflection factor is in agreement with the theoretical data for a conical yoke with taper ratio m (see Appendix):

$$F = 25 \cdot \tan \frac{\beta}{2} \cdot \frac{1 - 1/m}{\ln m} \quad \text{(volt/kilovolt-degree)}. \qquad (10)$$

Test results also check with the more convenient approximate formula

$$F = 25 \cdot \frac{D_m}{l} \quad [\text{volt/kv-degree}], \qquad (10a)$$
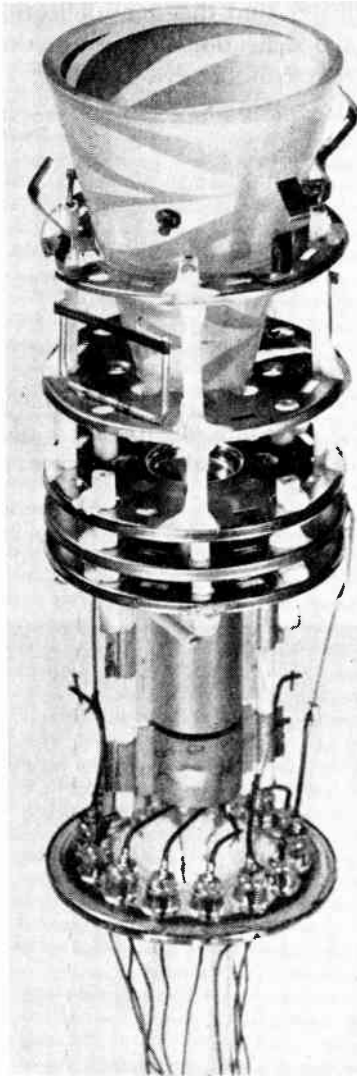
Fig. 5—Gun assembly with electrostatic yoke.

the 12LP4 type TV picture tube, to which a funnel section and 2-inch neck has been added. One stage of post-acceleration is used at a voltage step-up of 1.5:1 (7.5 kv at the screen, 5 kv in the deflecting space). Full scan occurs at 50 degrees of deflection which requires 2,300 volt peak to peak at each Deflectron terminal. In this operation, 75 per cent of the yoke aperture can be utilized, or one-half of the yoke window area, before scan distortion occurs. This compares favorably with the performance of magnetic deflection yokes. Fig. 6 shows the 12-inch Deflectronized tube to be no longer than a conventional 5-inch oscilloscope (16 inches). This relative compactness of the Deflectron is due to: 1) the wider deflection angle used, and 2) the 2:1 saving in length of the deflecting structure.
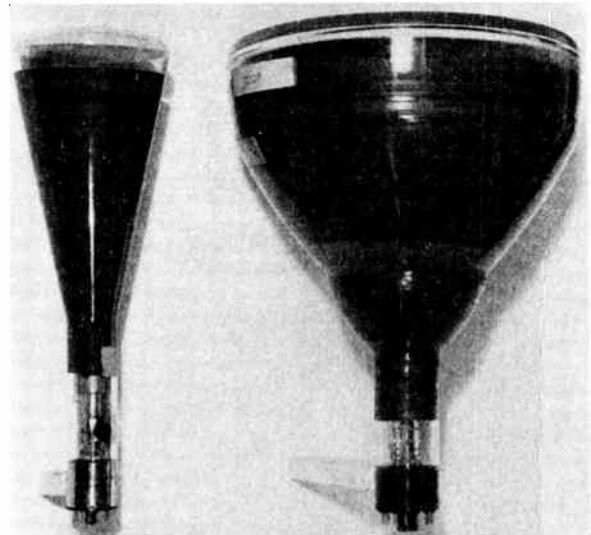
Fig. 6—5-inch, 25-degree conventional oscilloscope and 12-inch, 50-degree Deflectron tube using electrostatic yoke.

which holds for any unit with mean diameter d_m and length l regardless of taper (15% accuracy up to $m = 4$).

It is noteworthy that the sensitivity of both units is practically the same, despite the fact that the large unit handles twice as much deflection as the small one. This is in line with a general rule (see Appendix), whereby the transition from a parallel to a tilted structure has no first-order effect on sensitivity, as long as mean diameter and length are unaltered. However, since the exit aperture increases in the process, a conical unit has always greater over-all merit than a cylinder. The small pencil Deflectron is thus recommended only in cases where space is at a premium.

A 12-Inch "Deflectronized" Cathode-Ray Tube

Fig. 5 shows a gun assembly carrying a conical electrostatic yoke. Fig. 6 shows a finished tube using this system.[4] This tube employs a 12-inch blank as used in

---

[4] Built for use in a Radar-Indicator under BuShips Contract.

Performance Test Equipment

Fig. 7 shows a test set-up to check the performance of the finished tubes. The bulb is mounted vertically in the lower section which contains equipment for circular sweep. The signal generator is carefully filtered and employs inverse feedback to insure sweep waveforms with less than 1 per cent distortion.

An ultra-violet light source projects, onto the screen, the image of a photographic reference chart in polar coordinates. Since the yellow component of the P-7 phosphor responds to UV, we observe, on the screen, the superposition of the optical reference and the circular scan. Since both displays are in the same plane, the image can be viewed from any point without parallax.

The Circularity Problem

Fig. 8 shows a photograph obtained, with the above station, from one of the earlier tubes. At a sweep diameter of 10 inches (46 degrees), it is seen that deflection

at $\pm 45°$ off axis (diagonal) is slightly larger than on axis. This noncircularity amounts to about $\frac{1}{8}$-inch radial; *i.e.*, $2\frac{1}{2}$ per cent of the diameter. The error distribution is quadrantal; *i.e.*, it repeats itself four times per revolution.

It is possible to account for this quadrantal error by further analysis of the pattern geometry of Fig. 2.

Fig. 7—Optical test stand to check Deflectron circularity.

To this end, the computation of the effective wall potential, carried out above for the axes of deflection [(6a)–(6c)], has been repeated for diagonal deflection in the range:

$$\frac{\pi}{2} - \Delta \leqq \alpha \leqq \frac{\pi}{2} + \Delta.$$

Calling Φ_a the axial potential, as computed in (6c), we find, by the same methods, an expression for the diagonal potential $_d:\Phi_d = \Phi_a + \Phi_\Delta$, where the error term Φ_Δ is

$$\Phi_\Delta = \cos \omega t \cdot \frac{1 - \sin (\alpha - \Delta)}{4}$$
$$+ \sin \omega t \frac{1 - \sin (\alpha + \Delta)}{4} \cdot \quad (11)$$

Eq. (11) indicates that diagonal deflection is slightly greater than axial deflection because of the error term Φ_Δ/Φ_a. This term can be evaluated at the diagonal points of sweep by setting

$$\omega t = \frac{\pi}{4} \quad \text{and} \quad \alpha = \frac{\pi}{2}$$

in (11). The result is

$$\Phi_\Delta = 0.707 \cdot \frac{\Delta^2}{4} \cdot \quad (12)$$

That is, the error increases with the square of the dead angle Δ. Taking the value Φ_a for axial potential from (6c), we find the quadrantal error-percentage:

$$\frac{D - A}{A} = \frac{\Phi_\Delta}{\Phi_a} = \frac{\Delta^2}{4 \cdot \cos \Delta} \rho \sim \left(\frac{\Delta}{2}\right)^2 \cdot 100 \text{ per cent.} \quad (13)$$
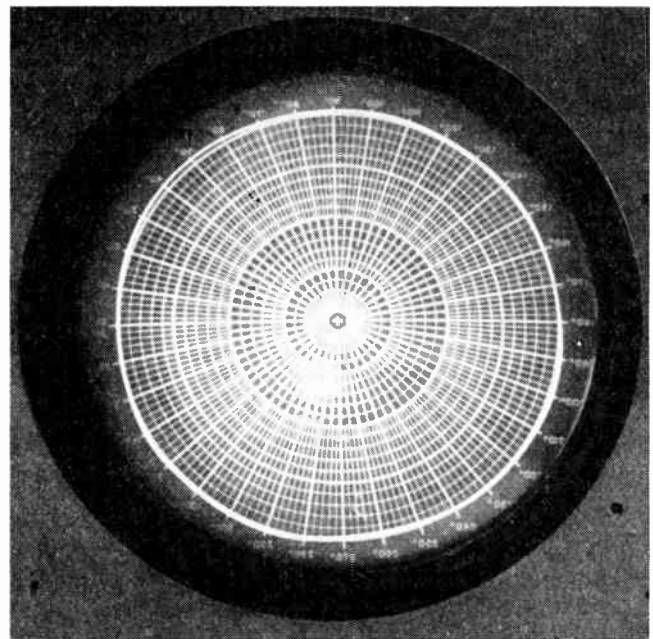
Fig. 8—Quadrantal error favoring diagonals.

Here, D and A are deflection diameters, read along the axes and diagonals of circular sweep, respectively. This theoretical noncircularity is evaluated in Table III for three values of dead angle Δ. It is seen that the theory gives a quantitative account for experience.

TABLE III

Dead angle	Quadrantal error	Correcting tabs height
12°	1.1 per cent	6 mils
15°	1.7 per cent	17 mils
18°	2.5 per cent	25 mils

CORRECTION OF QUADRANTAL ERROR

A cure for noncircularity suggests itself by inspection of (9) for the error term Φ_Δ. The factors

$$\frac{1 - \sin(\alpha - \Delta)}{4} \quad \text{and} \quad \frac{1 - \sin(\alpha + \Delta)}{4}$$

in this equation describe the triangular areas shown at (x) in Fig. 2, but in one-half of their actual height. It seems possible therefore to cancel the error term Φ_Δ by printing additional tabs of similar shape right above the dead angles $\pm\Delta$ of the pattern, and then connecting these tabs to signals of opposite polarity. This can be done readily in a pattern with an odd number of cycles, such as shown in Fig. 2 for $N = 3$. The required compen- pensating voltages $(-\sin wt)$ and $(-\cos wt)$ are then easily accessible on adjacent stripes. The height of the compensating tabs may be found from (11).

$$h = \frac{\Delta^2}{8} \cdot l \tag{14}$$

where l is the total length of the Deflectron pattern. This strip-width h of the tabs is listed in Table III and it is found to be quite small (approximately 20 mils). Even this small strip-width accrues only if the error is allowed to add up, without correction, over all cycles of the pattern. The sum total is then corrected by tabs at input and output of the yoke.
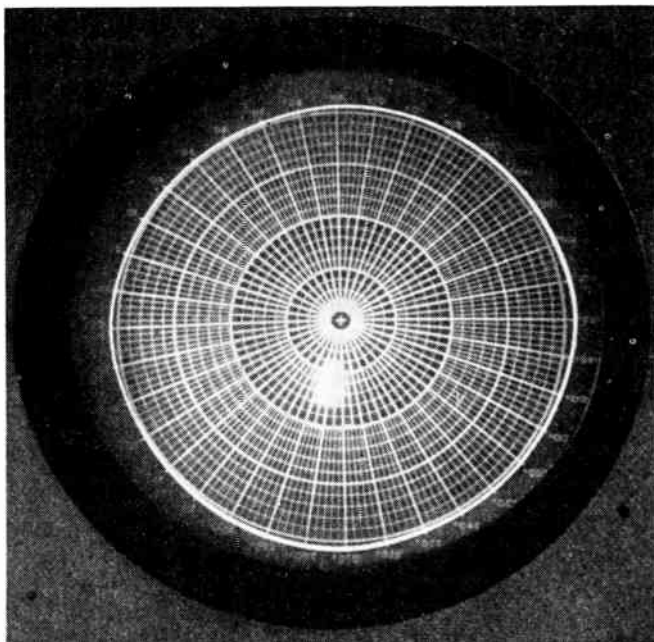
Fig. 9—Quadrantal error overcorrected favoring axials.

The photograph, Fig. 9, has been taken of one of the early Deflectrons compensated in that manner. It indicates that the quadrantal error has actually been over-compensated, the diagonals now being about 2 per cent shorter than the axials ($D/A < 1$). Further refinements in our printing technique will undoubtedly permit a more precise correction of residual noncircularity.

PROGRESS IN THE TECHNIQUE OF POST-ACCELERATION

Since the voltage demand for electrostatic deflection is directly proportional to the electron voltage in the deflecting region, any progress in the technique of post-acceleration is a great help in the development of electrostatic deflection.
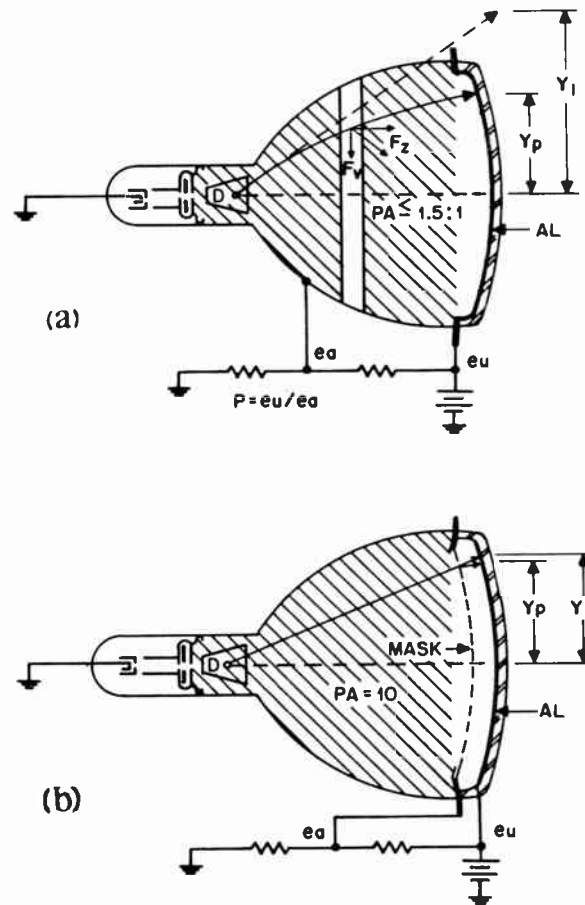
Fig. 10—Two types of intensifiers: (a) ring accelerator, (b) mask accelerator.

Conventional post-accelerators, also called intensifiers, operate with conductive coatings of band or spiral shape, plated on the inside of the bulb. In all of these accelerators, including the constant-gradient type, electron trajectories are not straight, but are bent back towards the axis. This causes considerable deflection loss [see Fig. 10(a)] partly offsetting the desired gain from post-acceleration. Another disadvantage of curved trajectories is the need to handle, in the deflecting unit, sweep angles in excess of those finally achieved. This increases deflection distortion in the yoke and forces a reduction of its ultimate efficiency by design.

In 1950, L. S. Allard published, in England, a paper on an "ideal" accelerator for CRT's.[5] He proposed a mask-and-screen assembly to achieve acceleration in a confined region close to the screen [see Fig. 10(b)]. Since this arrangement uses most of the bulb as a field-free drift space, trajectories are straight lines and deflection loss may be avoided entirely.

When experimenting with the mask-type of intensifier, we soon came to realize that the major, perhaps the only, obstacle was secondary emission (S.E.) from the mask. Fig. 11(a) shows the pictorial effects of S.E. observed. In these studies, we used a high transmission (50 per cent) mask of copper-nickel alloy, one inch away from the screen. The "ghost" image was comparable in brightness to the primary image, but was lagging behind it in deflection because of beam refraction in the plane mask-and-screen arrangement. Fig. 11(b) shows the same pictures after cancellation of secondary emission.
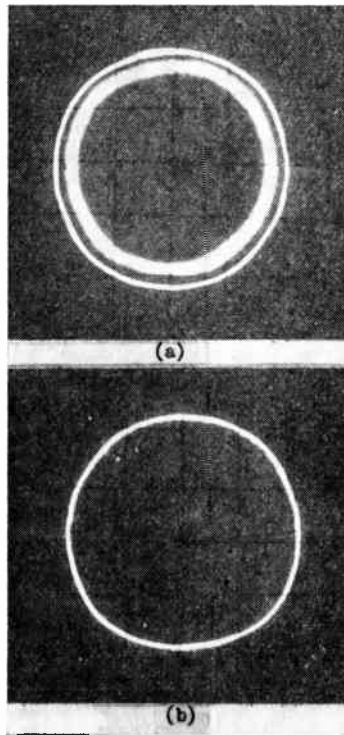
Fig. 11—Barrier-mask intensifier: (a) barrier bias removed, secondary image appears, (b) barrier mask in operation.

This improvement was obtained by a device, which we call a "barrier-mask" and which is explained in Fig. 12.

The inside surface of the intensifier-mask is coated with an insulating material having a high degree of secondary emission. The outer surface is left metallic and is connected to an external bias 100 volts below drift-space potential. When scanned, the insulating face soon adopts the potential of the drift space wall, while the second surface acts as a repeller, or "barrier," against secondary emission from the mask.

[5] L. S. Allard, "An 'ideal' post deflection accelerator CRT," *Electronic Engrg.*, vol. 22, pp. 461–463; November, 1950.

With this "barrier-mask intensifier," post-acceleration of 10:1 has been achieved readily. The portent of this development for electrostatic deflection lies in a considerable reduction of sweep voltage. In experimental tubes, deflection of a 20-kv beam by 62 degrees was done with only 1,300 v per plate, using a conical deflectron as shown in Fig. 4(b). The same sweep would have required 8,300 v per plate with one-step ring accelerator 1.5:1.
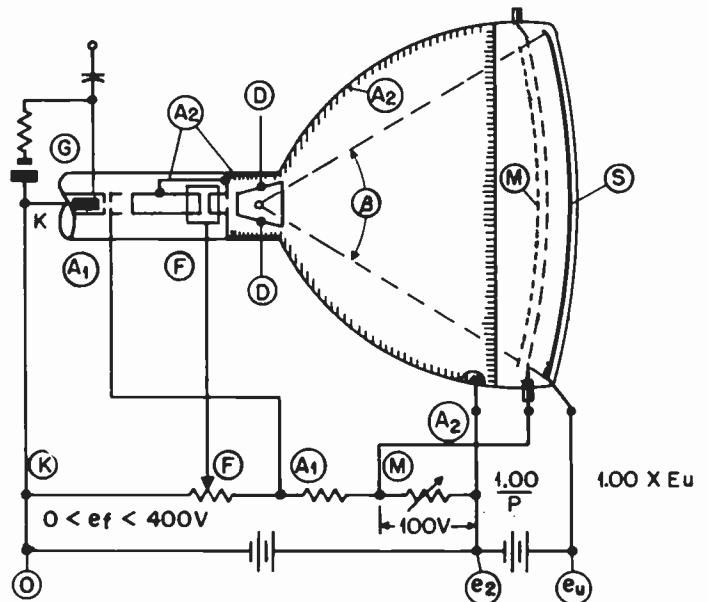
Fig. 12—CRT with electrostatic yoke and barrier-mask intensifier. K = cathode, G = control grid, A_1 = first anode, A_2 = second anode, F = focusing cylinder, D = Deflectron, M = barrier mask, S = metal-back screen. Typical operation is as follows: β = 62°, p = 10:1 post-acceleration, e_u = 20 kv, e_2 = 2 kv, e_M = 1.9 kv, e_D = 1,300 N, p-p = per plate.

The 12-inch tube, shown in Fig. 6, will sweep 50 degrees at 7.5 kv with only 500 v per terminal, if equipped with barrier mask acceleration 10:1. This is only 20 per cent of the voltage which we need now in connection with a conventional ring-accelerator.

In summing up, it appears at this time, that the combination of the Deflectron yoke with the "barrier-mask" intensifier presents a system for electrostatic deflection, which combines low distortion at wide angles with compactness, and has the ability to scan high ultor voltages with low deflection voltage. Work is under way to use this approach for high intensity CRT's, in the fields of specialty tubes,[6] as well as for television picture displays.

APPENDIX

Deflection Factor of Conical Deflectrons

For parallel plates, a well-known relation exists between structural dimensions (D, L) and voltage demand for a given deflection angle α:

$$e_d = 2 \cdot e_a \cdot \frac{D}{L} \cdot \tan \alpha. \tag{15}$$

Here, e_a is the anode voltage preceding the deflector. For small angles α, (15) may be transformed into a convenient expression for the voltage required per degree of deflection:

$$F = e_{d(v)}/e_{a(KV)} \cdot \alpha^0 = \frac{2 \cdot 10^3}{57.3} \frac{D}{L}$$

$$= 35 \frac{D}{L} \; [\text{volt per kilovolt} \cdot \text{deg.}]. \tag{16}$$
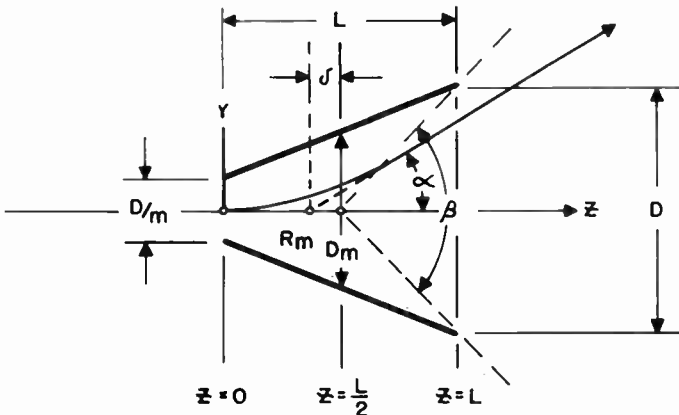
Fig. 13

This figure is used in the text as "deflection factor" [see (8)]. We now compare a pair of parallel plates to a pair with taper. The taper-ratio m is defined in the Fig. 13. The plate separation of the tapered pair is:

$$d = \frac{D}{m}\left[1 + (m - 1) \cdot \frac{z}{l} \right]. \tag{17}$$

The active field strength then becomes

$$E_z = E_1 \cdot \frac{1}{1 + (m - 1) \cdot \dfrac{z}{l}} \tag{18}$$

where

$$E_1 = \frac{e_d}{D} \cdot m$$

is the field at the input end of the structure. From electron ballistics, we get from the trajectory:

$$\frac{d^2 y}{dz^2} = \frac{E_z}{2e_a} \cdot . \tag{19}$$

Inserting (18) and integrating yields the exist angle of the beam:

$$\frac{dy}{dz_{(z=e)}} = \frac{e_d}{2e_a} \cdot \frac{L}{D} \cdot \frac{m \cdot \ln m}{m - 1} = \tan \alpha. \tag{20}$$

By comparison of (20) with (15), the sensitivity gain by taper is found as

$$g_T = \frac{\ln m}{1 - 1/m} \cdot . \tag{21}$$

For a cone with a 4:1 taper ratio, as shown in Fig. 4(b), the taper gain is 1.83:1.

Since the approximation:

$$\frac{1 - 1/m}{\ln m} \sim \frac{1}{2}\left[1 + 1/m \right] \tag{22}$$

holds within 10 per cent up to $m = 3.5$, the deflection factor from (20) may be written

$$F = \frac{e_d}{e_a \cdot \tan \alpha} \sim 2 \cdot \frac{D_m}{L} . \tag{16a}$$

This shows the invariance of sensitivity for units with equal mean diameter and length.

There is a slight reduction of aperture from tapering. The center of deflection R_m moves back from the geometrical center of the electrode by the amount δ.

$$\frac{\delta}{L} = \frac{1}{2} \frac{m + 1}{m - 1} - \frac{1}{\ln m} . \tag{23}$$

At a taper ratio of $m = 4$, as used in our Deflectrons, this shift is 11 per cent of the total length of the electrode.

IRE Standards on Audio Systems and Components: Methods of Measurement of Gain, Amplification, Loss, Attenuation, and Amplitude-Frequency-Response, 1956*

COMMITTEE PERSONNEL

Subcommittee on Methods of Measurement of Gain, Amplification, Loss, Attenuation, and Amplitude-Frequency-Response
1949–1955

I. M. KERNEY, *Chairman* 1954–1955
W. L. BLACK, *Chairman* 1953–1954
D. E. MAXWELL, *Chairman* 1949–1953

W. L. Black	R. H. Edmondson
W. W. Dean	I. M. Kerney
I. G. Easton	W. E. Stewart

Audio Techniques Committee
1954–1955

D. E. MAXWELL, *Chairman* 1954–1955   I. M. KERNEY, *Vice-Chairman* 1954–1955
C. A. CADY, *Chairman* 1952–1954   D. E. MAXWELL, *Vice-Chairman* 1952–1954

H. W. Augustadt	L. H. Good	R. C. Moody
O. C. Bixler	G. H. Grenier	L. D. Runkle
W. L. Black	F. K. Harvey	H. O. Saunders
R. L. Brown	F. L. Hopper	F. H. Slaymaker
D. H. Castle	R. A. Miller	W. E. Stewart

Standards Committee
1955–1956

E. WEBER, *Chairman*   R. F. SHEA, *Vice-Chairman*
M. W. BALDWIN, JR., *Vice-Chairman*   L. G. CUMMING, *Vice-Chairman*

W. R. Bennett	P. J. Herbst	H. R. Mimno
J. G. Brainerd	Hans Jaffe	M. G. Morgan
P. S. Carter	Henry Jasik	G. A. Morton
P. S. Christaldi	A. G. Jensen	H. L. Owens
A. G. Clavier	J. L. Jones	C. H. Page
J. E. Eiselein	J. G. Kreer, Jr.	P. A. Redhead
A. W. Friend	E. A. Laport	R. Serrell
V. M. Graham	A. A. Macdonald	R. M. Showers
R. A. Hackbusch	Wayne Mason	H. R. Terhune
H. C. Hardy	D. E. Maxwell	J. E. Ward
D. E. Harnett	K. R. McConnell	W. T. Wintringham

Measurements Coordinator

R. F. SHEA

PREFACE

The purpose of this standard is to indicate methods for making measurements on systems and components primarily intended for application or operation at audio frequencies. Audio systems and components are special forms of the more general term "transducer,"[1] and the basic methods of measurement described in this standard are, in general, broadly applicable to many types of transducers. Performance standards are avoided as being outside the scope of the Institute of Radio Engineers. Complete delineation of underlying theory is omitted, as such material is available from other sources. Several of these sources are referenced in the standards herein presented.

In general, the material on each type of measurement includes a brief discussion of the principles involved. There is usually a presentation of mathematical relations and measuring circuits, including, in some instances, specialized circuit arrangements considered representative of good audio-frequency measuring practices. In some cases, for background information, there is included a discussion of the requirements and characteristics of the measuring equipment. The measuring procedures are outlined and the factors which affect the accuracy of the obtained results are discussed. Methods of presentation of such results are given. The format is such that each of the following sections represents in itself as complete a treatment of its subject matter as seems practical, thereby reducing the amount of cross-referencing required by the reader.

Standard IRE letter symbols are employed throughout this document, and a knowledge of these symbols is essential to proper interpretation of the various mathematical expressions. A tabulation of pertinent symbol notation is given below:

Item	Form of Type	Example
Scalars	Italic	E
Vectors	Bold Roman	**E**
Phasors	Bold Italic	***Z***
Conjugate phasors	Bold Italic	***Z*****
Absolute magnitudes of vectors or phasors	Italic	E

1. GAIN, AMPLIFICATION, LOSS, ATTENUATION

In audio-frequency usage "gain" and "amplification" and the inverse terms "loss" and "attenuation" are general terms pertaining to the transmission characteristics of audio systems and components, and are commonly used to express significant power, voltage, or current ratios. In order to avoid ambiguity, it is recommended that the terms gain and loss be used only to express *power* ratios, while the terms amplification and attenuation should be limited to the expression of *voltage* or *current* ratios. Gain and loss are generally stated in decibels. Because of long established usage in the audio field, amplification and attenuation ratios are expressed in terms of decibels in this standard, although the more recently introduced term "decilog" is more appropriate. If the use of the terms attenuation and amplification is restricted to the expression of the results of measurements of *voltage* or *current* ratios, much of the confusion that has existed in the past usage will be avoided.

The standard methods of measurement set forth in the following sections are applicable, for the most part, only to those audio systems and components which are representable as linear three- and four-terminal networks with electrical inputs and outputs. Thus, they are not generally applicable to measurements of electroacoustical or electromechanical transducers, such as microphones, loudspeakers, and recording or reproducing transducers.

The measuring principles, while illustrated in this standard with unbalanced-to-ground circuit arrangements, are applicable to both balanced and unbalanced-to-ground systems.

1.1 Gain (Transmission Gain)

Gain (transmission gain) is a general term used to denote an increase in power in transmission from one point to another. Gain is usually expressed in decibels, and the term is widely used in audio practice to denote "transducer gain."

The measurement of several types of gain is outlined under specific headings in the material which follows. In every case gain is a ratio of powers. The type of gain to be measured will depend on the desired application. In each instance it is recommended that the stated result be identified by the full terminology (*e.g.*, Transducer Gain rather than Gain) unless, by context, otherwise, there appears to be no possible chance of ambiguous interpretation.

1.1.1 Bridging Gain

Bridging gain is the ratio of the power a transducer delivers to a specified load under specified operating conditions, to the power dissipated in the reference impedance across which the input of the transducer is bridged. This gain is usually expressed in decibels.

The application of bridging gain is ordinarily limited to a transmission system in which it is desired to furnish power to an auxiliary load circuit without appreciable influence on the main transmission circuit. For example, in a broadcasting audio system it is usually desirable to monitor an outgoing program line in such a way that

---

[1] **Transducer**: A device capable of being actuated by waves from one or more transmission systems or media and of supplying related waves to one or more other transmission systems or media. (*54 IRE 3. S1 Standards on Audio Techniques: Definitions of Terms, 1954.* PROC. IRE, vol. 42, pp. 1109–1112; July, 1954.)

the line level is not appreciably altered by the monitoring equipment. This requirement can be met by bridging a monitoring amplifier across the program line, providing the input impedance of the amplifier is very much higher (say, 10 times higher) than the terminating impedance of the line. The ratio of the power in the load circuit of the amplifier to the power in the line terminating impedance is the bridging gain of the amplifier.

1.1.1.1 Bridging Gain Relations
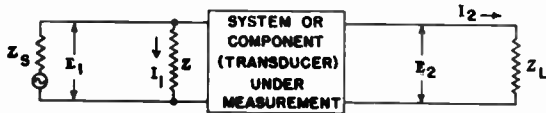
Fig. 1—Elementary circuit for bridging gain.

$$Z = R \pm jX = \text{Reference Impedance}.$$
$$Z_L = R_L \pm jX_L = \text{Load Impedance}.$$

$$\text{Bridging Gain in db} = 10 \log \left[\frac{(I_2)^2 R_L}{(I_1)^2 R} \right].$$

Since

$$I_1 = \frac{E_1}{Z}, \quad \text{and} \quad I_2 = \frac{E_2}{Z_L},$$

$$\text{Bridging Gain in db} = 10 \log \left[\left(\frac{E_2}{E_1}\right)^2 \left(\frac{Z}{Z_L}\right)^2 \left(\frac{R_L}{R}\right) \right].$$

If Z and Z_L are pure resistances R and R_L respectively, the above equations can be simplified to the following:

$$\text{Bridging Gain in db} = 10 \log \left[\frac{(E_1)^2 / R}{(E_2)^2 / R_L} \right].$$

Note: This equation is rigorously correct even if reactance is present in the reference impedance Z and load impedance Z_L, provided R and R_L represent the equivalent parallel resistance of Z and Z_L, respectively. Equivalent parallel resistance R_{par} can be computed from the series resistance R_{ser}, and series reactance X_{ser}, by the expression:

$$R_{par} = \frac{(R_{ser})^2 + (X_{ser})^2}{R_{ser}}.$$

1.1.1.2 Bridging Gain Measuring Circuits

The circuit of Fig. 1 used to illustrate bridging gain relations can also be considered as a measuring circuit by the addition of the meters necessary to measure the magnitudes of E_1, E_2, etc. If the impedance of the measuring devices are such as to affect the quantities being measured, proper allowance must be made for this effect. For information concerning the required

characteristics of the measuring devices, reference should be made to section 1.5.

In some instances it may prove impractical from the standpoint of operational convenience and accuracy to make measurements directly as described above. Therefore, suggested measuring circuits representative of good engineering practice and adaptable to a variety of gain measurements are shown in Fig. 5(a) through 5(c). The circuits of Fig. 5(a) and 5(b) though shown in the Transducer Loss Section, are also applicable to the measurement of bridging gain, particularly where the input impedance Z_i of the audio system or component is much higher than the impedance R_S'. The following conditions must be satisfied by the measuring equipment:

$R_S' = R_S =$ reference impedance Z (resistive) of the bridging system or component under measurement.

$R_L =$ specified load resistance of the system or component under measurement.

Then:

$$\text{Bridging Gain in db} = A + B + 10 \log \left[\frac{4(E_{V2})^2 R_A}{(E_{V1})^2 R_L} \right]$$
$$+ 20 \log \left[1 + \frac{R_S'}{2Z_i} \right].$$

If $R_S' \ll Z_i$, as is frequently the case, the above equation simplifies to:

$$\text{Bridging Gain in db} = A + B + 10 \log \left[\frac{4(E_{V2})^2 R_A}{(E_{V1})^2 R_L} \right]$$
$$= A + B + 6 + 10 \log \left[\frac{(E_{V2})^2 R_A}{(E_{V1})^2 R_L} \right].$$

1.1.2 Insertion Gain

The insertion gain of a transducer inserted in a transmission system is the ratio of the power delivered to that part of the system following the transducer to the power delivered to that same part before insertion of the transducer. This gain is usually expressed in decibels.

The above applies to the use of a three- or four-terminal transducer inserted in a transmission system, and to an impedance bridged across a transmission system. Insertion gain resulting from the bridging of an impedance across a transmission system must be carefully differentiated from bridging gain (see section 1.1.1).

Insertion gain is the inverse of insertion loss. It is suggested that reference be made to the discussion of insertion loss in section 1.3.2. In particular, it should be noted that, under some conditions, a passive transducer may produce insertion gain; and that an active transducer, such as an amplifier, may sometimes produce insertion loss.

1.1.2.1 Insertion Gain Relations
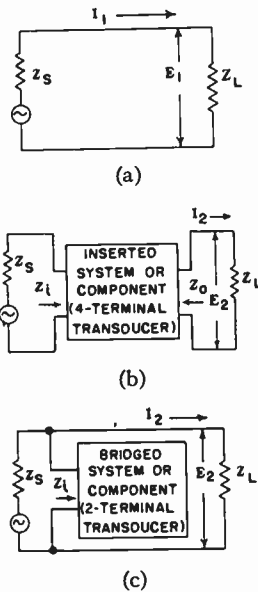
Fig. 2—Elementary circuits for insertion gain. (a) Circuit for determining reference power output before insertion or bridging. (b) Circuit for determining power output after insertion. (c) Circuit for determining power output after bridging.

$Z_i = R_i \pm jX_i =$ Input impedance of inserted or bridged system or component (transducer) under measurement.

$Z_L = R_L \pm jX_L =$ Impedance looking toward load at the point of insertion or bridging.

$Z_o = R_o \pm jX_o =$ Output impedance of inserted system or component.

$Z_S = R_S \pm jX_S =$ Impedance looking toward source at the point of insertion or bridging.

$$\text{Insertion Gain in db} = 10 \log \left[\frac{(I_2)^2 R_L}{(I_1)^2 R_L} \right]$$

$$= 20 \log \left[\frac{I_2}{I_1} \right].$$

Or, since E_1 and E_2 are proportional to I_1 and I_2,

$$\text{Insertion Gain in db} = 20 \log \left[\frac{E_2}{E_1} \right]$$

Note: The impedances Z_i, Z_L, Z_o and Z_S do not enter into the expression for insertion gain, although they obviously affect the numerical result. Therefore, the equations give a true power ratio even though all the above impedances may contain reactance.

1.1.2.2 Insertion Gain Measuring Circuits

The circuit of Fig. 2 can be considered as a measuring circuit by the addition of the voltmeter necessary to read the magnitudes of E_1 and E_2. If the impedance of the voltmeter is such as to affect the quantities under measurement, proper allowance must be made.

As noted in previous sections, insertion gain is the inverse of insertion loss, and the discussion under 1.3.2.2 applies equally well to this measurement.

The representative measuring circuits shown in Fig. 5 may be frequently found more convenient for the measurement of insertion gain when Z_S and Z_L are resistive. For insertion gain measurements, the following special conditions apply to the circuits of Fig. 5:

$R_S' = \infty$.

$R_S =$ Specified source resistance presented to audio system or component under measurement at point of insertion.

$R_L =$ Specified load resistance presented to audio system or component under measurement at point of insertion.

Then:

$$\text{Insertion Gain in db} = A + B + 10 \log \left[\frac{4(E_{V2})^2 R_A}{(E_{V1})^2 R_L} \right]$$
$$+ 10 \log \left[\frac{(R_S + R_L)^2}{4 R_S R_L} \right].$$

The term

$$\log 10 \left[\frac{(R_S + R_L)^2}{4 R_S R_L} \right]$$

in the above equation represents the transition loss of the measuring system at the insertion point. If $R_S = R_L$, this term becomes zero.

If the substitution method of making the insertion gain measurement is employed in conjunction with the measuring circuits of Fig. 5(a) and 5(b) it is possible to eliminate the absolute accuracy of the voltmeters V_1 and V_2 as a factor in the accuracy of the desired result. This can be effected simply by noting the reading of V_2 before the insertion, and then readjusting the source-circuit calibrated attenuator to give the same reading of V_2 after the insertion of the audio system or component. The insertion gain is then indicated directly by the difference in db of attenuation between the two settings of the source-circuit calibrated attenuator. In making an insertion gain measurement by the above method, it is necessary that E_{V1} be held constant before and after the insertion.

1.1.3 Power Gain

Power gain is the ratio of the power that a transducer delivers to a specified load, under specified operating conditions, to the power absorbed by its input circuit. This gain is usually expressed in decibels.

The power gain of an audio system or component is ordinarily of rather limited interest. A statement of the power gain of a particular audio system or component usually does not give the most useful information regarding the transmission gain which will result if this system or component is inserted in or bridged across a second audio transmission system. For example: The input impedance of a microphone preamplifier is often

very high compared to its specified source impedance. The power gain of the preamplifier may approach infinity, but this is not significant since the more useful gain of this amplifier is its transducer gain. (See section 1.1.4.)

1.1.3.1 Power Gain Relations
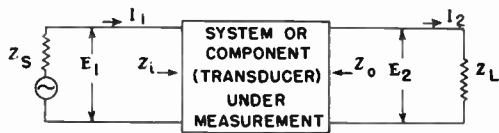
Fig. 3—Elementary circuit for power gain.

$Z_i = R_i \pm jX_i$ = Input impedance of system or component.
$Z_L = R_L \pm jX_L$ = Load impedance.
$Z_o = R_o \pm jX_o$ = Output impedance of system or component.
$Z_S = R_S \pm jX_S$ = Source impedance.

$$\text{Power Gain in db} = 10 \log \left[\frac{(I_2)^2 R_L}{(I_1)^2 R_i} \right].$$

Since

$$I_1 = \frac{E_1}{Z_i}, \quad \text{and} \quad I_2 = \frac{E_2}{Z_L},$$

$$\text{Power Gain in db} = 10 \log \left[\left(\frac{E_2}{E_1} \right)^2 \left(\frac{Z_i}{Z_L} \right)^2 \frac{R_L}{R_i} \right].$$

If Z_i and Z_L are pure resistances R_i and R_L respectively, the above equations can be simplified as follows:

$$\text{Power Gain in db} = 10 \log \left[\frac{(E_2)^2 R_i}{(E_1)^2 R_L} \right].$$

This equation is rigorously correct even if reactance is present in the input impedance Z_i and the load impedance Z_L, provided R_i and R_L represent the equivalent parallel resistance of Z_i and Z_L, respectively. Equivalent parallel resistance R_{par} can be computed from the series resistance R_{ser}, and series reactance X_{ser} by the expression:

$$R_{par} = \frac{(R_{ser})^2 + (X_{ser})^2}{R_{ser}}.$$

1.1.3.2 Power Gain Measuring Circuits

The circuit of Fig. 3 can be considered as a measuring circuit for power gain by addition of the meters necessary to determine the magnitudes of E_1 and E_2, or I_1 and I_2. If the impedances of the meters are such as to affect the quantities being measured, proper allowance must be made. For information concerning the required characteristics of meters, reference should be made to section 1.5.

1.1.4 Transducer Gain

Transducer gain is the ratio of the power that a transducer delivers to a specified load under specified operating conditions to the available power of a specified source, and is usually expressed in decibels. Stated in another manner, transducer gain is the ratio of the power that

a given transducer delivers to a specified load from a specified source to the power which would be delivered if the actual transducer were replaced by an ideal transducer.[2]

Transducer gain (or loss) is the most frequently employed measure of the transmission characteristics of audio systems or components. The transducer-gain concept is so widely used and so firmly established that it is often referred to loosely as simply "gain" (or "loss"). In order to avoid possible ambiguities, however, it is strongly recommended that the full terminology (*i.e.*, "transducer gain" rather than "gain") be used to express the results of measurements of transducer gain.

1.1.4.1 Transducer Gain Relations
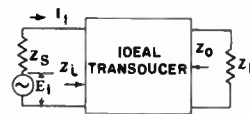
(a)
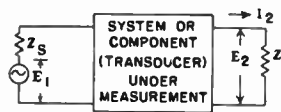
(b)

Fig. 4—Elementary circuit for transducer gain. (a) Circuit for determining reference power with ideal transducer. (b) Circuit for determining load power with system or component substituted for ideal transducer.

$Z_S = R_S \pm jX_S$ = Source Impedance.
$Z_i = Z_S{}^* = R_S \mp jX_S$.
$Z_L = R_L \pm jX_L$ = Load Impedance.
$Z_o = Z_L{}^* = R_L \mp jX_L$.

Since by definition an ideal transducer dissipates no energy, the reference power in Z_L of Fig. 4(a) above must equal the power in Z_i. Thus the power in $Z_L = (I_1)^2 R_i = (I_1)^2 R_S$.

Note that the reference power is the maximum available power of the source.

Then:

$$\text{Transducer Gain in db} = 10 \log \left[\frac{(I_2)^2 R_L}{(I_1)^2 R_S} \right]$$

or, since

$$I_1 = \frac{E_1}{2R_S} \quad \text{and} \quad I_2 = \frac{E_2}{Z_L}.$$

$$\text{Transducer Gain in db} = 10 \log \left[\frac{4(E_2)^2 R_L R_S}{(E_1)^2 (Z_L)^2} \right].$$

---

[2] **Ideal Transducer** (for connecting a specified source to a specified load): A hypothetical passive transducer which transfers the maximum possible power from the source to the load.
　Note: In linear transducers having only one input and one output, and for which the impedance concept applies, this is equivalent to a transducer which (a) dissipates no energy and (b) when connected to the specified source and load presents to each its conjugate impedance. (*54 IRE 3. SI Standards on Audio Techniques, Definitions of Terms, 1954;* PROC. IRE, vol. 42, pp. 1109–1112; July 1954.)

If Z_L is a pure resistance R_L, the above equation can be simplified as follows:

$$\text{Transducer Gain in db} = 10 \log \left[\frac{4(E_2)^2 R_S}{(E_1)^2 R_L}\right].$$

This equation is correct even if reactance is present in the load impedance Z_L, provided that R_L represents the equivalent parallel resistance of Z_L.

1.1.4.2 Transducer Gain Measuring Circuits

(a)

(b)

(c)
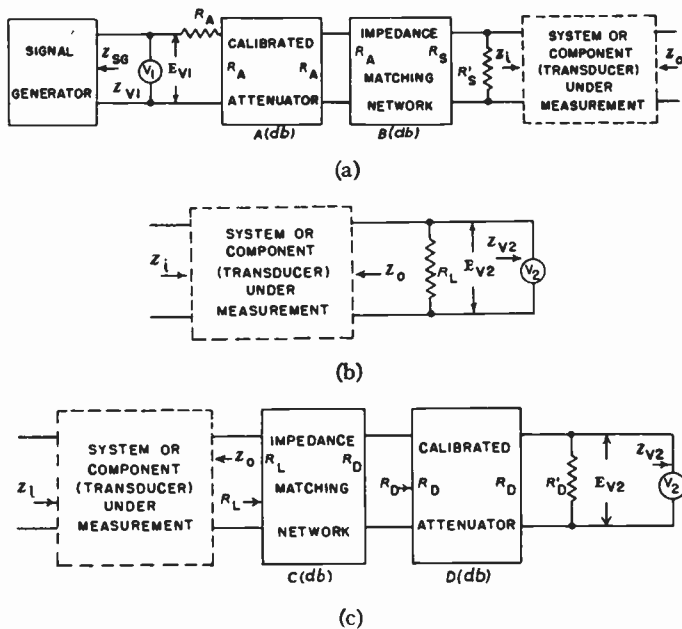
Fig. 5—Suggested circuits for gain measurement. (a) Source circuit arrangement. (b) Load circuit arrangement. (c) Alternate load circuit arrangement.

A—Transducer loss in db of the source-circuit calibrated attenuator.

B—Transducer loss in db of the source-circuit impedance-matching network when operated from a source impedance R_A into a load impedance R_S.

C—Transducer loss in db of the load-circuit impedance-matching network when operated from a source impedance R_L into a load impedance R_D.

D—Transducer loss in db of the load-circuit calibrated attenuator.

E_{V1}—Voltage output of signal generator, as indicated by voltmeter V_1.

E_{V2}—Voltage developed across R_L, as indicated by voltmeter V_2.

R_A—Iterative impedance of source-circuit calibrated attenuator; and input impedance of source-circuit impedance-matching network when the network is terminated in R_S.

R_D—Iterative impedance of the load-circuit calibrated attenuator.

R_D'—Resistance equal in value to R_D.

R_L—Load resistance of system or component under measurement.

R_S—Output impedance of source-circuit impedance-matching network when output terminals of audio signal generator are short-circuited.

R_S'—Shunting resistance across output of source-circuit impedance-matching network.

V_1—Source voltmeter.

V_2—Load voltmeter.

Z_i—Input impedance of system or component under measurement. May contain both resistance (R_i) and reactance (X_i).

Z_o—Output impedance of system or component under measurement. May contain both resistance (R_0) and reactance (X_0).

Z_{SG}—Output impedance of signal generator.

Z_{V1}—Impedance of voltmeter V_1.

Z_{V2}—Impedance of voltmeter V_2.

The circuit of Fig. 4(b) can be considered as a measuring circuit by the addition of the voltmeters necessary to determine the magnitudes of E_1 and E_2. If the impedances of the voltmeters are not sufficiently high so as to have negligible loading effect upon the circuit under measurement, proper allowance must be made.

In some instances it may prove impractical from the standpoint of operational accuracy or convenience to make measurements directly as described above. Therefore, suggested measuring circuits representative of good engineering practice and adaptable to a variety of gain measurements are shown in Fig. 5(a) and 5(b).

These circuits are particularly applicable when the reference source and load impedances of the audio system or component under measurement are resistive in nature, which condition obtains for the great majority of measurements required in audio engineering practice. However, these same circuits may also be used in cases where the source and load impedances of the system or component under measurement are reactive, providing the source-circuit and load circuit impedance-matching networks are suitably modified and calibrated at the measuring frequency.

The source circuits shown in Fig. 5(a) are assumed to include any requisite isolating transformers, as well as appropriate provision for the grounding of the audio system or component under measurement. The source-circuit impedance-matching network of Fig. 5(a) is required when the source-circuit calibrated attenuator does not provide the desired source impedance for the equipment under test.

The load circuits, Fig. 5(b) or 5(c), likewise are assumed to include any isolating transformers and grounding provisions required by the audio system or component under measurement. If the impedance Z_{V2} of Fig. 5(b) is not so high that its shunting effect on R_L can be neglected, then this impedance must be included as part of R_L.

The ability of the measuring circuit to accommodate a wide range of output levels and impedances may be increased by the addition of an impedance-matching pad and a second calibrated attenuator in the load circuit of the system or component under measurement. This is shown in the alternate load circuit of Fig. 5(c). In typical measuring practice, several elements shown in the circuits of Fig. 5(a) through 5(c) may frequently be combined in one physical instrument.

For the measurement of transducer gain the following special conditions apply to the circuits of Fig. 5(a) and 5(b):

$$R_S' = \infty.$$

R_S = Specified source resistance of system or component under measurement.

R_L = Specified load resistance of system or component under measurement.

Then:

Transducer Gain[3] in db $= A + B + 10 \log \left[\dfrac{4(E_{V2})^2 R_A}{(E_{V1})^2 R} \right].$

If as a matter of practical operating convenience the circuit additions of Fig. 5(c) are made, the transducer gain will then be given by the following expression:

Transducer Gain[3] in db
$$= A + B + C + D + 10 \log \left[\frac{4(E_{V2})^2 R_A}{(E_{V1})^2 R_D'} \right]$$
$$= A + B + C + D + 6 + 10 \log \left[\frac{(E_{V2})^2 R_A}{(E_{V1})^2 R_D'} \right].$$

In practice a further simplification is often made in that the meters V_1 and V_2 are calibrated to read level in db above or below some reference power (frequently 1 milliwatt). Such calibration of a meter must, of course, be associated with some specific resistance; a value of 600 ohms is often employed. Therefore, if R_A and R_D are equal in value respectively, to the calibrating resistances of the meters V_1 and V_2 the measurement of gain reduces to the relatively simple process of algebraic addition. For example, transducer gain under these conditions would be as follows:

Transducer Gain[3] in db
$$= (P_{V2}) - (P_{V1}) + 6 + A + B + C + D,$$

where

$P_{V1} =$ Power level in db indicated by voltmeter V_1
$P_{V2} =$ Power level in db indicated by voltmeter V_2.

Where the assembly of measuring equipment is of a permanent nature, a still further operational simplification is quite commonly made, in that the input meter V_1 is calibrated to include both the 6 db factor of the expression above as well as the loss of the source-circuit impedance-matching network, while the load meter V_2 is calibrated to include the loss of the load circuit impedance-matching network. In this case transducer gain would be as follows:

Transducer Gain in db $= (P_{V2}) - (P_{V1}) + A + D.$

1.2 Amplification

Amplification is a general term used to denote an increase of magnitude in transmission from one point to another. Amplification may be expressed as a numerical or logarithmic ratio. By long-standing audio practice amplification is frequently expressed in decibels by multiplying the common logarithm of the ratio by 20, although it would be more appropriate to express this ratio in decilogs.

In audio practice the term "attenuation" is employed for, and should be limited to, the expression of a *current*

[3] In this equation, the factor 4, or the 6 db term, derives from the fact that the reference voltage across the input of the source-circuit calibrated attenuator is one-half the voltage E_{V1} chosen as a reference.

or *voltage* ratio between any two points in a transmission system. When expressing a power ratio it is recommended that the term "loss" be used instead of attenuation. Conversely, the use of the term loss (or the inverse term "gain") to express current or voltage ratios is deprecated.

In the following sections, the measurements of voltage amplification and current amplification are outlined. In referring to the results of these measurements, it is recommended that the complete terminology be used (*e.g.*, "voltage amplification" rather than "amplification"), unless the context is such that there can be no ambiguity.

1.2.1 Current Amplification

Current amplification is the ratio of the magnitude of the current in a specified load impedance connected to a transducer to the magnitude of the current in the input circuit of the transducer. By custom this amplification is often expressed in decibels by multiplying the common logarithm of the ratio by 20.

1.2.1.1 Current Amplification Relations
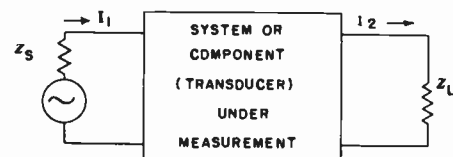
Fig. 6—Elementary circuit for current amplification.

$$\text{Current Amplification} = \frac{I_2}{I_1}.$$

$$\text{Current Amplification in db} = 20 \log \left[\frac{I_2}{I_1} \right].$$

1.2.1.2 Current Amplification Measuring Circuits

The circuit of Fig. 6 may be considered as a measuring circuit by the addition of ammeters or other current measuring devices necessary to determine the magnitudes of the currents I_1 and I_2. The impedance of the device used for measuring I_2 must be taken into consideration if it is significant compared to Z_L.

If the specified load impedance is resistive, a convenient way of determining the load current I_2 is to measure the voltage drop across the load resistance and to compute I_2 as the ratio of load voltage to load resistance. Similarly, for a complex load impedance, the current may be determined by measuring the voltage drop across a resistor inserted in series with the load, and computing I_2 as the ratio of this voltage drop to the value of the series resistor. The magnitude of the series resistor must be such that it will have a negligible effect on the load current.

The input current I_1 is often measured in terms of the voltage drop across a known resistance inserted in series with the input circuit.

1.2.2 Power Amplification

The use of the expression "power amplification" with reference to audio systems and components is deprecated. Power gain (section 1.1.3) is the preferred terminology.

1.2.3 Voltage Amplification

Voltage amplification is the ratio of the magnitude of the voltage across a specified load impedance connected to a transducer to the magitude of the voltage across the input of the transducer. By custom this amplification is often expressed in decibels by multiplying the common logarithm of the ratio by 20.

Voltage amplification is a particularly useful concept in connection with vacuum tube amplifiers, where measurements are frequently made without regard to input and output impedances. For example, the performance of an amplifier operating into the plates of a general-purpose cathode-ray oscilloscope is usefully expressed in terms of voltage amplification. The performance of a transformer connected between a low impedance microphone and the grid circuit of a vacuum tube may also be expressed in this manner.

1.2.3.1 Voltage Amplification Relations
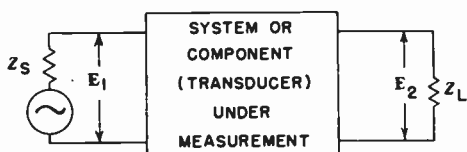
Fig. 7—Elementary circuit for voltage amplification.

$$\text{Voltage Amplification} = \frac{E_2}{E_1}.$$

$$\text{Voltage Amplification in db} = 20 \log \left[\frac{E_2}{E_1}\right].$$

1.2.3.2 Voltage Amplification Measuring Circuits

The circuit of Fig. 7 can be considered as a measuring circuit by the addition of the meters necessary to measure the magnitudes of the voltages E_1 and E_2. If the impedances of the measuring devices are such as to affect the quantities being measured, proper correction must be made. For information concerning the required characteristics of the measuring devices, it is suggested that reference be made to section 1.5.

1.3 Loss (Transmission Loss)

Loss (transmission loss) is a general term used to denote a decrease in power in transmission from one point to another. Loss is usually expressed in decibels, and the term is widely used in audio practice to denote "transducer loss."

There are several types of loss, and the measurement of each is treated under separate headings in the material which follows. In every case loss is a ratio of powers. The type of loss to be measured will depend on the desired application. It is recommended that any expression of loss be identified by the full qualifying terminology (*e.g.*, "transducer loss" rather than "loss") unless, by context, or otherwise, there appears to be no possible chance of ambiguous interpretation.

1.3.1 Bridging Loss

Bridging loss is the ratio of the power dissipated in the reference impedance across which the input of the transducer is bridged, to the power the transducer delivers to a specified load impedance under specified operating conditions. This loss is usually expressed in decibels. In telephone practice this term is synonymous with the insertion loss resulting from bridging an impedance across a circuit.

The application of bridging loss is ordinarily limited to a transmission system in which it is desired to furnish power to an auxiliary load circuit without appreciable influence on the main transmission circuit. For example, in a studio control room of a broadcasting system, the primary of the transformer associated with the input of the monitoring equipment is frequently bridged across the studio program bus. The shunting impedance of this transformer primary is usually much higher than the program bus impedance, so that the loading effect of the monitoring circuit can be considered as negligible. In such an application the transformer under discussion is spoken of as a bridging transformer. The ratio of the power in the main program bus across which this transformer is bridged, to the power at the transformer secondary terminals is taken as the bridging loss of the transformer.

1.3.1.1 Bridging Loss Relations
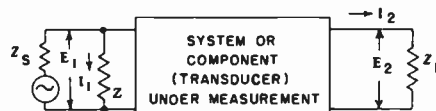
Fig. 8—Elementary circuit for bridging loss.

$Z = R \pm jX$ = Reference Impedance.
$Z_L = R_L \pm jX_L$ = Load Impedance.

$$\text{Bridging Loss in db} = 10 \log \left[\frac{(I_1)^2 R}{(I_2)^2 R_L}\right].$$

Since

$$I_1 = \frac{E_1}{Z}, \quad \text{and} \quad I_2 = \frac{E_2}{Z_L},$$

$$\text{Bridging loss in db} = 10 \log \left[\left(\frac{E_1}{E_2}\right)^2 \left(\frac{Z_L}{Z}\right)^2 \left(\frac{R}{R_L}\right)\right].$$

If Z and Z_L are pure resistance R and R_L, respectively, the preceding equations can be simplified to the following:

$$\text{Bridging Loss in db} = 10 \log \left[\frac{(E_1)^2/R}{(E_2)^2/R_L} \right].$$

Note: This equation is rigorously correct even if reactance is present in the reference impedance Z and load impedance Z_L, provided R and R_L represent the equivalent parallel resistance of Z and Z_L respectively. Equivalent parallel resistance R_{par} can be computed from the series resistance R_{ser} and series reactance X_{ser} by the expression:

$$R_{par} = \frac{(R_{ser})^2 + (X_{ser})^2}{R_{ser}}.$$

1.3.1.2 Bridging Loss Measuring Circuits

The circuit of Fig. 8 can be considered as a measuring circuit by the addition of the voltmeters necessary to read the magnitudes of E_1 and E_2, or the ammeters necessary to read the magnitudes of I_1 and I_2.

If the impedances of the voltmeters or ammeters are such as to affect the quantities under measurement, proper allowance for their presence must be made.

The circuits of Fig. 5(a) and 5(b) are also applicable to the measurement of bridging loss particularly where the input impedance Z_i of the system or component is much higher than the impedance R_S'. The following conditions must be satisfied by the measuring equipment:

$R_S' = R_S =$ Reference impedance Z (resistive) of the bridging system or component under measurement.

$R_L =$ Specified load resistance of the system or component under measurement.

Then:

$$\text{Bridging Loss in db} = 10 \log \left[\frac{(E_{V1})^2 R_L}{4(E_{V2})^2 R_A} \right]$$
$$- 20 \log \left[1 + \frac{R_S'}{2Z_i} \right] - A - B.$$

If $R_S' \ll Z_i$, as is frequently the case, the above equation simplifies to:

$$\text{Bridging Loss in db} = 10 \log \left[\frac{(E_{V1})^2 R_L}{4(E_{V2})^2 R_A} \right] - A - B$$
$$= 10 \log \left[\frac{(E_{V1})^2 R_L}{(E_{V2})^2 R_A} \right] - 6 - A - B.$$

1.3.2 Insertion Loss

Insertion loss, resulting from the insertion of a transducer in a transmission system is the ratio of the power delivered to that part of the system following the transducer, before insertion of the transducer, to the power delivered to that same part of the system after insertion of the transducer. This loss is usually expressed in decibels. The bridging of an impedance across a transmission system is considered one form of insertion loss.

Insertion usually implies the straight-through connection of a three or four terminal transducer at some point in a given two-wire transmission system. Bridging, on the other hand, ordinarily implies the connection of two terminals of a transducer across some point in a two-wire transmission system. Since the transmission loss in the main circuit resulting from either the insertion or bridging connection is of similar nature, the loss associated with either type of connection is designated "insertion loss." Note in the case of bridging that "insertion loss" is a measure of the effect of the bridging connection on the main transmission circuit, while "bridging loss" relates to the loss in the branch (bridging) circuit formed by the bridging connection.

Insertion loss gives a direct measure of the particular type of loss which occurs when a transducer is inserted or bridged at some point in a transmission system. The inserted or bridged transducer may have impedance characteristics which reduce a previously-existing transition loss in the system at the point of insertion, and it is possible for a completely passive transducer to cause an insertion gain when inserted or bridged at some point in a transmission system.

Note should be taken of the fact that the insertion loss due to a transducer is a function of not only the transducer itself, but also of the transmission circuit in which it is inserted. In other words, a transducer may reduce the received power in the load by dissipation within itself, by reducing the power received from the source, or by a combination of both. Therefore, when measuring insertion loss, it is necessary to specify circuit conditions fully.

1.3.2.1 Insertion Loss Relations

$$\text{Insertion Loss in db} = 10 \log \left[\frac{(I_1)^2 R_L}{(I_2)^2 R_L} \right]$$
$$= 20 \log \left[\frac{I_1}{I_2} \right].$$

Or, since E_1 and E_2 are proportional to I_1 and I_2,

$$\text{Insertion Loss in db} = 20 \log \left[\frac{E_1}{E_2} \right].$$

Note that the impedances Z_i, Z_L, and Z_S do not enter into the expression for insertion loss, although they obviously affect the numerical result. Therefore, the equations give a true power ratio, even though all of the above impedances may contain reactance.
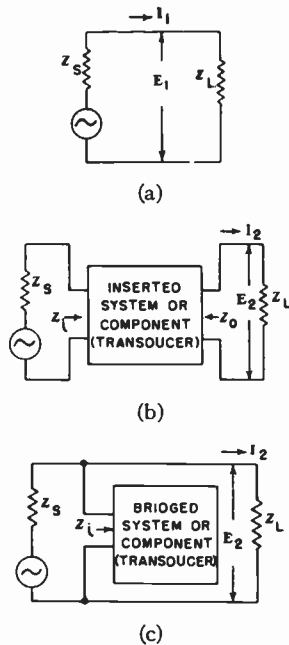
Fig. 9—Elementary circuits for insertion loss. (a) Circuit for determining reference power output before insertion or bridging. (b) Circuit for determining power output after insertion. (c) Circuit for determining power output after bridging.

$Z_i = R_i \pm jX_i =$ Input impedance of inserted or bridged system or component.

$Z_L = R_L \pm jX_L =$ Impedance looking towards output load at the point of insertion or bridging.

$Z_o = R_o \pm jX_o =$ Output impedance of inserted system or component.

$Z_S = R_S \pm jX_S =$ Impedance looking towards source at the point of insertion or bridging.

1.3.2.2 Insertion Loss Measuring Circuits

The circuits of Fig. 9 can be considered as measuring circuits by the addition of the voltmeter necessary to read the magnitudes of E_1 and E_2.

If the impedance of the voltmeter is such as to affect the quantities under measurement, proper allowance must be made.

In a linear transmission system, it is not necessary that insertion loss be measured at the exact point where the insertion or bridging occurs. Since the effects of an inserted or bridged transducer will be the same everywhere in the system after the insertion point, it frequently will be found advantageous to make the insertion loss measurement at the output terminals of the transmission system. This latter procedure may be especially desirable when the insertion occurs at a point in the transmission system where the signal level is too low to be conveniently read by available voltmeters, or where the circuit impedances at the point of insertion are comparable in magnitude to the impedance of the voltmeter.

The substitution method of measurement indicated by Fig. 9 is often the most practical one when Z_S and Z_L are complex, or when the signal level at the insertion point is very low. When Z_S and Z_L are resistive

it may prove convenient to make a direct measurement of the insertion loss of a system or component by means of the measuring circuits shown in Fig. 5(a) and 5(b). The usefulness of these latter circuits is generally restricted to applications involving inserted transducers rather than bridged transducers.

For the direct measurement of insertion loss of an inserted transducer, the following special conditions apply to the circuits of Fig. 5(a) and 5(b):

$R_{S'} = \infty$.

$R_S =$ Specified source resistance of system or component under measurement at point of insertion.

$R_L =$ Specified load resistance of system or component under measurement at point of insertion.

Then:

$$\text{Insertion Loss in db} = 10 \log \left[\frac{(E_{V1})^2 R_L}{4(E_{V2})^2 R_A} \right]$$

$$- 10 \log \left[\frac{(R_S + R_L)^2}{4 R_S R_L} \right] - A - B.$$

The term

$$10 \log \left[\frac{(R_S + R_L)^2}{4 R_S R_L} \right]$$

in the above equation represents the transition loss of the measuring system at the insertion point. If $R_S = R_L$ this term becomes zero.

If the substitution method of making the insertion loss measurement is employed in conjunction with the measuring circuits of Fig. 5(a) and 5(b) it is possible to eliminate the absolute accuracy of the voltmeters V_1 and V_2 as a factor in the accuracy of the desired result. This can be effected simply by noting the reading of V_2 before the insertion, and then readjusting the source-circuit calibrated attenuator to give the same reading of V_2 after the insertion of the system or component. The insertion loss is then indicated directly by the difference in db between the two settings of the source-circuit calibrated attenuator. In making an insertion loss measurement by the above method it is necessary that E_{V1} be held constant before and after the insertion.

In certain cases where the insertion loss is high, the alternate circuit of Fig. 10 may be found more convenient. This is also a substitution method, but in this case the calibrated attenuator and the transducer under measurement are in separate branches of the measuring circuits, so that a higher level is received at the voltmeter V_2.

The measuring procedure when using the circuit of Fig. 10 is as follows:
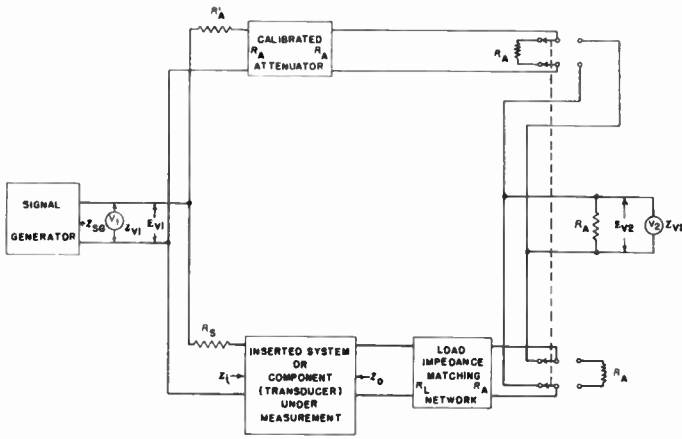
Fig. 10—Alternate circuit for insertion loss measurements by substitution method.

E_{V1}—Voltage output of signal generator, as indicated by voltmeter V_1.
E_{V2}—Voltage developed across R_A, as indicated by voltmeter V_2.
R_A—Load resistance of output indicator-circuit. Equal numerically to iterative resistance of the calibrated attenuator.
R_L—Load resistance of system or component under measurement.
R_S—Source resistance of system or component under measurement.
V_1—Input voltmeter.
V_2—Load voltmeter.
Z_i—Input impedance of system or component under measurement. May contain both resistance (R_i) and reactance (X_i).
Z_o—Output impedance of system or component under measurement. May contain both resistance (R_o) and reactance (X_o).
Z_{SG}—Output impedance of signal generator.
Z_{V1}—Impedance of voltmeter V_1.
Z_{V2}—Impedance of voltmeter V_2.

1) Before the transducer to be measured is inserted (*i.e.*, with R_S connected directly to the load impedance-matching network), operate the switch to first one position and then the other, and adjust the calibrated attenuator until E_{V2} is the same for the two positions. This procedure establishes the reference loss setting of the calibrated attenuator.

2) Insert the system or component as indicated in the figure, and while operating the switch to first one position and then the other readjust the calibrated attenuator until E_{V2} is again the same for both switch positions. A new loss setting of the calibrated attenuator will be obtained. The difference between this setting and that obtained in Step 1 above is the desired insertion loss. The accuracy of the result is not a function of the absolute accuracy of the voltmeters V_1 and V_2, but depends primarily upon the accuracy of calibration of the attenuator.

If the insertion loss is very high, it may be necessary to insert a calibrated amplifier after the system or component under measurement and ahead of the load circuit arrangement. A calibrated amplifier is one of which the gain (or amplification) and amplitude-frequency response are known. If the component under

test is reactive, sufficient isolation, loss, or attenuation should be introduced between the component and the amplifier to avoid reaction between the reactive elements of the component and the input transformer of the amplifier.

1.3.3 Power Loss

The power loss of an audio system or component is the ratio of the power absorbed by the input circuit of a transducer to the power delivered to a specified load impedance under specified operating conditions. This loss is usually expressed in decibels.

The power loss of an audio system or component is ordinarily of rather limited interest. A statement of the power loss of a particular audio system or component usually does not give the most useful information regarding the transmission loss which will result if this system or component is inserted in or bridged across a second audio transmission system. For example, when the system or component under measurement has an input impedance which is very high compared to its source impedance, the power loss may be extremely low, yet the transducer loss of that same system or component may be very high.

1.3.3.1 Power Loss Relations
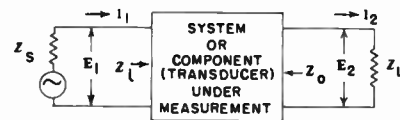
Fig. 11—Elementary circuit for power loss.

$Z_i = R_i \pm jX_i$ = Input impedance of system or component.
$Z_L = R_L \pm jX_L$ = Load impedance.
$Z_o = R_o \pm jX_o$ = Output impedance of system or component.
$Z_S = R_S \pm jX_S$ = Source impedance of system or component.

$$\text{Power Loss in db} = 10 \log \left[\frac{(I_1)^2 R_i}{(I_2)^2 R_L} \right].$$

Since

$$I_1 = \frac{E_1}{Z_i}, \quad \text{and} \quad I_2 = \frac{E_2}{Z_L},$$

$$\text{Power Loss in db} = \left[\left(\frac{E_1}{E_2} \right)^2 \left(\frac{Z_L}{Z_i} \right)^2 \frac{R_i}{R_L} \right].$$

If Z_1 and Z_2 are pure resistance R_i and R_L, respectively, the above equations can be simplified as follows:

$$\text{Power Loss in db} = 10 \log \left[\frac{E_1^2 R_L}{E_2^2 R_i} \right].$$

This equation is rigorously correct even if reactance is present in the input impedance Z_i and the load impedance Z_L provided R_i and R_L represent the equivalent parallel resistance of Z_i and Z_L. Equivalent parallel resistance R_{par} can be computed from the series re-

sistance R_{ser} and series reactance X_{ser} by the expression:

$$R_{par} = \frac{(R_{ser})^2 + (X_{ser})^2}{R_{ser}}.$$

1.3.3.2 Power Loss Measuring Circuits

The circuit of Fig. 11 can be considered as a measuring circuit for power loss by addition of the meters necessary to determine the magnitudes of E_1 and E_2, or I_1 and I_2. If the impedances of the meters are such as to affect the quantities being measured, proper allowance must be made. For information concerning the required characteristics of meters, reference should be made to section 1.5.

1.3.4 Transducer Loss

Transducer loss is the ratio of the available power of a specified source to the power that the transducer delivers to a specified load under specified operating conditions. This loss is usually expressed in decibels. Stated differently, transducer loss is the ratio of the power which an ideal transducer[4] would deliver to a specified load from a specified source to the power delivered by the actual transducer.

Transducer loss (or gain) is the most frequently employed measure of the transmission characteristics of audio systems or components. The transducer loss concept is so widely used and so firmly established in audio practice that it is often expressed loosely as simply "loss" (or "gain"). In order to avoid possible ambiguities, however, it is strongly recommended that the full terminology (*i.e.*, "transducer loss" rather than "loss") be used to express the results of the measurements of transducer loss.

1.3.4.1 Transducer Loss Relations

(a)

(b)
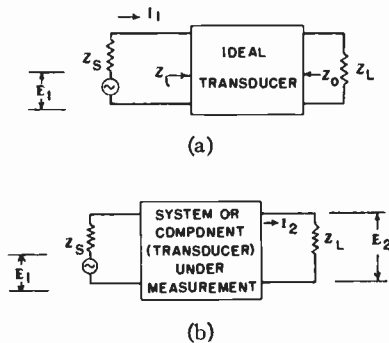
Fig. 12—Elementary circuit for transducer loss. (a) Circuit for determining reference power with ideal transducer. (b) Circuit for determining load power with system or component substituted for ideal transducer.

$$\begin{aligned}
Z_S &= R_S \pm jX_S = \text{Source impedance.} \\
Z_i &= Z_S^* = R_S \mp jX_S. \\
Z_L &= R_L \pm jX_L = \text{Load impedance.} \\
Z_o &= Z_L^* = R_L \mp jX_L.
\end{aligned}$$

[4] Ideal Transducer, *loc. cit.*

Since by definition an ideal transducer dissipates no energy, the reference power in Z_L of Fig. 12(a) above must equal the power Z_i. Thus, the power in $Z_L = (I_1)^2 R_i = (I_1)^2 R_S$.

Note that the reference power is the maximum available power of the source.

Then:

$$\text{Transducer loss in db} = 10 \log \left[\frac{(I_1)^2 R_S}{(I_2)^2 R_L}\right].$$

Or, since

$$I_1 = \frac{E_1}{2R_S}, \quad \text{and} \quad I_2 = \frac{E_2}{Z_L},$$

$$\text{Transducer Loss in db} = 10 \log \left[\frac{(E_1)^2 (Z_L)^2}{4(E_2)^2 R_L R_S}\right].$$

If Z_L is a pure resistance R_L, the above equation can be simplified as follows:

$$\text{Transducer loss in db} = 10 \log \left[\frac{(E_1)^2 R_L}{4(E_2)^2 R_S}\right].$$

This equation is correct even if reactance is present in the load impedance Z_L, provided that R_L represents the equivalent parallel resistance of Z_L.

1.3.4.2 Tranducer Loss Measuring Circuits

The circuit of Fig. 12(b) can be considered as a measuring circuit by the addition of the voltmeters necessary to read the magnitudes of E_1 and E_2. If the impedances of the voltmeters are not sufficiently high to have negligible loading effect upon the circuit under measurement, proper allowance must be made.

In some instances it may prove impractical from the standpoint of operational accuracy or convenience to make measurements directly as described above. Therefore, suggested measuring circuits representative of good engineering practice and adaptable to a variety of loss measurements are shown in Fig. 5(a) and 5(b).

For the measurement of transducer loss the following special conditions apply to circuits of Fig. 5(a) and 5(b):

$R_S' = \infty$.

R_S = Specified source resistance of system or component under measurement.

R_L = Specified load resistance of system or component under measurement.

Then:

$$\text{Transducer Loss in db} = 10 \log \left[\frac{(E_{V1})^2 R_L}{4(E_{V2})^2 R_A}\right] - A - B.$$

If as a matter of practical operating convenience the circuit additions of Fig. 5(c) are made, the transducer loss will then be given by the following expression:

Transducer Loss in db

$$= 10 \log \left[\frac{(E_{V1})^2 R_D'}{4(E_{V2})^2 R_A} \right] - A - B - C - D.$$

In practice a further simplification is often made in that meters V_1 and V_2 are calibrated to read level in db above or below some reference power (frequently 1 milliwatt). Such calibration of a meter must, of course, be associated with some specific resistance. A value of 600 ohms is often employed. Therefore, if both R_A and R_D are equal in value to the calibrating resistance of the meters V_1 and V_2, respectively, the measurement of loss reduces to the relatively simple process of algebraic addition. For example, the transducer loss under these conditions would be as follows:

Transducer Loss in db

$$= P_{V1} - P_{V2} - 6 - A - B - C - D.$$

Where

$P_{V1} = $ Power level in db indicated by voltmeter V_1,
$P_{V2} = $ Power level in db indicated by voltmeter V_2.

Where the assembly of measuring equipment is of a permanent nature, a still further operational simplification is quite commonly made, in that the input meter V_1 is calibrated to include both the 6 db factor of the expression above as well as the loss of the source impedance-matching network B, while the load meter V_2 is calibrated to include the loss of the load circuit impedance-matching network C. In this case transducer loss would be as follows:

Transducer Loss in db = $(P_{V1}) - (P_{V2}) - A - D.$

1.3.5 Transformer Loss

In audio techniques usage, transformer loss is the ratio of the power that would be delivered to a specified load impedance if an ideal transformer were substituted for the actual transformer, to the power delivered to the specified load impedance by the transformer, under the condition that the impedance ratio of the ideal transformer is equal to that specified for the transformer. This loss is usually expressed in decibels.

Note that any transition loss which might result from connecting a given transformer between specified source and load impedances is excluded by definition from the transformer loss expression.

The concept of transformer loss provides a useful measure of the efficiency of an audio transformer. One frequent application is found in high-level sound distribution systems, where it is the usual practice to bridge several loudspeakers across a constant-voltage signal bus. Speaker matching transformers are commonly employed to make the connections between the signal bus and the loudspeaker loads. In such a system, the transmission efficiencies of the speaker-matching transformers are of considerable importance, and the transformer loss concept provides a useful measure of performance.

1.3.5.1 Transformer Loss Relations
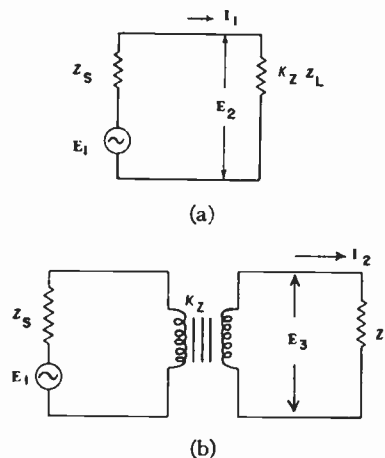
Fig. 13—Elementary circuits for transformer loss. (a) Circuit for determining reference power which would be delivered by an ideal transformer. (b) Circuit for determining load power delivered by actual transformer.

$K_Z = $ Ratio of specified primary impedance to specified secondary impedance of transformer under measurement; a scalar quantity.
$Z_S = R_S \pm J X_S$ Source impedance.
$Z_L = R_L \pm j X_L$ Load impedance.

$$\text{Transformer Loss in db} = 10 \log \left[\frac{K_Z(I_1)^2}{(I_2)^2} \right]$$

$$= 20 \log \left[\frac{\sqrt{K_Z} I_1}{I_2} \right].$$

Since

$$I_1 = \frac{E_2}{K_Z Z_L}, \quad \text{and} \quad I_2 = \frac{E_3}{Z_L},$$

$$\text{Transformer Loss in db} = 10 \log \left[\frac{(E_2)^2}{K_Z (E_3)^2} \right]$$

$$= 20 \log \left[\frac{E_2}{\sqrt{K_Z} E_3} \right].$$

Though the source and load impedances Z_S and Z_L, respectively, do not appear in the above equations for transformer loss, they will obviously affect the numerical result.

If Z_S and Z_L are pure resistances R_S and R_L, respectively, it is convenient from a measurement standpoint to write an expression for transformer loss directly in terms of E_1 and E_2 of Fig. 13(a), without the necessity of separately measuring the reference power which would be transmitted by an ideal transformer.

Thus when Z_S and Z_L are resistive, it can be shown that

$$\text{Transformer Loss in db} = 20 \log \left[\left(\frac{\sqrt{K_Z} R_L}{R_S + K_Z R_L} \right) \left(\frac{E_1}{E_3} \right) \right].$$

1.3.5.2 Transformer Loss Measuring Circuits

The circuit of Fig. 13 can be considered a measuring circuit by the addition of the voltmeters necessary

to read the magnitudes of E_1, E_2, and E_3, or the ammeters necessary to read the magnitudes of I_1 and I_2.

If the impedances of the voltmeters or ammeters are such as to affect the quantities under measurement, proper allowance for the presence of these meters must be made.

1.3.6 Transition Loss

In audio techniques usage the transition loss at any point in a transmission system is the ratio of the available power from that part of the system ahead of the point under consideration to the power delivered to that part of the system beyond the point under consideration. This loss is usually expressed in decibels.

Transition loss occurs at any point in an audio system or component where there is an impedance mismatch between the part of the system ahead of the point under consideration and the part of the system beyond the point under consideration. Transition losses are very common in audio systems and components, and may have a major effect upon the more-frequently measured transmission characteristics such as transducer gain or loss, insertion gain or loss, and bridging gain or loss. For example, in a transmission system where it is desired to furnish power to an auxiliary load circuit without appreciable influence on the main transmission circuit, a bridging transformer may be connected across the main transmission circuit. The input impedance of the bridging transformer in this case would normally be very high compared to the impedance of the main transmission circuit, and the power level in the load circuit of the bridging transformer will be very much less than that in the main circuit. A part of the bridging loss of such a transformer will be due to the transition loss between the relatively low impedance of the main transmission circuit and the very much higher input impedance of the bridging transformer.

1.3.6.1 Transition Loss Relations

$$\text{Transition Loss in db} = 10 \log \left[\frac{(I_1)^2 R_S}{(I_2)^2 R_L} \right],$$

or, since

$$I_1 = \frac{E_1}{2R_S}, \quad \text{and} \quad I_2 = \frac{E_2}{Z_L},$$

$$\text{Transition Loss in db} = 10 \log \left[\frac{Z_L^2}{4R_S R_L} \left(\frac{E_1}{E_2} \right)^2 \right].$$

If Z_S and Z_L are pure resistance R_S and R_L respectively,

$$I_1 = \frac{E_1}{2R_S} \quad \text{and} \quad I_2 = \frac{E_1}{R_S + R_L}.$$

In this case, the expression for transition loss reduces to

$$\text{Transition Loss in db} = 10 \log \left[\frac{(R_S + R_L)^2}{4R_S R_L} \right].$$
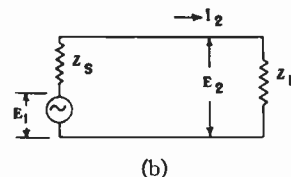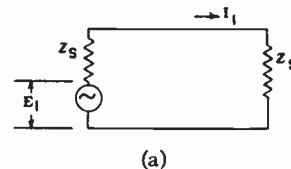
Fig. 14—Elementary circuits for transition loss. (a) Circuit for determining available power from that part of system ahead of the point under consideration. (b) Circuit for determining actual power delivered to that part of the system beyond the point under consideration.

E_1 = Open-circuit voltage of source at point under consideration.
$Z_S = R_S \pm jX_S$ = Source impedance at point under consideration.
$Z_S^* = R_S \mp jX_S$ = Conjugate of source impedance at point under consideration.
$Z_L = R_L \pm jX_L$ = Load impedance at point under consideration.

1.3.6.2 Transition Loss Measuring Circuits

The circuit of Fig. 14 can be considered a measuring circuit by the addition of the voltmeters necessary to read the magnitudes of E_1 and E_2. Unless the impedance of the voltmeter employed to read E_2 is very much higher than Z_L, proper allowance for its effect on E_2 must be made. The impedance of the voltmeter employed to read E_1 has no effect upon the accuracy of the measurement.

1.4 Attenuation

Attenuation is a general term used to denote a decrease in the magnitude of a current or voltage in transmission from one point to another. Attenuation may be expressed as a numerical or logarithmic ratio. By long-standing audio practice attenuation is frequently expressed in decibels by multiplying the common logarithm of the ratio by 20 although it would be more appropriate to express this ratio in decilogs.

In audio techniques the term "attenuation" is employed for, and should be limited to, the expression of a *current* or *voltage* ratio between any two points in a transmission system. When expressing a power ratio it is recommended that the term "loss" be used instead of attenuation. Correspondingly, the use of the term loss (or the inverse term "gain") to express current or voltage ratios is deprecated.

In the following sections, standard methods for the measurement of current attenuation and voltage attenuation are set forth. In referring to the results of such measurements, it is recommended that the complete terminology be used (*e.g.*, "voltage attenuation" rather than attenuation) unless the context is such that there can be no ambiguity.

1.4.1 Current Attenuation

Current attenuation is the ratio of the magnitude of the current in the input circuit of a transducer to the magnitude of the current in a specified load impedance connected to the transducer. By custom this attenuation is often expressed in decibels by multiplying the common logarithm of the ratio by 20.

1.4.1.1 Current Attenuation Relations
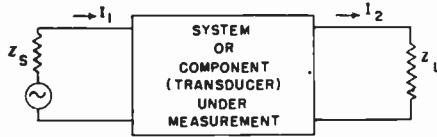
Fig. 15—Elementary circuit for current attenuation.

$$\text{Current Attenuation} = \frac{I_1}{I_2}.$$

$$\text{Current Attenuation in db} = 20 \log \left[\frac{I_2}{I_2} \right].$$

1.4.1.2 Current Attenuation Measuring Circuits

The circuit of Fig. 15 may be considered as a measuring circuit by the addition of ammeters or other current measuring means necessary to determine the magnitudes of the currents I_1 and I_2. The impedance of the device used for measuring I_1 must be taken into consideration if it is significant compared to the load impedance Z_L.

If the specified load impedance is resistive, a convenient way of determining the load current I_2 is to measure the voltage drop across the load resistance, and to compute I_2 as the ratio of this voltage drop to the value of the load resistance. Similarly, for a complex load impedance, the load current may be determined by measuring the voltage drop across a resistor inserted in series with the load, and computing I_2 as the ratio of this voltage drop to the value of the series resistor. The value of the series resistor must be such that it will have negligible effect on the load current.

The input current I_1 can also be measured in terms of the voltage drop across a known resistance inserted in series with the input circuit.

1.4.2 Power Attenuation

The use of the expression "power attenuation" is deprecated. The preferred terminology is "power loss" (section 1.3.3).

1.4.3 Voltage Attenuation

Voltage attenuation is the ratio of the magnitude of the voltage across the input of a transducer to the magnitude of the voltage across a specified load impedance connected to the transducer. By custom this attenuation is often expressed in decibels by multiplying the common logarithm of the ratio by 20.

1.4.3.1 Voltage Attenuation Relations
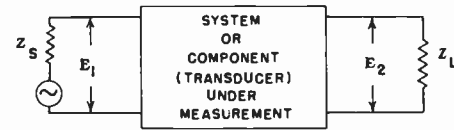
Fig. 16—Elementary circuit for voltage attenuation.

$$\text{Voltage Attenuation} = \frac{E_1}{E_2}.$$

$$\text{Voltage Attenuation in db} = 20 \log \left[\frac{E_1}{E_2} \right].$$

1.4.3.2 Voltage Attenuation Measuring Circuits

The circuit of Fig. 16 may be considered as a measuring circuit, by the addition of the meter necessary to measure the magnitudes of the voltages E_1 and E_2. If the impedances of the measuring devices are such as to affect the voltages being measured, proper correction must be made. For more information concerning the required characteristics of the measuring devices, it is suggested that reference be made to section 1.5.

1.5 Requirements and Characteristics of Measuring Equipment

The following material, while generally applicable to gain, loss, amplification or attenuation measurements, is more specifically related to the representative measuring circuits of Fig. 5(a) through 5(c).

1.5.1 Signal Generator

The signal generator should be adjustable in frequency, preferably continuously, over at least the useful frequency range of the system or component under measurement. For the majority of measurements it is desirable that the frequency calibration of the signal generator be accurate to at least within plus or minus 2 per cent for any frequency within the frequency range under measurement. The frequency of the signal generator should preferably be free from drift over long periods of operation, and should be independent of reasonable variations in power supply voltage. If the frequency drift is of substantial magnitude, means should be provided in the signal generator for convenient recalibration of the indicated frequency.

For measurements on systems or components which have reasonably uniform response over their useful frequency ranges, the total rms value of undesired components of the signal generator voltage, such as harmonics and hum, should not exceed 10 per cent of the total output voltage. However, when making measurements upon systems or components having nonuniform

response-frequency characteristics, the undesired content of the signal generator may have to be considerably less than 10 per cent in order to have a negligible effect on the measurement.

It is desirable from the standpoint of operating convenience that the output level of the signal generator be substantially constant over the useful frequency range of the system or component under measurement. In addition, it is desirable that the output level of the generator be continuously adjustable over at least a moderate range of values.

1.5.2 Indicating Devices

The type of meter available for audio measurement use generally consists of a dc instrument preceded by an input circuit which may contain one of the following devices: a rectifier, an amplifier-rectifier, or a thermocouple.

It is preferable that the input impedance of the indicating device be high enough so that most transmission circuits can be bridged without noticeable effect. However, a low impedance device may be used if its loading effect is taken into account.

The meter should be stable and accurate. Consecutive meter readings should be reproducible. Feedback-stabilized vacuum tube voltmeters can be obtained which are accurate to within ± 2 per cent of any logarithmic scale reading. Indicating devices using disk rectifier types, because of possible aging of the elements, are often conservatively rated at ± 5 per cent of the full scale reading. Thermocouple types are usually rated at ± 2 per cent full scale.

The meter scale and pointer structure should be such that level changes in the system or component under measurement are discernible to the precision desired.

The calibration of the indicating device should preferably be independent of frequency over the operating range of the system or component under measurement. Some conventional instruments using disk rectifiers may show a reduction in indication of 1 per cent per kc; however, vacuum tube voltmeters and thermocouples are usually constant within a few per cent over the entire audio range.

Susceptibility to external effects under unusual operating conditions is a factor to be considered when choosing an indicating device. Disk rectifiers and thermocouples are subject to some error under high ambient temperatures. Vacuum tube voltmeters may become erratic if the line voltage is poorly regulated. In the presence of a strong electromagnetic or electrostatic field, meters with metal shielded cases may be required.

The indicating device should be able to take a substantial momentary overload without damage. The thermocouple type should be protected by a limiter circuit. A meter should be capable of withstanding a reasonable amount of handling and physical shock without readjustment or recalibration.

1.5.3 Graphic Level Recorders

A graphic level recorder may be desirable as a load meter when a considerable number of repetitive measurements are to be made, and especially when non-uniform amplitude-frequency characteristics are anticipated. A logarithmic scale is preferable so that the readings can be obtained directly in decibels. Since many of these devices employ a stepped potentiometer in the moving system, the accuracy is dependent upon the size of the step increment which is generally not less than $\frac{1}{2}$ db. Otherwise the characteristics of a recorder should be similar to that required of a meter.

1.5.4 Attenuators

The accuracy of calibration of the attenuators and the increments of attenuation available have a major bearing on the accuracy with which absolute gain or loss can be determined. The accuracy of the attenuators should be such that both absolute and relative gains or losses are indicated within the desired limits of precision. The attenuators should have a flat response-frequency characteristic over the useful frequency range under measurement.

A total range of attenuation at least equal to that of the over-all gain to be measured is desirable. For greatest accuracy and operating convenience the calibrated attenuators should preferably be adjustable in small increments.

1.5.5 Impedance Matching Networks

Since the impedances of calibrated attenuators are fixed by design, it will be necessary to add impedance-matching networks if the source and load impedances of the system or component under measurement differ from those of the calibrated attenuators. The required accuracy of the values of the resistors used to make up the impedance-matching networks will be governed by the accuracy desired in determining the gain or loss of the system or component under measurement. The impedance-matching networks should have a flat response-frequency characteristic over the useful frequency range under measurement.

1.6 Measurement Procedure

On the assumption that the proper measuring equipment is available for testing the system or component, it becomes the responsibility of the technical personnel to use the equipment correctly.

1.6.1 Conditions

The conditions for the system or component under measurement having a bearing on the accuracy of the measured results include the following:

A. Frequency

The frequency at which gain or loss is measured may often have a substantial effect upon the result, especially for systems or components in which the transmission characteristics are nonuniform over the frequency range of interest (*e.g.*, filters and equalizers).

B. Impedances

The magnitude and phase angle of both the source and load impedance generally have a primary effect upon the measured value of gain or loss. Similarly, the input and output impedances of the system or component under measurement usually have a direct effect upon the measured results, and must be taken into account.

C. Level

Both the input level and the output level of the system or component under measurement will frequently have a bearing on the measured value of gain or loss. This is especially true when the system or component under measurement contains active elements such as vacuum tubes, or iron-cored devices such as transformers and reactors.

D. Distribution of Gains and Losses

When the system or component under measurement has more than one gain control or other provisions for various distributions of gains and losses within the system, the measured value of gain or loss will frequently be a function of the distribution.

E. Waveform Distortion and Noise

If the output of the system or component under measurement contains appreciable distortion and noise products, these may affect the measured value of gain or loss and should be taken into account.

F. Shielding and Grounding

The shielding and grounding of the source and load circuits should be the same as that contemplated for actual use. Care should be taken to prevent undesired coupling between source and load circuits, or serious errors in measurements may result.

G. Power Supply

The voltage, frequency, harmonic content and noise content of the required power supply may have a bearing on the measured results, and should be controlled if necessary.

H. Temperature

Ambient temperature may have an effect upon the system or component under measurement, and should be controlled when necessary. In addition, the internal temperature of the system or component should be stabilized. This latter condition may be accomplished by a preliminary period of operation prior to testing.

1.6.2 Technique

With reference to the typical measuring circuits of Fig. 5(a) through 5(c), the level of the source and the settings of the calibrated attenuators should be adjusted until the level in the load impedance of the system or component under measurement is at a desired value.

If a single voltmeter is alternately connected between the source and load positions, the calibrated attenuators should be adjusted until the voltmeter reading is identical in either position. This procedure will eliminate the calibration accuracy of the voltmeter as a factor governing the accuracy of the measured value. (Likewise, the response-frequency characteristic of the meter may also be neglected.) When switching a single voltmeter between source and load circuits, precautions should be taken to insure that levels throughout the measuring circuit are unaffected by the position of the voltmeter. If the input impedance of the voltmeter is not extremely high compared to the impedances across which it is bridged, it will be necessary to substitute an impedance for the voltmeter impedance when the voltmeter is removed from the circuit.

Where separate source and load voltmeters are used, the absolute value of the voltages enters into the various computations of gain or loss, and it is necessary that the voltmeter calibration be sufficiently accurate at all frequencies to insure the required degree of accuracy of the absolute gain or loss measurement. In addition, the response-frequency characteristics of the source and load voltmeters should be identical, in order that gain or loss measurements on the system or component will not reflect the frequency characteristics of the source and load voltmeters.

In cases where the shunting effect of a voltmeter across the load impedance is not negligible, the value of the load impedance should be altered to such an extent that the parallel impedance of the load and the voltmeter is equal to the rated load impedance of the transmission system at that point.

Adequate shielding of low-level interconnecting cables in the measuring circuit is essential for accurate results. These shields should be grounded at one end only, and in such a manner that ground loops are avoided.

The system or component under measurement should be grounded in the same way for measurement as for actual use. In particular, the grounding or isolation from ground of the source or load or both should be maintained. This necessitates particular attention to the method of grounding the measuring circuits to avoid errors in the results of the measurements.

Where very high values of attenuation are required, it may be desirable to divide the attenuation into sections, physically separated, to reduce coupling effects from input to output.

1.6.3 Presentation of Data

A measurement of gain or loss (and also amplification or attenuation) gives a number which expresses in db or as a ratio the gain or loss of the system or component at a specified frequency and under specified operating conditions.

Gain or loss is usually measured at a frequency in the middle portion of the pass band (or stop band) of the system or component. For systems or components which have reasonably uniform response over the middle range of the audio spectrum, gain or loss is generally measured at a frequency of 400 or 1,000 cps.

2. AMPLITUDE-FREQUENCY RESPONSE

2.1 Introduction

Amplitude frequency response is the amplitude transmission characteristic of a system or component as a function of frequency. The amplitude-response may be stated as actual gain, loss, amplification, or attenuation or as a ratio, of any one of these quantities, at a particular frequency, with respect to that at a specified reference.

2.1.1 Measuring Circuits

Amplitude-frequency response may be measured for systems exhibiting gain, loss, amplification, or attenuation. Typical referenced circuits which are applicable to these types of measurement are:

Insertion Gain	Fig. 2
Transducer Gain	Fig. 4
Insertion Loss	Figs. 9 and 10.

2.1.2 Requirements and Characteristics of Measuring Equipment

The requirements and characteristics for the measuring equipment are similar to those outlined for the measurement of gain, loss, amplification, or attenuation as given in section 1.5.

2.2 Measurement Procedures

2.2.1 Conditions

The considerations given in section 1.6 pertain to all measurements of amplitude-frequency response.

2.2.2 Techniques

2.2.2.1 Amplitude-Frequency Response for Systems or Components Exhibiting Gain or Amplification

With reference to Fig. 4, the output of the signal generator and source circuit calibrated attenuator should be adjusted to provide a convenient mid-scale reading on the output load voltmeter, using a voltmeter

having a scale in db. This should be done for a reference frequency, such as 400 or 1,000 cycles. The input voltage from the signal generator should be kept constant at all frequencies as determined by the source circuit voltmeter. Variations in frequency response for other frequencies may be read directly from the load voltmeter. In some cases it may be more meaningful to keep the load voltage constant while observing the variations of the input voltage as a function of frequency. If the variations are large, it may be necessary to readjust the source circuit calibrated attenuator, and to correct the readings of the load voltmeter for any change in attenuation.

The established reading for the load voltmeter at the reference frequency should be sufficiently above the noise output of the system involved, and sufficiently below the system overload level, to avoid errors due to the presence of noise or harmonic distortion.

2.2.2.2 Amplitude-Frequency Response for Systems or Components Exhibiting Loss or Attenuation

For high loss systems or those whose characteristics change rapidly with frequency, it may be necessary to include a calibrated amplifier as outlined in section 1.3.2.2. The gain or amplification of the amplifier should be at least equivalent to the greatest loss to be measured. Frequency response is then measured utilizing the technique outlined in 2.2.2.1, except that a much greater range of adjustment of the source circuit calibrated attenuator will be required. Components such as filters and equalizers may be measured in this manner. The system or component is generally located ahead of the calibrated amplifier in order to avoid overloading. To reduce interaction, an attenuator is frequently placed between the system or component under measurement and the calibrated amplifier.

2.2.2.3 Presentation of Data

Frequency response is often plotted to show the variation in gain, loss, amplification, or attenuation in db from the actual gain, loss, amplification or attenuation, at a specified reference frequency. It is, of course, permissible to plot actual gain, loss, amplification or attenuation as a function of frequency. Usually a logarithmic frequency scale is employed.

3. REFERENCES FOR GAIN, AMPLIFICATION, LOSS, ATTENUATION, AND AMPLITUDE-FREQUENCY RESPONSE

[1] IRE Standards on Audio Techniques: Definition of Terms, 1954. Standard 54 IRE 3. S1, PROCEEDINGS OF THE IRE, vol. 42, pp. 1109–1112; July, 1954.
[2] IRE Standards on American Recommended Practice for Volume Measurements of Electrical Speech and Program Waves, 1953. Standard 53 IRE 3. S2, PROCEEDINGS OF THE IRE, vol. 42, pp. 815–817; May, 1954.
[3] Johnson, K. S., *Transmission Circuits for Telephone Communication.* New York, D. Van Nostrand Co., Inc., 1925.
[4] Terman, F. E., *Measurements in Radio Engineering*, 1st ed. New York, McGraw-Hill Book Co., 1935.

[5] Pender, H., and McIlwain, K., ed., *Electrical Engineers Hand-book-Electric Communications and Electronics*, 3d ed. New York, John Wiley and Sons, 1936.

[6] Research Council of the Academy of Motion Picture Arts and Sciences, *Motion Picture Sound Engineering*. New York, D. Van Nostrand Co., 1938.

[7] *American Standard Definitions of Electrical Terms*, ASA-C42-1941, American Institute of Electrical Engineers, New York, N. Y. (Under revision by A.I.E.E. Communications Grp. 65—Proposed revision dated August 1953 available but not approved.)

[8] Terman, F. E., *Radio Engineers' Handbook*. New York, McGraw-Hill Book Co., 1943.

[9] Haefner, S. J., "Amplifier-Gain Formulas and Measurements," PROCEEDINGS OF THE IRE vol. 34, pp. 500–506; July, 1946.

[10] *RETMA Standard-Audio Facilities for Radio Broadcasting Systems*, TR-105A, May, 1948; Engineering Department, Radio Electronics and Television Manufacturers Association, Washington, D. C.

[11] *RETMA Standard-Amplifiers for Sound Equipment* SE-101A—July 1949; Engineering Department, Radio Electronics and Television Manufacturers Association, Washington, D. C.

[12] Black, W. L., and Scott, H. H., "Audio Frequency Measurement," PROCEEDINGS OF THE IRE, vol. 37, pp. 1108–1115; October, 1949.

[13] Karakash, J. J., *Transmission Lines and Filter Networks*. New York, The Macmillan Co., 1950.

[14] Johnson, W. C., *Transmission Lines and Networks*. New York, McGraw-Hill Book Co., 1950.

[15] Breazeale, W. B., *Lines, Networks and Filters*. Scranton, International Textbook Co., 1951.

[16] Terman, F. E., *Electronic Measurements*. New York, McGraw-Hill Book Co., 1952.

[17] Koehler, G., *Circuits and Networks*. New York, The Macmillan Co., 1955.

[18] Beranek, L. L., *Acoustic Measurements*. New York, John Wiley and Sons, Inc., 1949.

[19] Beranek, L. L., *Acoustics*. New York, McGraw-Hill Book Co., Inc., 1954.

[20] Sterling, G. E., and Monroe, R. B., *Radio Manual*, 4th ed. New York, D. Van Nostrand Co., Inc., 1950.

[21] Langford-Smith, F., *Radiotron Designers' Handbook*, 4th ed. Wireless Press, Sydney, Australia, 1952 (obtain from RCA, Harrison, N. J.)

[22] *Manual of Electric Instruments*. G. E. Co., Apparatus Dept., GET-1087B, 1954.

[23] Fletcher, H., *Speech and Hearing in Communications*, 2d ed. New York, D. Van Nostrand Co., Inc., 1953.

[24] Potter, R. K., Kopp, G. A., and Green, H. C., *Visible Speech*. New York, D. Van Nostrand Co., Inc., 1947.

Cascaded Feedthrough Capacitors*

H. M. SCHLICKE†, SENIOR MEMBER, IRE

Summary—Feedthrough capacitors built of a multiplicity of stacked disks are practically useless filter elements because they behave essentially like tubular feedthrough capacitors, namely exhibiting pronounced parallel resonances.

However, if washers of suitable, lossy ferrite are interspaced in the structure, the effective coupling impedance for the lower frequencies is identical with the $1/\omega C$, whereas at medium and higher frequencies the effective coupling impedance is reduced by a factor of 1,000 to 10,000 or more, as compared with the best discoidal feedthrough capacitors available now. In fact, the effective coupling impedance is so low that resonances of the disks (even large ones) themselves become negligible. The advantage of the discussed structures is the absence of dc losses.

The mathematical theory for all cases above is developed by matrix algebra and verified by experiments. The selection of the correct ferrite is analyzed.

The practical significance of this development for extremely effective miniaturized low-pass filters is presented.

ORIENTING CONSIDERATION

THIS PAPER is concerned with a new type of ceramic feedthrough capacitor. By incorporating lossy ferrites in a stacked structure of discoidal feedthrough capacitors, extremely effective filter capacitors not available heretofore are evolved. By proper utilization of magnetic losses, the capacity can be increased arbitrarily without introducing undesirable parallel resonances. In addition, at high frequencies the modified capacitors behave as if they were 1,000 to 10,000, or more, times the capacity measured at low frequencies. The new feedthrough capacitors are without losses at dc and low frequencies, since the losses only occur in the vhf and uhf range due to domain wall and gyromagnetic resonances.

This particular solution was sought after known or obvious approaches using dielectrics only failed to yield satisfactory solutions to the following essentially identical problems:

1) To increase the capacity,
2) To increase the voltage rating without decreasing the capacity of ceramic feedthrough capacitors while avoiding detrimental parallel resonances.

It has been shown[1] that discoidal feedthrough capacitors surpass standard tubular feedthrough capacitors in the vhf and uhf range as far as filtering performance is concerned. Hence, the investigation was confined to discoidal capacitors, though extension to tubular capacitors is permissible.

For large capacitances or large electrode spacings, even discoidal feedthrough capacitors become so large in diameter that parallel resonances occur in the vhf and uhf range. Mechanically stacking several small disks of high parallel resonance frequencies led to undesirable low coupling resonance frequencies. Hence, the occurrence of the unexpectedly low resonance frequencies must first be explained to allow finding means to circumvent them.

[1] H. M. Schlicke, "Discoidal vs tubular feedthrough capacitors," PROC. IRE, vol. 43, pp. 174–178; February, 1955.

Theoretical Analysis of Stacked Discoidal Feedthrough Capacitors

Single π-Networks

In Fig. 1(a), two discoidal feedthrough capacitors are shown electrically (as it seems) in parallel, and mechanically cascaded. To start with, resonances in the single-disk feedthrough capacitors are disregarded and assumed to be beyond the frequency range of interest. A closer inspection indicates that the equivalent circuit of Fig. 1(a) is Fig. 1(b); that is the two ideal capacitors are connected by an extremely short transmission line of characteristic impedance Z and of length l.
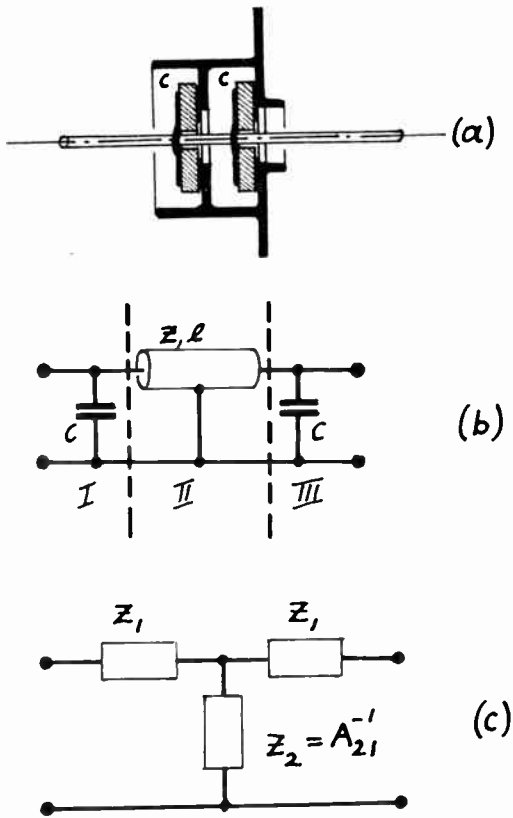
FIG. 1—Mechanical cascading of two discoidal feedthrough capacitors.

To determine what the effective, shunting, coupling impedance Z_2 [Fig. 1(c)] is, the cascade matrices of sections I, II, and III, in Fig. 1(b), have to be multiplied. Hence: with $b = 2\pi l f/3 \cdot 10^{10}$ (l in cm, f in cps)

$$\|A\| = \left\| \begin{array}{cc} 1 & 0 \\ j\omega C & 1 \end{array} \right\| \times \left\| \begin{array}{cc} \cos b & jZ \sin b \\ j \sin b/Z & \cos b \end{array} \right\|$$
$$\times \left\| \begin{array}{cc} 1 & 0 \\ j\omega C & 1 \end{array} \right\|, \tag{1}$$

or

$$\|A\| = \left\| \begin{array}{cc} A_{11} & A_{12} \\ A_{21} & A_{22} \end{array} \right\|$$
$$= \left\| \begin{array}{cc} \cos b - \omega CZ \sin b & jZ \sin b \\ j2\omega C \cos b - j \sin b/Z & \\ -j\omega^2 C^2 Z \sin b & \cos b - \omega CZ \sin b \end{array} \right\|. \tag{2}$$

Since $Z_2 = A_{21}{}^{-1}$ and since $b \ll 1$, the series expansion of $\sin b$ and $\cos b$ in (2) can be limited to the first two terms each, yielding

$$Z_2{}^{-1} = + j2\omega C(1 - (l/3 \cdot 10^{10})^2 \omega^2/2! + \cdots)$$
$$- j(Z^{-1} + Z\omega^2 C^2)((l/3 \cdot 10^{10}) \cdot \omega$$
$$- (l/3 \cdot 10^{10})^3 \omega^3/3! + \cdots). \tag{3}$$

For most practical cases this can be further simplified and approximated to

$$Z_2{}^{-1} \approx j2\omega C - j\omega^3 Z^2 Cl/3 \cdot 10^{10}. \tag{4}$$

A numerical sample indicates the order of magnitude involved. If $Z = 50\Omega$, $C = 500~\mu\mu f$, $l = .1$ cm, then $Z_2{}^{-1}$ is 0 at 780 mc. That means at this frequency the structure constitutes a shunting parallel resonance circuit; just the opposite of what is desirable for a filter capacitor.

Equating (4) with 0 results in the condition for parallel resonance

$$\omega_0 = \sqrt{6 \cdot 10^{10}/CZl}, \tag{5}$$

converting (4) into

$$Z_2{}^{-1} \approx j4.9 \times 10^5 \sqrt{C/Zl}[(\omega/\omega_0) - (\omega/\omega_0)^3]. \tag{6}$$
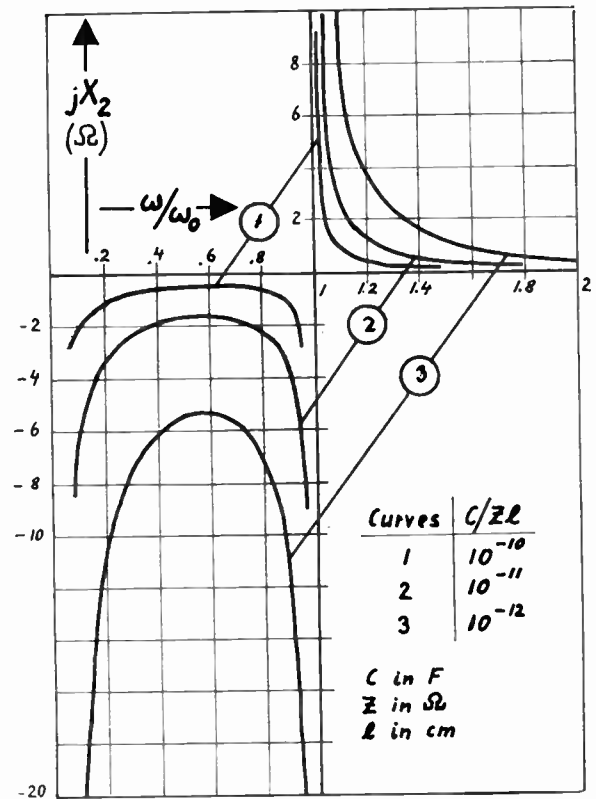
Fig. 2—X_2 vs frequency for two mechanically cascaded discoidal feedthrough capacitors.

For three different parameters, $C/Zl = 10^{-10}$, 10^{-11}, and 10^{-12}, (6) is plotted in Fig. 2. Losses are neglected.

n T-Networks

Stacking an arbitrary number of discoidal feedthrough capacitors by adding monotonously to Fig. 1(a) (π-networks) soon results in untractable expressions.

The following derivations are based on cascading individual T-sections as shown in Fig. 3 representing the equivalent circuit. The extreme shortness of the transmission line under consideration permits us to substitute for the transmission line a constant series inductance L, where $\omega L = Z \sin b \approx Zb$.
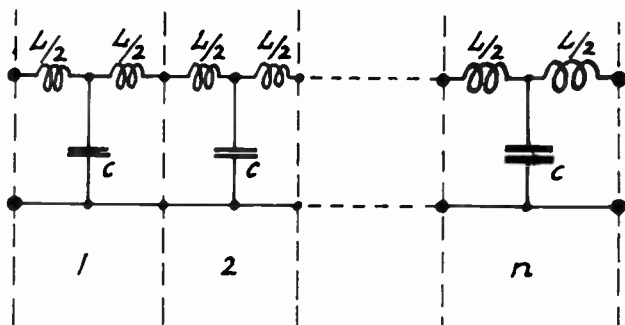
Fig. 3—n T-sections.

A single T-section of Fig. 3 has the matrix

$$\|A\| = \left\| \begin{array}{cc} 1 - \omega^2 LC/2 & j\omega(L/2)(2 - \omega^2 LC/2) \\ j\omega C & 1 - \omega^2 LC/2 \end{array} \right\|. \quad (7)$$

This can also be expressed as a modified transmission line for a frequency dependent characteristic impedance Z_T and phase measure a.

To avoid ambiguity, the latter is now being denoted by a; in (1), for the uniform transmission line, its designation was b. Hence,

$$\|A\| = \left\| \begin{array}{cc} \cos a & jZ_T \sin a \\ j \sin a/Z_T & \cos a \end{array} \right\|. \quad (8)$$

Equating A_{11} from (7) and (8) and using the identity for

$$\cos 2\alpha = 1 - 2 \sin^2 \alpha, \quad (9)$$

yields

$$\omega^2 LC/2 = 2 \sin^2 (a/2), \quad (10)$$

or

$$\omega = (2/\sqrt{LC}) \sin (a/2). \quad (11)$$

Cascading n T-Sections, according to transmission line theory, converts (8) into

$$\|A\|^n = \left\| \begin{array}{cc} \cos (na) & jZ_T \sin (na) \\ j \sin (na)/Z_T & \cos (na) \end{array} \right\|. \quad (12)$$

X_T^2 can be derived from A_{12}/A_{21} in (8). Substituting these terms from (7) yields

$$Z_T = \sqrt{L/C}\sqrt{2 - \omega^2 LC/2} \quad (13)$$

with

$$\omega_0 = 2/\sqrt{LC}. \quad (14)$$

Derived from (11) with $a/2 = \pi/2$, (13) can be rewritten as

$$Z_T = \sqrt{L/C}\sqrt{1 - (\omega/\omega_0)^2}. \quad (15)$$

That means $Z_T/\sqrt{L/C}$ is the quadrant of a circle with the radius one over the linear axis ω/ω_0.

By multiplying A_{12} and A_{21} in (8) and using the corresponding terms of (7),

$$\sin a = 2(\omega/\omega_0)\sqrt{1 - (\omega/\omega_0)^2}. \quad (16)$$

Since the effective coupling impedance Z_2 of the equivalent T-section [Fig. 1(c)], representing now the whole structure of Fig. 3, is

$$Z_2^{-1} = A_{21}. \quad (17)$$

A_{21} taken from (12) gives

$$\boxed{Z_2 = - jZ_T/\sin (na)}. \quad (18)$$

Hence poles of Z_2 are conditioned by

$$\sin (na) = 0, \quad (19)$$

and for

$$\sin (na) = 1 \quad (20)$$

$Z_2 = -jZ_T$ and is tangent to Z_T.

Eq. (19) is fulfilled for

$$a = r\pi/n \qquad (r = 0, 1, 2, \cdots n - 1), \quad (21)$$

(20) for

$$a = r\pi/2n \qquad (r = 1, 3, 5, 7 \cdots). \quad (22)$$

Inserting these values in (11) results in point sequences of extremes of Z_2 plotted in Fig. 4.
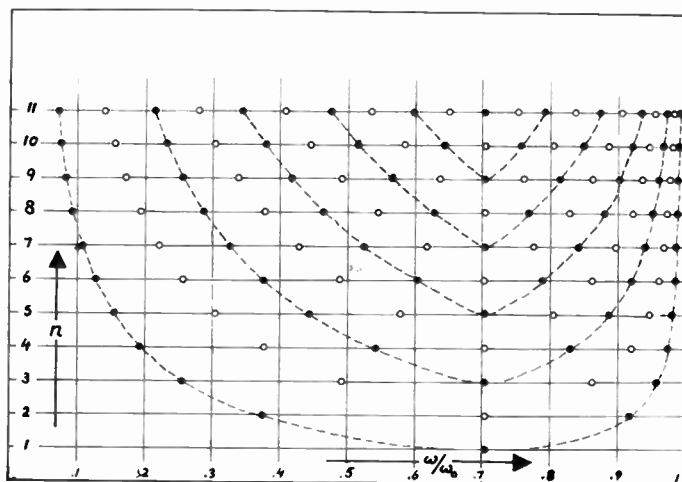
Fig. 4—Poles (dots) and "minima" (rings) for n mechanically cascaded T-Sections.

THEORY OF STACKED DISCOIDAL FEEDTHROUGH CAPACITORS WITH INTERSPACED FERRITE WASHERS

In the vhf and uhf range the effective impedance of a ferrite washer or bead strung on a wire, can by first approximation be considered as a constant impedance predominantly inductive at the low frequencies and essentially resistive at higher frequencies. There are cases where the impedance increases by $f^{.5}$ at most. This

would only mean an improved performance as compared with the one now to be calculated on the basis of nearly constant impedance. As will be confirmed in the next section, ferrite beads behave in the first approximation like equivalent constant resistors R at vhf and uhf. No dc losses occur.

(a)

(b)
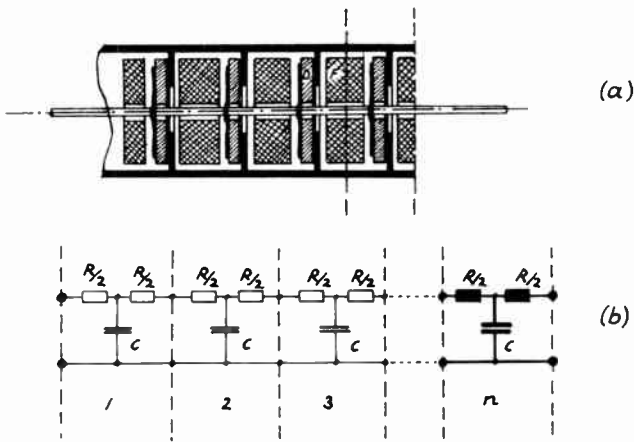
Fig. 5—Mechanically cascaded discoidal feedthrough capacitors with interspaced ferrite washers.

The cascade matrix of a single section of Fig. 5 is

$$\|A\| = \left\|\begin{array}{cc} j\omega C(R/2) + 1 & (R/2)((R/2)j\omega C + 2) \\ j\omega C & j\omega C(R/2) + 1 \end{array}\right\|. \quad (23)$$

The corresponding matrix of a generalized lossy transmission line is

$$\|A\| = \left\|\begin{array}{cc} \cosh g & Z \sinh g \\ \sinh g/Z & \cosh g \end{array}\right\|, \quad (24)$$

with g denoting the complex propagation measure.

Stipulating further,

$$j\omega CR/2 \gg 1 \quad (25)$$

yields

$$A_{11} = \cosh g = j\omega CR/2 = (1/2)(e^g + e^{-g}), \quad (26)$$

and neglecting e^{-g} for $g \gg 1$, in (26), defines

$$e^g/2 = j\omega RC/2, \quad (27)$$

or

$$\ln j\omega RC = g. \quad (28)$$

Thus, following the same reasoning as applied the preceding section for n-sections in cascade (Fig. 5), the equivalent coupling impedance

$$Z_2 = Z/\sinh g = j^{-(n-1)}(1/j\omega C)/(R\omega C/2)^{n-1}, \quad (29)$$

since for large g $\sinh g = \cosh g$.

From

$$A_{12}/A_{21} = Z^2 = (R/2)((R/2) + (2/j\omega C)) \quad (30)$$

or

$$Z \approx R/2. \quad (31)$$

COMPARISON WITH EXPERIMENTAL RESULTS AND CONCLUSIONS

The theory developed in the second section asserts that stacking of n discoidal feedthrough capacitors results in $(n-1)$ poles of the effective coupling impedance. Four $\frac{1}{4}$ inch discs each having a capacity of about 1,400 $\mu\mu f$ were assembled in a fashion shown in Fig. 1(a). The spacing was 0.05 cm accounting for the thickness of the disc and about 0.165 cm more for electrodes and insulation. The relative dielectric constant of the ceramic was 6,000. In Fig. 6, Curve $B1$ (solid) represents the theo-
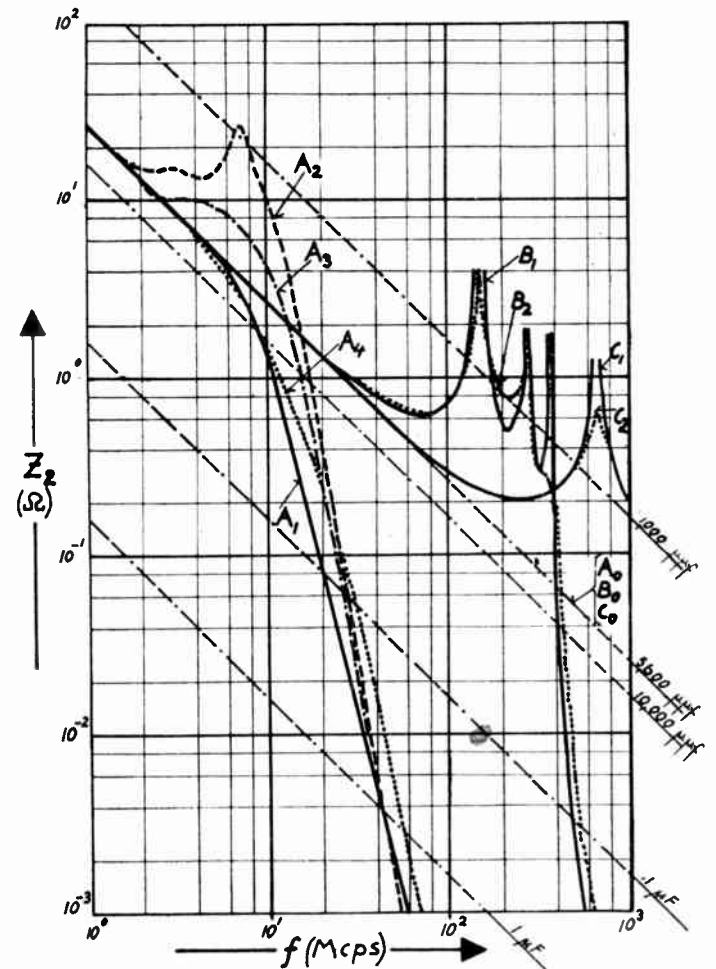
Fig. 6—$|Z_2|$ vs frequency for different filter capacitors of the same nominal capacity (coupling impedances below 1 milliohm are not shown).

retical curve for $n = 4$; Curve $B2$ (dotted) the measured values. The conformance of the curves is obvious. Naturally, the measured curves show no infinite impedance at the poles because of dielectric losses but the position of the poles is exactly as calculated. The third peak of $B2$ is hardly recognizable since the Q of the high ϵ dielectric used is less than 5 at the frequency in point (360 mc). The slight discrepancy between theoretical and experimental curves occurring at the sloping high frequency end is also explainable by the low Q of the dielectric, becoming dominant in the neighborhood of

the series resonance of the discoidal capacitor, occurring at about 800 mc.

The curves B for stacked discs of a total capacity of about 5,600 $\mu\mu f$ are juxtaposed to Curve $C1$ (solid) (theoretical) and $C2$ (dotted) (empirical) representing a single discoidal feedthrough capacitor of about $\frac{1}{2}$ inch diameter having a capacity of the same order of magnitude, namely 5,700 $\mu\mu f$. The parallel resonance of the latter is 680 mc.

It is therefore useless to try preventing parallel resonances of large discoidal feedthrough capacitors by stacking smaller discs of higher parallel resonance frequency. A single small disc capacitor of 1,400 $\mu\mu f$ used for Curve $B2$ has a parallel resonance at about 1,800 mc. Thus the splitting up introduces unavoidable coupling inductances which, though extremely small, bring about undesirably low coupling resonances.

The introducing of ideal lossless ferrites in form of interspaced washers or beads would only change the frequency scale of Curve $B1$, provided the permeability of the ferrite remained constant with frequency. The inductance would be increased and the peaks (poles of Z_2) would be shifted to lower frequencies by a factor of $\sqrt{\mu}$.
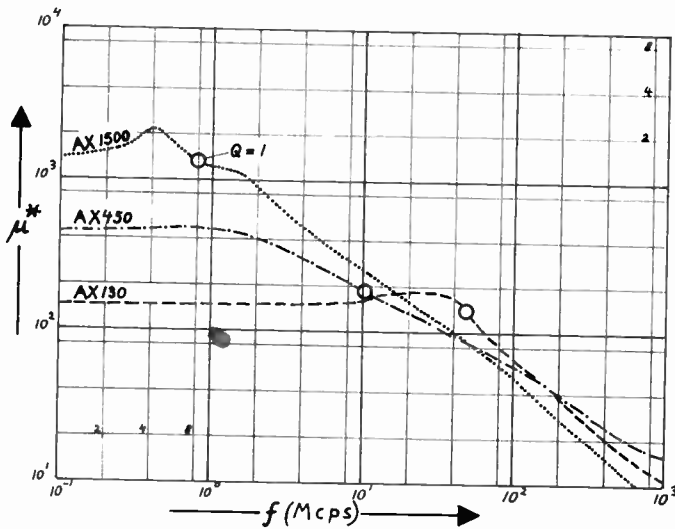
Fig. 7—$\sqrt{\mu'^2 + \mu''^2}$ vs frequency for some of the ferrites used.

However, ferrites are far from being ideal in the vhf and uhf range due to domain wall and gyromagnetic resonances. Fig. 7 represents the absolute value of the complex permeability of three different ferrites as function of frequency. On each curve the point $Q=1$ is marked, where $\mu'=\mu''$. For frequencies lower than the frequency for which $Q=1$ the ferrite is predominantly inductive, and for higher frequencies it is essentially resistive.

To avoid confusion in Fig. 7 and to illustrate in more detail, Fig. 8 brings separately μ' and μ'' for the low permeability ferrite for which $\sqrt{\mu'^2 + \mu''^2} = \mu^*$ is shown in Fig. 7.

Consideration will now be given to the curves $A1$, $A2$, $A3$, and $A4$ (in Fig. 6), representing the behavior of cascaded feedthrough capacitors with interspaced fer-

rite washers [Fig. 5(a)]. The dimensions of the ferrite washers are: height 0.38 cm; od 0.75 cm; and id 0.2 cm. If the slope of $\sqrt{\mu'^2 + \mu''^2}$ vs frequency in Fig. 7 were $-45°$, the impedance of the ferrite bead would be independent of frequency. Since the slope is less than 45°, the impedance increases slightly with frequency. This is the reason why Curve $A2$ (pertaining to ferrite AX 130) and Curve $A3$ (pertaining to ferrite AX 450) in Fig. 8 fall off more steeply than Curve $A1$. $A1$ (solid) is the theoretical curve for four T-sections with a constant magnetically induced R of 50 ohms, the C again being about 1,400 $\mu\mu f$ per section. The curves A, B, and C then have the same nominal capacity.
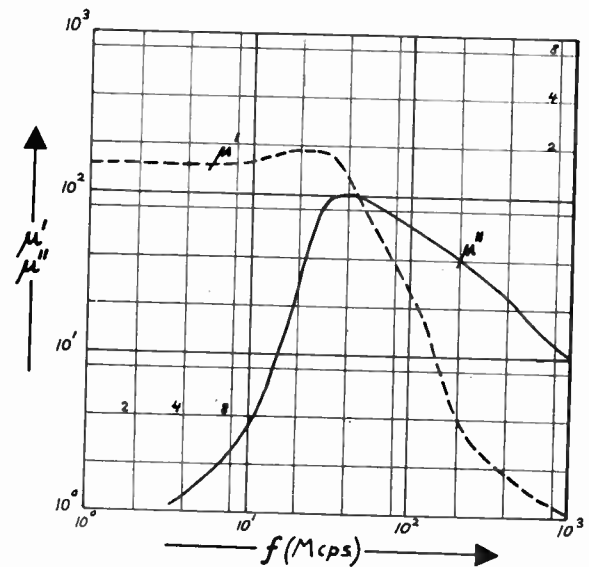
Fig. 8—μ' and μ'' vs frequency for AX 130.

There is another more significant difference in the Curves $A1$, $A2$, $A3$, and $A4$. Using ferrite AX 130, $A2$ shows noticeable deviation. Since $Q=1$ occurs at 40 mc for AX 130, the ferrite is inductive with appreciably high Q below 10 mc where the coupling resonances occur. In contrast, ferrite AX 450, having its $Q=1$ at 10 mc, shows hardly any deviations since heavy damping occurs, but still some variation from the theoretical curve takes place ($A3$).

Curve $A4$ (dotted) is obtained with washers of AX 1,500 ferrite. This ferrite, according to Fig. 7, has its $Q=1$ point at about 1 mcps. The coupling resonances are thus completely damped away. $A4$ is slightly shifted to the right since the washers were made a bit too small, resulting in effective $R < 50$ ohms.

The successive improvement demonstrated by comparing Curves $A2$, $A3$, and finally $A4$, proves conclusively the adequacy of the premises underlying the calculations, namely that the ferrite must behave predominantly resistive in the frequency range where coupling resonances can exist.

In Fig. 6 a few straight sloping dash-dot lines representing constant effective "capacity" are drawn. These curves correspond to $1/\omega C' = |Z_2|$. It is understood that according to (18) and (29), Z_2 may be either capacitive or inductive, at the peaks even resistive. Still, the lines

for effective capacity indicate that the filtering effect is the same as if an equivalent capacitor of capacity C' were used. For instance, at 150 mc for the $n=4$ structure having a low frequency capacity of 5,600 $\mu\mu f$, C' is reduced to 250 $\mu\mu f$ when no ferrite is used, but increased to 40,000,000 $\mu\mu f$ with ferrite washers (outside of range shown in Fig. 6). The single disc structure corresponds to 4,000 $\mu\mu f$ equivalent capacity at the same frequency.

The measurement of the resulting, extremely high insertion loss is rather difficult for two reasons:

1) The high input power required at the filter input to obtain a filter output above the noise level,
2) Leakage within the measuring setup has to be rigorously eliminated.

The curves A in Fig. 6 were validly based on calculations premised upon ideal capacitors in the structure. However, the tremendous transforming effect of the ferrite washers permit in practice the use of large discs (or even tubes) that have their parallel resonances in the operating frequency range. Thereby, large capacity values can be achieved, noticeably improving the performance at very high frequencies. This has been verified experimentally with stacked units consisting of 1 inch diameter discs of 12,000 $\mu\mu f$ each.

For $n=2$ the capacitance transformation is less than for $n=4$. Still, it is quite effective, as Fig. 9 illustrates. However, the reason why the case of $n=2$ is singled out in particular is to show two additional factors affecting the performance:

1) The straight line D_0 represents the behavior of the ideal capacitor of 2,600 $\mu\mu f$. $D1$ stands for two 1,300 $\mu\mu f$ capacitors stacked without a ferrite washer interspaced (theoretical). $D2$ is the theoretical curve of two 1,300 $\mu\mu f$ capacitors separated by a 50-ohm equivalent ferrite washer and two 25-ohm equivalent end sections. $D3$ is the measured curve pertaining to the same arrangement except that the outside cylindrical metal shell is replaced by brackets. A pronounced series resonance appears at 170 mc. In the case of a completely closed coax the outside metallic shell represents 0 impedance (otherwise A_{21} in (2) would have a pole). If the coaxial shell is replaced by brackets, they introduce an easily calculable inductance between the two ground connections of the capacitor C in Fig. 1(b), leading to a series resonance with the C of section I. Depending on the configuration of the bracket the series resonance can be shifted within certain limits, thus permitting a certain equalization of Z_2. For simple structures with n only 2, this may occasionally be quite desirable.

2) $D4$ is based on the same mechanical arrangement as $D3$, however, with three turns around the center ferrite washer. The series resonance frequency is maintained since the same bracket is used, but since the impedance of the decoupling ferrite is increased by 3^2, the filter effect is increased by the same amount. $D4$ is impaired in performance above the series resonance. It is useless to have more than three turns around the ferrite because winding capacitance would shunt the

toroid. For a closed shell even three turns are too much since the shell adds excessive capacity.

Another disadvantage of multiple turns is the reduction in filtering by biasing effects exerted by dc currents through the conductor. For one turn around the ferrite up to 5 amp dc current does not noticeably decrease the filtering performance if the proper ferrite is selected.
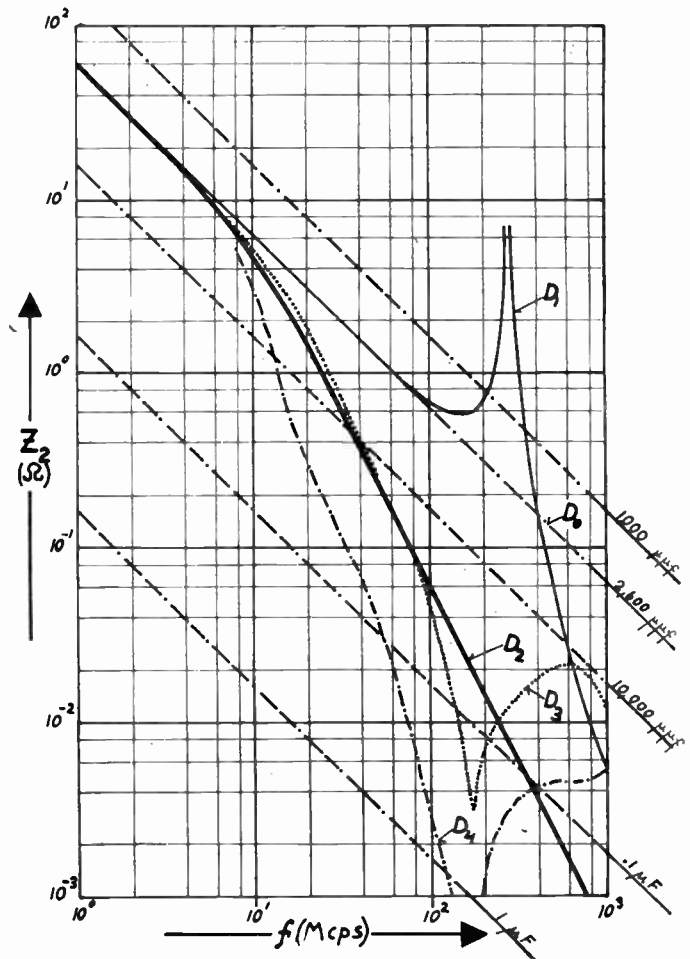
Fig. 9—The effect of brackets for $n=2$ T-Sections.

Finally the new feedthrough capacitors described in this paper act as a complete low-pass filter by themselves above about 20 mc. If the cutoff frequency has to be lowered, filter chokes must be added. Their parallel resonance now can be below 20 mc, thus providing high insertion losses at low frequencies without having to take ineffectiveness at higher frequencies into account.

Correspondence

Estimating the Ratio of Steady Sinusoidal Signal to Random Noise from Experimental Data*

The cumulative distribution of the envelope, R, of $I(t)$, where $I(t)$ is the sum of a steady sinusoidal signal, $P \cos bt$, and random noise, I_N, has been given by Rice[1] in terms of $a = P/$rms I_N, and $v = R/$rms I_N. Curves of this distribution have been presented by Rice[2] in terms of the three variables $p =$ probability that v is not exceeded, a, and $(v-a)$. More recently, curves and tables of this distribution have been presented by Norton, Vogler, Mansfield, and Short,[3] where the three variables considered are $(1-p)$, $K = 20 \log \sqrt{2}/a$, and $R = 20 \log v/a$. (R, in this case, is that used in reference 3, and is not the same as the R previously given, which conforms to the terminology of reference 1.)
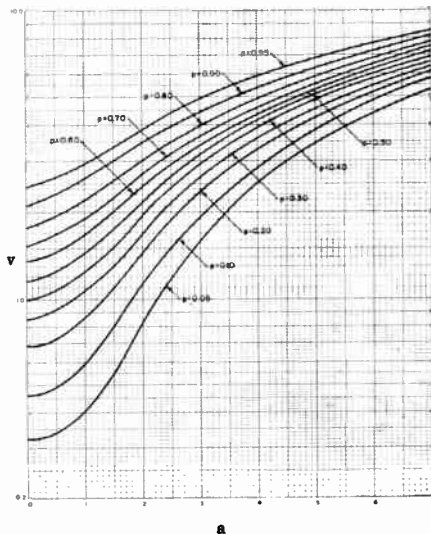
Fig. 1—Cumulative distribution function of the envelope, R, of $I(t)$: $I(t) = P \cos (bt) + I_N$, $p =$ Probability that $R/$rms $I_N < v$, $a = P/$rms I_N, and $v = R/$rms I_N.

Estimation of the ratio a, which is of particular interest in studies of scatter propagation, from observed values of the envelope of received field intensities, R, cannot be made readily from such curves and tables. It may be made directly, however, for the usual case of practical interest—that for which the rms I_N is approximately constant during the interval for which the distribution of R is tested—by suitable plotting of the variables a, v, and p. If v is plotted on a logarithmic scale vs a on any convenient function scale, a family of curves denotes convenient parametric values of p (Fig. 1 above). Observed values of R for conveniently chosen values of p are

plotted on a separate paper, with the same logarithmic scale as v; this plot, consisting of points on a line parallel to v, is superimposed on the set of p curves, so that the best determined values of R for a given p coincide with the curve for that value of p. (Usually the median values—those for $p = 0.5$—are the best determined.) The proper value of a is given by sliding the plot of R values, thus superimposed, along the family of p curves until the best fit of values is obtained. Judgment should be exercised in such fitting so that undue weight is not given to poorly determined values of R for a given p, such as those usually are for regions near the tails of the distribution.

This type of distribution is identical with a Rayleigh distribution for the case $a = 0$, departs rather little from a Rayleigh distribution for values of a between 0 and about 0.5, and rapidly approaches a Gaussian (or normal) distribution with a mean value of P and standard deviation equal to that of the instantaneous values of I_N for further increase of a, so that for most practical purposes the distribution may be considered as Gaussian for values of a higher than 3.

M. L. Phillips
Lincoln Laboratory
Lexington, Mass.

Russian Antenna Terminology*

The glossary given here is a list of some of the more representative types of radio antennas; no effort has been made to include radar or television antennas.

Russian antenna terminology follows closely that used in English; in most cases a literal translation is evident, although it may tend toward British rather than American usage. The adjectival form-образная, found in a number of terms, is equivalent to the English -shaped. Where the antenna is identified by the inventor's name, this is transliterated into Russian in the genitive case and placed following the word antenna. The terms as given are kept as simple as possible and it should not be difficult to determine then, for example, that горизонтальная ромбическая приемная антенна Бруса is the horizontal rhombic receiving antenna of Bruce.

Adcock antenna	антенна Адкока
Bellini-Tosi antenna	антенна Беллини-Този
Beverage antenna	антенна Бевереджа
broadside antenna	антенна "бродсайд"
Chireix and Mesny antenna	антенна Ширекса-Мени
Hertz antenna	антенна Герца
Marconi antenna	антенна Маркони
Zeppelin (Zepp) antenna	антенна "цеппелин"
airplane a.	аэропланная а.
automobile a.	автомобильная а.
aperiodic a.	апериодическая а.

artificial a.	искусственная а.
ball a.	шаровая а.
beam a.	лучевая а.
buried a.	закопанная а.
closed a.	замкнутая а.
condenser a.	емкостная а.
cone a.	коническая а.
cylindrical a.	цилиндрическая а.
dielectric a.	диэлектрическая а.
dipole a.	дипольная а.
direction-finder a.	пеленгаторная а.
extended a.	удлиненная а.
fan a.	веерообразная а.
frame (loop) a.	рамочная а.
ground a.	земная а.
grounded a.	заземленная а.
half-wave a.	полуволновая а.
harmonic a.	гармоническая а.
harp a.	арфообразная а.
horizontal a.	горизонтальная а.
horn a.	рупорная а.
indoor a.	комнатная а.
inverted-L (gamma) a.	Г-образная а.
inverted-V a.	двускатная а.
isotropic a.	изотропная а.
long-wave a.	длинноволновая а.
long-wire a.	длиннопроволочная а.
mast a.	мачтовая а.
monitoring (control) a.	контрольная а.
mobile (movable) a.	подвижная а.
multiple a.	многократная а.
nonradiating (mute) a.	неизлучающая а.
open a.	открытая а.
outdoor a.	наружная а.
parasitic a.	паразитная а.
periodic a.	периодическая а.
phantom a.	суррогатная а.
plain a.	простая а.
plane a.	плоская а.
prism a.	призматическая а.
quarter-wave a.	четверть-волновая а.
quiescent a.	молчающая а.
radiating a.	излучающая а.
receiving a.	приемная а.
reflecting a.	отражающая а.
rhombic a.	ромбическая а.
short-wave a.	коротковолновая а.
short-wire a.	короткопроволочная а.
spring a.	пружинная а.
symmetrical (doublet) a.	симметрическая а.
T a.	Т-образная а.
tier a.	ярусная а.
tower a.	башенная а.
transmitting a.	передающая а.
tuned a.	настроенная а.
umbrella a.	зонтичная а.
underground a.	подземная а.
underwater a.	подводная а.
unidirectional a.	однонаправленная а.
untuned a.	ненастроенная а.
vertical a.	вертикальная а.
wave a.	волновая а.
wire a.	проволочная а.
zigzag a.	зигзагообразная а.

G. F. Schultz
Indiana University
Bloomington, Indiana

Spurious Modulation of Electron Beams*

Cutler's summary of ion noise effects[1] is an excellent one, and badly needed. A few additional points are worth mentioning.

1) Situations which give rise to ion-trapping that is not pressure-sensitive over a wide range of pressures are frequently encountered in designing microwave beam tubes. The most common of these is when the electron beam passes through a drift tube which is gridded at each end. These grids may be necessary for rf reasons, and the resulting ion-trapping be unavoidable. Similar situations arise when the electron beam is scalloped, or when the drift tube wall is scalloped. When these situations exist, positive ions are trapped as they are formed. They can then collect in numbers sufficient to lead to serious ion noise effects even at the best vacuums attainable in commercial practice today.

2) Relaxation oscillations resulting from positive ions are frequently observed at low audio and even sub-audio frequencies. If, as Cutler suggests, the frequency of these relaxation oscillations is related to the build-up time of the positive ions, this serves to confirm 1) above. However, the frequency may be controlled by some other unknown factor.

3) The purpose of my 1952 paper[2] was not to "rediscover" ion noise effects. Instead, it was pointed out that even when reflex klystrons are free of discernible ion-modulation effects, attempts to externally-modulate the tubes at frequencies near the ion-plasma frequencies may lead to distortion and instabilities in the output signal. Effects that have been observed include severe harmonic distortion of the modulating signal, low-frequency jitter and relaxation oscillations induced by external modulation at the ion plasma frequencies, and carrier frequency shifts that are a function of the modulating frequency and can be as great as 0.1 per cent.

THEODORE MORENO
Varian Associates
Palo Alto, Calif.

A Note on the Root Locus Method*

If the transfer function of a closed-loop circuit is given by $KG(s)$, $K>0$, the zeros of $1+KG(s)$ determine the stability of the circuit. One normally wishes to find those values of the gain, $K>0$, for which the zeros of $1+KG(s)$ lie in the left-hand plane. If we

write $G(s)$ as the quotient of two polynomials, $G=\phi_1/\phi_2$, $1+KG(s)=0$ reduces to $\phi_2(s)/\phi_1(s)=-K$ or $\phi_2(s)+K\phi_1(s)=0$. A necessary and sufficient condition that s be a root of $\phi_2(s)/\phi_1(s)=-K$ is that arg $\phi_2(s)$ $-\arg \phi_1(s)=\arg (-K)=\pi$. The root-locus method uses graphical and analytical methods for determining those s for which arg $\phi_2(s)-\arg \phi_1(s)=\pi$.

One notes, however, that if $\phi_1(s)$ and $\phi_2(s)$ are simple polynomials then one can obtain an analytic expression for the locus of roots of $\phi_2(s)+K\phi_1(s)=0$, K real. From $\phi_2(s)/\phi_1(s)=-K$ we have

$$Im \frac{\phi_2(s)}{\phi_1(s)} = 0, \quad Im \phi_2(s)\overline{\phi_1(s)} = 0$$
$$Re\phi_2(s)/\phi_1(s) = -K. \quad (1)$$

The equation $Im\phi_2(s)\overline{\phi_1(s)}=0$ is the locus of complex points s for which $\phi_2(s)/\phi_1(s)$ is real. For each s on this curve we can compute K from $K=-Re\ \phi_2(s)/\phi_1(s)$ or from $K=-\phi_2(s)/\phi_1(s)$. As an example let

$$G(s) = [s(s+1)(s^2+4s+20)]^{-1}.$$

We wish to obtain the locus of points for which

$$Im\ s(s+1)(s^2+4s+20) = 0. \quad (2)$$

One writes $s=x+iy$, and after a few multiplications (2) yields $y=0$ and

$$y = \pm \sqrt{\frac{4x^3+15x^2+48x+20}{4x+5}}. \quad (3)$$

We note immediately that $4x+5=0$ is an asymptote. Two other asymptotes can be obtained as follows. From (3) we have $y\approx \pm\sqrt{x^2+5x/2}$ for x large, so that

$$y \approx \pm x\left(1+\frac{5}{2x}\right)^{1/2} = \pm x\left(1+\frac{5}{4x}\right)$$
$$= \pm \left(x+\frac{5}{4}\right).$$

Thus

$$y = \pm \left(x+\frac{5}{4}\right)$$

are the two remaining asymptotes. We note that the asymptotes intersect at $x=-5/4$. The zeros of $s(s+1)(s^2+4s+20)$ are $s_1=0$, $s_2=-1$, $s_3=-2+4i$, $s_4=-2-4i$ and

$$\sum_{i=1}^{4} s_i = -5.$$

The mean of these zeros is $-5/4$, and we will show that it is no coincidence that the asymptotes intersect at $x=-5/4$. We omit the graph of (3).

One can determine the slopes and the x-intercepts of the asymptotes for the general case as follows. If

$$\phi_2(s) = s^{m+n} + a_1s^{m+n-1} + \cdots$$
$$\phi_1(s) = s^m + b_1s^{m-1} + \cdots,$$

then $\phi_2(s)/\phi_1(s)=-K$ can be written as

$$s^n+(a_1-b_1)s^{n-1}+\cdots+c_n+\frac{r(s)}{\phi_1(s)}=-K \quad (4)$$

with $\phi_1(s)$ of higher degree than $r(s)$. For s large, which in turn implies that $-K$ is

large, the principal term of the left-hand side of (4) is s^n, so that $s^n\approx-K$, and n arg $s=\arg(-K)$, or

$$\arg s=\frac{\pi+2\pi p}{n}, \quad p=0,1,2,\cdots,n-1. \quad (5)$$

Thus

$$\tan\left(\frac{\pi+2\pi p}{n}\right)$$

yields the slopes of the intercepts. To find the x-intercepts of the asymptotes one considers

$$s^n + (a_1-b_1)s^{n-1} \approx -K \quad (6)$$

for s large. Factoring yields

$$s^n\left[1+\frac{a_1-b_1}{s}\right] \approx -K,$$

so that

$$s\left[1+\frac{a_1-b_1}{s}\right]^{1/n} \approx s\left[1+\frac{a_1-b_1}{ns}\right] \approx \sqrt[n]{-K},$$

and

$$s \approx \frac{b_1-a_1}{n} + \sqrt[n]{-K}. \quad (7)$$

Thus s is the vector sum of

$$s_1 = \frac{b_1-a_1}{n} \quad \text{and} \quad s_2 = \sqrt[n]{-K}.$$

Since $\sqrt[n]{-K}$ always has a constant direction, the vector s will appear to move along a straight line originating at

$$x = \frac{b_1-a_1}{n},$$

the x-intercept of the asymptotes. It is known that $-a_1$ is the sum of the zeros of $\phi_2(s)$ and that $-b_1$ is the sum of the zeros of $\phi_1(s)$. One can obtain this same result by an elegant method due to Robert M. Stewart of the California Institute of Technology. For $|s|$ large (4) can be written as

$$(s_1-s_1)(s-s_2)\cdots(s-s_n) \approx -K \quad (8)$$

with

$$\sum_{i=1}^{n} s_i = b_1 - a_1.$$

The log of (8) yield

$$\sum_{i=1}^{n} \log(s-s_i) \approx \log(-K).$$

However,

$$\sum_{i=1}^{n} \log(s-s_i)$$

is essentially the potential due to unit line charges placed at $s_1, s_2, \cdots, s_n$. It is known that if one is far removed from these charges that the field will approximate a field due to a charge placed at the center of charge, namely at

$$x = \sum_{i=1}^{n} \frac{s_i}{n} = \frac{b_1-a_1}{n}. \quad \text{Q.E.D.}$$

HARRY LASS
Motorola Research Lab.
Riverside, Calif.

The Radiation Pattern of an Antenna Mounted on a Surface of Large Radius of Curvature*

Flush mounted antennas on aircraft are now extensively utilized. The patterns are often calculated on the basis that the surface, on which the antenna is located, is flat, infinite in extent, and perfectly conducting. In the case of microwave radiating systems such as slots cut in wing and tail surfaces, these assumptions are not violated to any great extent if the observer is in the *illuminated* portion of space. On the other hand, if the observer is in the "shadow" region the field cannot be predicted unless the diffraction around the edges of wing or tail surfaces are considered. One possible approach from the theoretical standpoint is to represent the surface on which the antenna is located by an idealized shape such as a circular[1] or elliptic[2] cylinder or a sphere.[3] The computations can then proceed in a relatively straightforward manner if the radius of the curvature of the surface is not large compared to the wavelength. In fact, even when the radius of curvature is of the order of several wavelengths, the usual radial mode series solutions can be handled with facility by automatic computing methods. Such a technique was adopted recently in considering radiation patterns of a stub antenna on various cylindrical structures.[4] However, if the radius of curvature becomes quite large, say greater than about ten wavelengths, the summing of the radial mode series is an almost hopeless numerical task. An alternative approach is to transform this poorly converging series to one which is more rapidly varying at least in certain regions of space. This powerful technique was first successfully developed by G. N. Watson[5] and since it makes use of complex function theory, it has been labelled the "residue series." Watson's method was used with success by Van der Pol and Bremmer[5] to evaluate dipole field over a finitely conducting spherical earth. Present purpose is to extend and apply Van der Pol-Bremmer theory to calculate dipole or slot radiation pattern on conducting sphere of large radius.

As a starting point, source is considered to be a vertical (radial) electric dipole located at $r = b$, $\theta = 0$ with regard to a spherical coordinate system (r, θ, ϕ) centered at sphere of radius a. Hertz vector has only a radial component π_r and is given in terms of residue series apart from a constant factor as follows

$$\pi_r = \frac{2\pi i}{(ka)^3} \sum_{s=0}^{\infty} \frac{(\nu_s + \frac{1}{2}) h_{\nu_s}^{(2)}(kb) h_{\nu_s}^{(2)}(kr) P_{\nu_s}[\cos(\pi - \theta)]}{[h_{\nu_s}^{(2)}(ka)]^2 \left[\frac{\partial M(\nu)}{\partial \nu}\right]_{\nu = \nu_s}} \quad (1)$$

where $k = 2\pi/\text{wavelength}$, $h_\nu^{(2)}(x)$ is the spherical Hankel function of the second kind

* Received by the IRE, January 23, 1956.
[1] S. Silver and W. K. Saunders, "The radiation from a transverse slot in a circular cylinder," *J. App. Phys.*, vol. 21, pp. 745–749; August, 1950.
[2] J. R. Wait, "Field produced by an arbitrary slot on an elliptic cylinder," *J. App. Phys.*, vol. 26, pp. 458–463; April, 1955.
[3] C. T. Tai, "Some Electromagnetic Problems Involving a Sphere," Tech. Rep. No. 41, Contract AF 19(604)-266, Stanford Research Inst.; April, 1953.
[4] J. R. Wait and K. Okashimo, "Patterns of stub antennas on cylindrical (and semi-cylindrical) surfaces," *Can. J. Phys.* (in press).
[5] H. Bremmer, "Terrestrial Radio Waves," Elsevier Publishing Co., 1949, New York, N. Y. (The contributions of Watson, Van der Pol and Bremmer are concisely treated in this book.)

of order ν and argument z, $P_\nu[y]$ is the Legendre function of order ν of argument y,

$$M(\nu) = \left\{ \frac{1}{z} \frac{d}{dz} \log \left[z h_\nu^{(2)}(z) \right] \right\}_{z=ka}$$
$$- \left\{ \frac{1}{z} \frac{d}{dz} \log \left[z h_\nu^{(2)}(z) \right] \right\}_{z=k_1 a}, \quad (2)$$

$k_1 = Nk$ where N is the complex refractive index of the sphere, and ν_s is the sth zero of $M(\nu)$. The above expression for π_r given by Bremmer[5] is a rigorous representation for the first rainbow contribution of the field. The other rainbow terms are negligible for the case of a radio transmitter located on the earth. Furthermore, if the conductivity of the sphere becomes infinitely large, the contributions from the higher order rainbow terms vanish and π_r then a complete expression for the total field. In the reduction of the expression for π_r to a form applicable to ground wave propagation, Bremmer[5] makes use of the fact that the ratios b/a and r/a are near unity, that θ is small, and that ka is very large. In considering the radiation pattern of the dipole on a large sphere the ratio b/a can be replaced by unity, but r/a is considered to be a large number and θ is not necessarily restricted to small angles. Furthermore, since the conductivity of the sphere can be regarded as infinite, the quantity N can be replaced by $i^{-1/2} \infty$. Then, after utilizing asymptotic expansions for the spherical Hankel function $h_{\nu_s}^{(2)}(kr)$ and the Legendre function, the field of the dipole can be written $\pi_r = 2\pi_0 P(\theta)$ where π_0 is the primary Hertz potential and $P(\theta)$ is given by

$$P(\theta) = \left(\frac{\pi}{2 \sin \theta} \right)^{1/2} \sum_{s=0}^{\infty} (-1)^{s+1} \frac{\exp \cdot \left[-(ka)^{1/3}(i + \sqrt{3})(A_s/2)(\theta - \pi/2) \right]}{[2A_s]^{3/4}} \quad (3)$$

with $A_s = \frac{1}{2} [3\pi(s + 1/4)]^{2/3}$. The quantity A_s is actually the "tangent" approximation[5] for the quantity $(\nu_s - ka) \cdot (ka)^{-1/3} e^{i\pi/3}$.

The radiation pattern of the radial electric dipole is $\sin \theta \, P(\theta)$ where the $\sin \theta$ is the pattern of the dipole in free space. Furthermore, if the source was a rectangular slot cut in the surface of the sphere, the principal E-plane pattern (in the broadside direction of the slot) would be simply $P(\theta)$. Using the above formula $P(\theta)$ on a decibel scale is plotted in Fig. 1 as a function of θ from 90° to 150° which is the region in space below the tangent plane for various values of D/λ ($D = 2a$). The convergence of the series becomes very poor for θ near 90° and for θ less than 90° the series does not converge at all. At values of θ greater than about 110°, only 1 or 2 terms of the series is required; decibel level of field diminishes linearly with θ.

It is believed that a higher order geometrical optics approximation could be employed to characterize the field above the tangent plane ($\theta < 90°$). In any case the usual second order geometrical optics would simply yield a value of unity for $P(\theta)$ corresponding to the dipole or slot located on a flat per-

fectly conducting surface so that the three computed curves could be extrapolated towards 0 db in the region just less than 90°.

It is worthwhile to show in Fig. 1 some experimental values of the microwave field radiated in the E plane of a slot cut in a five foot diameter metal sphere. These results were obtained at Stanford Research Institute and have been reported by Bain,[6] and
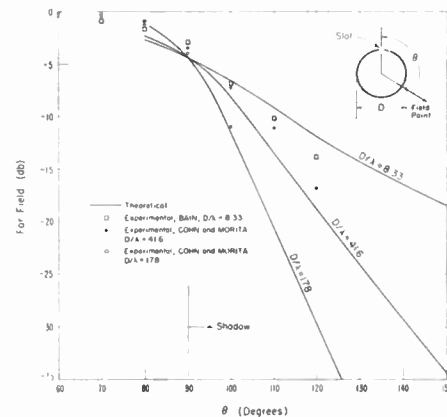
Fig. 1—Broadside radiation pattern of a slot on a large sphere.

Cohn and Morita.[7] The agreement for the electrically largest sphere ($D/\lambda = 178$) is very good; however, the agreement is only fair for the electrically smaller spheres. It is interesting to note, however, that the reduction of the measured field along the tangent plane is approaching the theoretical value of 4.2 db as the sphere diameter becomes large in terms of the wavelength. The discrepancy between the experimental and the calculated values can probably be attributed to the approximations implicit in the reduction of the residue series, the validity of which becomes better as ka becomes large. Furthermore, the experimental values are probably not accurate to better than a db or so, and for deep in the shadow zone, the effect of reflections from adjacent buildings and other structures could cause errors of several db.[8] Nevertheless, the experimental data generally confirm the theoretical prediction that the field is reduced by about 4 db in the tangent plane if the radius of curvature is larger than about 50 wavelengths. It is interesting to compare this value with the 6 db field strength reduction in the tangent plane from an abruptly truncated slot on a flat ground plane.[9,10]

J. R. WAIT
National Bur. of Standards
Boulder, Colo.
(Formerly at Def. Res. Bd., Ottawa, Can.)

[6] J. D. Bain, "Radiation Pattern Measurements of Stub and Slot Antennas on Spheres and Cylinders," Tech. Rept. 42, Contract No. AF 19(604)-266, Stanford Research Inst.; April, 1953.
[7] S. B. Cohn and T. Morita, "Microwave Radiation from Large Finite Bodies," Tech. Rep. 48, AF 19(604)-1296, Stanford Research Inst.; January, 1955.
[8] This is the considered opinion of Dr. S. B. Cohn (private communication).
[9] J. R. Wait and R. E. Walpole, "Calculated radiation characteristics of slots cut in metal sheets," *Can. J. Tech.*, vol. 33, pp. 211–227; 1955. Part I and Part II (in press).
[10] D. G. Frood and J. R. Wait, "An (experimental) investigation of slot radiators cut in metal plates," *Proc. IEE* (B), in press).

Comment on "Radar Polarization Power Scattering Matrix," by C. D. Graves*

I would like to call attention to an error in Mr. Graves' paper.[1] The power scattering matrix cannot "specify the polarization to be used for maximum power return" and at the same time "be completely specified by transmitting at horizontal, vertical, and the $\pm \pi/4$ plane polarization, and measuring the total power back-scattered." The polarization to be used for maximum power return will, in general, be elliptical with a certain sense of rotation. The proper sense of this elliptical polarization cannot be determined by any number of linearly polarized amplitude measurements. It follows that the power scattering matrix cannot be determined from linearly polarized measurements alone.

Mr. Graves has not shown explicitly how the power scattering matrix can be determined from these or similar measurements. A very simple construction on the Poincaré sphere eliminates a great deal of matrix algebra in the analysis of target scattering matrices (see Fig. 1). It is easy
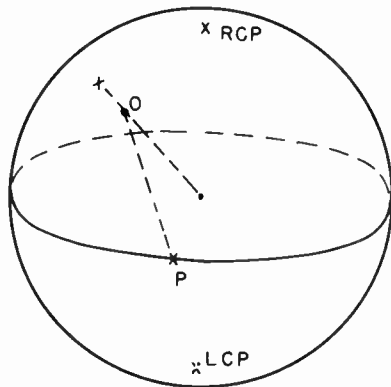
Fig. 1.—Determination of total back-scattered power for transmitter polarization P.

to prove that the total back-scattered power for any transmitting polarization P is equal to the square of the distance OP times a constant C, where C and the point O (lying on or within the polarization sphere) are determined by the target. Determination of the point O and the constant C is equivalent to the determination of the power scattering matrix for the target. This problem is similar to the determination of the polarization of a wave by use of different receiving antenna polarizations, as discussed by Deschamps.[2] No fewer than four measurements will suffice, and the polarizations used must not all lie on the same great circle of the Poincaré sphere.

The Poincaré sphere analysis can also be extended to the determination of echo area for identical transmitter-receiver polarization (see Fig. 2). It is found that two points, O_1 and O_2, on the Poincaré sphere define the antenna polarizations for which zero echo area is obtained. The echo area for any polarization P is proportional to the square of the chord product $O_1P \times O_2P$. The point O mentioned above is the mid-

point of the chord O_1O_2. The null-polarizations O_1 and O_2 and the constant C completely specify the polarization properties of a target.

I disagree with Mr. Graves' statement that the power scattering matrix is simpler to measure than the conventional scattering matrix, which, incidentally, was first applied
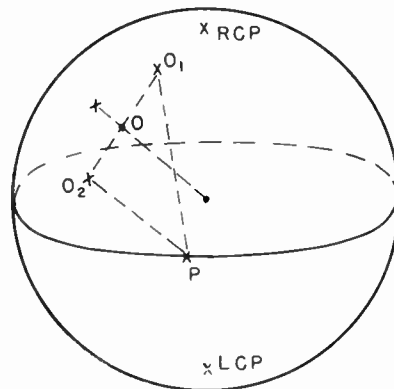
Fig. 2.—Determination of echo area for transmitter-receiver polarization P.

to problems of this sort by Sinclair.[3] It may be shown that seven echo amplitude measurements using identical transmitting-receiving polarizations suffice to determine the conventional scattering matrix. Only one of these measurements need use other than linear polarization. In contrast, measurement of the power scattering matrix actually involves eight measurements if four transmitter polarizations are used and the total back-scattered power in each case is measured, since in practice this would require measuring received power in two orthogonal receiving antennas for each transmission. At least one of the transmitter polarizations must be other than linear polarization in this instance, as well.

A complete discussion of the Poincaré sphere analysis of this problem is given in several unclassified reports.[4,5] This analysis was also presented before the 1951 National Convention. Unfortunately, this material has never been published, but a paper is now in preparation.

E. M. Kennaugh,
Antenna Laboratory,
Ohio State University,
Columbus, Ohio.

Rebuttal*

I would like to thank Mr. Kennaugh for noting an incorrect statement in my recently published paper. Mr. Kennaugh is correct in stating that the power scattering matrix cannot be specified by measuring the total back scattered power without transmitting at least one nonlinear polarization. For example, if the power scattering

matrix is referred to an x-y linearly polarized basis, then a measurement of the total back scattered power after: 1) transmitting at horizontal linear polarization yields directly the element a; 2) transmitting at vertical linear polarization yields directly the element c; 3) transmitting at $\pi/4$ linear polarization yields, after an addition, the real part of the element b; and 4) transmitting at circular polarization yields, after an addition, the imaginary part of the element b. The quantities a (real), c (real) and b (complex) are the elements of the power scattering matrix defined in my paper.

I cannot agree with Mr. Kennaugh's statement that the scattering matrix is simpler to measure than the power scattering matrix. It is to be noted that the scattering matrix can be completely determined by transmitting only two polarizations, both linear, if absolute phase as well as amplitude measurements are made. (Mr. Kennaugh's comment might seem to imply, if not carefully read, that at least one eliptically polarized transmission is always required to determine the scattering matrix.) Since absolute phase measurements are very difficult to make, it is customary to make a number of amplitude measurements at different transmitted polarizations and deduce the elements of the scattering matrix from these. Relative phase measurements, which are simpler to make, would specify the scattering matrix up to a phase angle. For example, if A_{ij} are the elements of the scattering matrix, then one could transmit at horizontal linear polarization and measure the amplitudes of A_{11} and A_{21} and their phase difference. One could then transmit at vertical linear polarization and measure the amplitudes of A_{22} and A_{12} and their phase difference. Since $A_{12} = A_{21}$, by reciprocity, a subtraction yields immediately the phase difference between A_{11} and A_{22}. However this method fails when A_{12} goes to zero. Hence if we restrict ourselves to amplitude measurements, then Mr. Kennaugh states that seven echo amplitude measurements using identical transmitting-receiving polarization suffice to determine the scattering matrix. Thus, seven transmissions, each at a different polarization, must be made and the resultant echo amplitude recorded. Furthermore these measurements yield only algebraic relations among the elements. The recorded data must then be analyzed to determine the elements of the scattering matrix. Hence this method may become impractical for examining several targets at many aspect angles. In contrast, to determine the power scattering matrix, only four transmissions, each at a different polarization, need be made. Only four quantities need be recorded which give directly the elements of the power scattering matrix. (Although practical considerations may dictate that the back-scattered echo be resolved into two orthogonal channels at the antenna, these can be summed giving a single output.) A moment's reflection shows that if one is concerned with measuring the polarization characteristics of a number of targets at all aspect angles, the advantage of the polarization power scattering matrix is considerable and it can indeed be a useful tool in radar polarization analysis.

C. D. Graves,
Engineering Research Institute,
University of Michigan,
Ann Arbor, Mich.

Oral Examination Procedure*

The purposes of an oral examination are few and simple. In these brief notes the purposes are set forth and practical rules for conducting an oral examination are given. Careful attention to the elementary rules is necessary in order to assure a truly successful examination. From the standpoint of each individual examiner the basic purposes of the oral examination are: to make that examiner appear smarter and trickier than either the examinee or the other examiners, thereby preserving his self esteem, and to crush the examinee, thereby avoiding the messy and time-wasting problem of post-examination judgement and decision.

Both of these aims can be realized through diligent application of the following time-tested rules:

1) Before beginning the examination, make it clear to the examinee that his whole professional career may turn on his performance. Stress the importance and formality of the occasion. Put him in his proper place at the outset.

2) Throw out your hardest question first. (This is very important. If your first question is sufficiently difficult or involved, he will be too rattled to answer subsequent questions, no matter how simple they may be.)

3) Be reserved and stern in addressing the examinee. For contrast, be very jolly with the other examiners. A very effective device is to make humorous comments to the other examiners about the examinee's performance; comments which tend to exclude him and set him apart (as though he were not present in the room).

4) Make him do it your way, especially if your way is esoteric. Constrain him. Impose many limitations and qualifications in each question. The idea is to complicate an otherwise simple problem.

5) Force him into a trivial error and then let him puzzle over it for as long as possible. Just after he sees his mistake but just before he has a chance to explain it, correct him yourself, disdainfully. This takes real perception and timing, which can only be acquired with some practice.

6) When he finds himself deep in a hole, never lead him out. Instead, sigh, and shift to a new subject.

7) Ask him snide questions, such as, "Didn't you learn that in Freshman Calculus?"

8) Do not permit him to ask you clarifying questions. Never repeat or clarify your own statement of the problem. Tell him not to think out loud, what you want is the answer.

9) Every few minutes, ask him if he is nervous.

10) Station yourself and the other examiners so that the examinee can not really face all of you at once. This enables you to bracket him with a sort of binaural crossfire. Wait until he turns away from you toward someone else, and then ask him a short direct question. With proper coordination among the examiners it is possible under favorable conditions to spin the examinee through several complete revolutions. This has the same general effect as item 2 above.

11) Wear dark glasses. Inscrutability is unnerving.

12) Terminate the examination by telling the examinee, "Don't call us; we will call you."

S. J. MASON
Research Laboratory of Electronics
Massachusetts Institute of Technology
Cambridge 39, Mass.

Phase Stabilization of Microwave Oscillators*

In the field of frequency multiplication there is a great deal of legend and some measurement[1] on so-called "multiplier phase noise." This is a kind of noise modulation of the multiplied carrier that arises because the onset of conduction of a hard-driven multiplier stage is determined not only by the driver carrier, but also by the grid-tank circuit noise. Although this phase modulation is trivial at the start, it is supposed to become predominant with large multiplication chains, since the modulation index is also multiplied in the process. A paper of the writer and one of his associates[2] on the phase stabilization of microwave oscillators has been called in question on the grounds of applicability because of possible limitation by this "phase noise." This letter is being written to banish such fear.

Two multiplier chains, driven from a single 5 mc source, are used to stabilize two X-band klystrons by the IF offset method (see Fig. 5).[2] The offset frequencies differ by about 900 cps. The outputs of the klystrons are then superposed and amplified by a stable X-band superheterodyne receiver that has an IF of 30 mc and a bandwidth of about 5 mc. The resulting beat displayed through a 0.2 mc video is shown in Fig. 1.

The noise with respect to the carrier was also measured by a GR type 736A wave analyzer. In the region about the carrier, from 0 to 16 kc, it is a constant 61 db below carrier per cps, indicating that no anomalous

[1] J. M. Shaull, "Frequency multiplier and converter for measurement and control," *Tele-Tech*, p. 86; April, 1955.
[2] M. Peter and M. W. P. Strandberg, "Phase stabilization of microwave oscillators," PROC. IRE, vol. 43, p. 869; July, 1955.

"phase noise" exists at low frequencies. This noise spectrum drops to a negligible amount at 100 kc from the carrier, its shape being determined by the high-frequency feedback cutoff. Thus, the effective noise bandwidth in Fig. 2 is about 50 kc, yielding an integrated noise of -61 db $+47$ db $= -14$ db with respect to the carrier, somewhat larger than is observed. In Fig. 2 the beat is shown through a narrow-band filter, approximately 50 cps wide, as essentially noiseless, which it should be for the uniform noise distribution. The signal-to-noise ratio is computed as 41 db, since the filter passes both sidebands.
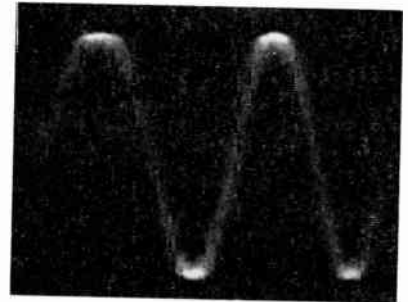
Fig. 1—900 cps beat between two independently phase-stabilized 3-cm klystrons. The display bandwidth is large compared to the carrier-noise spectral width.
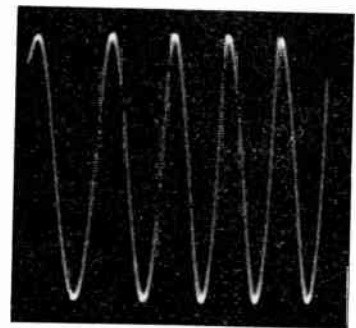
Fig. 2—900 cps beat between two independently phase-stabilized 3-cm klystrons. The display bandwidth is less than the carrier-noise spectral width.

Since the multiplier chain is very poor from the standpoint of minimizing "phase noise" (*i.e.*, it consisted of two quadruplers and one quintupler using 6AK5 pentodes with an over-all multiplication of 1,840 times), it must be concluded that the phase stabilization of microwave oscillators from low-frequency crystal references, or vice versa, is indeed possible (the beat patterns shown in the photographs compare favorably with those obtained from conventional RC oscillators), economical (self-powered units are conveniently assembled on a 10-inch by 12-inch chassis with 8 inches of rack space and they require eight envelopes of receiver type and a power supply), and capable of producing a microwave source with stability, control, and spectral purity not to be obtained by any other presently used means.

M. W. P. STRANDBERG
Dept. of Physics and Res. Lab. of Electronics
Massachusetts Institute of Technology
Cambridge, Mass.

Observations of Electroluminescence Excited by AC and DC Fields in Surface-Treated Phosphors*

Nicoll and Kazan[1] have described the excitation of electroluminescence by dc fields in crt phosphor screens by the application of a potential difference between the aluminium backing and the tube face. The effect was ascribed to the high fields produced across individual phosphor particles. It was also suggested that each particle is prevented from reaching destructive breakdown by the current limiting effect of an adjacent resistive layer.

We have been studying at these Laboratories effects of ac and dc fields on relatively thick compacted layers of phosphor compressed between two conducting surfaces.[2] The emission of light from cells of this type occurs at crystals adjacent to the conducting surfaces and has been observed by us for a number of electroluminescent and cathodoluminescent materials, at voltages considerably less than the breakdown value. Phosphors showing the effect include zinc sulphides, zinc silicates, cadmium borate, zinc phosphate, cadmium chlorophosphate, calcium-magnesium silicate, and calcium phos-

phate. The zinc sulphides used were activated by one of the elements, silver, copper, manganese, and phosphorus. The remainder of the phosphors were activated by manganese except calcium phosphate which was activated by dysprosium.

The essential feature of light production is the coating of the phosphor particles with a layer of an ionizable salt. We have used mainly potassium silicate for this purpose, but a number of the common alkali and alkaline-earth metal salts are also effective.

Taking as an example green electroluminescent zinc sulphide treated with potassium silicate, certain specific and repeatable phenomena occur. In a freshly prepared cell comprising a layer of the treated phosphor 2 square cm in area and about 0.5 mm thick, pressed tightly between two conducting glass surfaces, the application of a 500-v 50-cycle ac supply produces an electroluminescent type of glow from each surface but not from the body of the cell. The intensity of the glow builds up to a maximum in about one minute and is comparable with that from a conventional electroluminescent cell. During this time the cell current decreases from 3.5 ma to 1.0 ma.

Operation of a freshly prepared cell on dc produces light only at the positive face. The brightness is much lower than that observed on ac at a similar voltage. It reaches a maximum in about one second but the cell current decreases from 3 ma to 0.3 ma in about one minute. A cell polarized on dc in this way emits light on ac only at the surface

which was anode during polarization. After several minutes operation on ac there is a slow build-up of light emission at the other face until the luminance at both faces is again equal. The action of this type of cell appears to be primarily electrolytic in which a barrier is formed at the electrode surface of a type conducive to the excitation of luminescence. The presence of mobile ions in the region of the barrier also seems highly probable and in this connection the work of Ince and Oatley on ionic mobility in electroluminescent phosphors is of especial interest.[3]

The fact that cathodo-luminescent phosphors, which are inert in conventional electroluminescent devices, can be excited, indicates that the basic mechanism is akin to that of low-voltage cathode-ray excitation, as suggested by a number of workers in this field to whom Nicoll and Kazan have already referred. It is suggested that the phosphors used by Nicoll and Kazan in their experiments may have become contaminated with potassium silicate or other salts during the preparation of their screens and that the effects described by them are similar to those obtained in our own experiments.

J. N. Bowtell
H. C. Bate
Research Laboratories
The General Electric Company, Ltd.
Wembley, England

Contributors

W. R. Bennett (SM'45–F'56) was born in Des Moines, Iowa, on June 5, 1904. He received the degree of B.S. in electrical engineering from Oregon State College in 1925, and the degrees of M.A. and Ph.D. in physics from Columbia University in 1928 and 1949, respectively. He has been a member of the technical staff in the research department of the Bell Telephone Laboratories since 1925.

W. R. BENNETT

Dr. Bennett is the author of numerous papers related to multiplex telephony. He is a member of Tau Beta Pi, Eta Kappa Nu, Sigma Xi, the American Institute of Electrical Engineers, and the American Physical Society. He is secretary of the AIEE Committee on Communication Theory.

Marvin Chodorow (A'43–SM'47) was born on July 16, 1913, in Buffalo, N. Y. He received the B.A. degree in physics from the University of Buffalo in 1934, and the Ph.D. degree from the Massachusetts Institute of Technology in 1939.

During 1940 he was a research associate at Pennsylvania State College. Dr. Chodorow was an instructor of physics at the College of the City of New York

M. CHODOROW

from 1941 to 1943, when he became associated with the Sperry Gyroscope Co. as a senior project engineer. He remained at Sperry until 1947, when he joined the physics department of Stanford University, where he is now professor of applied physics and electrical engineering.

Dr. Chodorow is a member of the American Physical Society, and of Sigma Xi.

❖

E. J. Nalos (SM'54) was born in Prague, Czechoslovakia, on September 10, 1924. He received the degree of Master of Applied Science in 1947 from the University of British Columbia, and continued his graduate studies as a research and teaching assistant at the Microwave Laboratory at Stanford University under a Sperry Gyroscope Company fellowship. In 1951, he obtained the Ph.D. degree for his study on debunching of electron beams.

E. J. NALOS

Dr. Nalos worked as a research associate at the Microwave Laboratory, where he was

active in high-power microwave tube research leading to the development of megawatt pulsed TW tubes. In cooperation with Dr. Ginzton, he was active in the Microwave Measurements course, and the evolution of a laboratory manual under joint authorship. He is presently working on high-power traveling-wave tubes at the General Electric Microwave Laboratory in Palo Alto, Calif.

He is a member of Sigma Xi.

❖

J. R. Pierce (S'35–A'38–SM'46–F'48) was born in Des Moines, Iowa, on March 27, 1910. He received his Bachelor's and Master's

J. R. PIERCE

degrees in electrical engineering from the California Institute of Technology in 1933 and 1934 respectively. In 1936 he received his Ph.D. degree from the same institution.

Since 1936 he has been a member of the technical staff of the Bell Telephone Laboratories, Inc., where he has been concerned with various vacuum-tube problems. In January, 1952, he became director of Electronics Research at Bell Laboratories, and since August, 1955 he has been Director of Research for Electrical Communication.

In 1948 Dr. Pierce received the IRE Fellow Award for his "many contributions to the theory and design of vacuum tubes." Dr. Pierce is the recipient of the Eta Kappa Nu "Outstanding Young Electrical Engineer" award for 1942, and the IRE Morris Liebmann Memorial Prize for 1947. He is the author of two widely known books in his field, *Theory and Design of Electron Beams*, and *Traveling Wave Tubes*, and in addition has written many popular science articles for various magazines.

He is a member of the National Academy of Science, a Fellow of the American Physical Society, and a member of the American Institute of Electrical Engineers, the British Interplanetary Society, Tau Beta Pi and Sigma Xi. He was formerly Editor of the PROCEEDINGS OF THE IRE and a Director of the IRE during 1954–1955.

H. A. Samulon (A'46) was born in Graudenz, Germany, in 1915. He attended the Swiss Federal Institute of Technology

H. A. SAMULON

in Zurich, graduating with the degree of dipl. ing. in 1939. After doing postgraduate work at the Institute of High-Frequency Techniques, he was employed from 1943 to 1947 as an instructor and research engineer at the Institute of Communication Techniques and the Acoustical Laboratory of the Swiss Federal Institute of Technology.

In 1947, Mr. Samulon joined the Electronics Division of the General Electric Co., where he was engaged in TV problems, with special regard to transient phenomena as well as system problems in black-and-white and, as a member of Panel 13, NTSC, in color television.

Since 1955, Mr. Samulon has directed the analysis group of the Radar Department, Guided Missile Research Division of the Ramo-Wooldridge Corp.

❖

Kurt Schlesinger (A'41–SM'51–F'54) received the Doctor of Engineering degree in Berlin, and joined the Radio Research Laboratory of von Ardenne, in 1929.

KURT SCHLESINGER

From 1931 until 1938 he held the position of Chief Engineer in the television research department of Loewe Radio Berlin.

From 1938 through 1940, Dr. Schlesinger worked in Paris as a consultant to Radio-Gramont.

In the United States he first held a position with RCA Laboratories, located at Purdue University, from 1941 to 1944. During that time he developed a system for television sound multiplexing which employed frequency modulated wave bursts during the picture retrace. From 1944 through 1947, Dr. Schlesinger was consulting engineer in the color television department of CBS.

Since 1947 he has been in charge of television research with Motorola, Inc., Chicago, where he has been engaged in television receiver design for both monochrome and color. He also developed a system for increasing picture detail by scanning with arrested dots, and invented Motorola's Deflectron, an internal electrostatic yoke for cathode ray tubes.

Dr. Schlesinger has received more than two hundred U. S. patents, and has authored numerous technical articles and publications. Recently he contributed a section to the Handbook of Television Engineering edited by D. G. Fink. He has served on National Television System Committees studying dot interlace and color.

❖

H. M. Schlicke (M'49–SM'54) was born in Germany, on December 13, 1912. After graduation from the Staatsrealgymnasium

H. M. SCHLICKE

in Annaberg, he studied at the Institute of Technology in Dresden, majoring in electronics. In 1938 he received the degree of Doctor of Engineering Sciences with Professor Barkhausen as referent.

After several years as research engineer at the laboratories for large transmitters at Telefunken, Dr. Schlicke became head of the Naval Test Fields for communications, radar and infrared devices in Kiel, Germany. Later he originated, organized and supervised large-scale countermeasures projects. After the war, he was brought to this country by the U. S. Navy as a "paper clip" scientist. He worked as project engineer and special consultant on classified projects for the Office of Naval Research at Port Washington, Long Island, New York.

Since 1950 Dr. Schlicke has been with the Allen Bradley Co. in Milwaukee, Wis., where he is head of the High-Frequency Laboratory, working predominantly on the evaluation and application of ferrites and high K dielectrics.

1956 IRE CONVENTION HIGHLIGHTS AND PERSONALITIES

Above—Banquet scene at the Waldorf-Astoria. *Below*—Mr. Loughren, Herre Rinia, IRE Vice-President, and G. W. Bailey, IRE Executive Secretary, chat.

Above—1956 IRE President A. V. Loughren presents the Medal of Honor to J. V. L. Hogan at the annual March national convention of over 40,000 engineers and scientists in New York City.

Below, left to right—C. G. Suits, who spoke for the Fellows, and 1956 award winners J. E. Bridges, K. Bullington, J. V. L. Hogan, F. J. Bingley and W. S. Hinman, with A. V. Loughren (*fourth from left*). *Right*—The two surviving founders of the IRE, A. N. Goldsmith and J. V. L. Hogan.
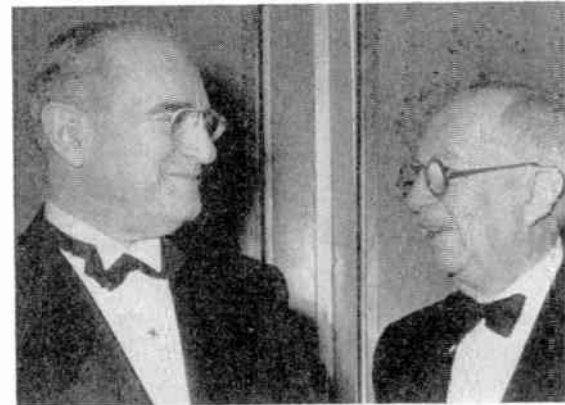
Above—Members of the 1956 general convention committee were (*left to right, standing*): B. F. Tyson, Cocktail Party; J. F. Bisby, Registration; R. R. Law, Technical Program; R. P. Burr, Banquet; J. S. Saby, Convention Record; L. G. Cumming, IRE Activities; W. C. Copp, Exhibits; J. B. Buckley, Finance; W. A. Baston, Facilities; H. Atwood, Jr., Hospitality. *Seated*—L. Petranek, Exhibits; E. Sirjane, Secretary; G. W. Bailey, Chairman; S. L. Bailey, Vice-Chairman; and E. K. Gannett, Publicity. *Right*—Cocktail hour at the Waldorf.

Above—Only one of the most popular sessions on the convention calendar, this symposium on the United States earth satellite program broke all attendance records. *Below*—Chairman W. R. G. Baker is at the microphone while his colleagues (*left to right*) J. A. Van Allen, J. T. Mengel, D. G. Mazur, M. W. Rosen, J. P. Hagen, and L. V. Berkner listen to his remarks on the earth satellite program. Arrangements are being made to publish the entire symposium in an early issue of PROCEEDINGS.

Left—The administrative committee of the PG on Ultrasonic Engineering. *Left to right* —J. F. Herrick. Vice-Chairman, A. L. Lane, C. M. Harris, O. E. Mattiat, M. D. Fagen, Chairman, J. E. May, Jr., Secretary, J. K. Hilliard, W. P. Mason, and Julius Bernstein, Treasurer.

Above—The PG on Broadcast Transmission Systems sponsored a session on TV transmitting equipment and techniques. At the speakers' table (*left to right*) are: W. B. Harris, R. E. Rohrer, J. B. Epperson, C. B. Mayer, C. A. Cady, and H. H. Leach. *Below*—The administrative committee of the PG on Vehicular Communications held a dinner meeting during the convention. Shown (*left to right*) are: A. B. Buchanan, S. C. Bartlett, Secretary, M. E. Kennedy, N. Monk, Chairman, C. M. Heiden, Vice-Chairman, L. E. Kearney, Treasurer, and W. A. Shipman.

Above, right—A glimpse of the many exhibits on view at the Kingsbridge Armory in New York City, March 19–22. *Above, left*—An engineer shows how, through the utilization of transistors and diodes, this electronic robot system decodes messages on punched tape and spells out words in lighted letters.

Above—This self-supporting, oscillograph-record camera is the first recorder specifically designed for use with three-inch cathode-ray oscillographs. It offers full binocular vision and produces prints one minute after exposure. *Below*—These dual-tube carts for aluminizing TV picture tubes can evacuate and coat two tubes with a single vacuum-pumping system. The standard five-cart continuous system, operating on a circular track seventeen feet in diameter, will turn out 96 finished 21-inch picture tubes per hour.

Above—Shown enlarged next to a match is a midget hermetically-sealed electric condenser, ¾" in diameter by ½" in length, to be used in the miniaturized electronic circuits of guided missiles. *Below*—This electronic memory system reduces the contents of sixteen thousand conventional file cabinet drawers to less than three cubic feet of space by automatically sequencing, selecting, collating and separating information recorded on magnetic tape. The tape is fed to a companion electronic computer.

IRE News and Radio Notes

PGANE Offers Free Copies of its Transactions to All

The Professional Group on Aeronautical and Navigational Electronics has an active membership of over 1,900. The Group has published at least four Transactions each year covering the application of electronics to navigation, traffic control and landing of aircraft and to navigation of all craft. If you are not a member of PGANE, you are missing out on sharing the latest developments in this field with your fellow engineers.

In order that you may get acquainted with the Transactions and judge for yourself the value of membership in PGANE, the Administrative Committee has arranged to send you, free of cost, a copy of a PGANE Transactions. Send your name and address to: Miss Emily Sirjane, IRE, 1 East 79 St., New York 21, N. Y. and ask for a copy of a PGANE Transactions.

National Telemetering Conference Is Slated for Aug. 20–21 at Los Angeles

The National Telemetering Conference will be held at the Biltmore Hotel, Los Angeles, California, August 20–21. The conference will be sponsored by the IRE, the American Institute of Electrical Engineers, the Institute of Aeronautical Sciences, and the Instrument Society of America.

Papers will be presented on novel industrial or military applications of telemetering in remote measurement systems, flight test data, remote guidance systems, remote monitoring, and air traffic control. New component developments such as transducers, multiplexers, data recorders, transmitters and receivers, pickoffs, and telemetering filters will also be discussed at the conference. The program will also cover telemetering and remote control system problems of coding, loop response, computers in remote links, microwave relay lines, and noise in telemetering channels.

The executive committee of the conference includes: R. R. Dexter, *Chairman;* L. G. Cumming, C. H. Hoeppner and R. E. Rawlins, *IRE Representatives;* R. S. Gardner, G. M. Thynell and A. J. Hornfeck, *AIEE Representatives;* K. C. Black and E. W. Robischon, *IAS Representatives;* W. H. Kushnick and R. E. Wendt, Jr., *ISA Representatives;* and Kipling Adams, *1955 NTC Chairman.* Conference committee members are: H. L. Hull, *Chairman;* L. W. Gardenhire, *Vice-Chairman;* F. Rucker, *Treasurer;* D. M. Culler, *Secretary;* R. E. Rawlins, *Program Chairman;* E. L. Gruenberg, *Program Vice-Chairman;* and John Spargo, *Publicity.*

H. Chait and N. Sakiotis Get PGMTT Award for Best Paper

H. N. Chait and N. G. Sakiotis, Associates of the IRE, have won the first annual award for an outstanding contribution to the microwave art published in the Transactions of the Professional Group on Microwave Theory and Techniques. Both men are electronic scientists at the Naval Research Laboratory, and members of the Washington Section.

Their prize-winning paper, "Properties of Ferrites in Waveguides," was published in the Transactions of the Professional Group on Microwave Theory and Techniques for November, 1953. The award of $100 was presented to the two men at the banquet of the Microwave Ferrites Symposium in Cambridge, Mass., April 2–4.

Early Submission of Papers Urged for PGED Meeting

The Second Annual Technical Meeting of the IRE Professional Group on Electron Devices will be held October 25–26, at the Shoreham Hotel in Washington, D. C., it has been announced by T. M. Liimatainen of Diamond Ordnance Fuze Laboratories, general chairman for the meeting.

A call for titles and abstracts of 100–200 words on papers to be offered for presentation is being issued by R. L. Pritchard of the Research Laboratory, General Electric Co., Schenectady, N. Y., in charge of the meeting's technical program. The deadline for receiving titles and abstracts is August 1, but the earlier submission of titles to facilitate planning is requested.

Some Highlights of the Recent Southwestern Conference at Oklahoma City

Shown (*left to right*) are: C. E. Harp, Conference Chairman; D. J. Tucker, Region Six Director; A. V. Loughren; A. P. Challenner, Oklahoma City Section Chairman. Oklahoma State Governor Raymond Gary also attended.

Redstone Arsenal Plays Host to IRE Visitors

Shown (*left to right*) are: Col. George Levings, assistant commander of the Arsenal, which is located at Huntsville, Ala., T. A. Hunter, a director of the IRE and editor of its STUDENT QUARTERLY, and P. H. Nelson, chairman of IRE Region Three Education Subcommittee. Dr. Hunter spoke at a chapter meeting at the Arsenal.

Professional Groups Tour NIKE Installation
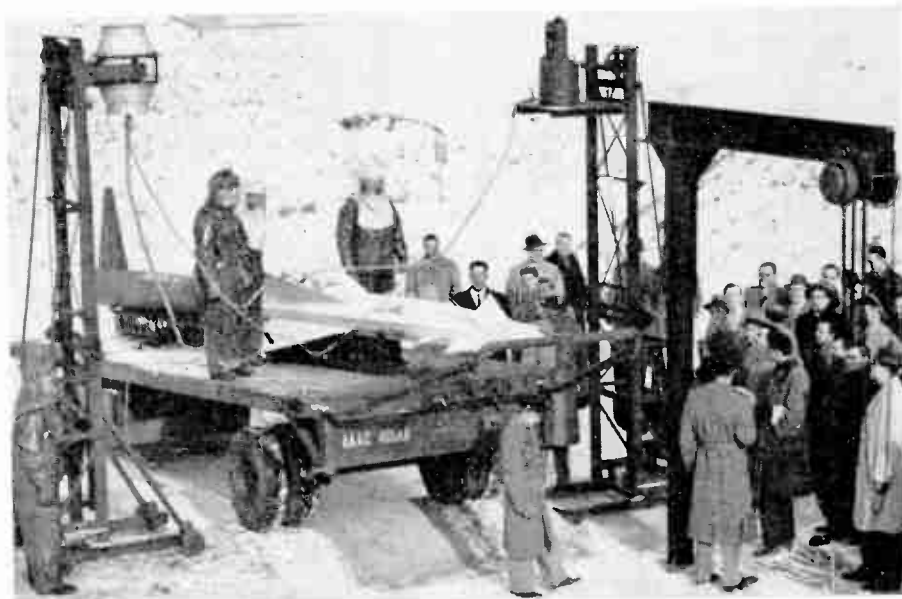
In Chicago, Professional Groups on Microwave Theory, Antenna Propagation, and Telemetry toured a NIKE installation and radar control area. A demonstration of enemy air attack defense measures was given.

Stanton De Forest Allaben, Lee De Forest's twelve-year old grandson, builds his first amateur receiver.

IRE President A. V. Loughren (*right*) congratulates G. K. Teal, Fellow award recipient, at the banquet of the recent Southwest Regional Conference.

Shown at left table (*left to right*) are: L. A. McCabe, John MacNeil, William Jaquish, A. O. Mann, Reed Stoveall, and Edward Fasho. Shown at head table (*left to right*): H. N. Ringer, J. C. Hetrick, J. W. Leas, L. A. Brothers, and George Laurent. At right table (*left to right*): Sally Des Rosiers, Irving Cohen, Edward Hawthorne, C. A. Slocum, and Herbert Gurk. They participated in an Operations Research symposium at the University of Pennsylvania recently.

Loughren Chats with Iowa Student Members

1956 IRE President A. V. Loughren chats with M. S. Coover and the officers of the Joint AIEE-IRE Student Branch at Ames, Iowa. *Left to right*—Mr. Loughren, M. S. Coover, J. L. Neese, B. L. Sewell, Dean Van Zuuk, Thomas Proctor, C. L. Scholefield. *Seated*—K. W. Jenkins and J. S. Barnett.

WAYNE OFFERS SUMMER COURSES

The Computation Laboratory of Wayne University is offering, for the fourth time, an intensive summer training program of three weekly courses.

The first course, which will be held July 23–28, will cover automatic computers, computer principles and organization, fundamentals of programming, and coding. Lectures, discussions, tutorial sessions, laboratory periods, and field trips to computation centers will be features of this course.

For the second course, electronic data processing in business and government, students are expected to have taken the first course, or have had similar training or experience. The course, which will be offered from July 30 to August 4, will cover recent developments in the application of electronics to business, programming and flow charting of business applications, and data processing from the standpoint of optimization in terms of mathematical programming. Major data processing systems in the Detroit area will be available for demonstration and running of sample programs.

The third and final course, to be held August 6–11, will cover computer applications with emphasis on numerical methods and advanced programming techniques. The Burroughs UDEC and the IBM 650 will be available to students during laboratory sessions.

The final program and further information may be obtained from A. W. Jacobson, Director, Computation Laboratory, Detroit 1, Michigan.

CALL FOR PAPERS ISSUED FOR SECOND RADOME SYMPOSIUM

The Second Annual Radome Symposium, sponsored by the Ohio State University and the Electronics Components Laboratory of Wright Air Development Center, will be held June 4–6, at the Student Union on the campus of the Ohio State University.

The proposed technical program includes the following subjects: future radome requirements, microwave research, electro-optical design, aerodynamics, structural, and environmental design, radome test methods and equipment, and radome materials and fabrication.

Material will be presented in two forms. First, formal papers will be presented. Second, one session each day will include a panel discussion conducted in a manner similar to the "Meet the Press" television program. At these sessions an effort will be made to assemble a panel of experts in the particular field. Preselected questions will be asked by designated representatives. Questions and comments will also be taken from the floor if time permits.

Interested persons are urged to contribute questions for the panel sessions and to submit one or more papers for possible inclusion in the program. Classified material is acceptable for presentation.

To facilitate the selection of papers, please send an abstract of not more than one hundred words before March 1 to T. E. Tice, Antenna Lab., Ohio State Univ., Columbus 10, Ohio. The abstract should be typed (single spaced) in duplicate on $8\frac{1}{2} \times 11$ paper. Please furnish titles which are unclassified so they may be used in an unclassified program. Papers of any classification through secret will be acceptable. It will be the responsibility of the author to establish whatever security classification and clearance is necessary through his own cognizant security agency.

The questions for the panel discussions relating to current and future problems should be sent to Mr. Tice before April 1. These questions will be arranged and forwarded to the questioners and the panel experts. In this way both may be prepared and lead the discussion so that all radome investigators may receive the benefit of their considered judgment.

In view of the classified nature of this symposium, a secret clearance must be furnished to attend. All persons must initiate clearance requests through security officers before April 16, with a request that they be sent to C. H. Everhart, (WCREA) Administrative and Security Officer, Electronics Components Laboratory, WADC, Wright Patterson Air Force Base, Ohio. All requests for security clearances for attending the symposium will be processed upon receipt and confirmation will come directly from Mr. Everhart. If the confirmation is not received in a reasonable length of time the security officer should contact Mr. Everhart. Personal identification will also be required upon arrival for the conference. Further information on details of the symposium may be obtained from Mr. Tice.

INFORMATION THEORY ANNOUNCEMENT

The Research Laboratory of Electronics of M.I.T. and the PG on Information Theory of the IRE will hold a Symposium on Information Theory at Cambridge, Mass., Sept. 10–12. Co-sponsors will be the Office of Naval Research, Air Research and Development Command, Signal Corps Engineering Labs., and U.R.S.I.

The TRANSACTIONS of the symposium will be mailed as a PGIT publication to all members of the sponsoring organizations at the same price Sept. 1.

The deadline for submission of papers not previously submitted in abstract form is June 15. Papers should be prepared on paper suitable for photo-offset reproduction and sent to P. Elias, Research Lab. of Elec., M.I.T., Cambridge 39, Massachusetts.

1956 IRE President Visits Dallas Section

D. J. Tucker *(left)*, Region Six Director and managing director of Radio Station WRR interviewed IRE President A. V. Loughren *(center)*. Later Mr. Loughren gave a newspaper interview, toured Continental Electronics and Texas Instruments, made two television appearances, and attended a meeting of the Dallas Section.

TUTORIAL LECTURES HIGHLIGHT TRANSISTOR CIRCUITS MEETING

The 1956 Transistor Circuits Conference was held under the joint auspices of the IRE, the AIEE, and the University of Pennsylvania at the Irvine Auditorium and the University Museum Auditorium in Philadelphia on February 16–17, 1956. A total of 1,164 people attended the conference.

This year's conference program had one change from that offered in past years: two additional sessions consisting of two tutorial lectures each were given on the first day of the conference simultaneously. Only contributed papers were heard in single sessions on Feb. 17.

Nineteen technical papers were delivered in addition to the four tutorial papers. Moreover, the authors in many cases plan to offer their papers to various technical journals for publication.

The opening session of the conference offered an address by Mr. George W. Haller, Chairman of the Conference and Director of the Laboratories Department, Electronics Division of General Electric Company, Syracuse, New York. In addition a presentation of one hundred dollars worth of library text books relating to transistors was presented on behalf of the conference to the university by D. G. Fink, Chairman of the 1955 Transistor Circuits Conference and one of the Directors of Research of the Philco Corporation. These books were accepted by J. Grist Brainerd, Professor of Electrical Engineering at the Moore School of Electrical Engineering of the University of Pennsylvania.

There still remain additional copies of the conference program which contains the abstracts for all of the contributed papers. As no proceedings are to be published, persons desiring copies of these abstracts may obtain them by writing to J. D. Chapline, c/o Research Division, Philco Corporation, "C" and Tioga Streets, Philadelphia 34, Penna.

MAGNETIC CONFERENCE INVITES AUTHORS TO SUBMIT PAPERS

A Conference on Magnetism and Magnetic Materials will be held at Hotel Statler in Boston on October 16–17–18, by the American Institute of Electrical Engineers in cooperation with the American Physical Society, the American Institute of Mining and Metallurgical Engineers, and the IRE. Authors should submit titles of proposed papers by June 15 and abstracts by August 1. For further details write T. O. Paine, Measurements Laboratory, General Electric Company, West Lynn, Mass.

SECOND IRE INSTRUMENTATION CONFERENCE INVITES PAPERS

The Professional Group on Instrumentation and the Atlanta Section of the IRE will sponsor the Second IRE Instrumentation Conference at the Biltmore Hotel in Atlanta on December 5–7, 1956. B. J. Dasher, Director of the School of Electrical Engineering, Georgia Institute of Technology, will again serve as conference chairman.

Sessions will be devoted to industrial applications, missile range instrumentation, and the application of solid-state devices, as well as to other fields of instrumentation. Prospective authors are invited to submit abstracts of 200 words or less not later than September 1 to the program chairman, M. D. Prince, Engineering Experiment Station, Georgia Institute of Technology, Atlanta, Georgia.

PURDUE ANNOUNCES JULY COURSE ON SYSTEMS ENGINEERING

Purdue University offers for the second time a ten-day short course in linear automatic control system synthesis July 9–20. The course will treat feedback theory from the signal-flow viewpoint, root locus methods, approximations in time and frequency, transform theory beyond the elementary level, synthesis through pole-zero configurations, and admittance parameter synthesis of multi-input systems. The course is intended for engineers who are interested in advanced control system theory and for teachers in this field. It will also be of particular interest to engineers working with circuits, control and system dynamics who have not had an opportunity to study the modern literature in detail.

The course will be presented by the staff of the Purdue School of Electrical Engineering. *Control System Synthesis* will be used as a text, and students will need a background of Laplace transform theory and frequency design techniques in closed loop systems. Instruction will be on the graduate level.

A brochure giving the details of the course and information as to fee, reservations, etc., may be had by writing to the Division of Adult Education, Engineering Administration Building, Purdue University, Lafayette, Indiana.

TEMPORARY MEMBERSHIPS ARE AVAILABLE AT INSTITUTE OF MATHEMATICAL SCIENCES AT NYU

The Institute of Mathematical Sciences of New York University offers temporary memberships to mathematicians and other scientists holding the Ph.D. degree who intend to study and do research in the fields in which the Institute is active. These fields include functional analysis, ordinary and partial differential equations, mathematical physics, fluid dynamics, electromagnetic theory, numerical analysis and digital computing, and various specialized branches, such as group theory, topological methods of analysis, hydromagnetics, reactor theory.

Requests for information and for application blanks should be addressed to the Membership Committee, Institute of Mathematical Sciences, 25 Waverly Place, New York 3, New York.

Shown are *(left to right, seated)*: H. J. Woll, Chairman of Program Committee; G. L. Haller, Chairman of National Committee; W. P. West, Chairman of Local Arrangements Committee; C. W. Hargens, Chairman of Registration Subcommittee. *(Standing, left to right)*: A. P. Stern, Secretary of National Committee; H. E. Tompkins, IRE Representative, Philadelphia PGCT and Member of Program Committee; J. D. Chapline, Chairman of National Publicity Committee; I. L. Auerbach, Treasurer of National Committee; and W. J. Popowsky, Chairman of Luncheon Arrangements Subcommittee. They headed the 1956 Transistor Conference.

February Western Joint Computer Conference Stressed New Trends and Devices

The Western Joint Computer Conference and Exhibit was held in San Francisco, February 7–9. The three-day session was managed by Chairman Oliver Whitby of Stanford Research Institute. In the keynote address N. H. Taylor, Computer Systems Engineer with the Lincoln Laboratory, Massachusetts Institute of Technology, reviewed the development of the automatic computer industry from infancy to its present early adolescence and then gave some predictions of things to come. Among these was the prediction that within the next ten years computers will automatically control all transport aircraft with pilots as moderators.

A number of sessions on programming and coding of large scale scientific and business computers included a number of papers on automatic programming and supervising systems, which emphasized those techniques which will be helpful in applying computers to business problems. A team of RCA engineers described the new "BIZMAC" computer system which has recently been installed for military inventory control.

Novel uses of digital computers as simulators for studying traffic control systems, planning new roadways, and baseball forecasting were described.

Papers on analog computing techniques included several on combined analog and digital systems.

Among papers describing new advances in hardware were descriptions of auxiliary equipment such as magnetic recording heads the relatively new Charactron display tube, new magnetic tape handles, and a system for data transmission over telephone circuits. Among new circuit components described is a device known as the "transfluxor." This can best be described as a variable setting magnetic gate in contrast to the customary vistable devices used in computer design.

Copies of the proceedings are available through the three sponsoring organizations: the A.I.E.E., the IRE, and the A.C.M.

OBITUARY

Heinrich G. Barkhausen (A'26–F'30), Professor Emeritus of the Institute of Technology, Dresden, Germany, died recently.

H. G. BARKHAUSEN

In 1907 he took his doctorate with a thesis on the generation of fast electrical oscillations which dealt with the principle of feedback. In 1911 he became professor of electrotechnique at the Institute of Technology, Dresden, Germany. Under his leadership grew the Institute for Low-Current Technique, and after World War II when the Institute was rebuilt, the building was named after Dr. Barkhausen.

Dr. Barkhausen's research and investigations of vacuum tubes had culminated in a four-volume book entitled *Electron Tubes*.

For many decades its numerous editions were kept up to date and the book was one of the standard handbooks of electronics, not only in Germany, but all over the world. The parameters of vacuum tubes, e.g. the "Durchgriff D" (inverse amplification factor) and the methods for their direct measurement with alternate current were conceived and developed by Dr. Barkhausen. His other contributions include the Barkhausen equation $(S \cdot R_p \cdot D = g_m \cdot R_p/\mu = 1)$, the Barkhausen clicks, the Barkhausen-Kurz oscillations, and his investigations of transit-time regions in vacuum tubes. In addition, he created the "phon" as the European unity for the intensity of sound.

During recent years, Dr. Barkhausen had headed the editorial board of the German *Zeitschrift für Hochfrequenztechnik und Elektroakustik*.

Dr. Barkhausen was a member of the German Academy of Science, the Saxonian Academy of Science, and an honorary member of the German Technical Academy, the Japanese Institute of Electrical Engineers and the Acoustical Society of America. Among his numerous awards the most outstanding were the German National Award, the Golden Heinrich-Hertz Medal, and the Morris Liebmann Memorial Prize of the IRE for 1933.

He had been a Director and Vice-President of the IRE in 1935.

PROFESSIONAL GROUP NEWS

Five New Chapters Announced

The IRE Executive Committee, at its meeting on March 1, approved the following chapters: Fort Wayne Section, PG on Military Electronics; Hawaii Section, PG on Audio; San Diego Section, PG on Antennas and Propagation, and PG on Microwave Theory and Techniques; Pittsburgh Section, PG on Nuclear Science.

The Princeton Section was officially included in the Joint New York Metropolitan Area Chapter of the Professional Group on Medical Electronics.

TECHNICAL COMMITTEE NOTES

The **Audio Techniques** Committee met at IRE Headquarters on February 21 with Chairman D. E. Maxwell presiding. It was announced that I. M. Kerney was appointed chairman of the Audio Techniques Committee for the term May 1, 1956 to April 30, 1957. The committee discussed the possibility of increasing the membership of the committee. The chairman suggested that it might prove fruitful to insert a notice in the IRE Transactions on Audio, describing the work of the Audio Techniques Committee and soliciting new members.

The chairman advised the committee that at the January meeting of the Standards Committee, a motion was passed which will allow the publication of proposed standards in the IRE Transactions. This will give the committee a chance to receive comments from experts in the respective fields before a standard is approved.

The remainder of the meeting was devoted to the review of the Proposed Standards on Audio Techniques: Definitions of

Terms, which is being prepared by Subcommittee 3.1 on Definitions.

Chairman W. R. Bennett presided at a meeting of the **Circuits** Committee at IRE Headquarters on February 24. The Proposed Definitions Standard, that is being prepared by Subcommittee 4.2 on Linear Lumped-Constant Passive Circuits, was discussed and some definitions amended. The remainder of the meeting was devoted to the discussion of the Proposed Standard on Linear Active Networks: Definitions of Terms Related to Basic Feedback Theory.

The **Facsimile** Committee met at the Times Building on February 17 with Chairman K. R. McConnell presiding. The chairman reported that the Standards on Facsimile: Definitions of Terms had been approved at the last meeting of the Standards Committee, and are now ready for publication.

The committee discussed the Temporary Test Standards issued in 1943, with a view toward revising it and bringing it up-to-date.

Chairman A. W. Friend presided at a joint meeting of the Ad Hoc Subcommittee on High Fidelity and the **Recording and Reproducing** Committee at IRE Headquarters on March 2.

Dr. Friend introduced D. E. Maxwell as the chairman-elect of the Recording and Reproducing Committee for the term May 1, 1956 to April 30, 1957.

The chairman said that the objective of the Ad Hoc Subcommittee on High Fidelity is to find standards on high fidelity that would be applicable for reference on the subject. He said that there are numerous standards relating to this subject, but people do not know just what they are or where they can be obtained. The purpose of this meeting is to compile a list of standards applicable to high fidelity and the organizations where they can be acquired.

The committee reviewed the Proposed Standard on Sound Recording and Reproducing: Methods of Calibration of Mechanically-Recorded Frequency Records, which was prepared by Subcommittee 19.2 on Mechanical Recording.

R. C. Moyer, Chairman of Subcommittee 19.1 on Magnetic Recording, said that they will have the Proposed Standard on Definitions ready in a couple of months.

The **Symbols** Committee met at IRE Headquarters on February 17 with Chairman H. R. Terhune presiding. The committee reviewed and approved a Proposed Standard on Graphical Symbols for Semiconductors.

An IRE Standard on Letter Symbols for Feedback-Control Systems has just been issued. The Standards Committee is considering a report on letter symbols for semiconductors. Subcommittee 21.7 on Letter Symbols should, therefore, review the letter symbols and mathematical signs in the Standards on Abbreviations, Graphical Symbols, Letter Symbols, and Mathematical Signs—1948 with the thought of recommending that all these reports be consolidated into a single document on letter symbols and mathematical signs. This will make the entire contents of the 1948 standard obsolete because all the other material in it has already been revised.

NATIONAL CONFERENCE ON AERONAUTICAL ELECTRONICS

BILTMORE HOTEL, DAYTON, OHIO
MAY 14–16, 1956

The Eighth Annual National Conference on Aeronautical Electronics will be held under the joint sponsorship of the Professional Group on Aeronautical and Navigational Electronics and the Dayton Section of the IRE at the Biltmore Hotel, Dayton, Ohio, May 14–16.

The welcome address will be given by Conference President R. J. Framme, Wright Air Development Center. An outstanding feature of the conference will be a forum entitled "How to Accelerate Research and Development of Aeronautical Electronics" on May 15. On the same day a session on human engineering will be sponsored by the Institute of the Aeronautical Sciences.

Luncheons will be held on May 14 and 16 at which winners of the Dayton Section Student Award and the United States Air Force Institute of Technology Subsection Student Award will be announced. The "Pioneer in Aeronautical Electronics" annual award will be presented at the banquet and dance on May 15.

Advance registration for IRE and IAS members will be accepted at a reduced rate of $1.50. Non-members can register in advance at a reduced rate of $2.50. Regular registration will begin on Sunday, May 13, at a rate of $2.50 for IRE and IAS members, and $3.50 for non-members. The official mailing address for the conference is P. O. Box 621, Far Hills Branch, Dayton 9, Ohio

9:00–11:30 a.m., Monday, May 14

Main Ballroom—Dayton Biltmore Hotel

MAGNETICS I

Moderator: R. A. Ramey, Westinghouse Electric Corp.

New Type Miniaturized Power Transformers for High Temperature Airborne Applications, H. S. Feder and A. B. Haines, Bell Telephone Labs.

High Performance Magnetic Amplifier Type Regulator-Exciter for AC Generator, H. S. Sechrist and H. G. Carlson, General Electric Co.

Core Volume Derivation for Magnetic Pulse Modulators, J. E. Sunderlin, Westinghouse Electric Corp.

Use of Constant Current Flux Reset Testing in the Design of Self-Saturating Magnetic Amplifiers, H. D. Faram, Emerson Television & Radio.

English Room—Dayton Biltmore Hotel

COMPONENTS I

Moderator: F. E. Wenger, Air Research & Development Command.

Hermetic Sealed Composition Resistors, A. C. Pfister, Allen-Bradley Co

Application and Selection of Accurate Film Type Resistors, Paul Nuyl, International Resistance Co.

Application and Selection of Power Resistors, G. M. Stapleton, Ward Leonard Electric Company.

The Use of Magnetic Clutches and Precision Potentiometers in Strain Gauge Measurements, Leo Woerner, International Resistance Co.

Auditorium—Engineers Club

SEMICONDUCTORS

Moderator: J. S. Saby, General Electric Company

The Microwave Diode, C. T. McCoy, Philco Corporation.

Investigation of Power Gain and Transistor Parameters as Functions of Both Temperature and Frequency, A. B. Glenn and I. Joffe, Radio Corporation of America.

High-Power Switching Characteristics of Conjugate Emitter Transistors, J. J. Suran, General Electric Company.

Characteristics of Silicon P-N-P Junction Transistors, J. Spanos, A. Caggiano and R. D. Greene, Raytheon Mfg. Co.

Silicon Tetrode Transistors for the 5 to 40 MC Region, R. R. Webster, Texas Instruments, Inc.

Italian Room—Engineers Club

CIRCUITS

Moderator: F. C. Collings, Radio Corporation of America.

PCM Frame Synchronization, P. J. Tapernoux, Stromberg-Carlson Company.

The Neon Tube Switch as a New Method of Highspeed Multiplexing, R. C. Givens, Radio Corporation of America.

Crystal Controlled Pulse Generators, D. C. Howard, Radiation, Inc.

A Precision Memory Delay Generator, Harvey Bush, Radiation, Inc.

Low Level Detection in the UHF Region, E. M. P. Rutz, Emerson Television & Radio.

2:00–5:00 p.m., Monday, May 14

Main Ballroom—Dayton Biltmore Hotel

MANAGEMENT

Moderator: George Rappaport, Wright Air Development Center.

Management of Research and Development, Paul Clark, Radio Corporation of America.

Management of a Development Engineering Enterprise, O. H. Winn, General Electric Company.

Managing an Engineering Research Center, R. L. Shetler, General Electric Co.

The Role of the Design Engineer in the Field Support of Complex Airborne Electronic Equipment, H. W. Brown, Radio Corporation of America.

The Questions are Easy, Donald Friedman, Avion Division of ACF Industries.

Skull to Skull Communication of Technical Ideas, Philip Klass, Aviation Week.

English Room—Dayton Biltmore Hotel

ENVIRONMENT

Moderator: J. R. Grimm, Wright Air Development Center.

The Problem of Electronic Components in Nuclear Power Plants, R. D. Shelton, Admiral Corporation.

Direct and Indirect Forced Air Cooling Techniques for Electronic Equipment, Melvin Mark and M. Stephenson, Jr., Raytheon Mfg. Company.

A Fusion Type Seal for Large Repairable Airborne Electronic Equipment, Robert Einfeldt and F. J. Biltz, Remington Rand.

A Note on Forced Convection Tube Cooling with Chimneys, Melvin Mark, Raytheon Mfg. Company.

Evaluation of Hermetic Sealing Terminals, G. A. Forster, Armour Research Foundation.

Auditorium—Engineers Club

ELECTRON TUBES I

Moderator: Walter Greer, Navy Bureau of Ships.

Receiving Tube Reliability Studies, G. H. Gage, General Electric Company.

Display Tubes, Jenny Bramley, Allen B. DuMont Lab., Inc.

Traveling-Wave Tubes: Applications and Application Considerations, F. R. Arams, Radio Corporation of America.

Beam Switching Tube Circuit Design in Aircraft Applications, Rudolph Cola, Haydu Brothers of N. J.

Using Viewing Storage Tubes in Aircraft Indicators, H. O. Hook, Radio Corporation of America.

Reduction of Vibration Output in Miniature Tubes, Melvin Levine and D. O. Holland, Raytheon Mfg. Co.

Italian Room—Engineers Club

TESTING AND TEST EQUIPMENT

Moderator: G. G. Brown, Inland Testing Laboratories.

New Testing Concepts for the Advancement of Electro-Mechanical Component Reliability, W. H. Grument, Rototest Laboratories.

Automatic Testing of Fire Control Systems, Allen Borck, Emerson Television & Radio.

A Dielectrometer for Millimeter Wavelengths, M. J. Ehrlich, Microwave Radiation Co.

The Design and Development of Precision Signal Generators in the VHF and UHF Regions, A. DiNardo and E. Fuller, Sperry Gyroscope Co.

High Voltage R-F Generator, J. O. Stenoien, Boeing Airplane Co.

New Developments in Liquid Loads for Use in Waveguide and Coaxial Systems, Samuel Freedman, Chemalloy-Electronics Corp.

The Discovery of a Realistic Dynamotor Brush Test, L. V. McNamara, Wright Air Development Center.

9:00–11:30 a.m., Tuesday, May 15

Main Ballroom—Dayton Biltmore Hotel

COMPUTERS I

Moderator: Lewis Imm, Librascope.

Redundancy in Complex Computers, M. Cohn, Remington Rand.

A High Accuracy, High Speed Shaft Position to Digital Converter, G. W. Oberle, Glenn L. Martin Company.

An Analog-to-Digital Converter with Decimal Output, R. P. Bishop, Radiation, Inc.

A High Speed Digital Translating-Recording System, G. F. Anderson, Radiation, Inc.

A Multipurpose Electronic Switch for Analog Simulation and Auto-Correlation Applications, N. D. Diamantides, Goodyear Aircraft Corporation.

English Room—Dayton Biltmore Hotel

COMPONENTS II

Moderator: J. T. Brothers, Philco Corporation.

Ceramic Capacitors and Their Applications, Nello Coda, Erie Resistor Corporation.

Typical Expected Performance Characteristics of Extreme Temperature Range Tantalum Capacitors, J. W. Maxwell, P. R. Mallory & Co., Inc.

Tantalum Solid Electrolytic Capacitors, E. A. McLean, Bell Telephone Labs., Inc.

Time Delay Relay Applications, J. J. Dietz, Thomas A. Edison, Inc.

Fluxless and Corrosionless Soldering of Aluminum and Attachment of Copper Thereto, Samuel Freedman, Chemalloy-Electronics Corporation.

Auditorium—Engineers Club

SEMICONDUCTOR CIRCUITS I

Moderator: Dan Noble, Motorola.

Communication Circuits Using Germanium Transistors, R. E. Wilson, Radio Corporation of America.

Low Level Transistor Amplifiers, F. L. Putzrath, Radio Corporation of America.

A Transistorized Automatic Gain Control for Variable Gain AC Servos, Ralph Gittleman, W. L. Maxson Corporation.

A Transistor Demodulator Limiter, N. L. Johanson, Boeing Airplane Company.

Italian Room—Engineers Club

ANTENNAS I

Moderator: L. E. Raburn, Crosley Div., AVCO.

Pattern Shaping with Surface Wave Antennas, R. S. Elliot, Hughes Aircraft Co.

Shunt-Fed and Notch-Fed Aircraft H-F Antennas, R. L. Tanner, Stanford Research Institute.

Study of Feasibility of H-F Airborne Direction-Finding Antenna Systems, P. S. Carter, Jr., Stanford Research Institute.

The Collins 37X-1 Marker Beacon Receiving Antenna, J. P. Shanklin, Collins Radio Company.

2:00–5:00 p.m., Tuesday, May 15

Auditorium—Engineers Club

FORUM

Moderator: J. W. McRae, President, Sandia Corporation.

Subject: "How to Accelerate Research and Development of Aeronautical Electronics."

Participants: Brigadier General T. L. Bryan, Jr., Wright Air Development Center; D. H. Ewing, David Sarnoff Labs.; K. H. Martinez, Boeing Airplane Company; Thomas Meloy, Melpar, Inc.; Julian Sprague, Sprague Electric Co.; R. J. Shank, Hughes Aircraft Company.

Italian Room—Engineers Club

HUMAN ENGINEERING

Moderator: J. M. Christenson, Wright Air Development Center.

The Use of Mock-Ups in Airborne Equipment Designing, G. W. Michalec, General Precision Lab.

Integrated Cockpit Presentation, T. J. Thomas, Kearfott Co., Inc.

New Engineering Techniques in Flight Display Evaluation, Frank Klimowski, Jr., Stavid Engineering, Inc.

Collapsing Loss in Airborne Radar Displays, L. E. Mertens, P. N. Nesbeda and J. P. Mayberry, Radio Corp. of America.

The PPI Display as a Linear Filter, Daniel Levine, Goodyear Aircraft Corporation.

On Flight Instrument Quantization, L. J. Fogel and D. Jagerman, Stavid Engineering, Inc.

9:00–11:30 a.m., Wednesday, May 16

Main Ballroom—Dayton Biltmore Hotel

MAGNETICS II

Moderator: Paul Russell, General Electric Company.

Design for Magnetic Switch, Norman Rubenfeld, W. L. Maxson Corporation.

Design Techniques for Extremely High Powered Broad Band Ferrite Isolators from 3,000 to 36,000 MC, T. N. Anderson, Airtron, Inc.

An Amplitude Regulator for Microwave Signal Sources, Philip Fire and Perry Vartanian, Electronic Defense Lab of Sylvania.

The Development of a 36 KMC High Power Rotational Ferrite Duplexer-Switch Isolator for Radar Services, T. N. Anderson, Airtron, Inc.

English Room—Dayton Biltmore Hotel

RADIO INTERFERENCE AND R-F CABLES

Moderator: Robert Lewis, Consulting Engineer.

An Approach to Designing Interference Free Electronic Systems, F. S. Scarborough and F. E. Garlington, Sprague Electric Company.

Grounding and Bonding, A. G. Berbert, Burndy Engrg. Co., inc.

Adaptive and Distribution-Free Filters, L. E. Mertons, Radio Corporation of America.

Guide to the Selection of Radio Frequency Cables, C. C. Camillo and G. J. Mares, American Phenolic Corp.

Recent Improvements in R-F Cable Assemblies, J. M. Caller, Sandia Corporation.

Auditorium—Engineers Club

SEMICONDUCTOR CIRCUITS II

Moderator: Lloyd De Vore, Stewart-Warner Corp.

Design and Application of Transistorized Regulated Power Supplies, S. Sherr, P. Levy and T. Kwap, General Precision Lab.

A Transistorized DC to AC Inverter with Good Regulation, R. M. Hubbard, Boeing Airplane Co.

Operation of a Saturable Core Square Wave Oscillator, D. C. Mogen, Minneapolis-Honeywell.

A Four-Quadrant Voltage Multiplier, G. L. Keister, Boeing Airplane Company.

A Fixed Tuned 12.5 MC FM Transistor Receiver, A. M. Boothe, Crosley Div. of AVCO.

Italian Room—Engineers Club

ANTENNAS II

Moderator: Thomas Tice, Ohio State University Research Foundation.

The Probe Excited Airframe as a High Frequency Antenna, T. G. Dalby, Boeing Airplane Company.

Antenna Coupler Efficiency Considerations in Airborne Liaison Communication Systems, M. Shoquist and L. E. Sabine, Remington Rand.

Decoupling of Small Horn Antennas, W. S. Carley, Emerson Television and Radio.

Automatic Boresight Measuring Equipment, J. B. Damonte, Dalmo Victor Company.

2:00–5:00 p.m., Wednesday, May 16

Main Ballroom—Dayton Biltmore Hotel

COMPUTERS II

Moderator: R. C. Newhouse, Bell Telephone Laboratories, Inc.

Digital Computer System for Airborne Applications, W. J. Moe, Remington Rand.

Logic Circuits for a Transistor Digital Computer, G. W. Booth and T. P. Bothwell, Radio Corporation of America.

An "All Transistor" Buffer Unit Using Coincident Current Storage, J. A. Kershaw, Remington Rand.

Precision Analog Computer Amplifier Utilizing Silicon Transistors, C. R. DeWeese, Texas Instruments, Inc.

Applications of Transistorized Binary Counters in Digital Timing Systems, C. W. Skelton, Texas Instruments, Inc.

English Room—Dayton Biltmore Hotel

ANALYSIS TECHNIQUES

Moderator: A. B. Carson, United States Air Force Institute of Technology.

Analysis and Prediction of Servo Gearing Performance, P. R. Jones, Collins Radio Company.

A Digital Technique for Rapid and Accurate Evaluation of Trigonometric Functions, G. W. Oberle, Glenn L. Martin Company.

The Mathematical Theory of Straight Line Approximations to Logarithmic Curves, Harold Goldberg, Emerson Television and Radio.

Plotting "Success-or-Failure" Test Results by Means of a Cumulative Performance Chart, Morten Gale, Emerson Television and Radio.

2:00–5:00 p.m., Wednesday, May 16

Auditorium—Engineers Club

ELECTRON TUBES II

Moderator: W. C. Kirk, Consulting Engineer.

The Unreliable Universal Component, M. A. Acheson, Sylvania Electric Products, Inc.

A New Magnetron for Commercial Airborne Weather Radar, W. F. Beltz and R. W. Kissinger, Radio Corp. of America.

Development of a 5-inch, Direct-View Storage Tube, E. M. Smith, Radio Corporation of America.

The Relation Between Performance and Reliability in Tubes, G. D. O'Neill and M. A. Acheson, Sylvania Elec. Prod. Inc.

A Comprehensive Quality Control Program Designed to Improve Subminiature Tube Reliability, H. H. Hoyle and H. J. Davis, Raytheon Mfg. Company.

Life Test Performance of Reliable Tubes at Maximum Ratings, T. J. White, Raytheon.

Italian Room—Engineers Club

EQUIPMENT

Moderator: P. G. Wulfsberg, Collins Radio Company.

A Precision Long Range Radio Navigation System, W. Dean, R. Frank and W. P. Frantz, Sperry Gyroscope Company.

An Airborne Single Sideband Transceiver, E. L. Martin, Collins Radio Company.

Locally-Generated-Keying-Tone Squelch. L. M. Harris, Jr., Stromberg-Carlson Co.

True Mass Liquid Quantity Gage, Willis Lindemann, Minneapolis-Honeywell Regulator Company.

Streamlining a Radar Data Distribution Unit, H. A. Bleam, Admiral Corporation.

A 20 to 70 MC Stable Radio Receiver Tuner, W. R. Harter, Crosley Div. of AVCO.

SYMPOSIUM ON RELIABLE APPLICATIONS OF ELECTRON TUBES

UNIVERSITY OF PENNSYLVANIA, PHILADELPHIA, PA., MAY 21–22, 1956

The RETMA Engineering Department is sponsoring a two-day symposium on Reliable Applications of Electron Tubes which will stress *how* to obtain reliable operation rather than reiterate the need for reliability. In preparing the program for this symposium the planning committee selected papers covering design engineering where reliability can be effected efficiently. This symposium, therefore, is intended primarily for design engineers and others directly concerned with this phase of engineering. Managers and other supervisory personnel can profit by attendance at this meeting by gaining a better understanding of the problems facing the designer and thus facilitate the implementation of his designs.

The program material has been grouped into sessions covering field experience, design planning, and circuits. In addition there will be a panel discussion on Monday evening, May 21, on "Can Tube Specifications Produce Equipment Reliability?". The panel will be composed of a group of men representing tube manufacturers, equipment manufacturers, and the military services. This discussion will also encompass audience participation insofar as is possible.

Advance registration may be had by sending a check or money order for $3.00 for each person registering. Registration at the door will be $4.00. All checks and money orders should be made payable to, and mailed no later than May 15, 1956 to: RETMA Engineering Dept., 11 W. 42nd St., New York 36, N. Y.

The Sylvania and John Bartram Hotels have reserved blocs of rooms for symposium registrants, and all hotel reservations should be made directly to the hotels, not to the RETMA office.

Proceedings of the symposium will be made available at some time after the meeting. Orders for copies of the proceedings will be taken by a publisher's representative at the registration desk.

Additional information may be obtained at the hotels and symposium registration desk.

TENTATIVE PROGRAM

Monday, May 21

Welcoming Address, C. C. Chambers, University of Pennsylvania.

Keynote Address, J. M. Bridges, Office of Assistant Secretary of Defense.

10:15 a.m.

FIELD EXPERIENCE AS AN AID TO RELIABLE EQUIPMENT DESIGN

Chairman: T. B. Perkins, RCA

Field Trial Techniques as a Tool to Improve Reliability and Life in Electron Tubes, L. F. Moose, Bell Telephone Labs.

Electron Tube Misapplication When Uncovered Through Field Surveillance, M. Norton, Aeronautical Radio Inc.

Defective Tubes—Manufacturer or User Responsibility?, R. B. Wilson, Cornell University.

2 p.m.

CIRCUIT SESSION

Chairman: R. J. E. Whittier, Raytheon.

Keyed Phase Sensitive Demodulator, O. Berger, Glenn L. Martin Company.

Reliable Design of Flip-Flop, H. W. Boyd, Lincoln Labs. M.I.T.

Series String Applications of Electron Tubes (Commercial and Military), R. G. Rauth, RCA.

Series Regulators, J. H. Muncy, National Bureau of Standards.

8 p.m.

PANEL SESSION

Can Tube Specifications Produce Reliable Equipment?—W. R. G. Baker, Chairman, M. A. Acheson, N. Aram, J. M. Bridges, F. Q. Gemmill, W. Kirk, and C. G. Walance.

Tuesday, May 22
10 a.m.

PLANNING FOR RELIABLE DESIGN

Chairman: R. W. Jamieson, Litton Industries.

Designing for Reliability Through the Proper Application of Tubes, C. M. Ryerson, RCA.

Application Techniques Leading to Reliable Tube Performance, Project Hi, J. J. Hofler, IBM.

Management and Engineering Responsibility for Design in Reliability, G. Beck, Bendix Aviation.

Mathematical Tools for Reliable Design, E. E. Brewer, Convair.

2 p.m.

RECEIVING TUBES

Chairman: A. L. Dolnick, Sylvania Electric Products, Inc.

JETEC Industry Standardization Towards Reliability, C. E. Coon, Tung Sol Electric, Inc.

Tube Acceptance Specifications for Television Applications, R. G. O'Faullin, Motorola, Inc.

Reliability in Dissimilar Section Tubes, R. W. Slinkman, Sylvania Electric Products, Inc.

Receiving Tube Reliability Studies, G. H. Gage, General Electric.

Professional Groups†

Areonautical & Navigational Electronics— James L. Dennis, General Technical Films, 3005 Shroyer, Dayton, Ohio.

Antennas & Propagation—Delmer C. Ports, Jansky & Bailey, 1339 Wisconsin Ave., N.W., Washington 7, D. C.

Audio—D. W. Martin, The Baldwin Piano Company, 1801 Gilbert Ave., Cincinnati 2, Ohio.

Automatic Control—Robert B. Wilcox, Raytheon Manufacturing Co., 148 California St., Newton 58, Mass.

Broadcast & Television Receivers—L. R. Fink, Research Lab., General Electric Company, Schenectady, N. Y.

Broadcast Transmission Systems—O. W. B. Reed, Jr., Jansky & Bailey, 1735 DeSales St., N.W., Washington, D. C.

Circuit Theory—H. J. Carlin, Microwave Res. Inst., Polytechnic Inst. of Brooklyn, 55 Johnson St., Brooklyn 1, N. Y.

† Names listed are Group Chairmen.

Communications Systems—A. C. Peterson, Jr., Bell Labs., 463 West St., New York 14, N. Y.

Component Parts—A. W. Rogers, Electronic Parts & Materials Branch, Signal Corps Engineering Labs., Fort Monmouth, N. J.

Electron Devices—J. S. Saby, Electronics Laboratory, G.E. Co., Syracuse, N. Y.

Electronic Computers—J. H. Felker, Bell Labs., Whippany, N. J.

Engineering Management—Max Batsel, Engineering Products Dept., RCA Victor Div. Bldg. 10-7, Camden, N. J.

Industrial Electronics—George P. Bosomworth, Engrg. Lab., Firestone Tire & Rubber Co., Akron 17, Ohio.

Information Theory—Louis A. DeRosa, Federal Telecommunications Lab., Inc., 500 Washington Avenue, Nutley, N. J.

Instrumentation—F. G. Marble, Boonton Radio Corporation, Intervale Road, Boonton, N. J.

Medical Electronics—V. K. Zworykin, RCA Labs., Princeton, N. J.

Microwave Theory and Techniques—A. C. Beck, Box 107, Red Bank, N. J.

Military Electronics—C. L. Engleman, 2480 16 St., N.W., Washington 9, D. C.

Nuclear Science—M. A. Schultz, Westinghouse Elec. Corp., Commercial Air Power, P.O. Box 355, Pittsburgh 30, Pa.

Production Techniques—R. R. Batcher, 240-02—42nd Ave., Douglaston, L. I., N. Y.

Reliability and Quality Control—Victor Wouk, Beta Electric Corp., 333 E. 103rd St., New York 29, N. Y.

Telemetry and Remote Control—C. H. Hoeppner, Stavid Engineering, Plainfield, N. J.

Ultrasonics Engineering—M. D. Fagen, Bell Labs., Whippany, N. J.

Vehicular Communication—Newton Monk, Bell Labs., 463 West St., N. Y., N. Y.

Sections*

Akron (4)—H. L. Flowers, 2029—19 St., Cuyahoga Falls, Ohio; H. F. Lanier, 49 West Lowell Ave., Akron, Ohio.

Alberta (8)—J. W. Porteous, Alberta Univ., Edmonton, Alta., Canada; J. G. Leitch, 13024—123A Ave., Edmonton, Alta., Canada.

Albuquerque-Los Alamos (7)—T. G. Banks, Jr., 1124 Monroe St., S.E., Albuquerque, N. Mex.; G. A. Fowler, 3333—49 Loop, Sandia Base, Albuquerque, N. Mex.

Atlanta (3)—M. D. Prince, 3821 Stoland Dr., Chamblee, Ga.; P. C. Toole, 605 Morningside Dr., Marietta, Ga.

Baltimore (3)—C. F. Miller, Johns Hopkins University, 307 Ames Hall, Baltimore 18, Md.; H. R. Hyder, 3rd, Route 2, Owings Mills, Md.

Bay of Quinte (8)—J. C. R. Punchard, Elec. Div., Northern Elec. Co. Ltd., Sydney St., Belleville, Ont., Canada; M. J. Waller, R.R. 1, Foxboro, Ont., Canada.

Beaumont-Port Arthur (6)—W. W. Eckles, Jr., Sun Oil Company, Prod. Laboratory, 1096 Calder Ave., Beaumont, Tex.; E. D. Coburn, Box 1527, Beaumont, Tex.

Binghamton (4)—O. T. Ling, 100 Henry Street, Binghamton, N. Y.; Arthur Hamburgen, 926 Glendale Dr., Endicott, N. Y.

Boston (1)—T. P. Cheatham, Jr., Hosmer St., Marlborough, Mass.; R. A. Waters, 4 Gordon St., Waltham, Mass.

Buenos Aires—J. M. Rubio, Ayachucho 1147, Buenos Aires, Argentina; J. L. Blon, Transradio Internacional, San Martin 379, Buenos Aires, Argentina.

Buffalo-Niagara (1)—D. P. Welch, 859 Highland Ave., Buffalo 23, N. Y.; W. S. Holmes, 1961 Ellicot Rd., West Falls, N. Y.

Cedar Rapids (5)—A. H. Wulfsberg, 3235—14 Ave., S.E., Cedar Rapids, Iowa; W. B. Bruene, 2769 Franklin Ave., N.E., Cedar Rapids, Iowa.

Central Florida (3)—K. A. West, 1345 Indian River Dr., Eau Gallie, Fla.; J. M

Kaeser, 1453 Thomas Barbour Dr., Loveridge Heights, Eau Gallie, Fla.

Chicago (5)—J. S. Brown, 9829 S. Hoyne Ave., Chicago 43, Ill.; D. G. Haines, 17 West 121 Oak Lane, Bensenville, Ill.

China Lake (7)—B. B. Jackson, 54-B Rowe St., China Lake, Calif.; H. W. Rosenberg, 217-B Fowler St., N.O.T.S., China Lake, Calif.

Cincinnati (4)—D. W. Martin, The Baldwin Company, 1801 Gilbert, Cincinnati 2, Ohio; F. L. Wedig, Jr., 3819 Davenant Ave., Cincinnati 13, Ohio.

Cleveland (4)—R. H. DeLany, 5000 Euclid Ave., Cleveland 3, Ohio; J. F. Keithley, 22775 Douglas Rd., Shaker Heights 22, Ohio.

Columbus (4)—W. E. Rife, 6762 Rings Rd., Amlin, Ohio; R. L. Cosgriff, 2200 Homestead Dr., Columbus, Ohio.

Connecticut Valley (1)—P. F. Ordung, Dunham Laboratory, Yale University, New Haven, Conn.; H. M. Lucal, Box U-37, University of Connecticut, Storrs, Conn.

Dallas (6)—M. W. Bullock, 6805 Northwood Rd., Dallas 25, Texas; C. F. Seay, Jr., Collins Radio Company, 1930 Hi-Line Dr., Dallas, Texas

Dayton (4)—M. A. McLennan, 304 Schenck Ave., Dayton 9, Ohio; N. A. Nelson, 408 Lewiston Road, Dayton 9, Ohio

Denver (6)—J. W. Herbstreit, 2000 E. Ninth Ave., Boulder, Colo; R. S. Kirby, 455 Hawthorne Ave., Boulder, Colo.

Des-Moines-Ames (5)—A. D. Parrott, 1515—45 St., Des Moines 11, Iowa; W. L. Hughes, E. E. Department, Iowa State College, Ames, Iowa.

Detroit (4)—M. B. Scherba, 5635 Forman Dr., Birmingham, Mich.; R. H. Reust, 20078 Westbrook, Detroit 19, Mich.

Egypt—H. M. Mahmoud, Faculty of Engineering, Fouad I University, Giza, Cairo, Egypt; E. I. El Kashlan, Main E.S.B. Stations, 4 Sherifein, Cairo, Egypt.

Elmira-Corning (1)—R. A. White, 920 Grand Central Ave., Horseheads, N. Y.; R. G. Larson, 220 Lynhurst Ave., Windsor Gardens, Horseheads, N. Y.

El Paso (6)—J. C. Nook, 1126 Cimarron St., El Paso, Texas; J. H. Maury, 3519 Fort Blvd., El Paso, Texas.

Emporium (4)—D. A. Dander, 22 S. Cherry St., Emporium, Pa.; R. J. Bisso, 99 Meadow Rd., Emporium, Pa.

Evansville-Owensboro (5)—E. C. Gregory, 1120 S.E. First St., Evansville, Ind.; A. K. Miegl, 904 Kelsey Ave., Evansville, Ind.

Fort Worth (6)—G. C. Sumner, 3900 Spurgeon, Fort Worth, Texas; C. W. Macune, 3132 Forest Park Blvd., Fort Worth, Texas.

Fort Wayne (5)—C. L. Hardwick, 2905 Chestnut St., Fort Wayne 4, Ind.; Paul Rudnick, Farnsworth Electronics Company, Fort Wayne 1, Ind.

Hamilton (8)—G. F. Beaumont, 6 Tallman Ave., Burlington, Ont., Canada; C. N. Chapman, 40 Dundas St., Waterdown, Ont., Canada.

Hawaii (7)—H. E. Turner, 44-271 Mikiola Dr., Kaneohe, Hawaii; G. H. Hunter, Box 265, Lanikai, Oahu, T. H.

Houston (6)—L. W. Erath, 2831 Post Oak Rd., Houston, Texas; R. W. Olson, Box 6027, Houston 6, Texas.

Huntsville (3)—A. L. Bratcher, 308 E. Holmes St., Huntsville, Ala.; W. O. Frost, Box 694, Huntsville, Ala.

Indianapolis (5)—A. J. Schultz, 908 E. Michigan St., Indianapolis, Ind.; H. L. Wisner, 5418 Rosslyn Ave., Indianapolis 20, Ind.

Israel—Franz Ollendorf, Box 910, Hebrew Inst. of Technology, Haifa, Israel; A. A. Wulkan, P.O. B. 1, Kiryat Motzkin, Haifa, Israel.

Ithaca (1)—Benjamin Nichols, School of Electrical Engineering, Cornell University, Ithaca, N. Y.; H. L. Heydt, General Electric Advanced Electronics Center, Cornell University Airport, Ithaca, N. Y.

Kansas City (6)—Richard W. Fetter, 8111 W. 87 St., Overland Park, Kan.; Mrs. G. L. Curtis, Radio Industries, Inc., 1307 Central Ave., Kansas City 2, Kan.

* Numerals in parentheses following Section Designate Region number. First name designates Chairman, second name, Secretary.

(Sections cont'd)

Little Rock (6)—J. E. Wylie, 2701 N. Pierce, Little Rock, Ark.; D. L. Winn, Tenth and Spring Sts., Little Rock, Ark.

London (8)—C. F. MacDonald, 328 St. James St., London, Ont., Canada; J. D. B. Moore, 27 McClary Ave., London, Ont., Canada.

Long Island (2)—Paul G. Hansel, Addison Lane, Greenvale, L. I., N. Y.; W. P. Frantz, Sperry Gyroscope Co., Great Neck, L. I., N. Y.

Los Angeles (7)—Walter E. Peterson, 4016 Via Cardelina, Palos Verdes Estates, Calif.; John K. Gossland, 318 E. Calaveras St., Altadena, Calif.

Louisville (5)—O. W. Towner, WHAS Inc., 525 W. Broadway, Louisville 2, Ky.; L. A. Miller, 314 Republic Bldg., Louisville, Ky.

Lubbock (6)—H. A. Spuhler, Electrical Engineering Department, Texas Technological College, Lubbock, Texas; J. W. Dean, 1903—49 St., Lubbock, Texas.

Miami (3)—C. S. Clemans, Station WSWN, Belle Glade, Fla.; H. F. Bernard, 1641 S.W. 82 Place, Miami, Fla.

Milwaukee (5)—Alex Paalu, 1334 N. 29 St., Milwaukee 8, Wis.; J. E. Jacobs, 6230 S. 116 St., Hales Corner, Wis.

Montreal (8)—Sydney Bonneville, Room 1427, 1050 Beaver Hall Hill, Montreal, Que., Canada; R. E. Penton, 2090 Claremont Ave., N.D.G., Montreal, Que., Canada.

Newfoundland (8)—E. D. Witherstone, 6 Cornell Heights, St. John's, Newfoundland, Canada; R. H. Bunt, Box H-182, St. John's, Newfoundland, Canada.

New Orleans (6)—J. A. Cronvich, Dept. of Electrical Engineering, Tulane University, New Orleans 18, La.; N. R. Landry, 620 Carol Dr., New Orleans 21, La.

New York (2)—A. C. Beck, Box 107, Red Bank, N. J.; J. S. Smith, 506 East 24 St., Brooklyn 10, N. Y.

North-Carolina-Virginia (3)—J. C. Mace, 1616 Jefferson Park Ave., Charlottesville, Va.; A. L. Comstock, 1404 Hampton Drive, Newport News, Va.

Northern New Jersey (2)—P. S. Christaldi, Box 111, Clifton, N. J.; W. C. Moore, 130 Laurel Hill Rd., Mount. Lakes, N. J.

Northwest Florida (3)—B. H. Overton, Box 115, Shalimar, Fla.; G. C. Fleming, 579 E. Gardner Dr., Ft. Walton Beach, Fla.

Oklahoma City (6)—A. P. Challenner, University of Oklahoma, Norman, Oklahoma; Frank Herrmann, 1913 N.W. 21 St., Oklahoma City, Okla.

Omaha-Lincoln (5)—M. L. McGowan, 5544 Mason St., Omaha 6, Neb.; C. W. Rook, Dept. of Electrical Engineering, University of Nebraska, Lincoln 8, Neb.

Ottawa (8)—George Glinski, 36 Granville Ave., Ottawa, Ont., Canada; C. F. Pattenson, 3 Braemar, Ottawa 2, Ont., Canada.

Philadelphia (3)—C. R. Kraus, Bell Telephone Co. of Pa., 1835 Arch St., 16 Floor, Philadelphia 3, Pa.; Nels Johnson, Philco Corp., 4700 Wissahickon Ave., Philadelphia 44, Pa.

Phoenix (7)—W. R. Saxon, 641 E. Missouri, Phoenix, Ariz.; G. L. McClanathan, 509 East San Juan Cove, Phoenix, Ariz.

Pittsburgh (4)—J. N. Grace, 112 Heather Dr., Pittsburgh 34, Pa.; J. B. Woodford, Jr., Box 369, Carnegie Tech. P.O., Pittsburgh 13, Pa.

Portland (7)—J. M. Roberts, 4325 N.E. 77, Portland 13, Ore.; D. C. Strain, 7325 S. W. 35 Ave., Portland 19, Ore.

Princeton (2)—G. C. Sziklai, Box 3, Princeton, N. J.; L. L. Burns, Jr., R.C.A. Labs., Princeton, N. J.

Rochester (1)—G. H. Haupt, 48 Van Voorhis Ave., Rochester 17, N. Y.; B. L. McArdle, Box 54, Brighton Sta., Rochester 10, N. Y.

Rome-Utica (1)—H. F. Mayer, 60 Fountain St., Clinton, N. Y.; R. S. Grisetti, 67 Root St., New Hartford, N. Y.

Sacramento (7)—R. C. Bennett, 3401 Chenu Ave., Sacramento 21, Calif.; R. A. Poucher, Jr., 3021 Mountain View Ave., Sacramento 21, Calif.

St. Louis (6)—F. A. Fillmore, 5758 Itaska St., St. Louis 9, Mo.; Christopher Efthim, 1016 Louisville Ave., St. Louis 10, Mo.

Salt Lake City (7)—A. L. Gunderson, 3906 Parkview Dr., Salt Lake City, Utah; S. B. Hammond, Engineering Hall, Univ. of Utah, Salt Lake City 1, Utah.

San Antonio (6)—Paul Tarrodaychik, 215 Christine Dr., San Antonio 10, Texas;

J. B. Porter, 647 McIlvaine St., San Antonio 1, Texas.

San Diego (7)—R. A. Kirkman, 3681 El Canto Dr., Spring Valley, Calif.; A. H. Drayner, 4520—62 St., San Diego, Cal.

San Francisco (7)—B. M. Oliver, 275 Page Mill Rd., Palo Alto, Calif.; Wilson Pritchett, Div. of Electrical Engineering, University of California, Berkeley 4, Calif.

Schenectady (1)—C. C. Allen, 2064 Baker Ave., Schenectady 9, N. Y.; A. E. Rankin, 833 Whitney Dr., Schenectady, N. Y.

Seattle (7)—W. C. Galloway, 5215 Pritchard St., Seattle 6, Wash.; J. M. Scovill, 7347—58 Ave., N.E., Seattle 15, Wash.

Syracuse (1)—G. M. Glasford, Electrical Engineering Dept., Syracuse University, Syracuse 10, N. Y. (Secretary).

Tokyo—Hidetsugu Yagi, Musashi Kogyo Daigaku, 2334 Tamagawa Todoroki 1, Setagayaku, Tokyo, Japan; Funio Minozuma, 16 Ohara-Machi, Meguro-Ku, Tokyo, Japan.

Toledo (4)—L. R. Klopfenstein, Portage, Ohio; D. F. Cameron, 1619 Milburn Ave., Toledo 6, Ohio.

Toronto (8)—A. P. H. Barclay, 2 Pine Ridge Dr., Toronto 13, Ont., Canada; H. W. Jackson, 352 Laird Dr., Toronto 17, Ont., Canada

Tulsa (6)—Glen Peterson, 502 S. 83 East Ave., Tulsa, Okla.; D. G. Egan, Research Laboratory, Carter Oil Company, Box 801, Tulsa 2, Okla.

Twin Cities (5)—N. B. Coil, 1664 Thomas Ave., St. Paul 4, Minn.; A. W. Sear, 5801 York Ave. S., Minneapolis 10, Minn.

Vancouver (8)—J. E. Breeze, 5591 Toronto Rd., Vancouver 8, B. C., Canada; R. A. Marsh, 3873 W. 23 Ave., Vancouver, B. C., Canada.

Washington (3)—H. I. Metz, U. S. Government Dept. of Commerce, CAA, Room 2076, T-4 Bldg., Washington 25, D. C.; R. M. Page, 5400 Branch Ave., Washington 23, D. C.

Williamsport (4)—G. B. Amey, 968 N. Market St., Williamsport, Pa.; W. H. Bresee, 818 Park Ave., Williamsport, Pa.

Winnipeg (8)—R. M. Simister, 179 Renfrew St., Winnipeg, Man., Canada; G. R. Wallace, 400 Smithfield Ave., Winnipeg, Man., Canada.

Subsections

Berkshire (1)—Gilbert Devey, Sprague Electric Company, Marshall St., Bldg. 1, North Adams, Mass.; R. P. Sheehan, Ballou Lane, Williamstown, Mass.

Buenaventura (7)—W. O. Bradford, 301 East Elm St., Oxnard, Calif.; M. H. Fields, 430 Roderick St., Oxnard, Calif.

Centre County (4)—W. L. Baker, 1184 Omeida St., State College, Pa.; W. J. Leiss, 1173 S. Atherton St., State College, Pa.

Charleston (3)—W. L. Schachte, 152 Grove St., Charleston 22, S. C.; Arthur Jonas, 21 Madden Dr., Dorchester Terr., Charleston Heights, S. C.

East Bay (7)—J. M. Rosenberg, 1134 Norwood Ave., Oakland 10, Cal.; C. W. Park, 6035 Chabolyn Terrace, Oakland, Cal.

Erie (1)—R. S. Page, 1224 Idaho Ave., Erie 10, Pa.; R. H. Tuznik, 905 E. 25 St., Erie, Pa.

Fort Huachuca (7)—B. V. Blom, Box 682, Benson, Ariz.; J. H. Homsy, Box 123, San Jose Branch, Bisbee, Ariz.

Lancaster (3)—R. B. Janes, Radio Corporation of America, Tube Dept., Lancaster, Pa.; H. F. Kazanowski, 108 Mackin Ave., Lancaster, Pa.

Mid-Hudson (2)—R. E. Merwin, 13 S. Randolph Ave., Poughkeepsie, N. Y.; P. A. Bunyar, 10 Morris St., Saugerties, N. Y.

Monmouth (2)—G. F. Senn, Orchard Rd.-River Plaza, Red Bank, N. J.; C. A. Borgeson, 82 Garden Rd., Little Silver, N. J.

Orange Belt (7)—F. D. Craig, 215 San Rafael, Pomona, Calif.; C. R. Lundquist, 6686 De Anza Ave., Riverside, Calif.

Palo Alto (7)—W. W. Harman, Electronics Research Laboratory, Stanford University, Stanford, Calif.; W. G. Abraham, 611 Hansen Way, c/o Varian Associates, Palo Alto, Calif.

Pasadena (7)—H. A. Curtis, 5193 La Canada Blvd., La Canada, Calif.; Jennings David, 585 Rim Rd., Pasadena 8, Calif.

Piedmont—Officers to be elected.

Quebec (8)—Maurice Boisvert, 1340 De Buisson, Sillery, P. Q., Canada; G. J. E. Fortin, 57 Fraser St., Quebec 6, P. Q., Canada.

Richland (7)—R. G. Clark, 1732 Howell, Richland, Washington; R. E. Connally, 515 Cottonwood Dr., Richland, Wis.

Tucson (7)—R. C. Eddy, 5211 E. 20 St., Tucson, Ariz.; P. E. Russell, Elect. Eng. Dept., Univ. Ariz., Tucson, Ariz.

USAFIT (5)—J. J. Gallagher, Box 3482 USAFIT, Wright-Patterson AFB, Ohio (Secretary).

Westchester County (2)—Joseph Reed, 52 Hillcrest Ave., New Rochelle, N. Y.; D. S. Kellogg, 9 Bradley Farms, Chappaqua, N. Y.

Wichita (6)—M. E. Dunlap, 548 S. Lorraine Ave., Wichita 16, Kan.; English Piper, 1838 S. Parkwood Lane, Wichita, Kan.

Books————

Fundamentals of Electroacoustics
by F. A. Fischer

Published (1955) by Interscience Publishers, Inc., 250 5th Ave., N. Y. 1, N. Y. 175 pages+2 page index +2 page bibliography+xii pages. 102 figures. 8¼×5¼. $6.00.

This readable textbook of modest size comprises a collection of theoretical principles of sound transduction and radiation. The reader is assumed to possess a good working knowledge of differential and integral calculus and to have a fundamental grasp of the theory of oscillations and alternating currents.

The first part presents a thorough review of oscillations and a brief treatment of electromechanical analogies. The author employs the concepts of "resistance reciprocity" (correspondence between the resistance-current and conductance-voltage relationships), "tonpilz" (coupled masses), and "tonraum" (coupled volumes), and shows the application thereof to electrical, acoustical, and mechanical configurations. There is a good fundamental discussion of the forces exerted on matter by electric and magnetic fields and of electroacoustic energy conversion principles. The usually omitted "tangential" case is very satisfactorily treated for both the electric and magnetic case. The mathematics and equivalent circuits of elementary electroacoustic transducers are clearly set forth; however, practical examples of electroacoustic apparatus are largely absent.

The latter part of the text deals briefly with radiation of sound from a piston, including the derivation of Rayleigh's equations. One might wish for a somewhat more extended discussion of this important phase of electroacoustics as well as for a treatment of the subject of sound transmission. The sensitivity and efficiency of transducers is thoroughly outlined. There is a short discussion of the "contact" (carbon) microphone. The text ends with an extensive list of symbols and units, a satisfactory bibliography and an adequate index. There are no problems.

The book will constitute a fine addition to the reference library, and because of its specialized nature it should appeal to those who are engaged in transducer design.

B. B. BAUER
Shure Brothers, Inc.
Chicago, Ill.

Electric Network Synthesis: Image Parameter Method by M. B. Reed

Published (1955) by Prentice-Hall, Inc., 70 5 Ave., N. Y. 11, N. Y. 247 pages+4 page index+x pages Illus. 9¼×6¼. $8.00.

Professor Reed presents a systematic evolution of the classical image parameter procedure of designing passive filters based upon his personal experience as a former member of the technical staff of the Bell Telephone Laboratories. The method stems from contributions made by Campbell, Bode, Dietzold, and others. It represents a classical approach to the design of filters by a step-wise procedure which results in physical structures that correspond rather closely to specified characteristics. Useful charts and tabulations are available as practical aids to simplify the design problem.

In Chapter 1, the reader is introduced to two-terminal L-C networks and equivalences of the Foster and Cauer types. Inverse networks are also described.

In Chapter 2, general properties of passive four-terminal networks are considered and related to the *T*-equivalent representation. Its electrical behavior is evaluated in terms of open-circuit, short-circuit, and iterative parameters. From the latter, the image impedance parameters and the image transfer function are derived.

Chapter 3 concerns itself with image parameters for reactive symmetric lattice sections. These lattice image parameters serve as the basis for designing filters. The specific quantities used are the image impedance parameter and the ratio function. The latter relates to the transfer loss. These quantities make it possible to design a filter for image impedance and transfer impedance requirements independently. The low-pass filter is utilized as the prototype and various functional properties are graphically illustrated.

In Chapter 4, low-pass lattices are treated extensively with emphasis on control frequencies and design criteria.

In Chapter 5, conversion techniques are applied for deriving ladder equivalences in many possible forms including the constant-k, m-derived and various multiple-m-derived variety.

Chapter 6 considers the tandem arrangements of half-sections for realizing image impedance match. By using different half-sections, filters with different image impedances at the input and output may be formed. This method generally reduces the complexity of the final network.

Chapter 7 stresses the widely used insertion loss approach. The insertion function is defined and related to reflection, transfer, and interaction functions. Graphical plots are given which cover many practical situations.

Chapter 8 is devoted to a brief treatment of dissipative effects and methods for incorporating such effects into the design of filters.

In Chapter 9, the design of low-pass filters is completely described. The main topics include filter requirements, location of cut-off, location of image impedance controls, poles of the transfer loss, reflection loss, determination of element values, transfer phase, and pass-band insertion loss.

Chapter 10 concerns itself with frequency transformations useful for converting the low-pass prototype filter into high-pass, symmetrical band-pass, and symmetrical band-block filters.

In Chapter 11, the main topic centers around the constant-resistance insertion loss equalizer and design techniques for incorporating it in the filter design to realize a desired pass-band insertion loss.

On the whole, this book is very well conceived and should prove to be of great value to engineers interested in designing image parameter filters. It is also most suitable as a college textbook. Each chapter is well supplemented with an excellent set of problems.

A. B. GIORDANO
Polytechnic Inst. of Brooklyn
Brooklyn, N. Y.

Introduction to Electronic Analogue Computers by C. A. A. Wass

Published (1955) by McGraw-Hill Book Co., Inc., 330 W. 42 St., N. Y. 36, N. Y. 220 pages+9 page index+6 page appendix+x pages. 149 figures. 8¼×5¼. $6.50.

This is a book primarily about real-time electronic analog computers (*i.e.*, "differential analyzers" and "simulators," the distinction being more a point of view than a difference in equipment). Network, repetitive, and a-c simulators are touched on only lightly. It is a book for people who use machines of this type and want to understand them rather than for those who design them. Two of the early chapters and one of the late ones are given over to discussions of ways of using analog computers. These discussions center on a series of increasingly complex problems and should be helpful to those who are not already experts.

Two features of the book merit special notice. First, the author analyzes major problems in the design of d-c operational amplifiers and points out many limitations on amplifier performance. He derives expressions that enable the reader to compute the magnitudes of certain errors made by practical amplifiers. These include errors caused by finite gain, grid current, and equivalent drift voltage, referred to input grid. The consequences of phase shift in the forward open-loop gain are touched lightly. Summing-junction capacitance and the errors it creates are not dealt with. Some readers may be surprised to learn that, percentage-wise, feedback makes one kind of error worse and does nothing to reduce another. For gains less than unity, one may want to use a pot instead of more feedback.

Secondly, the book contains descriptions of English analog computers which differ in interesting ways from American computers.

Both terminology and symbols are, of course, British, but they offer no problem to the American reader. It is apparent, however, that English practice differs in some respects from the American. The author takes a strong stand in the controversy over "open-shop" vs "post-box" methods of using computers.

This reviewer liked the "spiral" organization of the book, its up-to-dateness, and its information on British computers. It is well written and easy to read. Recommended.

STANLEY ROGERS
Convair
San Diego, California

Nuclear Radiation Detectors by J. Sharpe

Published (1955) by John Wiley & Sons, Inc., 440 4 Ave., N. Y. 11, N. Y. 179 pages+4 page index. 51 figures. 6¼×4¼. $2.50.

The entire science of nuclear physics is critically dependent on the ability of the experimenter to detect and measure the radiations resulting from nuclear reactions. This is the narrow window through which the physicist can peer into the vastly complex world of the nucleus. J. Sharpe's excellent treatise, one of Methuen's monographs on physical subjects, is intended to serve as a reference and handbook for the designer of nuclear radiation detectors. Its approach is basic, in that the physical processes in-

volved are discussed at considerable length and in great detail. The book is replete with graphs and tables giving characteristics of materials of interest and describing physical phenomena important to the operation of detectors. The discussion is limited essentially to the physics pertinent to the operation of scintillation counters, geiger counters, and ionization devices. The technical aspects of detector design, and of associated electronic equipment, are only briefly remarked upon. Photographic emulsions, chemical detectors, and cloud chambers are not covered. Chapters on the interaction of nuclear radiation with matter, detection media, efficiency of detectors, secondary emission and scintillation counters, and ionization devices serve to cover the intended subject material in a commendably complete fashion. The experimental nuclear physicist, who is almost inevitably concerned with the characteristics, if not the actual design, of such detectors will find this a convenient and highly useful handbook, which brings together an enormous amount of material otherwise available only by diligent search through a very extensive literature. References to published papers and to project reports are given in great abundance.

<div style="text-align:right">

J. W. COLTMAN
Westinghouse Research Labs.
Pittsburgh 35, Pa.

</div>

Network Analysis by M. E. Van Valkenburg

Published (1955) by Prentice-Hall, Inc., 70 Fifth Ave., N. Y. 11, N. Y. 433 pages+6 page index+vii pages. Illus. 9¼×6¼. $13.00.

Within perhaps the last decade the concepts of the complex frequency and of the pole-zero representation have become of increasingly widespread application in the study of network theory. With the growing use of the concept of the complex frequency and its ramifications, the older concepts of the steady-state and transient domains in network theory have largely been replaced by the concepts of the time and frequency domains.

Dr. Van Valkenburg in his book *Network Analysis* has addressed himself to the problem of showing the unity of the time and frequency domains by means of the pole-zero representation. He begins with the circuit concept by means of the linear differential equations that relate the currents and the potential differences in the network. The first six chapters are devoted to this classical approach. In the sixth chapter, the concept of the complex frequency is implicitly anticipated by means of graphical diagrams that show the complex roots that are the modes of transient oscillation of a simple network. In Chapter 7, the Laplace transformation is introduced and illustrated by means of numerous simple examples. In Chapter 8, the time and frequency relationships are established by the use of Fourier theory in order to lay a foundation of physical significance for the exploitation of the power of the Laplace transformation. With the background thus established, the concept of the complex frequency is explicitly introduced in Chapter 9 where it is used in expressing the impedance and admittance functions of a network. The use of the complex frequency in Chapter 9 leads directly to the pole-zero representation of network functions in Chapter 10, where, by means of a geometrical argument, the unity of the time and the frequency behavior of networks is developed. This unity is further expanded in Chapter 11 where the steady-state response of networks is studied by means of the pole-zero representation. In the last four chapters, Chapters 12 through 16, the pole-zero representation is used to study the properties of one-terminal pair and two-terminal pair networks, amplifying networks, and feedback networks.

This book is well conceived and well written. It is to be recommended to both the student who is first learning of the relationship of the time and frequency domains and to the engineer who wishes to refresh his knowledge of network phenomena. Perhaps the most severe criticism of the book is that the initial chapters on the classical analysis are somewhat more extensive than necessary and that in these chapters the concept of the complex frequency has not been more explicitly anticipated.

<div style="text-align:right">

P. F. ORDUNG
Dept. of Elec. Engrg.
Yale University
New Haven, Conn.

</div>

RECENT BOOKS

Canning, R. G., *Electronic Data Processing for Business and Industry*. John Wiley & Sons, Inc., 440 Fourth Ave., N. Y. 16, N. Y. $7.00.

Cohen, A. B., *Hi-Fi Loudspeakers and Enclosures*. John F. Rider Publisher, 480 Canal St., N. Y. 13, N. Y. $4.60.

Crichlow, W. Q., Smith, D. F., Morton, R. N., and Corliss, W. R., *Worldwide Radio Noise Levels Expected in the Frequency Band 10 Kilocycles to 100 Megacycles*. National Bureau of Standards Circular, Government Printing Office, Washington 25, D. C. $0.30.

Eckert, W. J. and Jones, R., *Faster, Faster*. McGraw-Hill Book Co., Inc., 330 W. 42 St., N. Y. 36, N. Y. $3.75.

Kaufman, M. and Thomas, H., *Introduction to Color TV*. John F. Rider Publisher, 480 Canal St., N. Y. 13, N. Y. $2.70.

Orr, W. I., editor, *Radio Handbook*, 14th ed. Editors and Engineers Ltd., Summerland, Calif. $7.50.

Rybner, Jorgen, *Nomograms of Complex Hyperbolic Functions*. Jul. Gjellerups Forlag, Copenhagen, Denmark. Dan. Kr. 44.00.

Schure, Alexander, *Multivibrators*. John F. Rider Publisher, 480 Canal St., N. Y. 13, N. Y. $0.90.

Tremaine, H. M. and Teffeau, G. K., *Attenuators, Equalizers and Filters*. Howard W. Sans & Co., Inc., Indianapolis 5, Indiana. $2.75.

Abstracts of IRE Transactions

The following issues of "Transactions" have recently been published, and are now available from the Institute of Radio Engineers, Inc., 1 East 79th Street, New York 21, N. Y. at the following prices. The contents of each issue and, where available, abstracts of technical papers are given below.

Sponsoring Group	Publication	Group Members	IRE Members	Non-Members*
Aeronautical & Navigational Electronics	Vol. ANE-2, No.	$1.40	$2.10	$4.20
Aeronautical & Navigational Electronics	Vol. ANE-3, No. 1	1.30	1.95	3.90
Antennas & Propagation	Vol. AP-4, No. 1	2.65	3.95	7.95
Audio	Vol. AU-4, No. 1	0.75	1.10	2.25
Electron Devices	Vol. ED-3, No. 1	2.10	3.15	6.30
Engineering Management	Vol. EM-3, No. 2	0.55	0.80	1.65
Industrial Electronics	PGIE-3	1.70	2.55	5.10
Medical Electronics	PGME-4	1.95	2.90	5.85
Nuclear Science	Vol. NS-3, No. 1	0.90	1.35	2.70

* Public libraries and colleges may purchase copies at IRE Member rates.

Aeronautical & Navigational Electronics

VOL. ANE-2, No. 4, DECEMBER, 1955

Chairman's Report—E. A. Post

ADF—J. V. N. Granger

The Automatic Radio Direction Finder— F. L. Moseley

The convenience, ease of operation and inherent reasonableness of a direction finding system which culminates in a simple needle pointing to the selected radio station must make it seem to the late-comer that things were always thus in the plane's front office. Not so. Much anguish was experienced, many brains overtaxed, and considerable ingenuity exercised to place this apparently simple device in the hands of the pilot. It will be the purpose of this paper to give the history of the development of the automatic direction finder, to give a condensed explanation of its mode of operation, and to describe its use in the navigation of aircraft.

Airline Requirements for Airborne Automatic Direction Finders and the Program of Equipment Development—W. T. Carnes, Jr.

A Magnetic Radio Compass Antenna Having Zero Drag—A. A. Hemphill

The use of high speed aircraft has accentuated the requirements for low drag antennas and has made the precipitation static problem much more severe. A radically new loop design using ferrite materials makes it possible to exceed the performance of the present external loop antenna in a submerged magnetic antenna that has zero drag. Among its important characteristics are lower weight, less mechanism, and rejection of precipitation static interference as well as reduction of the drag to zero.

The antenna consists of a small ferrite-core goniometer with four radial collector bars of the same material. The design includes a novel quadrantal error compensating scheme in which the loop is compensated by attaching selected end pieces to the collector bars.

ADF Sense Antenna Requirements and Design—J. T. Bolljahn

Analysis of the Over-Station Behavior of Aircraft Low Frequency ADF Systems—H. H. Ward, 3rd

A theoretical investigation has been made of the behavior of low-frequency automatic direction finder systems in aircraft on courses near and over the radio station. This behavior is explained in the light of electromagnetic field theory and the equipment characteristics. An equation is derived for the locus of all points where the ADF indicator will start to reverse due to sense-antenna signal phase shift with respect to the loop-antenna signal as the station axis is approached and passed. The equation contains six geometrical and electrical variables. The locus thus defined is similar to a cone or paraboloid, apex down, with the apex located at the radio station in most cases.

The equation predicts that for a phase advance of the loop signal, relative to the sense-antenna signal, of slightly more than the 90° value applied by the basic ideal receiver, the apex of the cone-like space figure locus rises off the ground, and that it would be possible to fly under this apex, producing but one reversal of ADF indicator needle with this single reversal starting exactly over the radio station. The altitude of this apex is a relatively simple function of the variables.

The results of the flight tests verifying the theoretical findings are given together with some requisites for the use of the findings to eliminate the effects due to improper sense antenna location, provided the location error is not too extreme.

The Marconi AD.7092 Series of ADF Receivers—L. R. Mullin

This paper traces briefly the history of the development of the AD.7092 series of automatic radio direction finders and describes the special features of the AD.7092C which was designed to suit the requirements of North American operators. Novel features include an electrical remote control system and a tuned remote sense amplifier which permits the use of long feeders using small sense antennas. The suppressed loop antenna and method of

error compensation are described and the trend of future ADF developments in Great Britain is indicated.

Contributors

PGANE News

VOL. ANE-3, No. 1, MARCH, 1956

James L. Dennis

The Practical Combination of Air Navigation Techniques—H. J. Galbraith and N. Braverman

Neither airborne self-contained nor ground-based air-navigation systems can by themselves completely meet the requirements of present day aircraft for both accuracy and continuity or positional and steering data. It is shown how dead-reckoning, providing continuity and reliability through the use of air-derived acceleration or velocity data, combined with intermittent "fixing" by employment of accurate position data obtained through the use of ground and stellar referenced sources, can increase operational capability without "pressing the state of the art" in any of the components of a system. Methods of inserting position fixes and of instrumenting the associated wind-computation and wind-memory functions are described and system errors are analyzed.

The Problems of Transition to Single Sideband Techniques in Aeronautical Communications—J. F. Honey

Reliability Through Redundancy—R. H. Hershey

As requirements for automaticity cause airborne electronic systems to grow in complexity, reliability tends to become a limiting factor to system success. Because of the small probability that a large number of components will all operate successfully at once, even though individual reliabilities are high, complex systems are inherently unreliable. Efforts to better system reliability through improvement of component reliability rapidly reach the point of diminishing returns. A more fruitful solution to the problem is the redundant use of parts of the system in such a way that the function of a malfunctioning assembly is assumed by another assembly. The "probability of no failure" barrier is by-passed by this method, and a large improvement of in-flight reliability can be obtained with relatively small increase of system complexity. The potential of method is illustrated by a reliability analysis of a theoretical system, its application in design of a system is outlined, and techniques of detecting system failures and initiating corrective action are discussed.

Some Operational Advantages of Pictorial Navigation Displays—F. S. McKnight

In the preparation of an evaluation program for several pictorial navigation displays, developed under sponsorship of the Air Navigation Development Board, it was necessary to make a study of possible operational advantages of the use of such displays. When compared to conventional symbolic instrumentation for displaying navigation information, the pictorial displays appear to have three primary advantages: 1) Continuous usable navigation information is supplied to the pilot in all airspace within range of the ground radio facilities. 2) Navigation workload on the flight crew is materially reduced. 3) A reduction in number of ground radio aids should be possible if most aircraft were equipped with pictorial navigation displays. Brief description of several pictorial computers is included.

An Evaluation of High Frequency Antennas for a Large Jet Airplane—O. C. Boileau, Jr.

The ability of aircraft cap-type high frequency antennas to act as efficient radiators is a subject of much current interest. In most instances the fixed-wire type hf antenna is incorrectly assumed to be superior to flush cap-type antennas. In this paper a performance comparison of five different hf communication antenna configurations for a large high speed aircraft is presented. These antennas include two fixed-wire types, a conventional tail-cap type, and two "L-gap" tail-cap configurations. The impedance vs frequency characteristic is explored over the 2–24 mc range for each antenna. The antenna system efficiency of each antenna is computed using the antenna impedance characteristic and considering the transmission line, coupling network, antenna feed and lightning protection system, and the antenna radiation pattern. This antenna system efficiency is used as a basis for comparison of five antennas.

Experimental Determination of TACAN Bearing and Distance Accuracy—E. deFaymoreau

Radio Beam Coupler System—H. Hecht and G. F. Jude

The radio beam coupler system has been recently developed as an en route navigation and approach aid for modern transport and bombing aircraft. It is applicable to both military and commercial operations.

The system comprises an electronic amplifier and cockpit switching elements for coupling the automatic pilot to VOR and ILS radio facilities. Accuracy and efficiency of control is improved over previous systems while automatic sequencing and sensing simplify the human pilot's operating procedures. Design features such as magnetic components and hermetic sealing enhance the reliability of the amplifier unit.

Contributors

Antennas & Propagation
VOL. AP-4, No. 1, JANUARY, 1956

News and Views
Contributions—Exterior Electromagnetic Boundary Value Problems for Spheres and Cones—L. L. Bailin and Samuel Silver

The problem of determining a harmonic time-varying electromagnetic field where the electric vector assumes prescribed values for its tangential components over given spherical or conical boundaries and which has proper radiation characteristics at infinity is considered by a procedure very much like that used in the theory of slots in waveguide walls. The technique used in solving this type of boundary value problem is to establish, by an application of the Lorentz Reciprocity Theorem, a Green's function which represents the electric and magnetic fields of a point generator (infinitesimal dipole) applied at an arbitrary position on the conducting surface where the fields satisfy homogeneous boundary conditions. The total fields for an arbitrary source are then obtained by superposition; *i.e.*, direct integration over the aperture.

Since detailed results for the case of a sphere have been obtained by many authors, we confine the details of the technique to the infinite cone. It is assumed that in each case the tangential components of the electric vector are given functions over the entire boundary surface. The results apply directly to the theory of radiating apertures in a perfectly conducting spherical wall or a cone, since the tangential components of the electric vector are different from zero only in the area of the aperture, where it is presumed they are known. The results are also applicable to scattering by conducting spheres and cones, since the tangential electric field components over the boundary surfaces are the negative of those of the incident field.

To illustrate the applicability and the limitations of the results, we shall present the formal solutions for arbitrarily shaped apertures on cones and apply them to the several types of delta slots which are usually discussed in connection with other radiating structures.

Analysis of a Terminated-Waveguide Slot Antenna by an Equivalent Circuit Method—L. B. Felsen

The pattern in a half-space of a slot in the wall of a waveguide is a function of the terminating impedance. The description of the far fields in such a configuration is simplified considerably by the adoption of a network viewpoint, whereby the half-space is represented approximately by two (or more) spherical transmission lines, the feeding waveguide by a single uniform transmission line, and the slot by a coupling network which is directly analogous to that for a hybrid junction. For a given waveguide termination, the spherical mode voltages are computed by a simple network calculation, and the gain pattern is obtained by modal synthesis. The slot equivalent circuit parameters are obtained readily by simple measurements or from available theoretical formulas. Described in detail both theoretically and experimentally is a symmetric rectangular slot cut in either the broad or narrow face of a rectangular waveguide.

An Experimental Study of the Disk-Loaded Folded Monopole—E. W. Seeley

Data is presented to show the reduction in size and increase in radiation resistance and bandwidth of the disk-loaded folded monopole as compared with a disk-loaded monopole of the same electrical length. The ratio of diameters of the folded part to the diameter of the driven part was varied for one series of impedance measurements and the axial spacing between the driven part and folded part was varied for another series. The resonant radiation resistance and resonant length may be varied almost independently. The radiation resistance depends upon the ratio of diameter of the folded part to the diameter of the driven part, and the resonant length depends upon axial spacing. The radiation resistance multiplication factor relative to a disk-loaded monopole of the same electrical length is approximately the same as the multiplication factor of a folded dipole relative to a dipole. The disk-loaded folded monopole has a greater bandwidth than an unloaded monopole of the same wavelength-to-diameter ratio. Where the effective diameter of the folded antenna is $\sqrt{2D_dS}$, its radiation pattern is essentially that of an unloaded monopole.

Some Data for the Design of Electromagnetic Horns—E. H. Braun

Using an idea recently suggested by the author, a table is presented from which the gain of all electromagnetic horns may be calculated with substantially the same accuracy obtainable using the gain formula.

The exact parameters of an optimum horn are given, and a simple procedure for the design of optimum horns with a specified gain and other desirable properties is described.

Measured Performance of Matched Dielectric Lenses—E. M. T. Jones, T. Morita, and S. B. Cohn

Two microwave lenses whose surfaces have been matched respectively by embedded capacitive walls and by simulated quarter-wave transformers were built and compared experimentally to an unmatched lens of identical aperture and focal length. At the design frequency, the matched lenses exhibited reductions in side-lobe level of 14 and 10 db with respect to the unmatched lens, and increases in over-all gain of 0.35 and 0.1 db. The input vswr of the feed horn was reduced from 1.6 for the unmatched case to 1.02 and 1.05 for the matched cases. The bandwidth of good performance for the two lenses ranged from 16 per cent to at least 44 per cent.

Microwave Lens Matching by Simulated Quarter-Wave Transformers—T. Morita and S. B. Cohn

The reflections from the surface of a dielectric lens may be cancelled by a quarter-wavelength layer of refractive index intermediate between that of air and the lens medium. The possibility of simulating a quarter-wave matching section by perturbing the boundary of the lens is described in this paper. Some of the configurations considered are corrugated surfaces, arrays of dielectric cylinders, and arrays of holes in the dielectric surface. In each case, a match may be obtained at a given frequency and angle of incidence by the proper adjustment of the depth of the perturbation, and of one other parameter such as the width of a groove.

Surface Currents Excited by an Infinite Slot on Half-Planes and Ribbons—J. R. Wait and M. O'Grady

The distribution of surface current density on a perfectly conducting half-plane excited by an infinite axial slot is determined. The slot is assumed to be of small width and it is excited throughout its length by a uniform transverse voltage. It is shown that the surface currents which flow toward the edge of the half-plane are somewhat smaller than they would be if they were on an infinite plane. For sake of comparison the surface currents of an infinite axial slot on a thin elliptic cylinder or ribbon are also examined.

Radar Back-Scattering Cross Sections for Nonspherical Targets—P. N. Mathur and E. A. Mueller

Studies were made of the scattering of electromagnetic waves from nonspherical targets by making exact determination of the nose-on radar back-scattering cross sections of conducting prolate spheroids of various sizes and shapes. Curves are given for the back-scattered cross sections as a function of dimensionless size and shape parameters for prolate spheroids. The results are compared with the Rayleigh-Gans first-order approximation and Stevenson's third-order approximation, and the range of applicability of these approximations is evaluated.

An Experimental Investigation of Cavity-Mounted Helical Antennas—A. Bystrom, Jr., and D. G. Berntsen

This paper presents the results of an experimental investigation which led to the development of cavity-mounted helical antennas for airborne applications. The effects on patterns and impedance of various antenna parameters, such as number of turns, cavity size and shape, helix pitch angle, and conductor size, were investigated.

Methods of feeding the helix which produce an input impedance near 50 ohms, without external compensation, throughout the axial mode frequency range are discussed. Some of the types of cavity-mounted helices developed and typical performance data are described.

Radiation Patterns of Unsymmetrically Fed Prolate Spheroidal Antennas—H. A. Myers

This paper describes the radiation pattern of the unsymmetrically-fed prolate spheroidal transmitting antenna. Maxwell's equations are solved in prolate spheroidal coordinates subject to the boundary conditions. The prolate spheroidal functions are expressed in the form of power series and Laurent series. Radiation patterns have been obtained for antennas of three different lengths up to about one wavelength long, for length/thickness ratios of about 5/1, 10/1, 22/1, and 316/1, and for nine unsymmetrical gap locations as well as for the symmetrically-fed cases. It was found that the two most important factors affecting the radiation pattern of a fairly thin antenna were the location of the gap and the electrical length. For antennas less than a half wavelength long, the pattern was the usual symmetrical figure eight and was essentially independent of the

location of the gap (except for magnitude changes due to the different gap impedances). For antennas two-thirds to three-quarters of a wavelength long the figure eight patterns could be "bent" in the direction of the longer element, and for antennas one wavelength long or longer minor lobes began to appear.

Optical Fresnel-Zone Gain of a Rectangular Aperture—Charles Polk

An equation for the on-axis gain of a uniformly illuminated rectangular aperture is derived which is valid in the "Optical Fresnel Zone." This equation is formulated in terms of the ordinary radiation field gain multiplied by a correction factor which depends upon the aperture dimensions and the distance, R, from the aperture at which the gain is measured. A table of the function $[C^2(v) + S(v)]/v^2$ is given; $C(v)$ and $S(v)$ being the Fresnel integrals. The gain of a square aperture ($L \times L$ meters) in the Fresnel-zone region is compared with the gain of a circular aperture and it is shown that for apertures of equal area $G_{square} < G_{circle}$ when $(L^2/\lambda) < R \leq (2L^2/\lambda)$; it is also shown that G_{square} has minima, but not zeros at $R = L^2/7.30\lambda$, $R = L^2/15.24\lambda$. Furthermore it is shown that for $R \geq L^2/2\lambda$ the first order gain correction factor of a square aperture is equal to the gain correction factor of a circular aperture having a diameter equal to 1.208 times the sidelength of the square. An approximate formula for the Fresnel-zone gain of a long and narrow aperture is also given.

Some Relationships between Total Scattered Power and the Scattered Field in the Shadow Zone—J. T. Bolljahn and W. S. Lucke

Equations are derived which relate the far-zone scattered field, as measured in the shadow zone of an electromagnetic scatterer, to the total energy scattered and absorbed by the scatterer. In the case of a perfectly conducting scatterer, the energy stored in the fields about the scatterer is also related to the far-zone scattered field in the shadow zone.

Long Range Meteoric Echoes via F-Layer Reflections—J. T. deBettencourt and W. A. Whitcraft, Jr.

This note reports HF observations of meteoric back-scatter echoes at ranges greatly exceeding radio line-of-sight. The observations were part of a program of measurements on backscatter using COZI equipment.

Examples are given of observations at South Dartmouth, Massachusetts in 1949 on 16 mc and of more recent observations in 1954 on 12 and 16 mc using improved equipment. Short duration echoes are observed in advance at ranges shorter than those of the ground backscatter. No such meteoric echoes are observed when the ground backscatter disappears. The meteoric echo ranges move with time of day just as the range to the ground backscatter moves. A plausible explanation for the observed meteoric echo ranges exceeding 1,000 miles is that they are due to backscatter from the trail, ionospherically propagated to and fro via the F region, just as the ground backscatter. Other possible ionospheric propagation modes are discussed.

"Fresnel Antenna Patterns"—L. W. Lechtreck

Correlation in VHF Propagation over Irregular Terrain—R. S. Kirby and F. M. Capps

A study has been made of the correlation in transmission loss observed over irregular-terrain paths. Simultaneous mobile measurements were made of two pairs of VHF broadcasting stations in the Washington, D. C.–Baltimore, Maryland area. The correlation coefficients derived from sample sets of transmission loss data indicate that when reception is from opposite directions, no significant correlation is evident, and when the paths of propagation are the same even though the frequencies are separated considerably, the correlation appears to be significantly high.

Communications—Control of Surface Cur-

rents by the Use of Channels—W. K. Saunders

The Impossibility of Certain Desirable Luneberg Lens Modifications—A. F. Kay

Summary of Normal Mode Theory Symposium

Contributors

IRE Transactions on Antennas and Propagation. Index to Volume AP-3—1955

Audio

Vol. AU-4, No. 1, January–February, 1956

Why Engineers Should Write Technical Papers—M. S. Corrington

PGA News

Miniaturized Audio Transformer Design for Transistor Applications—H. H. Kajihara

The electrical and physical parameters which are of concern in audio transformer design and their relationships to the problems of miniaturization are discussed. A detailed design of two typical audio transformers for transistor application is presented to illustrate the application of the design information obtained in the SCEL investigation on the subject. Several methods of sealing these miniature units and the effect on the ultimate size are reviewed. General information pertinent to the design of miniaturized audio transformers is assembled in the appendix.

Efficiency and Power Rating of Loudspeakers—R. W. Benson

The specification of the performance of loudspeakers is a subject of international controversy at the present time. Several groups in this country are concerned with standardized methods of evaluating the performance of loudspeakers in order to have a basis for comparison. Several European countries are also concerned with similar problems.

The measurement of the response-frequency characteristic and directional characteristics of loudspeakers is routinely performed by various laboratories. Sufficient agreement can be attained by the various laboratories to standardize this measure of performance. It is important to have a measure of the efficiency, that is sound power output vs electrical power input, and also a method of specifying the power handling capacity of a loudspeaker. Various methods are in use at the present time to indicate the characteristics of a loudspeaker concerning these two measures. The method of using a reverberation chamber to integrate acoustic power output and thus determine the efficiency will be discussed in comparison to the more tedious method of analytical integration of measurements performed in free space. Power handling capabilities of loudspeakers as determined by distortion measurements and mechanical or electrical failure will also be discussed. A summary of the various methods of specifying both efficiency and power handling capacity as used in various laboratories in both the United States and Europe will be included.

Bells, Electronic Carillons, and Chimes—F. H. Slaymaker

Bells and chimes, unlike the more familiar string and wind instruments, produce tones in which the overtone structure cannot be expressed as a series of harmonics. The accuracy of tuning of the various overtones varies widely but the better cast bell carillons, electronic carillons, and tubular chimes do have very accurately tuned overtones. This paper describes the results of measurements on cast bells, electronic carillons, and tubular chimes. Data will be given on relative amplitude and decay rates of the various overtones. The reaction of "out-of-tuneness" will be discussed and explained. A new type of tone source for electronic carillons will be described. With this new tone source, a rod of carefully controlled rectangular cross section is used. This rod can give in a single unified

structure essentially the same overtone array as that of an accurately tuned cast carillon bell.

Contributors

Correction

Electron Devices

Vol. ED-3, No. 1, January, 1956

Current-Voltage Characteristic and Hole Injection Factor of Point Contact Rectifiers in the Forward Direction—K. Lehovec, A. Marcus, and K. Schoeni

Theoretical curves are given showing the current-voltage relationship for a germanium point contact rectifier biased in the forward direction, and the dependence of the hole injection factor on current. The curves were obtained by graphical solution of equations similar to those derived by Swanson.

Large Signal Behavior of High Power Traveling-Wave Amplifiers—J. J. Caldwell, Jr. and O. L. Hoch

The results of an experimental investigation on the large signal behavior of a kilowatt power level helix type traveling-wave amplifier tube are presented. Operation with and without attenuators was investigated using a movable electromagnetic probe to measure power level along the tube.

Quite different effects of drive power and beam voltage on the saturation level were found for operation with and without attenuators. The maximum power level is lower for attenuator operation. Also, power levels do not continue to increase with increasing beam voltage and drive power. In contrast, attenuator-less operation produces the highest efficiency, and the power levels continue to rise with increasing beam voltage and drive power. Conversion efficiencies as high as 25 per cent are obtained with an attenuator and as high as 40 per cent without an attenuator. Efficiency calculations based on small-signal theory can be made to agree reasonably well with the experimental attenuator-less operation efficiencies by assuming an appropriate ratio of the ac component of beam current to the dc component of beam current, i/I_0.

Wave Propagation On Multifilar Helices—H. R. Johnson, T. E. Everhart, and A. E. Siegman

The modes of the sheath helix are shown to be related closely to the space harmonics of real helices. Multiwire helices propagate many modes, the principal space-harmonic component of each approaching more closely the appropriate sheath helix mode as the number of wires is increased. Each mode can be excited by a certain phase sequence of exciting currents for the wires in one transverse plane. Experimental verification of the theory is reported using a bifilar helix tube. Phase velocities and impedances are measured, using Kompfner's null method and the start of backward-wave oscillations for the principal forward and backward components respectively.

An Approximation to Alpha of a Junction Transistor—R. D. Middlebrook and R. M. Scarlett

In this paper, a new approximation for the frequency dependence of the short-circuit current gain of a theoretical junction triode is derived, which is a rational function of frequency and convenient to use. It is shown that the approximation is in excellent agreement with the frequency response of the theoretical expression for alpha in both magnitude and phase to above the alpha cutoff frequency. The approximation is also considered in the time domain, where it is in good agreement except for small values of time corresponding to frequencies well above alpha cutoff.

A Step-Type, Broadband, X-Band Ceramic Waveguide Window—H. K. Jenny and F. E. Vaccaro

This paper describes a broadband-type ce-

ramic output window for use in X-band microwave power tubes. This vacuum-tight window is capable of passing average cw power outputs of more than 250 watts, and can withstand temperatures as high as 750°C. The window introduces a standing-wave ratio of less than 1.2 over a frequency range of more than 2,000 megacycles per second, and, due to lengthening of the arc path, shows little tendency toward arcover.

Scalloped Beam Amplification—T. G. Mihran

Scalloped beam amplification occurs when an rf signal propagates along an electron beam of periodically varying diameter whose scallop wavelength is adjusted to be one-half the effective plasma wavelength in the beam. The dependence of this gain mechanism on frequency, magnetic field, voltage, and current has been investigated experimentally, and over two db gain per scallop has been measured. In the particulr setup used, positive ion oscillations caused smearing of true scalloped beam amplification effects.

A Large-Signal Analysis of the Traveling-Wave Amplifier: Theory and General Results—J. E. Rowe

Equations are derived describing the large-signal operation of the traveling-wave amplifier including the effects of ac space charge and attenuation along the helical slow-wave structure. The equations constitute a system of nonlinear partial-differential-integral equations valid with reasonable approximations for all values of the parameters which are encountered in typical high-power traveling-wave amplifiers. The parameters which appear in the equations are the relative injection velocity b, the gain parameter C, the large-signal space-charge parameters K and B, the loss parameter d, and the input-signal level A_0.

The working equations were programmed for and solved on the Michigan Digital Automatic Computer, MIDAC, located at the University of Michigan's Willow Run Research Center. The rf voltage amplitude $A(y)$, the phase lag of the rf wave relative to the electron stream $\theta(y)$, and the velocity deviation $2Cu(y, \phi_0)$, were computed and plotted for several values of C, K, b, and B at $A_0 = 0.0025$, and $d = 0$. Also, distance-phase plots are presented for each of the above cases. These flight-line diagrams for the traveling-wave amplifier are similar to the well-known "Applegate diagram" associated with klystrons. Zero-space-charge solutions are presented for $C = 0.05$, 0.1, and 0.2 with b as the parameter in order to determine the value of b which gives the maximum saturation gain and the optimum tube length. For $C = 0.1$ similar solutions are obtained for several values of the space-charge parameter K. Presented in graphical form, the results of these various solutions shed a considerable amount of light on the high-level operation of the traveling-wave amplifier.

New Beam Power Tubes for UHF Service—W. P. Bennett

This paper is, in effect, a progress report on the continuing development of high-power, grid-driven, uhf beam power tetrodes similar to the 6448. It is divided into four main parts: 1) a brief history of the development and field usage of the 6448; 2) a review of the basic design philosophy and construction of the 6448; 3) a description of a new developmental 27-kilowatt uhf beam power tube; 4) a discussion of other new uhf beam power tubes for pulse service.

A UHF Traveling-Wave Amplifier Tube Employing an Electrostatically Focused Hollow Beam—S. B. Crumly

The increasing importance of beam-type microwave devices has stimulated interest in focusing methods other than the usual uniform magnetic field. One such method applicable to hollow cylindrical beams, proposed by L. A. Harris, utilizes a radial electric field acting on a spinning beam to counterbalance the space-charge divergence forces. A traveling-wave amplifier operating in the 300 to 600 mc region, employing this focusing method, was designed and constructed. Experimental results obtained with this tube are presented. Beam transmissions as high as 90 per cent and net gain over 15 db were obtained. Practical considerations and tube design factors are discussed. The primary advantage of this kind of focusing is in the elimination of the solenoid, and consequent reduction in power supply requirements and weight, accessibility of rf connections to the tube, and elimination of capsule and aligning adjustments. This focusing method appears to have great potential usefulness in hollow-beam applications, and particularly in devices where the spiral motion of the beam can be made to interact with a spirally traveling wave.

Recent Dark-Trace Tube Developments—S. Nozick

Dark-trace tubes or skiatrons have certain advantages over bright display tubes which make their use desirable for information displays. These advantages are the ability to integrate visually, to store information, and daylight and sunlight viewing. Since World War II, at the time the 4AP10 was used, several of the basic disadvantages have been corrected in part, such as erase time, writing speed, contrast and color. Several experimental tube types have been evolved and others are under development. Some radical improvements in one or more of the limiting characteristics have been achieved. These were accomplished in several ways, including low heat capacity screens, conductive film techniques, different screen compositions, special electron optics, and other techniques. The characteristics and limitations are summarized for different tube types together with several suggestions for possible further research and development in the field.

The equipment design factors peculiar to these tubes, such as stringent voltage requirements, sweep failure protection, beam current limiting circuitry, and other items are discussed to aid preliminary equipment designers in the use of these tubes.

Light-Weight Aluminum Foil Solenoids for Traveling-Wave Tubes—W. G. Worcester, A. L. Weitzmann, and R. J. Townley

Most traveling-wave tubes use solenoids to constrain their electron beams. Each tube requires a certain diameter, length, and strength of magnetic field, which are the basic specifications for the solenoid. In addition, for airborne applications it becomes important to minimize weight and power, and to provide suitable cooling.

Methods have been developed for winding coils of aluminum foil, together with a suitable insulation. The ends of the coils can be machined, then bonded to a heat-conducting plate or cooled by an air stream. There is only one insulating boundary; thus heat is readily removed from the winding. This design permits operation at high current densities without exceeding safe hot-spot temperatures, so that aluminum coils can be made about the same size, for given characteristics, as copper wire coils. The saving in weight is thus proportional to the densities of the two materials.

A further interesting feature of the aluminum foil solenoids is that the ends of the coils can be machined to almost any desired shape. Slots or holes can be cut in the coils to permit the introduction of power leads or mechanical devices.

Engineering Management

Vol. EM-3, No. 2, March, 1956

Management in Production Engineering—Charles Blahna

The Research and Development Stockroom—Leo Rosen

The Soul of an Organization—E. A. Laport

Is the Yardstick for Estimating Individual Engineering and Scientific Potential Reliable?—Allen Schooley

This paper is based on the case histories of twelve persons who were hired as B.S. degree graduates about twelve years ago to do electronic work at the Naval Research Laboratory. The potential value of the employees, based on information available at the time they were hired, is compared with their now established record. It is concluded that no reliable means existed for estimating the engineering and scientific potential of the individuals considered.

Managers: When Do We Get More Engineers?—P. S. Wessels

From the figures presented, it has been demonstrated that engineers will be in short supply for the next twenty years. The effects on industry have been shown to be threefold: (1) a shortage of development engineers; (2) a shortage of engineers to serve a necessary function of management; and, (3) a far reaching effect on the military preparedness program. The possible solutions to this problem have been widely discussed in the literature. They are not as clearly presented as is the statement of the problem. At least, we have compiled the first phase of an engineering solution to a tough problem: a statement of the problem. We are now searching for possible solutions. If we proceed with the engineering approach, we will next choose one of these solutions and develop it to its fullest extent. At the end of this development period, we will be ready to apply the solution to an industrial situation to achieve the desired end result.

Industrial Electronics

PGIE-3, March, 1956

A Miniature Strobe Light for a 60,000 RPM Bearing Tester—John Patraiko

A strobe light system for high speed machinery has been developed with the following specifications—Flashing Rate: 3,000 to 60,000 fpm (flashes per minute); Light Pulse Width: 1 microsecond at one third intensity points; Light Intensity: 10 candle power max. at 60,000 rpm.

This paper presents the circuitry with a discussion emphasizing the design of the strobe light pulser.

Electronic Instrumentation of a Device to Automatically Count and Size Particles in a Gas—E. S. Gordon, D. C. Maxwell, Jr., and N. E. Alexander

This paper describes the electronic instrumentation of a device called an aerosoloscope for automatic counting and sizing of aerosol particles. This device relieves the chemist of the tedious and time-consuming job of counting the particles collected on a slide under the microscope. It has wide potential application in analyzing dusts, fogs, smokes, etc.

Particles from one to 64 microns in diameter and counting rates up to 100 particles per second are handled by the instrument. The aerosol is diluted and drawn across a high intensity light beam; a multiplier phototube receives a portion of the light energy scattered by each particle. The resulting electrical pulses are amplified and classified by size into twelve groups by a unique pulse height discriminator. Glow-transfer tubes and registers are used to count the pulses within the various groups. Dynamic range problems and system noise are briefly discussed.

How Can Industry Use Television?—H. F. Schneider

Capacitive Measurements of High Sensitivity and Their Applications to Industrial Testing and Control—George Revesz

Some Applications of Capacity Micrometers to High Speed, High Temperature Measurements—R. E. Condit

A capacity micrometer for the measurement of blade clearance in a turbine is described. The calibration of the instrument is nonlinear with displacement, and clearances of the order of .030 to .001 inch may pe measured with a nominal accuracy of ±10 per cent of the indicated reading.

Measurements may be made at temperatures up to 1,500°F by the use of water-cooled pickup probes, and with a frequency response from dc to 200,000 cycles per second.

The stability of the measurement depends on the temperature stability of the pickup dielectric material. Pickup drift may be measured during operation and may be counteracted by a control on the instrument.

Stable reference capacitors provide a means for checking zero drift and calibration independent of the pickup and cable.

Examples of the application of the instrument to a variety of other displacement measurements are provided.

Principles of Radioactive Gauging as Applied to Measurement and Control in the Process Industries—D. C. Brunton

A Frequency-Modulated Magnetic Recorder—Walther Richter

Limitations of tape recording of amplitude modulated signals are:

1. Inherent frequency response of magnetic recording systems is not flat, necessitating compensation networks.

2. D-C signals cannot be recorded with conventional recording heads and circuits.

3. A variation of about 1 db (12 per cent) can be expected in the characteristics of the magnetic material used on the tape.

These limitations are overcome by using the signal to be recorded to change the frequency of an oscillator, which is in turn recorded on the tape. This f-m signal can be played back—if desired at a lower speed (and hence lower frequency)—to a demodulator, which retranslates the f-m signal into an a-m signal for direct writing recorders.

Problems in the Control of a Nuclear Reactor—Steam Electric Power Plant—William Kerr

Linear Accelerators and Radioactive Waste as Practical Sources for Industrial Sterilization Processes—M. R. Jeppson

Programming Chemical Kinetics Problems for Electronic Analogue Computers—R. C. H. Wheeler and G. F. Kinney

A Numerically Controlled Cam-Milling Machine—E. C. Johnson

A special machine tool built by the Bendix Aviation Corporation utilizes numerical control techniques to simplify the manufacture of small three-dimensional cams. The machine is designed to produce master cams and engineering prototypes directly from numerical control information recorded on a punched plastic tape. This information is derived from dimensional data appearing on an engineering drawing by means of automatic punched-card office accounting equipment.

The machine resembles a small lathe in basic configuration, except that a high-speed ballend milling cutter is substituted for the tool. The cutter is positioned radially by a high-performance hydraulic servo in response to incremental control signals generated electronically from the punched tape. An over-all accuracy of approximately 0.001 inch is achieved from drawing to finished cam.

A Two Motion Duplicator for Machine Tools—A. J. Carr, Jr.

The Raytheon Two Motion Duplicator for machine tools is discussed with emphasis on the vector operations performed by the electronic circuitry to accomplish constant velocity tracing of a two dimensional contour.

Two low level 60 cycle voltages are obtained from the follower (an electro magnetic transducer) when its stylus is brought in contact with a templet which represents the contour to

be traced. These two voltages, representing the resolved components of stylus deflection, are the input vectors to the system and are operated on to produce, eventually, two dc voltages of complementary magnitudes, which determine the speeds of two motors through thyratron power stages. The motors drive lead screws which continuously position the machine element carrying both follower and cutting tool. The relative motor speeds are so controlled and corrected by interpreting amplitude and phase information of follower output signals that the path of the follower and cutting tool duplicates the templet contour.

The Principal Mechanical and Electrical Features of a Hysteresis Clutch—L. R. Brown

The hysteresis loss that occurs in magnetic devices subjected to changing magnetic fields usually represents a detrimental condition. One exception, however, is the hysteresis clutch where this loss is utilized to perform a useful function. One particular type of clutch is described and its chief mechanical and electrical features are summarized. Its utility as a variable speed drive is also illustrated.

IRE Professional Group on Industrial Electronics Membership Directory

Medical Electronics

PGME-4, February, 1956

(*Symposium on Physiologic and Pathologic Effects of Microwaves, Mayo Clinic and Mayo Foundation, September 23–24, 1955*)

Foreword

Address of Welcome—F. H. Krusen

Problems Which Are Challenging Investigators in Industry—B. L. Vosburgh

Military Aspects of the Biological Effects of Microwave Radiation—S. I. Brody

Problems Which Are Challenging Investigators in Medicine—J. F. Herrick and F. H. Krusen

Correction

Energy Densities of Microwave Radiating Systems—W. E. Tolles and W. J. Horvath

An Exploration of the Effects of Strong Radio-Frequency Fields on Micro-Organisms in Aqueous Solutions—G. H. Brown and W. C. Morrison

Protective Measures for Microwave Radiation Hazards: 750 to 30,000 Mc—H. R. Meahl

Biologic Effects Studies on Microwave Radiation: Time and Power Thresholds for the Production of Lens Opacities by 12.3-Cm Microwaves—D. B. Williams, J. P. Monahan, W. J. Nicholson, and J. J. Aldrich

This study is essentially an extension of the work of Daily, *et al.* and Richard, *et al.*, who demonstrated that 12.3-cm radiation could produce lens opacities in the eyes of animals. Because of the broader implication of their findings in terms of human analogy, this present investigation was designed to gain some idea of what microwave power densities should be considered dangerous for human exposure. Both wavelength and power densities used for this purpose are of interest in the applied fields of microwave diathermy, radar communications, and microwave research.

The Use of Biological Simulants in Estimating the Dose of Microwave Energy—F. G. Hirsch

The Effects of Microwave Diathermy on the Eye—L. Daily, K. G. Wakim, J. F. Herrick, E. M. Parkhill, and W. L. Benedict

Microwave Energy in Food Procedures—D. A. Copson

Power input up to 1.6 kw is used in electronic ovens operating at 2,450 mc for cooking, heating, and defrosting foods. Some important considerations in microwave cooking are sizes of food masses, comparable processing time, residual cooking, normalcy in results, special surface effects, the relation between process

time and food load size, and the effect on nutrients.

Paramagnetic Resonance Methods in Biological Research—Scott Blois

Heat Exchange Characteristics of Animals Exposed to 10-Cm Microwaves—T. S. Ely and D. E. Goldman

Work now in progress on the biological effects of high intensity 10-cm microwave fields has been accompanied by studies on heat exchange characteristics of rats, rabbits, and dogs irradiated under relatively free field conditions. These studies include measurements of field intensity and distribution as well as of body temperatures. Determination of initial heating rates, steady-state body temperatures, and cooling rates permitted estimation of thermal characteristics including absorption and certain heat exchange parameters as an aid in interpretation of biological effects.

Physical Evaluation of Personnel Exposed to Microwave Emanations—C. I. Barron, A. A. Love, and A. A. Baraff

The Mechanism of Absorption of Ultrahigh Frequency Electromagnetic Energy in Tissues, as Related to the Problem of Tolerance Dosage—H. P. Schwan and Kam Li

List of Attendees

Nuclear Science

Vol. NS-3, No. 1, February, 1956

Editorial

Pulsed Geiger Counters—A. B. Witzel

Naval Research Laboratory High-Current Photomultiplier—J. D. Shipman and M. R. McCraven

Automatic Start-Up of Nuclear Reactors—R. J. Cox

Some Remarks on Nuclear Reactor Instrumentation—J. Walker

(*Abstracts of Papers at the Second Annual Meeting of the Professional Group on Nuclear Science*)

An Analogue of the Alternating Gradient Synchrotron—R. R. Kassner

The Microtron, a Nuclear and Elctronic Research Instrument—H. F. Kaiser

Proton Beam Studies in a Fixed-Frequency Cyclotron—F. L. Green

An Approximate Method for Obtaining the VSW on Cyclotron Dees—M. R. Donaldson

Phototube Voltage Regulations for Scintillation Counters—O. R. Harris and Bruce d'E. Flagge

Recent Advances in the Modular Design of Electronics—W. G. James

Multichannel Time Interval Analyzer—J. H. Neiler, H. E. Banta, W. M. Good and E. C. Smith

The "Hard-Bottoming" Technique in Nuclear Instrumentation Circuit Design—C. C. Harris

Four-Channel Counting System—D. W. Scott

Electronic Analog Devices for Design of Reactor Controls—E. R. Mann

Some Considerations in the Control of a Boiling Reactor—John MacPhee

The Ornl Serial Memory 120 Channel Pulse Height Analyzer—T. L. Emmer

Circuits for Pulse Analysis—G. G. Kelley

Medical Radiation Instrumentation with Scintillation Spectrometers—P. R. Bell

Measurement of Radioactive Fallout—J. H. Harley

Present Status of Halogen Quenched GM Tubes Using Transparent, Nonmetallic, Electrically Conducting Cathodes—L. B. Clark, Sr.

A Direct Current Integrator—F. M. Glass

Instrument Requirements for Routine Medical Radioisotope Techniques—Theodore Fields

A Dual Function Gamma Monitor—R. E. Connally

The Secretary's Notebook

IRE Professional Group on Nuclear Science Membership Directory

Abstracts and References

Compiled by the Radio Research Organization of the Department of Scientific and Industrial Research,
London, England, and Published by Arrangement with that Department and the
Wireless Engineer, London, England

NOTE: The Institute of Radio Engineers does not have available copies of the publications mentioned in these pages, nor does it
have reprints of the articles abstracted. Correspondence regarding these articles and requests for their
procurement should be addressed to the individual publications, not to the IRE.

The number in heavy type at the upper left of each Abstract is its Universal Decimal Classification number and is not to be confused with the Decimal Classification used by the United States National Bureau of Standards. The number in heavy type at the top right is the serial number of the Abstract. DC numbers marked with a dagger (†) must be regarded as provisional.

The Index to the Abstracts and References published in the PROC. IRE from February, 1954 through January, 1955 is published by the PROC. IRE, April, 1955, Part II. It is also published by *Wireless Engineer* and included in the March, 1955 issue of that journal. Included with the Index is a selected list of journals scanned for abstracting with publishers' addresses.

ACOUSTICS AND AUDIO FREQUENCIES

534.12   **961**
The Principal Frequencies of Vibrating Systems with Elliptic Boundaries—S. D. Daymond. (*Quart. J. Mech. appl. Math.*, vol. 8, Part 3, pp. 361–372; September, 1955.) Analysis involving Mathieu functions is presented.

534.121.1   **962**
On Upper and Lower Bounds of the Eigenvalues of a Free Plate—Y. Nakata and H. Fujita. (*J. phys. Soc. Japan*, vol. 10, pp. 823–824; September, 1955.) A brief mathematical note on the vibration of a thin elastic plate.

534.2-8   **963**
New Methods for rendering Ultrasonic Waves Visible—F. Hauer and G. Keck. (*Naturwissenschaften*, vol. 42, pp. 601–602; November, 1955.) Both traveling and standing waves in liquids can be made visible by using a specially prepared photographic plate; the sensitive material is dissolved at a rate depending on the strength of the ultrasonic field.

534.612.082.72-8   **964**
Capacitance Analyser of Sound Field—V. A. Zverev, V. M. Bokov, and I. E. Lur'e. (*Akust. Zh.*, vol. 1, pp. 218–220; July/September, 1955.) A circuit arrangement is described in which a capacitance change corresponding to the fractional change of the dielectric constant of water due to a sound field of frequency of 85 kc is caused to modulate a rf signal; the change in the dielectric constant is of the order of 1 part in 10^6 for a pressure change of 10^5 bar.

534.833:534.75   **965**
Apparatus for the Protection of the Hearing from the Damaging Effects of Noise—I. M.

Polkovski. (*Akust. Zh.*, vol. 1, pp. 249–256; July/September, 1955.) Low-pass mechanical sound filters to be worn over the ears are described. Their attenuation is low up to 1 kc but increases rapidly to about 35 db at 3.5 kc.

534.845   **966**
Measurement of the Absorption Coefficient of Acoustic Materials by the Reverberation-Chamber Method—R. Lamoral. (*Ann. Télécommun.*, vol. 10, pp. 206–217; October, 1955.) Formulas for reverberation time developed by Sabine, Eyring, and Millington are compared; values calculated from the two later formulas may differ by as much as 25 per cent for fairly "dead" studios. Details are given of the test method and installation used by the RTF organization; the volume of the reverberation chamber is 246 m³, and the excitation sound is a frequency-modulated tone. An electro-optical system for interrupting the sound without producing transients is described. Measurements are reported on panels of various materials either in one piece or divided up and variously arranged; material is most effective when located near the microphone. The results are embodied in graphs suitable for design purposes.

534.86   **967**
Conference on Electroacoustics, Kiev, 1st–5th July 1955—(*Akust. Zh.*, vol. 1, pp. 294–296; July/September, 1955.) Brief notes on 17 papers presented at the conference.

534.86:534.76   **968**
Secondary Field in Stereophonic Two-Channel Transmission for Various Positions of the Sound Source in the Primary Field—P. G. Tager. (*Akust. Zh.*, vol. 1, pp. 286–293; July/September, 1955.) The effect of varying one or more parameters in a system comprising two separate electroacoustic transmission channels on the stereophonic effect at various positions in an auditorium is considered theoretically, reverberation effects being neglected. The principal parameters are the differences of energy levels and time. These are taken into account in calculations by (a) the stereophonic-transmission factor $\beta\mu$ and (b) the delay factor τ, where β is a function of the directivity of the sound source, microphones, and loudspeakers, the amplification factors of the two channels, and the constructional factors of the microphones and loudspeakers, and μ is the ratio of distances between the source and the microphones. Curves and tables are given to facilitate calculations.

534.861.1   **969**
Broadcast Studio Redesign—L. L. Beranek. (*J. Soc. Mot. Pict. Telev. Engrs.*, vol. 64, pp. 550–559; October, 1955.) "A review is made of psychoacoustic and audience-opinion informa-

tion of recent and older sources from which criteria for studio design are drawn. New criteria are proposed for reverberation time for studios and auditoriums used for speech, music, and general purposes. Examples of three types of existing studios that need revision are discussed."

621.395.61   **970**
A New Cardioid Microphone—N. Friedman and C. Macpherson. (*Tele-Tech & Electronic Ind.*, vol. 14, pp. 70–72, 133; October, 1955.) A cardioid polar diagram and flat frequency characteristic are achieved by an arrangement of entrance ports and acoustically coupled cavities which also substantially eliminates proximity effect and susceptibility to mechanical shock.

621.395.612.4   **971**
Design of a [pressure-type] Ribbon Microphone—A. V. Rimski-Korsakov. (*Akust. Zh.*, vol. 1, pp. 257–263; July/September, 1955.) Design formulas are given.

ANTENNAS AND TRANSMISSION LINES

621.315.213   **972**
Polythene-Insulated Video-Pair Cables—(*Elect. Commun.*, vol. 32, pp. 165–168; September, 1955.) Constructional features and electrical characteristics are described for cables with four, six, and eight video pairs.

621.315.687   **973**
Electrical Resistance of Joints in Copper Cables—K. Sagel. (*Nachrichtentech. Z.*, vol. 8, pp. 541–544; October, 1955.) Experimental results show that soldered joints (solder composition 40 per cent Sn, 2.7 per cent Sb, remainder Pb) have a lower resistance, and lower scatter of resistance values, than spliced or welded joints. Results are tabulated and microphotographs are reproduced.

621.372   **974**
A Method of launching Surface Waves—J. D. Lawson. (PROC. IRE, vol. 44, p. 111; January, 1956.) The principle used is to maintain the phase velocity of the wave constant throughout the launching system; tapered-horn arrangements are illustrated.

621.372.21:621.315.213   **975**
Strip Transmission Lines—C. Bowness. (*Electronic Engng.*, vol. 28, pp. 2–7; January, 1956.) Practical production techniques for strip transmission lines are investigated and the construction of typical component parts of a rf system is described. The system has advantages, especially as regards cost, in cases where some stray radiation can be tolerated.

621.372.22   **976**
A Transmission-Line Taper of Improved

Design—R. W. Klopfenstein. (PROC. IRE, vol. 44, p. 31–35; January, 1956.) Discussion of the design of a line with Dolph-Tchebycheff taper, which is optimum in the sense that for a given taper length the reflection coefficient is minimum throughout the pass band, while for a specified upper limit to the reflection coefficient the length of the taper is a minimum. Values of transcendental functions used in the design are tabulated.

621.372.22:621.314.2   **977**
A Tapered Strip Line for Pulse Transformer Service—Primozich, Schatz, and Woodford. (See 993.)

621.372.8   **978**
Circular and Rectangular Waveguides with Longitudinal Diaphragms—E. G. Solov'ev. (Zh. tekh. Fiz., vol. 25, pp. 707–710; April, 1955.) The propagation of em waves in waveguides with infinitely thin conducting diaphragms, equally spaced along the guide, is considered. The problem is solved by the method of matching the fields at the boundary between two regions. The electric field between the diaphragms is evaluated approximately. One of the dispersion equations obtained for the propagation constant is analyzed for the case when the length of the wave in the waveguide is much greater than the space-period of the diaphragm structure.

621.372.8:537.226   **979**
Media rendered Artificially Anisotropic—Ya. B. Fainberg and N. A. Khizhnyak. (Zh. tekh. Fiz., vol. 25, pp. 711–719; April, 1955.) An anisotropic medium can be obtained by arranging dielectric disks periodically along the axis of a waveguide, as suggested by Harvie (1744 of 1949). A mathematical discussion shows that the system is equivalent to a waveguide completely filled with an anisotropic dielectric, not only in respect of retarding properties but also in respect of the mean values of the electric and magnetic fields.

621.396.67   **980**
Distribution of Current along a Cylindrical Transmitting Aerial—P. Poincelot. (Ann. Télécommun., vol. 10, pp. 186–194, September, and pp. 219–228; October, 1955.) Detailed analysis. See 932 of 1955 and back references.

621.396.67   **981**
Method for Calculation of the [input] Conductance of Cylindrical Aerials—G. Barzilai. (Alta Frequenza, vol. 24, pp. 339–355; August/October, 1955.) The method consists essentially in evaluating separately the input voltage and the radiated power for a given value of current in the vicinity of the maximum point. First and second-order calculations are made. For an abbreviated account in English see TRANS. IRE, vol. AP-3, pp. 29–32; January, 1955.

621.396.67.012.12   **982**
Radiation Diagrams of Ring Arrays with Rotationally Symmetrical Horizontal Characteristics—H. W. Fastert. (Tech. Hausmitt. NordwDtsch. Rdfunks, vol. 7, pp. 157–165; 1955.) Long-wave antenna systems with sky-wave suppression are discussed. An examination is made of the number of radiators required in practice to give a constant-current system. Analysis for multi-ring systems is simplified by stipulating additional conditions; e.g. maximum gain.

621.396.677   **983**
Synthesis of Aerial Arrays—A. Fernandez Huerta. (Rev. Telecomunicación, Madrid, vol. 9, pp. 3–13; September, 1955.) A theoretical study of linear uniformly spaced arrays. By resolving the characteristic polynomial into binomial expressions the radiation diagrams are found rapidly; broadside and end-on arrays are thus treated. Use of Tchebycheff polynomials to obtain optimum distribution and of small spacings to obtain superdirectivity are discussed.

621.396.677.3.012.12   **984**
Design of Line-Source Antennas for Narrow Beamwidth and Low Side Lobes—T. T. Taylor. (TRANS. IRE, vol. AP-3, pp. 16–28; January, 1955.) The effect of nonuniform field distributions across the antenna aperture on the radiation pattern is discussed mathematically. The ideal compromise between beam width and side-lobe level is given by a space factor $\cos \pi \sqrt{u^2 - A^2}$, where $u = (2a/\lambda) \cos \theta$, θ being the angle of radiation and a the half-length of the line source, and $\cosh \pi A$ is the side-lobe ratio. Practical approximations to this ideal pattern are discussed.

621.396.677.833   **985**
Double-Parabolic-Cylinder Pencil-Beam Antenna—R. C. Spencer, F. S. Holt, H. M. Johanson, and J. Sampson. (TRANS. IRE, vol. AP-3, pp. 4–8; January, 1955.) Radiation from a point source on the focal line of one cylinder is reflected in turn from this cylinder and from a second one arranged so that its focal line coincides with the directrix of the first, resulting in the production of a parallel beam. Production advantages of such systems are stressed.

AUTOMATIC COMPUTERS

681.142   **986**
Electronic Computing Machines and their Uses—J. H. Wilkinson. (J. sci. Instrum., vol. 32, pp. 409–415; November, 1955.) Basic design of digital computers is described. Programming for suitable types of problem is discussed and illustrated by examples.

681.142   **987**
A Simple Electronic Fourier Synthesizer—H. B. Mohanti and A. D. Booth. (J. sci. Instrum., vol. 32, pp. 442–444; November, 1955.) An experimental model of a machine for two-dimensional Fourier synthesis is described which incorporates magnetic drum storage of the required sine and cosine functions.

681.142   **988**
Simplified Analog Computer—V. B. Corey. (Electronics, vol. 29, pp. 128–131; January, 1956.) A differential analyzer is described, based on ten identical operational amplifiers which may be used for integration, multiplication, etc., as required by the particular problem. The arrangement is very flexible and may be used with external circuitry for the generation of special functions required in synthesizing particular input analogs.

681.142:621.375.2.024   **989**
Some Aspects of the Design of a D.C. Amplifier for Use with a Slow Analogue Computer—H. Fuchs. (Electronic Engng., vol. 28, pp. 22–25; January, 1956.) "The errors introduced as a result of an ht resistance common to several amplifiers is calculated, and a criterion for the accuracy of a linear computer stated."

681.142:621.375.43   **990**
Transistor Amplifiers for Use in a Digital Computer—Simkins and Vogelsong. (See 1014.)

CIRCUITS AND CIRCUIT ELEMENTS

621.3.011.21   **991**
Contribution on the Calculation of the Total Impedance of Parallel-Connected Impedances—W. Boesch. (Rev. gén. Élect., vol. 64, pp. 517–520; October, 1955.) A method of calculation involving use of a special transparent rule and a simple nomogram is described and illustrated by a numerical example.

621.3.016.35:621–526   **992**
Stability Criteria for an Electrical or Mechanical System with Distributed Parameters —A. S. Gladwin. (Brit. J. appl. Phys., vol. 6, pp. 400–402; November, 1955.) For electrical or mechanical systems with distributed parameters, or with an element producing a finite time delay, to be stable all the roots of the appropriate characteristic equation must be negative or have negative real parts. If the equation is expressed in the form $C_0 + C_1 z + (C_2 + C_3 z) \tanh z = 0$, then for C_0 positive, C_1 and C_3 must be positive and C_2/C_1 must be greater than a certain critical value which is a function of C_0/C_3. An example is given of the application of these criteria to a servomechanism.

621.314.2:621.372.22   **993**
A Tapered Strip Line for Pulse Transformer Service—F. G. Primozich, E. R. Schatz, and J. B. Woodford. (Elect. Engng., N.Y., vol. 74, p. 908; October, 1955.) Digest of paper in Communication and Electronics, pp. 158–161; May, 1955. A rolled-up construction is described for an exponential-line impedance transformer. The impedance is 25Ω at one and of the 10-m line and $1,000\Omega$ at the other; pulses as long as 36 mμs can be handled.

621.316.825+[621.314.632:546.289   **994**
The Turnover Phenomenon in Thermistors and in Point-Contact Germanium Rectifiers—R. E. Burgess. (Proc. phys. Soc., vol. 68, pp. 908–917; November 1, 1955.) The turnover power in thermistors increases as the square of the absolute ambient temperature. The similarity in form between the reverse characteristic of a point-contact Ge rectifier and the static characteristic of a thermistor suggests a thermal hypothesis for rectifier turnover; but in the latter case the turnover power decreases approximately linearly with ambient temperature. The type of function necessary to reproduce the rectifier characteristics at turnover is discussed; such a function cannot be derived from existing theories of rectification.

621.318.424:621.318.134   **995**
A Survey of the Application of Ferrites to Inductor Design—R. S. Duncan and H. A. Stone, Jr. (PROC. IRE, vol. 44, pp. 4–13; January, 1956.)

621.318.435:621.375.3   **996**
Influence of I.D.-O.D. [inside-diameter /outside-diameter] Ratio on Magnetic Properties of Toroidal Cores—R. W. Roberts and R. I. Van Nice. (Elect. Engng., N.Y., vol. 74, pp. 910–914; October, 1955.) The optimum design of cores for magnetic amplifiers is discussed. A theoretical result is obtained assuming a parallelogram-shaped hysteresis loop, and an experimental investigation is reported. The dependence of the optimum ratio on the magnetic properties of the core material is indicated.

621.318.57+621.314.7+621.385   **997**
Design of Electronic Devices for Production—Thomson. (See 1249.)

621.319.4:621.387   **998**
Electrically Variable-Gas-Dielectric Capacitor—J. F. Gordon. (Electronics, vol. 29, pp. 158–160; January, 1956.) A neon tube placed between the plates of an air-dielectric capacitor gives a variation in dielectric constant proportional to the tube current. Maximum variation of capacitance is about 10 per cent. The device may be used for frequency control of self-excited oscillators.

621.372   **999**
A Simplified Method of solving Linear and Nonlinear Systems—R. Boxer and S. Thaler. (PROC. IRE, vol. 44, pp. 89–101; January, 1956.) The method described uses the z transform [363 of 1955 (Ragazzini and Bergen)] directly to determine the responses of linear and nonlinear systems approximately. The solutions are given as time series representing

the values of the response at equally spaced instants. Both constant and time-varying systems are considered.

621.372.413 1000
The Harmodotron—a Beam Harmonic Higher-Order-Mode Device for producing Millimeter and Submillimeter Waves—P. D. Coleman and M. D. Sirkis. (*J. appl. Phys.*, vol. 26, pp. 1385–1386; November, 1955.) High-power oscillations are generated by exciting a single higher-order TM mode in a cylindrical cavity by means of a bunched beam of 1–1.5-mev electrons.

621.372.542.2.01 1001
Simultaneous Approximation for the Amplitude and Delay Time of an Ideal Low-Pass Filter using the Flow Analogy—J. Peters. (*Arch. elekt. Übertragung*, vol. 9, pp. 453–459; October, 1955.) Analogies between transmission phenomena in networks and current flow in a potential field are discussed [2370 of 1951 (Darlington)]. A distortion-free low-pass filter can be represented by two superposed fields, one with parallel flow, corresponding to the distortion-free aspect, and the other with radial flow, corresponding to the filter aspect. Such a representation involves a finite residual error which cannot be eliminated without introducing instability, but which can be reduced indefinitely by increasing the delay time.

621.372.543.2:538.652 1002
Electromechanical Filters for 100-kc/s Carrier and Sideband Selection—R. W. George. (PROC. IRE, vol. 44, pp. 14–18; January, 1956.) Torsional-type filters comprising $\lambda/2$ cylindrical resonators with $\lambda/4$ coupling necks are discussed. Descriptions are given of two filters with bandwidths of 50 cps and 3.1 kc respectively. Using a particular Fe-Ni-Cr-Ti alloy known as Ni-Span-C, the temperature variation of frequency is <2 parts per million. Magnetostrictive transducers made of this alloy or of ferrite are used. Spurious modes of vibration are reduced by a balanced arrangement of the transducers and by mechanical damping in the end supports.

621.372.56 1003
A Push-Button Attenuator for Frequencies up to 10 Mc/s—H. Paardekooper. (*Commun. News*, vol. 16, pp. 10–22; October, 1955.) Details are given of a resistance attenuator providing attenuation up to 99.5 db in 1-db steps with an interpolation step of 0.5 db. Each section comprises a *T*-network with the shunt arm bridged by capacitance to compensate the inductance of the series arms.

621.373.4.029.65 1004
Cherenkov Radiation—J. G. Linhart. (*Research, Lond.*, vol. 8, pp. 402–406; October, 1955.) A brief explanation is given of the mechanism of Čerenkov radiation, which may find application in mm-λ oscillators.

621.373.421 1005
Cathode-Follower Phase-Shift Oscillator—J. C. Samuels. (*Elect. Commun.*, vol. 32, pp. 198–202; September, 1955.) Analysis indicates that better frequency stability is obtained by connecting the phase-shifting network between grid and cathode than by connecting it in the anode circuit. Calculations are made for three typical circuits.

621.373.431.1 1006
Investigations of the D.C. and A.C. Characteristics of Bi-stable Multivibrators—K. Gosslau and H. J. Harloff. (*Nachrichtentech. Z.*, vol. 8, pp. 521–530; October, 1955.) The characteristics are discussed theoretically with reference to the design of reliable counting and switching units. Design procedure is illustrated by two numerical examples, one of a binary counting unit with counting rate up to 1 mc at supply voltages between 50 and 350 v, the

other for a pulse-counting rate of 10 mc at supply voltages between 60 and 300 v. A modification of the latter circuit using a Type-E88CC double-triode, instead of Type-E90CC, was used at counting rates up to 30 mc.

621.374.3:621.318.57 1007
The Diode Pump Integrator—J. B. Earnshaw. (*Electronic Engng.*, vol. 28, pp. 26–30; January, 1956.) The design of a diode circuit for integrating a train of pulses is discussed and conditions are established for linear and nonlinear operation. An application to a frequency-sensitive relay with quick "on-off" characteristics is described.

621.374.32 1008
A Logarithmic Voltage Quantizer—E. M. Glaser and H. Blassbalg. (*Tele-Tech & Electronic Ind.*, vol. 14, pp. 73–75, 128; October, 1955.) Details are given of an analog-to-digital converter which provides an output pulse whose duration is proportional to the logarithm of the input voltage, the output pulse duration being determined by counting the number of fixed-frequency pulses occurring in the same interval. Range of input voltage is 3.3–100 v, with a threshold input pulse length of 0.5 μs.

621.374.32 1009
Analog-to-Digital Data Converter—S. Rigby. (*Electronics*, vol. 29, pp. 152–155; January, 1956.) The required conversion is performed by arranging an oscillator generating pulses at a repetition rate proportional to the analog voltage to feed a digital counter for a fixed period. The oscillator described has a range of four decades; stability is better than 0.1 per cent of maximum pulse frequency.

621.375.221 1010
The Compensation of Wide-band Amplifiers at High Frequencies—P. Rohan and J. Weislitzer. (*Proc. IRE, Aust.*, vol. 16, pp. 354–362; October, 1955.) Analysis is given for various coupling arrangements including RC, RCL, and special two- and four-terminal networks.

621.375.23:621.3.018.78 1011
Distortion in Feedback Amplifiers—R. W. Ketchledge. (*Bell Syst. tech. J.*, vol. 34, pp. 1265–1285; November, 1955.) Analysis is presented for frequency-dependent feedback. Consideration is restricted to cases where the distortion products are comparatively small and the nonlinear element can be described by a power series with only a few terms. Formulas are derived for a number of third-order products.

621.375.4:621.314.7 1012
Analysis of the Common-Base Transistor Circuit—R. L. Pritchard. (*Electronic Engng.*, vol. 28, p. 40; January, 1956.) Mathematical errors in a paper by Oakes (1600 of 1955) are pointed out.

621.375.4:621.314.7 1013
Transistor Circuit for Resonance-Coefficient Multiplier—M. Soldi and M. Valeriani. (*Alta Frequenza*, vol. 24, pp. 375–389; August /October, 1955.) Use of transistors in *Q*-multiplier circuits [2678 of 1951 (Harris)] is discussed. The input admittance is calculated and the conditions for stabilization against self-oscillation are derived. Design and performance of experimental arrangements are described; composite transistors [927 of 1956 (Pearlman)] may be used.

621.375.43:681.142 1014
Transistor Amplifiers for Use in a Digital Computer—Q. W. Simkins and J. H. Vogelsong. (PROC. IRE. vol. 44, pp. 43–55; January, 1956.) Pulse-regenerative amplifiers for a 3-mc synchronous binary computer are based on use of external feedback, so that a negative-resistance transistor characteristic is not required. By

using semigated feedback, allowance can be made for the slow recovery of Ge diodes incorporated in the circuit.

621.372+621.317].029.63/.64 1015
Schaltungstheorie und Messtechnik des Dezimeter- und Zentimeterwellengebietes [Book Review]—A. Weissfloch. Publishers: Birkhäuser, Basel, 308 pp., 1954. (*Bull. schweiz. elektrotech. Ver.*, vol. 46, p. 1092; October 29, 1955.) Theory and applications of four-, six-and eight-pole networks are covered. Circle-diagram representation is used to show transformation properties of four-pole networks.

GENERAL PHYSICS

535.325:538.566.2.029.6 1016
The Refractive Indices of Water Vapour, Air, Oxygen, Nitrogen and Argon at 72 kMc/s —K. D. Froome. (*Proc. phys. Soc.*, vol. 68, pp. 833–835; November 1, 1955.) Experiments indicate that the refractive indexes of water vapor, air, and oxygen are modified at microwave frequencies in the manner to be expected from dipole theory; the values for nitrogen and argon should not vary with frequency, and this is confirmed.

537.122 1017
The Dielectric Theory of Electronic Interactions in Solids—J. Hubbard. (*Proc. phys. Soc.*, vol. 68, pp. 976–986; Nobember 1, 1955.) The long-range part of the Coulomb interaction of the electrons in solids is treated by regarding the solid as a homogeneous dielectric. Sustained oscillations are shown to be possible in metals and are identified with the plasma oscillations discussed by Bohm and Pines (1375 of 1954).

537.21 1018
The Capacity and Field of a Cylindrical Trough with a Plane Conductor in the Axial Plane of Symmetry—H. J. Peake and N. Davy. (*Brit. J. appl. Phys.*, vol. 6, pp. 404–408; November, 1955.)

537.21:517.9 1019
Poisson's Partial Difference Equation—H. Davies. (*Quart. J. Math.*, vol. 6, pp. 232–240; September, 1955.) The Green's functions and their asymptotic behavior for Poisson's partial difference equation in two and three dimensions are discussed and the distribution of potential and current in a regular grid of wires is calculated. The method may also be applied to nonisotropic grids and can be extended to triangular and hexagonal grids in two dimensions and probably to more complicated patterns in three dimensions.

537.311.31 1020
Theory of Electrical Conductivity in Metals —P. S. Zyryanov. (*Zh. eksp. teor. Fiz.*, vol. 29. pp. 193–200; August, 1955.) The fluctuations in the potential in the electron-ion plasma of a metal and the electrical resistance due to the scattering of electrons by these fluctuations are calculated.

537.311.31 1021
Number of States and the Magnetic Properties of an Electron Gas—A. W. Sáenz and R. C. O'Rourke. (*Rev. mod. Phys.*, vol. 27, Part I, pp. 381–398; October, 1955.) A theoretical investigation of the thermodynamic properties of conduction electrons in metals.

537.311.33:538.614 1022
The Infrared Faraday Effect due to Free Carriers in a Semiconductor—E. W. J. Mitchell. (*Proc. phys. Soc.*, vol. 68, pp. 973–974; November 1, 1955.)

537.52:546.11 1023
Growth of Pre-breakdown Ionization Currents in Hydrogen—R. W. Crompton, J. Dutton, and S. C. Haydon. (*Nature, Lond.*, vol. 176, p. 1079; December 3, 1955.) Experiments

are briefly reported, the results of which indicate that the mechanism of primary ionization is the same over a range of pressures from a few mm to 150 mm Hg.

537.52 : 621.317.729.2   **1024**

Theory of Langmuir Probes—Yu. M. Kagan and V. I. Perel'. (*Zh. eksp. teor. Fiz.*, vol. 29, pp. 261–263; August, 1955.) A note contrasting results of Langmuir's theory with those of the authors' precise theory of the spherical probe at low pressures and negative probe potential (*C.R. Acad. Sci. U.R.S.S.*, vol. 95, pp. 765–768; 1954. In Russian.)

537.525 : 621.385 833   **1025**

Electric "Microdischarges" in a Dynamic Vacuum—R. Arnal. (*Ann. Phys., Paris*, vol. 10, pp. 830–873; September/October, 1955.) Account of an experimental and theoretical investigation of undesired discharges occurring as a result of surface imperfections in vacuum apparatus operated at high voltage. Experimental electrode systems similar to those in electron microscopes were used. The phenomena are distinguishable from field emission, and involve repeated secondary emission of electrons and H ions. For voltages applied in very short pulses the upper limit before onset of microdischarges is higher than for continuous voltages.

537.533   **1026**

Some Factors influencing Field Emission and the Fowler-Nordheim Law—T. J. Lewis. (*Proc. phys. Soc.*, vol. 68, pp. 938–943; November 1, 1955.) "Departures from the normal Fowler-Nordheim law which have been observed at fields up to 7×10^7 v cm⁻¹ have previously been ascribed to space-charge field distortion. It is shown that certain other effects due to failure of the image law, nonuniformity of work function and to possible surface irregularities could produce similar effects."

537.533   **1027**

Electron Emission from Metal Surfaces after Mechanical Working—J. Lohff and H. Raether. (*Z. Phys.*, vol. 142, pp. 310–320; October 1, 1955.) A fuller account of work described previously (2265 of 1955). Electron multiplication by secondary emission was used to facilitate the observations.

537.533 : 539.211   **1028**

A Study of the Structure of Abraded Metal Surfaces—L. Grunberg and K. H. R. Wright. (*Proc. roy. Soc. A.*, vol. 232, pp. 403–423; November 8, 1955.) A report is presented of an experimental investigation of the spontaneous

and photoelectric electron emission from abraded surfaces in various atmospheres. All the metals investigated responded to radiation in the near ultraviolet; Al, Mg, and Zn, which form "excess metal" oxides, responded to wavelengths in the visible range also. From the observed rate of decay of emission it is inferred that both thermal and oxidation phenomena are involved. Previous theories that the emission depends on exothermal processes [2301 of 1953 (Kramer)] are considered untenable.

537.56 : 536.2   **1029**

Theory of Thermal Conductivity of a Plasma—H. Schirmer. (*Z. Phys.*, vol. 142, pp. 116–126; September 12, 1955.) The treatment is similar to that used previously for investigating the electrical conductivity of plasma (382 of 1956).

537.562 : 538.6   **1030**

Particle Transport, Electric Currents, and Pressure Balance in a Magnetically Immobilized Plasma—P. Stehle. (*Phys. Rev.*, vol. 100, p. 443; October 15, 1955.) The problem discussed by Tonks (2595 of 1955) is treated without detailed analysis of particle trajectories; qualitatively similar results are obtained.

538.222   **1031**

A Note on the Paramagnetic Relaxation—M. Yokota. (*J. phys. Soc. Japan*, vol. 10, pp. 762–768; September, 1955.) The theory given explains experimental results obtained by Gorter (*Paramagnetic Relaxation*, 1947) for the dependence of the spin-spin relaxation time on the static field strength.

538.3   **1032**

Electromagnetic Theory of Moving Matter: Part 2—E. J. Post. (*Tijdschr. ned. Radiogenoot.*, vol. 20, pp. 307–321; September, 1955. In English.) Part 1: 3230 of 1955.

538.311   **1033**

Magnetic Field due to Circular Current—R. Cazenave. (*Rev. gén. Élect.*, vol. 64, pp. 510–512; October, 1955.) Analysis is simplified by applying recent work on elliptic integrals.

538.561 : 537.533   **1034**

Production of Millimetre Waves by a Magnetic Undulator—R. Combe and T. Frelot. (*C.R. Acad. Sci., Paris*, vol. 241, pp. 1559–1560; November 28, 1955.) Measurements have been made on a device of a type described previously [1037 of 1954 (Combe and Feix) and back references] using an electron beam from a pulsed linear accelerator. With a mean beam intensity of 0.3 μa, the output power was about 1 mw, intermediate between the values corresponding to complete incoherence and complete coherence of the elementary vibrations. The spectrum extended from 4.8 to 8 mm with a maximum at 5.75 mm.

538.566 : 537.226.2   **1035**

Transmission of Electromagnetic Waves through Inhomogeneous Layers—H. G. Haddenhorst. (*Z. angew. Phys.*, vol. 7, pp. 487–496; October, 1955.) Layers are considered in which the dielectric constant is graded from the value unity at each face to a maximum value at the midplane, the variation being either linear or exponential. Dielectrics are prepared satisfying this specification by forming ordinary homogeneous materials into a series of wedges or the like, thus producing a space-periodic structure. Reflection-factor measurements made in free space and in waveguides are reported. Variation of reflection factor with layer thickness is shown graphically for moltopren, paraffin, and trolitul; variation with angle of incidence is shown for trolitul. The experimental results are compared with values of the reflection factor calculated from solutions of Maxwell's equations for the appropriate conditions. Such structures can give good transmission of microwaves over a wide frequency band.

538.566.029.6   **1036**

Generation of Submillimeter Waves—H. Motz and K. B. Mallory. (*J. appl. Phys.*, vol. 26, p. 1384; November, 1955.) Brief preliminary note describing radiation observed unexpectedly when a bunched high-energy beam of electrons was passed through a simple rectangular waveguide.

538.569.4 : 535.33   **1037**

Pulse Techniques in Microwave Spectroscopy—R. H. Dicke and R. H. Romer. (*Rev. sci. Instrum.*, vol. 26, pp. 915–928; October, 1955.) "Methods are described for exciting gases to states from which they emit coherent spontaneous radiation in the microwave frequency region. The excitation is produced by the application of short pulses of microwave power. The power subsequently radiated by the gas is calculated for several cases, and experimental methods used to detect the radiation are described. The problem of sensitivity is discussed and compared to the sensitivity obtainable in a continuous absorption experiment. The operation of a high resolution microwave spectrometer, which produces lines substantially narrower than the usual Doppler width,

is described. The method used to stabilize the klystron used in these experiments, which is a modification of the Pound IF method, is given." See also 92 of 1956 (Romer and Dicke).

538.569.4 : 539.152.2   **1038**

Spin Echo Serial Storage Memory—A. G. Anderson, R. L. Garwin, E. L. Hahn, J. W. Horton, G. L. Tucker, and R. M. Walker. (*J. appl. Phys.*, vol. 26, pp. 1324–1338; November, 1955.) Methods are discussed for storing information in the form of pulses in a nuclear-magnetic-resonance system, by use of the free-induction spin-echo technique [see also 1962 of 1955 (Fernbach and Proctor)]. The storage capacity in liquids is expressed in terms of the thermal noise of the detecting apparatus, the self-diffusion of the molecules, and the relaxation times. Undesired echoes arising from the interaction of input pulses are eliminated by frequency- and magnetic-field-modulation techniques. Glycerin and solutions of paramagnetic ions in water provide storage times of 10–50 ms, with a storage capacity of the order of 1,000 echoes. Larger capacities expected from liquids with long relaxation times are not realized owing to self-diffusion.

538.632   **1039**

The Hall Effect in Metals at High Frequencies—B. Donovan. (*Proc. phys. Soc.*, vol. 68, pp. 1026–1032; November 1, 1955.) Theory is developed in terms of a "surface Hall coefficient"; calculations are made for a metal with two overlapping energy bands, and the variations with frequency and with field strength are shown graphically for some special cases. At very low frequencies the Hall coefficient is constant; over a range of higher frequencies it increases as the square root of the frequency and then becomes constant again. The frequency variation of the phase angle between current and Hall emf is also investigated.

538.652   **1040**

Quantum Theory of Magnetostriction—A. A. Gusev. (*Zh. eksp. teor. Fiz.*, vol. 29, pp. 181–192; August, 1955.) The theory of magnetostriction in hexagonal single crystals is developed on the basis of a polar model (Bogolyubov and Tyablikov, *ibid.*, vol. 19, pp. 256, 261; 1950) by considering the magnetic and magnetoelastic interaction of electrons in the lattice. The energy spectrum of the crystal at low temperatures, the free energy, and the temperature dependence of magnetostriction constants are calculated.

538.652 : 537.312.62   **1041**

Some Consequences of the Influence of Elastic Deformations on Superconductivity: Magnetostriction—C. Grenier. (*C.R. Acad. Sci., Paris*, vol. 241, pp. 1275–1277; November 7, 1955.) Analysis of conditions at the transition from the normal-conduction to the superconduction state in tin indicates that magnetostriction mainly in the direction of the quaternary axis is to be expected. Conditions for Hg are more complex.

548.0 : 53   **1042**

Effects of Defects on Lattice Vibrations—E. W. Montroll and R. B. Potts. (*Phys. Rev.*, vol. 100, pp. 525–543; October 15, 1955.) "The theory of the effect of localized defects such as impurities, holes, and interstitials on the vibrations of crystal lattices is developed."

GEOPHYSICAL AND EXTRATERRESTRIAL PHENOMENA

523.16   **1043**

International Research in Radio Astronomy—R. L. Smith-Rose. (*Nature, Lond.*, vol. 176, pp. 1110–1111; December 10, 1955.) Special Reports Nos. 3, 4, and 5 published by the International Scientific Radio Union, and entitled respectively "Discrete Sources of Extra-

terrestrial Radio Noise," "The Distribution of Brightness on the Solar Disk," and "Interstellar Hydrogen" are noticed.

523.16 1044
Results of Observations of Discrete Emitters of Cosmic Radio Emission on Wavelength $\lambda = 3.2$ cm—N. L. Kaidanovski, N. S. Kardashev, and I. S. Shklovski. (*C.R. Acad. Sci. U.R.S.S.*, vol. 104, pp. 517–519; October 1, 1955. In Russian.) Results are given of a determination of the em flux at 3.2 cm λ originating from the Omega nebula (NGC 6618), Orion nebula (NGC 1976), Cassiopeia A (supernova A.D. 369), Taurus A (NGC 1952, supernova A.D. 1054), and a source near the galactic center Sagittarius X (possibly supernova A.D. 827). When these values are plotted together with observations at other radio wavelengths and, in the case of the Crab nebula, also at optical wavelengths, the results suggest that one mechanism may be responsible for radiation both at optical and radio wavelengths.

523.165:550.385 1045
The 27-Day Recurrence Tendency of Cosmic-Ray Intensity—I. J. van Heerden and T. Thambyahpillai. (*Phil. Mag.*, vol. 46, pp. 1238–1251; November, 1955.) The 27-day-cycle variations of cosmic-ray intensity precede those of magnetic activity by about five days; it is tentatively suggested that the same solar disturbances are associated with both phenomena.

523.5:621.396.11 1046
Diurnal Variations in the Number of Shower Meteors detected by the Forward-Scattering of Radio Waves: Part 2—Experiment—P. A. Forsyth, C. O. Hines, and E. L. Vogan. (*Canad. J. Phys.*, vol. 33, pp. 600–606; October, 1955.) "The theory developed in Part 1 [738 of 1956 (Hines)] is applied to derive the expected diurnal variations of the meteor signal rate for four showers as observed by means of a particular forward-scatter transmission path (Cedar Rapids–Ottawa). These results are then compared with the experimental signal rates. The good agreement obtained indicates that the approximations inherent in the theory are sufficiently accurate for practical purposes. The results also indicate that very few meteors, if any, are observed under conditions which do not satisfy the requirements for specular reflection."

523.746.5 1047
The Decreasing Phase of the Last Solar Cycle, as indicated by Measurements at the Astronomical Observatory at Rome—T. Fortini. (*R.C. Accad. naz. Lincei*, vol. 19, pp. 131–136; September/October, and pp. 272–276; November, 1955.) Detailed observations are compared with those obtained at Zurich.

551.510.535 1048
Thermal Upward Flow in the Ionosphere—Syun-ichi Akasofu. (*Sci. Rep. Tohoku Univ., 5th. Ser., Geophys.*, vol. 6, pp. 150–161; June, 1955.) The possibility of atmospheric waves due to heating effects of solar radiation is established; vertical thermal flow in the F_2 region may give rise to ion drift along the magnetic lines of force; this may explain anomalous diurnal variations in the F_2 layer. By applying the theory to observed ionospheric data for the North American zone, estimates are obtained for the velocity of the ions and of the thermal flow.

551.510.535 1049
The Detection of the S_q Current System in Ionospheric Radio Sounding—E. V. Appleton, A. J. Lyon, and A. G. Pritchard. (*J. atmos. terr. Phys.*, vol. 7, pp. 292–295; October, 1955.) Anomalies found in the application of Chapman's theory of ionosphere layer formation to E-layer phenomena are explicable if it is accepted that the S_q current system modifies the

diurnal variation of electron density in the layer, most probably by some form of vertical-drift mechanism. Similar phenomena are found in the F_1 layer.

551.510.535:621.396.11 1050
The Night-Time Lower Ionosphere as deduced from a Theoretical and Experimental Investigation of Coupling Phenomena at 150 kc/s—R. W. Parkinson. (*J. atmos. terr. Phys.*, vol. 7, pp. 203–234; October, 1955.) Experimental work over the period March, 1953, to January, 1954, is described and the results are compared with theoretical results given by Davids and Parkinson (1192 below). Curves show seasonal and diurnal variations of the night time D layers in the coupling region. D-E-region models for the sunset period for July and November, 1953, are proposed; the variation of electron distribution during the night is deduced from a recombination-coefficient model suggested by Mitra (*Scientific Report No. 68*, Ionospheric Research Laboratory, State College, Pennsylvania). All available experimental data tend to confirm the theoretical analysis.

551.510.535:621.396.11 1051
On the Variation of Ionospheric Absorption at Different Stations—W. R. Piggott. (*J. atmos. terr. Phys.*, vol. 7, pp. 244–246; October, 1955.) "The possibility that the day-to-day changes in absorption at Slough, Swansea, and Freiburg are identical is examined statistically. After allowing for known sources of error, it is considered that the residual differences in summer months are too small to be significant, but that it is probable that real differences occur in winter. In both cases the minimum probable correlation for the Swansea-Slough comparison is very high—about 0.92."

551.510.535:621.396.11 1052
Selective Annotated Bibliography on Ionospheric Propagation—M. Rigby and M. L. Rice. (*Met. Abstracts Bibliography*, vol. 6, pp. 489–547; April, 1955.) Includes some 300 references covering the period 1902–1955.

551.594.5:551.51 1053
Measurements of the Mean Lifetime of the Metastable ^1S-state of the Oxygen Atom in the Upper Atmosphere during Auroral Displays—A. Omholt and L. Harang. (*J. atmos. terr. Phys.*, vol. 7, pp. 247–253; October, 1955.) The mean lifetime of the OI ^1S level is found to vary between 0.45 and 0.75 a second.

LOCATION AND AIDS TO NAVIGATION

621.396.93 + 621.396.96 1054
Contributions of the Siemens Company to Air-Safety Technique and Air-Navigation Electronics in the Years 1930–1945—H. J. Zetzmann. (*Frequenz*, vol. 9, pp. 351–360; October, and pp. 386–395; November, 1955.) A detailed illustrated account covering radar equipment, altimeters, navigation aids, and transmission technique.

621.396.96 1055
Shore-Based Radio Aids to Navigation on Centimetric Wavelength—J. M. F. A. van Dijk, N. Schimmel, and E. Goldbohm. (*Tijdschr. ned. Radiogenoot.*, vol. 20, pp. 271–279; September, 1955. In English.) "The problem of shore-based radar as a navigational aid for shipping is discussed from the system engineering point of view. A short review of the work carried out in the Netherlands, Belgium, and Western Germany is given."

621.396.96 1056
A Ramark Beacon for Use with Marine Radars—J. M. F. A. van Dijk, N. Schimmel, and E. Goldbohm. (*Tijdschr. ned. Radiogenoot.*, vol. 20, pp. 281–290; September, 1955. In English.) Description of wide-band 3-cm-λ equipment with a range of 30 miles. A diversity system of transmitting antennas is used. The

ramark signal can be eliminated from the ship's ppi by switching on the fast-time-constant anticlutter circuit provided in the marine radar. Results of trials are discussed.

MATERIALS AND SUBSIDIARY TECHNIQUES

535.215 + 537.311.33 1057
Ultrashort Light and Voltage Pulses Applied to Silver Halide Crystals by Turbine-Driven Mirror and Spark-Gap Switch—J. H. Webb. (*J. appl. Phys.*, vol. 26, pp. 1309–1314; November, 1955.) Technique for studying electron mobility at room temperature is described.

535.215 1058
Photoelectric Yields in the Vacuum Ultraviolet—W. C. Walker, N. Wainfan, and G. L. Weissler. (*J. appl. Phys.*, vol. 26, pp. 1366–1371; November, 1955.) Measurements are reported on polycrystalline specimens of Ni, Cu, Pt, Au, W, Mo, Ag, and Pd exposed to radiation of wavelengths 473–1,400 Å.

535.215:538.221 1059
Photoelectron Emission in a Ferromagnetic Material—A. Z. Veksler. (*Zh. eksp. teor. Fiz.*, vol. 29, pp. 201–208; August, 1955.) Formulas are derived for the velocity distribution of photoelectrons and the temperature dependence of the photocurrent near the Curie point. The calculations are made on the basis of Vonsovski's s-d exchange model (*ibid.*, vol. 16, p. 981; 1946.) Results show that the photocurrent varies quadratically with magnetization.

535.215:546.482.21 1060
Infrared Quenching of Cadmium Sulfide—S. H. Liebson. (*J. electrochem. Soc.*, vol. 102, pp. 529–533; September, 1955.) "Infrared quenching of CdS has been investigated as a function of applied voltage and both infrared and exciting light intensities. Infrared quenching of photoconductivity due to light of wavelengths shorter than that corresponding to the absorption edge increases as the voltage is increased. The quenching spectrum is found to shift with temperature in approximately the same amount as the corresponding shift of the absorption edge. An explanation of infrared quenching is offered based on infrared freed holes recombining with trapped electrons within the crystal."

535.215:546.482.2 1061
Nonstationary Processes in Photoconductors: Part 1—Slow Build-Up of Photoconduction in CdS Single Crystals as a Method for Analysis of Disturbed States—K. W. Böer and H. Vogel. (*Ann. Phys., Lpz.*, vol. 17, pp. 10–22; October, 15, 1955.) Observed photoconductivity build-up curves obtained with weak illumination exhibit inflection points from whose positions the concentration of acceptor impurities can be determined.

535.3 1062
Optical Properties of Cadmium Sulfide and Zinc Sulfide from 0.6 Micron to 14 Microns—J. F. Hall, Jr. and W. F. C. Ferguson. (*J. opt. Soc. Amer.*, vol. 45, pp. 714–718; September, 1955.)

535.33/.34:537.228.1 1063
[Optical] Vibration Spectrum of Piezoelectric Crystals: Part 5—Lithium Sulphate and Potassium Sulphate—J. P. Mathieu, L. Couture, and H. Poulet. (*J. Phys. Radium*, vol. 16, pp. 781–785; October, 1955.) A study was made of the Raman and infrared-absorption spectra of single crystals with various orientations.

535.37 1064
Oxidation States of Europium in the Alkaline Earth Oxide and Sulfide Phosphors—P. M. Jaffe and E. Banks. (*J. electrochem. Soc.*, vol. 102, pp. 518–523; September, 1955.)

535.37 1065

Preliminary Studies of the Perovskite-Type Ternary Oxides as Luminophors—S. Terol and R. Ward. (*J. electrochem. Soc.*, vol. 102, pp. 524–528; September, 1955.) Report of an investigation of phosphors with $LaAlO_3$ base and various activators.

535.37 1066

Yellow Luminescence caused by Titanium in Magnesium Silicate containing Fluoride—H. Dziergwa and H. Panke. (*Z. Phys.*. vol. 142, pp. 259–265; October 1, 1955.) Quantum yield, temperature dependence, absorption, and afterglow are investigated for $MgF_2 \cdot MgO \cdot SiO_2$ phosphors containing TiO_2 alone or with MnO.

535.37:546.412.84 1067

The Influence of the Crystal Structure on the Luminescence of Calcium Silicate (Mn, Pb)—H. Lange and G. Kressin. (*Z. Phys.*, vol. 142, pp. 380–386; October 15, 1955.)

535.376 1068

Electroluminescence. Absolute Brightness Waves and Mean Lifetime of Excited Centres—G. Destriau. (*J. Phys. Radium*, vol. 16, pp. 798–800; October, 1955.) The frequency variation of the alternating and steady components of brightness was studied for ZnS with various activators; the dependence of the relative amplitudes of the two components on the mean lifetime of the excited centers was demonstrated.

535.376 1069

Thermoluminescence Measurements of Electroluminescent ZnS:Mn Films—R. E. Freund. (*Phys. Rev.*, vol. 100, pp. 760–761; October 15, 1955.) A typical glow curve is shown for a film which emitted light on application of an alternating or direct field; the measurements were made over the temperature range $-196°$ to $+25°C$.

535.376:537.534.9 1070

Deterioration of Luminescent Phosphors under Positive-Ion Bombardment—J. R. Young. (*J. Appl. Phys.*, vol. 26, pp. 1302–1306; November, 1955.) "The reduction of cathodoluminescence efficiency of phosphors has been observed after bombarding with H^+, H_2^+, He^+, Ne^+, N_2, and A^+ ions having energies from 1 to 25 kev. Detectable deterioration could be observed after a bombardment of less than 10^{-9} coul/mm² of ions (5×10^{11} ions/cm²). The deterioration could be annealed out at temperatures between 450° and 700°C. Results indicate that light 25-kev ions probably penetrate 0.1μ to 0.2μ into the phosphor." The phosphors studied were mainly ZnS:Ag.

535.376:546.472.21 1071

Edge Electroluminescence from ZnS Single Crystals—R. W. Smith. (*Phys. Rev.*, vol. 100, p. 760; October 15, 1955.) Experimental results are presented which indicate that both free electrons and holes may contribute to the electroluminescence of ZnS.

537.226/.227:546.431.824–31 1072

Single-Crystal Neutron Analysis of Tetragonal $BaTiO_3$—B. C. Fraser, H. R. Danner, and R. Pepinsky. vol. 100, pp. 745–746; October 15, 1955.)

537.227/.228.1 1073

Properties of Piezoelectric Ceramics in the Solid-Solution Series Lead Titanate-Lead Zirconate-Lead Oxide: Tin Oxide and Lead Titanate-Lead Hafnate—B. Jaffe, R. S. Roth, and S. Marzullo. (*J. Res. nat. Bur. Stand.*, vol. 55, pp. 239–254; November, 1955.) Results of a detailed investigation are reported. Ferroelectric ceramics with composition close to a morphotropic phase boundary exhibit high dielectric constant and relatively good piezoelectric properties. Where polymorphic inversions below the Curie temperature do not occur, these

desirable properties are stable over a wide temperature range. The significance of the results for transducer materials is indicated.

537.227:546.431.824–31 1074

Observations on Etched Crystals of Barium Titanate—D. S. Campbell. (*Phil. Mag.*, vol. 46, pp. 1261–1262; November, 1955.) Observations similar to those reported by Hooton and Merz (2990 of 1955) have been made using hydrochloric acid and phosphoric acid on crystals direct from the melt, with no polarizing treatment. Photomicrographs are reproduced.

537.228.2:546.431.824–31 1075

Temperature Dependence of Electrostrictive and Elastic Properties of Ceramic Barium Titanate—N. A. Roi. (*Akust. Zh.*, vol. 1, pp. 264–271; July/September, 1955.) An experimental investigation over the temperature range 15°–150°C is reported. Results are presented graphically.

537.311.31:537.311.62 1076

Surface Resistance and Reactance of Metals at Infrared Frequencies—J. R. Beattie and G. K. T. Conn. (PROC. IRE, vol. 44, pp. 78–81; January, 1956.) Properties of Ag, Al, Cu, and Ni surfaces have been studied over the frequency range $2.5–15 \times 10^{13}$ cps. Experimental results are compared with predictions from theory.

537.311.33 1077

Reflectivity of Several Crystals in the Far Infrared Region between 20 and 200 Microns—H. Yoshinaga. (*Phys. Rev.*, vol. 100, pp. 753–754; October 15, 1955.) Results of measurements on Ge, Si, ZnS, InSb, PbS, PbSe, and TlCl are shown graphically.

537.311.33 1078

Surface Potential and Surface Charge Distribution from Semiconductor Field Measurements—W. L. Brown. (*Phys. Rev.*, vol. 100, pp. 590–591; October 15, 1955.) "It is possible from measurements of the change in conductance of a semiconductor with application of an electric field normal to its surface to determine both the electrostatic potential of the surface and the distribution of charge in surface states. Such determinations depend upon the uniqueness of the minimum in conductance which can be observed in these experiments, and its independence of the surface state charge."

537.311.33 1079

Ambipolar Thermodiffusion of Electrons and Holes in Semiconductors—P. J. Price. (*Phil. Mag.*, vol. 46, pp. 1252–1260; November, 1955.) If a temperature gradient is maintained in a semiconductor then, since the equilibrium concentrations of electrons and holes increase with temperature, there will be a concentration gradient of both in the direction of the temperature gradient and a diffusion of both down this gradient ("ambipolar thermodiffusion"). A formula is derived for the magnitude of this effect and is used to determine the electronic contribution to the thermal conductivity and to the Nernst effect.

537.311.33 1080

An Easy Derivation of the Hole Lifetime in an n-Type Semiconductor with Acceptor Traps—F. W. G. Rose and D. J. Sandiford. (*Proc. phys. Soc.*, vol. 68, pp. 894–897; November 1, 1955.) The relations between the constants of recombination, generation, and the mass-action laws are described and used for the calculation of hole lifetime in the case of steady-state injection, the concentrations of electrons and holes being assumed sufficiently low for Boltzmann statistics to apply. The result agrees with that given by Shockley and Read (420 of 1953). Lifetime at the commencement of injection is different from the steady-state value.

537.311.33 1081

The Use of a Modulated Light Spot in Semiconductor Measurements—D. G. Avery and J. B. Gunn. (*Proc. phys. Soc.*, vol. 68, pp. 918–921; November 1, 1955.) Modifications to the theory of the "traveling-light-spot" method for the measurement of minority-carrier lifetime τ, which become necessary when the light spot is intensity modulated at a frequency $\omega/2\pi$, are discussed and experimentally verified. A necessary condition for accurate determinations is $\omega^2\tau^2 \ll 1$. Measurement of the phase of the collector signal as well as its amplitude enables the diffusion constant, and hence the drift mobility, of minority carriers to be determined directly.

537.311.33:535.215 1082

Method for determining the Mobility of Minority Current Carriers injected by Light—S. M. Ryvkin and R. V. Khar'yuzov. (*Zh. tekh. Fiz.*, vol. 25, pp. 563–568; April, 1955.) A detailed description of the apparatus is given and results of measurements are presented, including a number of oscillograms. A comparison of the results obtained with those published in the literature indicates that the method can be applied with advantage to investigations of the photoelectric properties of semiconductors.

537.311.33:537.32:546.873.241 1083

Investigation of the Thermoelectric Properties of Bismuth Telluride—R. M. Vlasova and L. S. Stil'bans. (*Zh. tekh. Fiz.*, vol. 25, pp. 569–576; April, 1955.) Report of an extensive investigation of the dependence of the thermo-emf, electrical conductivity, concentration, and mobility of current carriers of Bi_2Te_3 on temperature and on departure from stoichiometric composition.

537.311.33:537.533 1084

The Effect of Field Emission on the Behaviour of Semiconductor Contacts—R. W. Sillars. (*Proc. phys. Soc.*, vol. 68, pp. 881–893; November 1, 1955.) Quite a low potential across a semiconductor contact may be sufficient to produce field emission around the area of contact. This condition is investigated theoretically and experimentally for semiconductors with negligible surface barrier; the current due to field emission varies as the square or three-halves power of the applied voltage. Similar effects are found with metals which are not quite in contact.

537.311.33:546.28 1085

Lifetime of Electrons in p-Type Silicon—G. Bemski. (*Phys. Rev.*, vol. 100, pp. 523–524; October 15, 1955.) Measurements of the temperature variation of the lifetime of electrons in the vicinity of a p-n junction give results consistent with theory developed by Hall (3453 of 1952) and Shockley and Read (420 of 1953), assuming the level of recombination centers to be 0.2 ev above the valence band.

537.311.33:546.28 1086

Broadening of Impurity Levels in Silicon—M. Lax and E. Burstein. (*Phys. Rev.*, vol. 100, pp. 592–602; October 15, 1955.) Calculations of infrared absorption based on a hydrogen-type energy-level scheme are compared with experimental results on boron-doped Si. Results confirm the hypothesis that the broadening of absorption lines observed as temperature increases from that of liquid helium to that of liquid nitrogen is due to the interaction of trapped electrons with acoustic lattice vibrations.

537.311.33:546.28 1087

Trapping of Minority Carriers in Silicon: Part 2—n-Type Silicon—J. R. Haynes and J. A. Hornbeck. (*Phys. Rev.*, vol. 100, pp. 606–615; October 15, 1955.) Complementary investigation to that described previously [2013 of 1955 (Hornbeck and Haynes)]. Evidence is obtained of hole trapping at two or more levels; the

heights of the trap levels deduced from photoconductivity decay curves for a range of temperatures are consistent with accepted values of the energy gap.

537.311.33:546.28:535.37 1088
Visible Light from a Silicon *p-n* Junction—R. Newman. (*Phys. Rev.*, vol. 100, pp. 700–703; October 15, 1955.) "When low-voltage silicon *p-n* junctions are biased in the reverse direction to breakdown, visible light is emitted from the junction region. The effects of surface treatment on the phenomenon are discussed. Two typical light output vs reverse current curves are shown. A typical spectral distribution curve in the 1.8–3.4 ev range is shown. The observations suggest that the light results from a radiative relaxation mechanism involving the high-energy carriers produced in the avalanche breakdown process."

537.311.33:546.28:621.396.822 1089
The Effect of Illumination on the Excess Noise of Silicon Filaments—C. A. Hogarth and W. Bardsley. (*Proc. phys. Soc.*, vol. 68, pp. 968–970; November 1, 1955.) Experiments indicate that the excess noise in Si filaments due to trapping effects is reduced by irradiation with white light. This is interpreted as showing that the free minority carriers produced by the absorbed light keep the traps occupied and so reduce their effectiveness.

537.311.33:546.289 1090
Precipitation of Copper in Germanium—R. A. Logan. (*Phys. Rev.*, vol. 100, pp. 615–617; October 15, 1955.) "The density of dislocations is shown to have a marked effect on the rate of anneal of copper in germanium. At 500°C samples containing high dislocation density ($\sim 10^6/cm^2$) anneal in about 1 hour in contrast to material of low dislocation density ($\sim 10^4/cm^2$) which requires about 24 hours. When copper-doped germanium is cooled from a high temperature in regions of high dislocation density, significant precipitation occurs in a cooling cycle of only a few seconds. In this case, in order to prevent precipitation the sample must be quenched from the high temperature in a time of the order of 0.1 second."

537.311.33:546.289 1091
Properties of Germanium Doped with Manganese—H. H. Woodbury and W. W. Tyler. (*Phys. Rev.*, vol. 100, pp. 659–662; October 15, 1955.) "The temperature dependence of the electrical resistivity and Hall coefficient in *p*- and *n*-type manganese-doped germanium crystals indicates that manganese introduces two acceptor levels in germanium at $0.16+0.01$ ev from the valence band and $0.37+0.02$ ev from the conduction band. The distribution coefficient for manganese in germanium is $(1.0\pm0.2) \times 10^{-6}$. Comparison is made with other fourth-row metals (V, Fe, Co, and Ni) as impurities in germanium."

537.311.33:546.289 1092
Classical Theory of Cyclotron Resonance for Holes in Ge—J. M. Luttinger and R. R. Goodman. (*Phys. Rev.*, vol. 100, pp. 673–674; October 15, 1955.)

537.311.33:546.289 1093
Observation of Quantum Effects in Cyclotron Resonance [in Ge]—R. C. Fletcher, W. A. Yager, and F. R. Merritt. (*Phys. Rev.*, vol. 100, pp. 747–748; October 15, 1955.) Observations of new cyclotron resonance lines at very low temperatures are interpreted as confirming theoretical predictions by Luttinger and Kohn (2316 of 1955).

537.311.33:546.289 1094
Restoration of Resistivity and Lifetime in Heat Treated Germanium—R. A. Logan and M. Schwartz. (*J. appl. Phys.*, vol. 26, pp. 1287–1289; November, 1955.) "Experiments are described in which minority carrier lifetime and

resistivity of germanium are altered by the addition of copper by diffusion, under conditions where extraneous chemical contamination is minimized. This copper is then gettered by heating the samples in contact with liquid lead or gold, and the resistivity and lifetime are substantially restored. The gettering process is interpreted in terms of the low distribution coefficient of copper in the ternary system which copper and germanium form with the getter."

537.311.33:546.289 1095
The Influence of Pressure on Metal/Germanium Contacts—J. Lees and S. Walton. (*Proc. phys. Soc.*, vol. 68, pp. 922–928; November 1, 1955.) Variation of the resistance of Ge with pressure is measured by comparing the areas of these contacts as given by electrical and by optical methods.

537.311.33:546.289 1096
Some Measurements connected with Carrier Deficit Phenomena in Germanium—A. Many, D. Gerlich, and E. Harnik. (*Proc. phys. Soc.*, vol. 68, pp. 970–972; November 1, 1955.) Carrier exclusion was studied in *n*-type Ge filaments composed of two sections, one containing a higher proportion of donor impurities than the other, separated by a sharp transition region. Results are in accordance with theory.

537.311.33:546.289:535.215 1097
Temperature Dependence of Photocurrent in Ge *p-n* Junctions—R. Wiesner and E. Groschwitz. (*Z. angew. Phys.*, vol. 7, pp. 496–499; October. 1955.) Measurements were made of the photocurrent at temperatures between 10° and 60°C; results are consistent with the recombination mechanism proposed by Hall (3453 of 1952), the temperature dependence being determined mainly by the carrier diffusion length. The production of carriers by the illumination is nearly independent of temperature. With the specimens investigated, surface recombination contributed little to the temperature variation of the photocurrent, hence the problem could be treated with sufficient accuracy as unidimensional.

537.311.33:546.289:538.614 1098
Faraday Effect in Germanium at Room Temperature—R. R. Rau and M. E. Caspari. (*Phys. Rev.*, vol. 100, pp. 632–639: October 15, 1955.) Room-temperature measurements were made of the Faraday rotation of plane-polarized microwaves traversing 4-mm-thick samples of Ge inserted in a circular waveguide; for a longitudinal magnetic field of 1,400 G the angle of rotation is about 3°. Values of 3,780 and 3,300 cm per v/cm were deduced for the electron and hole mobilities in *n*- and *p*-type specimens respectively, based on analysis using the Drude-Zener model. For small losses, the ellipticity of the polarization of the transmitted wave is proportional to the relaxation time.

537.311.33:546.289:548.0 1099
Some Aspects of Slip in Germanium—R. G. Treuting. (*J. Metals, N.Y.*, vol. 7, Section 2, pp. 1027–1031; September, 1955.) Experiments are reported indicating that slip in Ge crystals subjected to tension at 600°C is in the ⟨100⟩ direction.

537.311.33:546.289:621.317.331 1100
Surface Preparation and Resistivity Measurements on Semiconductor Crystals—R. Manfrino. (*Alta Frequenza*, vol. 24, pp. 390–420; August/October, 1955.) The main chemical and electrolytic etching processes suitable for Ge single crystals are described; micrographs illustrating results are reproduced. Apparatus for resistivity measurements by the four-probe method [1502 of 1954 (Valdes)] is described. A resistivity map obtained with a crystal surface of area 150 mm² is shown.

537.311.33:546.289:621.396.822 1101
Hall Effect Noise—J. J. Brophy and N. Rostoker. (*Phys. Rev.*, vol. 100, pp. 754–756; October 15, 1955.) Hall-effect measurements were made on Ge "bridge" specimens exhibiting excess noise with the usual $1/f$ spectrum. A magnetic-field-dependent noise voltage was observed; this is interpreted as indicative of carrier density fluctuations.

537.311.33:546.3.171 1102
Production of Metal Nitrides by Glow Discharge, and some of their Properties—W. Janeff. (*Z. Phys.*, vol. 142, pp. 619–636; October 26, 1955.) The preparation of nitrides of Ag, Cu, Zn, Cd, Sb, Bi, Pb, Sn, Fe, and Ni and measurements of their resistivities are described in detail. The temperature coefficient of resistance was also determined. No photoelectric effect was observed.

537.311.33:546.361.31 1103
Conductance Mechanisms and the Thermal Transition in Caesium Chloride—W. W. Harpur and A. R. Ubbelohde. (*Proc. roy. Soc. A.*, vol. 232, pp. 310–319; November 8, 1955.)

537.311.33:546.46.814 1104
Electrical and Optical Properties of Intermetallic Compounds: Part 4—Magnesium Stannide—R. F. Blunt, H. P. R. Frederikse, and W. R. Hosler. (*Phys. Rev.*, vol. 100, pp. 663–666; October 15, 1955.) Measurements over a temperature range indicate that the value of the energy gap is 0.33 ev at 0°K, and room-temperature mobilities are 320 and 260 cm per v/cm for electrons and holes respectively. Appreciable photoconductivity is observed at 85° and 5°K. Part 3: 1405 of 1955 (Blunt, *et al.*).

537.311.33:546.47-31 1105
The Electrical Conductivity at the Surface of Zinc Oxide Crystals—G. Heiland. (*Z. Phys.*, vol. 142, pp. 415–432; October 15, 1955.) Continuation of experiments reported previously (159 of 1955). The effects of exposure to an oxygen atmosphere and to light and electron irradiation were studied using single-crystal specimens. Both reversible and irreversible variations of conductivity are produced by irradiation at low temperature; this is interpreted as indicating that thin surface layers are effective in absorbing the radiation as well as in the oxygen interaction.

537.311.33:546.621.86 1106
Effect of Impurities on the Electrical Conduction Mechanism of AlSb—A. R. Regel and M. S. Sominski. (*Zh. tekh. Fiz.*, vol. 25, pp. 768–770; April, 1955.) Experimental evidence shows that an admixture of Ge does not alter the conduction mechanism of AlSb while admixtures of Sn, Pb, As, Bi, Se, and Te transform it into *n*-type. The rectifying properties of AlSb are also greatly affected by impurities. A theoretical interpretation of the results is presented.

537.311.33:[546.682.86+546.681.86 1107
Nuclear Magnetic Resonance in Semiconductors: Part 1—Exchange Broadening in InSb and GaSb—R. G. Shulman, J. M. Mays, and D. W. McCall. (*Phys. Rev.*, vol. 100, pp. 692–699; October 15, 1955.) Experimental work is reported.

537.311.33:546.682.86 1108
Plasma Resonance in Crystals: Observations and Theory—G. Dresselhaus, A. F. Kip, and C. Kittel. (*Phys. Rev.*, vol. 100, pp. 618–625; October 15, 1955.) Observations are reported of magnetic resonance observed in *n*-type InSb at 9 and 24 kmc, at temperatures of 4° and 77°K. Theory presented previously in relation to resonance in Si and Ge (2995 of 1955) is extended to deal with this case. The influence of specimen shape and the possibility of detecting minority-carrier cyclotron reso-

nance in the presence of a majority-carrier plasma are examined and eddy-current effects are discussed.

537.311.33:546.817.221:621.396.822   **1109**
Measurements of Current Noise in Lead Sulphide at Audio Frequencies—D. Barber. (*Proc. phys. Soc.*, vol. 68, pp. 898–907; November 1, 1955.) The mean square noise voltage per unit bandwidth, $v_n{}^2$, was found to vary as the square of the exciting current and to increase with decreasing frequency in a manner which varied from cell to cell, being directly dependent on cell resistance. Temperature and illumination affected $v_n{}^2$ only through their effect on resistance.

537.311.33:[546.873.231+546.873.241   **1110**
Diffusion of Tin and Antimony in the Semiconducting Compounds Bi_2Se_3 and Bi_2Te_3—B. Boltaks. (*Zh. tekh. Fiz.*, vol. 25, pp. 767–768; April, 1955.) Experimental data are presented graphically. The activation energy in the case of Sb is two or three times greater than in the case of Sn.

537.311.33:621.396.822   **1111**
Relative Influence of Majority and Minority Carriers on Excess Noise in Semiconductor Filaments—L. Bess. (*J. appl. Phys.*, vol. 26, pp. 1377–1381; November, 1955.) "An experiment has been devised whereby excess noise is measured along various different directions in a germanium filament after the directions of current flow for the majority and minority carriers had been altered by a magnetic field. From this experiment it is possible to determine that whereas shot noise is caused by both majority and minority carrier fluctuation, $1/f$ noise is essentially produced only by majority carrier fluctuation."

537.323:546.56–1   **1112**
Effect of Point Imperfections on the Electrical Properties of Copper: Part 2—Thermoelectric Power—F. J. Blatt. (*Phys. Rev.*, vol. 100, pp. 666–670; October 15, 1955.) Calculations are presented of the variation of thermoelectric power due to the presence of interstitials and vacancies and small concentrations of As. Part 1: 790 of 1956.

538.214:546.26–1   **1113**
Theory of the Magnetic Susceptibility of Graphite—J. E. Hove. (*Phys. Rev.*, vol. 100, pp. 645–649; October 15, 1955.)

538.22   **1114**
Neutron Diffraction Study of the Magnetic Properties of the Series of Perovskite-Type Compounds $[(1+x)La, xCa]MnO_3$—E. O. Wollan and W. C. Koehler. (*Phys. Rev.*, vol. 100, pp. 545–563; October 15, 1955.) "This series of compounds exhibits ferromagnetic and antiferromagnetic properties which depend upon the relative trivalent and tetravalent manganese ion content. The samples are purely ferromagnetic over a relatively narrow range of composition ($x\sim0.35$) and show simultaneous occurrence of ferromagnetic and antiferromagnetic phases in the ranges ($0 < x < 0.25$) and ($0.40 < x < 0.5$). Several types of antiferromagnetic structures at $x = 0$ and $x > 0.5$ have also been determined." The results are in good agreement with Goodenough's predictions (1115 below).

538.22   **1115**
Theory of the Role of Covalence in the Perovskite—Type Manganites [La, $M(II)$] MnO_3—J. B. Goodenough. (*Phys. Rev.*, vol. 100, pp. 564–573; October 15, 1965.) The structure of these manganites is studied using the concept of semicovalent exchange [3016 of 1955 (Goodenough and Loeb)]. Predicted properties are consistent with experimental results (*e.g.*, 1114 above).

538.22   **1116**
Magnetic Moment Arrangements and Magnetocrystalline Deformations in Antiferromagnetic Compounds—Yin-Yuan Li. (*Phys. Rev.*, vol. 100, pp. 627–631; October 15, 1955.)

538.22   **1117**
Considerations on Double Exchange—P. W. Anderson and H. Hasegawa. (*Phys. Rev.*, vol. 100, pp. 675–681; October 15, 1955.) Calculations are presented of interactions between magnetic ions, of the type discussed by Zener (2441 of 1951).

538.22:621.318.134   **1118**
Properties of Lithium Ferrite $FeLiO_2$—R. Collongues. (*C.R. Acad. Sci., Paris*, vol. 241, pp. 1577–1580; November 28, 1955.) Structural changes observed at temperatures up to 670°C are described.

538.22:621.318.134   **1119**
Micrographic Study of the Cubic→Quadratic Transformation in Copper Ferrite—I. Behar. (*C.R. Acad. Sci., Paris*, vol. 241, pp. 1580–1581; November 28, 1955.)

538.22:621.318.134   **1120**
Influence of Substitutions on Quadratic Deformation in Copper Ferrite and Chromite—C. Delorme. (*C.R. Acad. Sci., Paris*, vol. 241, pp. 1588–1589; November 28, 1955.)

538.221   **1121**
A Simple Method for rendering Elementary Magnetic Domains Visible by use of Dry Powder—W. Andrä and E. Schwabe. (*Ann. Phys., Lpz.*, vol. 17, pp. 55–56; October 15, 1955.) The specimen is exposed to smoke from ignited iron pentacarbonyl.

538.221   **1122**
Solutions of the Equations of Ferrimagnetic Resonance—B. Dreyfus. (*C.R. Acad. Sci., Paris*, vol. 241, pp. 1270–1272; November 7, 1955.) A detailed study is made of the four solutions of the resonance equation derived previously (185 of 1956) in the light of the fact that only two resonances are observed experimentally and one of these is generally very weak [2335 of 1955 (McGuire)].

538.221   **1123**
Irreversible Magnetic After-Effect and its Influence on the Form of the Magnetization Curve—O. Yamada. (*Z. Phys.*, vol. 142, pp. 225–240; September 12, 1955.) Results of an experimental investigation on alnico (24 per cent Co; 13.5 per cent Ni; 8.5 per cent Al; 3 per cent Cu; 51 per cent Fe) are reported and discussed.

538.221   **1124**
Results and Problems of the Quantitative Theory of Coercive Force—R. Brenner. (*Z. angew. Phys.*, vol. 7, pp. 499–507; October, 1955.) A critical survey of published theoretical work on the nature of the coercive force in ferromagnetic materials, in relation to physical and practical aspects.

538.221   **1125**
Theory of Remagnetization of Thin Tapes—H. Ekstein. (*J. appl. Phys.*, vol. 26, pp. 1342–1343; November, 1955.) Analysis based on domain-wall displacements is given for the reversal of magnetization of ferromagnetic tapes with rectangular hysteresis loops, subjected to an external field parallel to the surface.

538.221   **1126**
Influence of Pulsed Magnetic Fields on the Reversal of Magnetization in Square-Loop Metallic Tapes—D. S. Rodbell and C. P. Bean. (*J. appl. Phys.*, vol. 26, pp. 1318–1323; November, 1955.) Report of experiments confirming results obtained previously [1706 of 1955 (Bean and Rodbell)] and illuminating the process of domain formation. The "intrinsic mobility" of domain walls is evaluated; for a

particular permalloy specimen the value is about 100 cm per oersted.

538.221   **1127**
Electrical Analog of the Eddy-Current-Limited-Domain Boundary Motion in Ferromagnetics—G. Brouwer. (*J. appl. Phys.*, vol. 26, pp. 1297–1301; November, 1955.) When a ferromagnetic material is magnetized by domain-boundary displacement, the dispersion region of the permeability/frequency curve shifts towards lower frequencies with increasing domain size, in consequence of the inhomogeneous distribution of the permeability at the domain boundaries. This corresponds to the eddy-current phenomenon in laminated materials. Analysis based on equivalent networks is presented for some idealized cases. Successive stages in the magnetization process are illustrated by field maps with boundary movements indicated.

538.221   **1128**
Hysteresis Loops of Mixtures of Ferromagnetic Micropowders—C. P. Bean. (*J. appl. Phys.*, vol. 26, pp. 1381–1383; November, 1955.) The mixtures considered are dilute compacts with <1 per cent of the volume occupied by the ferromagnetic powders, so that the total magnetization can be determined simply from the magnetization of the constitutents. The latter comprise particles in three different size ranges: large (multidomain), medium (single-domain), and small (single-domain "super-paramagnetic"). Experimental results are discussed in relation to theories regarding the coercive force of such mixtures.

538.221   **1129**
The Remanent Magnetization of Haematite Powders—E. P. Wohlfarth. (*Phil. Mag.*, vol. 46, pp. 1155–1164; November, 1955.) "Calculations are described of the remanent magnetization and the remanence after demagnetization as a function of field strength for powders of haematite, αFe_2O_3. The calculations are based on the assumptions that the powder particles are single domains and that their hysteretic properties are due to magnetocrystalline anisotropy with threefold symmetry in the basal crystal plane. The calculations are intended for eventual comparison with experiments now in progress."

538.221   **1130**
The Thermal Effects associated with the Magnetization of High-Coercivity Materials—L. F. Bates and A. W. Simpson. (*Proc. phys. Soc.*, vol. 68, pp. 849–858; November 1, 1955.) Experiments with alloys of the Fe_2NiAl type, over a field range of 4,000 oersteds, give results in accordance with the theory advanced by Stoner and Rhodes (*Phil. Mag.*, vol. 40, p. 481; 1949).

538.221+549.514.51]:534.22–8   **1131**
Variation of Elastic-Wave Velocity with Frequency in Fused Quartz and Armco Iron—D. S. Hughes and J. M. Kennel. (*J. appl. Phys.*, vol. 26, pp. 1307–1309; November, 1955.) Using small cylindrical samples specially built up to transmit only torsional waves, the propagation velocity was observed to be constant within ±1 m over the frequency range 0.6–3 mc for fused quartz; for armco the velocity was constant within ±2 m from 0.5 to 1.5 mc and decreased by about 10 m between 1.5 and 3 mc.

538.221:539.234   **1132**
Magnetic Domains in Thin Films of Nickel-Iron—C. A. Fowler, Jr., and E. M. Fryer. (*Phys. Rev.*, vol. 100, pp. 746–747; October 15, 1955.) Photographs of the domain pattern on both faces of an evaporated film are reproduced.

538.221:621.318.132   **1133**
Relation of Magnetic Characteristics of Magnetically Soft Alloys to Thickness of Lami-

nation—E. I. Gurvich and E. Kondorski. (*C. R. Acad. Sci. U.R.S.S.*, vol. 104, pp. 530–532; October 1, 1955. In Russian.) Experimental results indicate that the change in the frequency characteristics of the permeability and loss angle with change in the thickness of the specimen is probably due to a greater penetration, during the heat treatment, of impurities from the surface into the material in thinner specimens. Molybdenum permalloy and 50 per cent permalloy were investigated.

538.221:621.318.134 **1134**
Ferrimagnetic Resonance in Single Crystals of Manganese Ferrite—J. F. Dillon, Jr., S. Geschwind, and V. Jaccarino. (*Phys. Rev.*, vol. 100, pp. 750–752; October 15, 1955.) Report of experiments at frequencies of 5.9, 9.3, and 24 kmc, using temperatures up to 300°K. Resonance curves and line-width/temperature characteristics are shown.

538.221:621.318.134 **1135**
Transient Phenomena in a Ferrite—S. Matz. (*Rev. gén. Élect.*, vol. 64, pp. 491–509; October, 1955.) Detailed account of an investigation, previously described briefly (3605 of 1954), of the complex-permeability variations of ferrites in a hf magnetic field. Results are discussed in relation to theory and measurements of magnetic after-effect.

538.221:621.318.134 **1136**
Low-Magnetic-Saturation Ferrites for Microwave Applications—L. G. Van Uitert. (*J. appl. Phys.*, vol. 26, pp. 1289–1290; November, 1955.) Values of Curie temperature, coercive force, magnetic saturations at 25° C, and initial permeability at 0.1 mc are given for six MgAlMn ferrites

538.652 **1137**
Calculation of Magnetostriction Constants for Nickel—G. C. Fletcher. (*Proc. phys. Soc.*, vol. 68, pp. 1066–1071; November 1, 1955.) Calculations for Ni at 0°K, based on the collective electron model, give values of the magnetic constants rather larger than the latest figures obtained experimentally at 120°K.

548.0:537.311.33 **1138**
Symmetry Properties of the Energy Nands of the Zinc Blende Structure—R. H. Parmenter. (*Phys. Rev.*, vol. 100, pp. 573–579; October 15, 1955.) Analysis is based on group theory, first excluding and then including spin-orbit coupling. Character tables and compatibility tables are presented. The degeneracies and gradients of the various possible energy bands are studied at lines and points of symmetry in the Brillouin zone. The results are compared with those for the equivalent energy bands in crystals of diamond structure.

548.0:537.311.33 **1139**
Spin-Orbit Coupling Effects in Zinc Blende Structures—G. Dresselhaus. (*Phys. Rev.*, vol. 100, pp. 580–586; October 15, 1955.) "Character tables for the 'group of the wave vector' at certain points of symmetry in the Brillouin zone are given. The additional degeneracies due to time reversal symmetry are indicated. The form of energy vs wave vector at these points of symmetry is derived."

548.5 **1140**
Single Crystals with Pure Surfaces—E. Menzel, W. Stössel, and M. Otter. (*Z. Phys.*, vol. 142, pp. 241–244; October 1, 1955.) A method is outlined for producing spherical single crystals of metals by congelation from the molten state on to a plane base material in a vacuum.

548.5:669.046.54/.55 **1141**
Contribution to Mathematics of Zone Melting—L. Burris, Jr., C. H. Stockman, and I. G. Dillon. (*J. Metals, N. Y.*, vol. 7, Section 2, pp. 1017–1023; September, 1955.)

548.5:669.046.54/.55:537.311.33 **1142**
Temperature Gradient Zone Melting—W. G. Pfann. (*J. Metals, N. Y.*, vol. 7, pp. 961–964; September, 1955.) "Under certain conditions, a molten zone can be made to move through a solid by impressing a stationary temperature gradient across the solid. This phenomenon can be utilized in fabricating semiconductive devices, growing single crystals, joining, boring fine holes in solids, measuring diffusivities in liquids, small scale alloying, and purification. Fundamentals and exemplary applications are outlined."

621.315.56:621.315.616 **1143**
Rubber as an Electrical Conductor in Engineering: Properties, General and Special Applications—S. de Meij. (*Bull. schweiz. elektrotech. Ver.*, vol. 46, pp. 1067–1069; October 29, 1955.) The electrical and mechanical properties of rubber containing furnace black are briefly reviewed. Applications mentioned include use in antistatic devices, cable sheaths, panel heating, noise-free cables, and electromechanical transducers. Use of conducting rubber for semiconductor diodes and triodes is suggested, but no details are given.

621.315.614.64 **1144**
Acetylized Paper as an Insulating Material in Electrical Engineering—W. Dieterle. (*Bull. schweiz. elektrotech. Ver.*, vol. 46, pp. 1045–1065; October 29, 1955.) A comprehensive survey is presented of the electrical properties of paper treated with acetic acid. The treatment reduces the hygroscopicity. Impregnation with chlorinated oils of high dielectric constant further improves the insulating qualities. 26 graphs, 3 tables of properties of papers, fibers, and oils, and 43 references are given.

621.315.616 **1145**
The Mechanical Engineering of Dielectrics—B. Maxwell. (*Elect. Engng., N. Y.*, vol. 74, pp. 870–873; October, 1955.) The mechanical properties of polymeric plastics are discussed; the importance of their variation with time and with temperature is illustrated by results of measurements.

621.315.616 **1146**
Electric Strength of Irradiated Polythene—K. H. Stark and C. G. Garton. (*Nature, Lond.*, vol. 176, pp. 1225–1226; December 24, 1955.) Measurements were made at temperatures up to 220°C on molded disks recessed to a thickness of about 50μ, irradiated with 4-mev electrons. Results are compared with those obtained by Bird and Pelzer for unirradiated material (1696 of 1949).

621.318.2:621.385.029.6 **1147**
Permanent Magnets for Microwave Electron Valves—de Bennetot. (See 1254.)

621.357 **1148**
Micromachining with Virtual Electrodes—A. Uhlir, Jr. (*Rev. sci. Instrum.*, vol. 26, pp. 965–968; October, 1955.) An electrolytic etching method is described which has been used to drill very small holes in Ge, Mo, Fe, etc., and to plate small areas. The technique involves use of a glass tube drawn to a fine tip to localize the current.

537.311.33 **1149**
Poluprovodniki v Sovremennoi Fizike (Semiconductors in Contemporary Physics). [Book Review]—A. F. Ioffe. Publishers: Izd. A.N. S.S.S.R. (Acad. Sci. U.S.S.R.), Moscow-Leningrad, 355 pp., 1954. (*Uspekhi fiz. Nauk.* vol. 57, pp. 165–169; September, 1955.) A monograph written for physicists, chemists and engineers. Chapters are included on (*a*) solid electrolytes, (*b*) metals, (*c*) electronic semiconductors, (*d*) quantum theory of semiconductors, (*e*) physical phenomena in semiconductors, and (*f*) experimental results.

MATHEMATICS

512 **1150**
Vectors, Matrices and Determinants, Tensors—R. Fortet. (*Bull. Soc. franc. Elect.*, vol. 5, pp. 710–726; October, 1955.) An introductory article for electrical engineers.

517.522.2 **1151**
A Simple Method for the Numerical Calculation of Time Functions for Given Broken Rational Transform Functions—R. Hofmann and W. Walcher. (*Arch. elekt. Übertragung*, vol. 9, pp. 475–478; October, 1955.) The method described is useful in analysis involving Laplace transforms. The required time function is presented in the form of a rapidly converging power series.

517.9:537.21 **1152**
Poisson's Partial Difference Equation—(See 1019.)

MEASUREMENTS AND TEST GEAR

531.761+529.7 **1153**
Definition of the Second of Time—G. M. Clemence. (*Nature, Lond.*, vol. 176, p. 1230; December 24, 1955.) Attention is directed to certain undesirable consequences involved in the adoption of a "physical second" in place of the astronomical second [3686 of 1955 (Bullard)]. It is suggested that if a new physical unit is adopted it should be given a name other than "second," to avoid confusion. See also 513 of 1956 (Jones).

621.317.331:537.311.33:546.289 **1154**
Surface Preparation and Resistivity Measurements on Semiconductor Crystals—Manfrino. (See 1100.)

621.317.335:621.315.61 **1155**
Measurement of ϵ' and tan δ of a Solid Dielectric at Centimetre Wavelengths in the Temperature Range from $-100°$ to $+100°C$—P. F. Veselovski (*Zh. tekh. Fiz.*, vol. 25, pp. 601–609; April, 1955.) A new method is described in which use is made of a rectangular resonator designed for oscillations of the H_{10} type. The resonator consists of two waveguide sections separated by a sheet of mica and closed by movable pistons at the ends. Results of measurements on polythene and other insulating materials are given in tables and curves.

621.317.335:621.317.755 **1156**
A Precision Resonance Method for measuring Dielectric Properties of Low-Loss Solid Materials in the Microwave Region—S. Saito and K. Kurokawa. (*Proc. IRE*, vol. 44, pp. 35–42; January, 1956.) A disk sample is inserted into a cylindrical cavity resonator; the dielectric constant is found from the difference between the lengths for resonance with and without the sample, and the loss factor is found from the difference between the Q factors. Good precision is obtained by using a differentiated resonance curve as a frequency marker on the oscilloscope.

621.317.335.3 **1157**
The Measurement of Dielectric Constants of Liquids at Decimetre Wavelengths—T. Jäkel. (*Ann. Phys., Lpz.*, vol. 17, pp. 42–54; October, 1955.) Detailed description of a coaxial-line method in which the evaluation of the results does not involve transcendental functions.

621.317.336 **1158**
Reflection and Impedance Measurements by means of a Long Transmission Line—J. C. van den Hoogenband and J. Stolk. (*Philips tech. Rev.*, vol. 16, pp. 309–320; May, 1955.) Description of a variable-frequency stationary-detector method using a line about 60 m long. Direct visual indication of matching is given by means of an oscilloscope. For quick meas-

urements a wobbulator is used, for more accurate measurements a variable-frequency oscillator is preferred, in conjunction with a dc microammeter.

621.317.34 : 621.373.42.025.3 1159
Wide-Band Three-Phase *RC*-Generators for Complex Measurements of Two-Poles and Four-Poles—G. Thirup. (*J. Brit. IRE*, vol. 15, pp. 597–605; December, 1955.) "From a 3-phase RC oscillator two voltages are derived, the complex ratio of which can be varied. The complex ratio is independent of the frequency. The two voltages are used in a compensation circuit for measuring the parameters of two-poles and four-poles. Two equipments are described covering the frequency ranges 20 cps–22 kc and 22 kc–10 mc. The possible error is ±0.5 db and ±2° in the frequency range 100 cps–3 mc. Outside this range the phase error may increase about 3 times while the amplitude error remains nearly the same."

621.317.715 1160
Very-High-Sensitivity Screened Galvanometer—W. Meissner and R. Doll. (*Z. angew. Phys.*, vol. 7, pp. 461–468; October, 1955.)

621.317.722 1161
Design for a Sensitive Self-Recording Gold-Leaf Electroscope—P. Goodman. (*J. sci. Instrum.*, vol. 32, pp. 439–440; November, 1955.) An electrode system is used such that the leaf deflection passes through 90° and the leaf then discharges; the output is in the form of voltage pulses whose frequency is proportional to current for low values and logarithmically related for higher values. Steady electron currents of the order of 10^{-14} A can be measured.

621.317.733 : 621.314.7 1162
A D.C. and A.C. Balance Detector with Automatic Protection from Overload—C. Morton. (*J. sci. Instrum.*, vol. 32, pp. 437–439; November, 1955.) Two junction transistors in a balanced bridge circuit give a current gain of 50. The input resistance approaches infinity for input voltages >150 mv, thus providing automatic protection. For ac working the application of an auxiliary voltage of about 4 v, of the same frequency as the bridge voltage, gives a sensitivity of 15 ma/v (rms).

621.317.75.029.3 1163
Audio Frequency Spectrum Analyzer—E. F. Feldman. (*Tele-Tech & Electronic Ind.*, vol. 14, pp. 78–81, 135; October, 1955.) The heterodyne-type equipment described displays the Fourier analysis of complex waveforms, providing either logarithmic or linear frequency and amplitude indications. Points of the design are discussed, particularly the IF stages. the bandwidth of which is varied in synchronism with the log-frequency scan to maintain optimum resolution.

621.317.755 1164
Voltage Coincidence Oscilloscope—R. J. D. Reeves. (*Wireless World*, vol. 62, pp. 85–87; February, 1956.) A method of presenting multichannel displays on a single-beam cro uses a voltage-coincidence circuit in place of a *Y* amplifier, with a normal timebase voltage on the *X* plates. A number of co-phased outputs are taken from an independent af oscillator and one of them is applied to the *Y* plates to give a full-scale deflection; the others are used as reference signals in the voltage-coincidence circuit to explore the waveforms under examination, a bright spot appearing on the screen whenever the two signals are equal. The method is not useful for very fast displays, and care is necessary to avoid erroneous interpretation of the display.

621.317.755 : 621.3.015.3 1165
New Circuits for Recurrent Surge Oscillography—D. D. Davis. (*Elect. Engng.*, N. Y., vol. 74, pp. 919–923; October, 1955.)

621.317.772 1166
Measuring Phase at R.F. and Video Frequencies—Y. P. Yu. (*Electronics*, vol. 29, pp. 138–140; January, 1956.) A continuously variable delay line is used in conjunction with a balanced phase detector to indicate the phase difference between two input signals. The frequency range is 10 kc–20 mc; a delay of 5×10^{-10} second can be measured. Accuracy is within ±0.1° of phase angle, or ±1 per cent of indicated time delay.

621.317.772.029.3 : 621.314.7 1167
Direct-Indicating Audio-Frequency Phase-Angle Meters using Transistors—K. Homilius. (*Arch. tech. Messen*, pp. 221–224; October, 1955.) Circuits are described based on the technique of converting the sinusoidal signals whose phase difference is unknown into constant-amplitude pulses. Use of both point-contact and junction transistors is indicated.

621.317.784 1168
Wattmeters—H. D. Hawkes and A. H. M. Arnold. (*J. Instn. elect. Engrs.*, vol. 1, pp. 676–683; November, 1955.) A review of commercial instruments, including one torsion-head microwave type.

621.317 + 621.372].029.63/.64 1169
Schaltungstheorie und Messtechnik des Dezimeter- und Zentimeterwellengebietes [Book Review]—Weissfloch. (See 1015.)

OTHER APPLICATIONS OF RADIO AND ELECTRONICS

534.1–8 : 621.9 1170
Ultrasonic Machining of Brittle Materials—M. S. Hartley. (*Electronics*, vol. 29, pp. 132–135; January, 1956.) High-speed cutting is achieved by means of a correctly shaped tool vibrating above the specimen at a frequency of 25 kc. The tool face and the specimen do not come into contact; an abrasive powder in a liquid suspension is fed between the two and cutting is done by impact of the powder on the specimen surface.

550.837 1171
Geophysical Prospection of Underground Water in the Desert by means of Electromagnetic Interference Fringes—M. A. H. El-Said. (PROC. IRE, vol. 44, pp. 24–30; January, 1956.) A variable-frequency and a variable-distance method are described. Interference patterns obtained at two places in the Egyptian deserts are shown; results are in good agreement with information regarding the water table obtained from boring.

621–52 : 621.9 1172
An Electronically Controlled Machine Tool—(*Electronic Engng.*, vol. 28, p. 37; January, 1956.) A fully automatic copy milling machine for the production of cams is described. Coded design information is fed on plastic tape to a control unit and information store which also contains provision for enabling smooth profile curves to be deduced from a relatively small number of stored marker points.

621–526(083.7) 1173
IRE Standards on Terminology for Feedback Control Systems, 1955—(PROC. IRE, vol. 44, pp. 107–109; January, 1956.) Standard 55 IRE 26. S2.

621.365.5 : 621.385 1174
Brown Boveri Transmitting and Rectifier Tubes in Industrial Generators for R.F. Heating—R. Hübner. (*Brown Boveri Rev.*, vol. 42, pp. 370–387; September, 1955.) Brief illustrated descriptions are given of induction and dielectric heating apparatus for various purposes.

621.374.3 : 621.316.86 : 77 1175
Precision Photographic Timer—J. G. Thomason. (*Wireless World*, vol. 62, pp. 71–74;

February, 1956.) An electronic timing circuit based on the Miller integrator is described. Compensation for variations in mains voltage is obtained by use of a feed resistor in which the current passed varies approximately as the fifth power of the applied voltage.

621.384.613 1176
Energy Stability of the 22-MeV Betatron at the University of Illinois—B. M. Spicer and A. S. Penfold. (*Rev. sci. Instrum.*, vol. 26, pp. 952–953; October, 1955.) The greatest energy fluctuation observed over a period of eighteen months was 40 kev at 17 mev.

621.385.83.032.2 1177
Some Anomalous Emission Effects in Low-Energy Electron Beams—W. W. H. Clarke and L. Jacob. (*Proc. phys. Soc.*, vol. 68, pp. 805–816; November 1, 1955.) Cathode emission in a specially made electron gun, using accelerating voltages in the range 18–30 v, was found to vary in a periodic manner over the cathode surface, variations being greatest in the central region where the emission pattern was critically dependent on accelerating voltage and on cathode temperature. Variation of total emission was also periodic. The wavelength of the standing-wave pattern across the emitter was 0.01 mm; the electrons are assumed to oscillate in the field resulting from the effects of the initial velocities and the space charge.

621.385.833 1178
An Investigation of the Electron-Optical Properties of Straight Magnetic Gaps—S. N. Baranovski, D. L. Kaminski, and V. M. Kel'man. (*Zh. tekh. Fiz.*, vol. 25, pp. 610–624; April, 1955.) The system considered consists of two magnetic pole pieces greatly extended in one direction; electrons are subjected to the action not of the field in the gap but of the "dissipation field" in front of it. A theoretical as well as experimental investigation into the operation of the system is presented.

621.385.833 1179
The Scanning Electron Microscope and its Fields of Application—K. C. A. Smith and C. W. Oatley. (*Brit. J. appl. Phys.*, vol. 6, pp. 391–399; November, 1955.) The advantages of the scanning electron microscope, due especially to the large angles of incidence and reflection which can be used, are discussed and examples are given of applications for which the conventional electron microscopes are unsuitable. Bombardment of the specimen is much less severe than with conventional types. A resolution of 200 Å has been attained and a value of <100 Å may be attainable.

621.385.833 1180
A Possible Chromatic Correction System for Electron Lenses—G. D. Archard. (*Proc. phys. Soc.*, vol. 68, pp. 817–829; November 1, 1955.) It is shown that a combination of two two-pole groups of electrodes can provide axial chromatic correction in one plane. Applications to practical correction systems are discussed and curves are given for the chromatic and focal properties of the corrective electrode group considered.

621.385.833 1181
Chromatic Aberration and Aperture Error of Cylindrical Electron-Optical Lenses—M. Rheinfurth. (*Optik, Stuttgart*, vol. 12, pp. 411–416; 1955.) Expressions are derived for the two types of error, and it is shown that they cannot both be eliminated.

621.385.833 1182
Use of a Cylindrical Lens for reducing Image Distortion in Reflection Electron Microscopy—C. Fert and B. Marty. (*C. R. Acad. Sci., Paris*, vol. 241, pp. 1454–1456; November 21, 1955.)

621.385.833 : 535.767 1183
Theory and Technique of Electron-Micro-

scope Stereograms—(*Optik, Stuttgart*, vol. 11, pp. 562–577; 1954, and vol. 12, pp. 253–272; 1955.)

Part 1: 3657 of 1954.
Part 2: Errors in the Determination of Depth of Electron-Microscope Stereograms—J. G. Helmcke and H. J. Orthmann.
Part 3: Methods for determining the Depth of Objects and Requirements for a Photogrammetric Apparatus—J. G. Helmcke.

621.385.833:537.525   **1184**
Electric "Microdischarges" in a Dynamic Vacuum—Arnal. (See 1025.)

621.396.934:621.396.96   **1185**
Radar-Guided Missiles—(*Wireless World*, vol. 62, pp. 67–70; February, 1956.) A brief survey of the principles of command-guidance, homing and beam-riding control systems used with ground-to-air missiles.

621.396.934:621.398   **1186**
Fuel Cut-Off Control for Guided Missiles—G. L. Zomber and D. Macmillan. (*Electronics*, vol. 29, pp. 126–127; January, 1956.) The input circuit of the control relay comprises a parallel-T network tunable over the range 88–154 cps, and is designed for use with a radar beacon system. The operating potential of a neon-tube voltage regulator in the switching circuit is stabilized by radiation from a radium pellet.

621.398   **1187**
The New Centralized Telecontrol System on 175 c/s adopted by Électricité de France—F. Cahen and H. Prigent. (*Rev. gén. Élect.*, vol. 64, pp. 475–484; October, 1955.)

621.384.6   **1188**
High-Energy Accelerators [Book Review]—M. S. Livingston. Publishers: Interscience, New York and London, 157 pp., 1954. (*Phil. Mag.,*, vol. 46, p. 1264; November, 1955.) Recommended as a useful introduction to and survey of particle accelerators.

PROPAGATION OF WAVES

538.566.2:551.510.535   **1189**
Reflection of a Plane Electromagnetic Wave from a Stratified Ionized Gas—P. Poincelot. (*C.R. Acad. Sci., Paris*, vol. 241, pp. 1272–1275; November 7, 1955.) Continuation of analysis presented previously (3725 of 1955). The conditions for total reflection are indicated and expressions are derived for the phase shift of the reflected wave and the group propagation time in terms involving the apparent height of reflection. Results are discussed briefly in relation to ionosphere soundings.

621.396.11   **1190**
Measurements of the Propagation Time of Standard Time Signals—M. Boella and C. Egidi. (*Alta Frequenza*, vol. 24, pp. 309–338; August/October, 1955.) Report of experiments made in May, 1951, using transmissions in both directions between Turin, Italy, and Beltsville, U.S.A. Because the signals become distorted during transmission, an arbitrary criterion must be adopted for the moment at which the signal is considered to be received. Various criteria are compared on the basis of a statistical analysis of results. With a series of about 60 observations in 1 minute the accuracy of the determination is within about 0.1 ms, using photographic technique. On comparing the results with data obtained by ionospheric soundings at points near the propagation path, the most probable number of hops is deduced to be 4 or 5, the corresponding single-hop distance being 1,670 or 1,340 km respectively. Discrepancies between this result and the values usually assumed are discussed.

621.396.11:537.56   **1191**
Theory of Radio Reflections from Electron-Ion Clouds—V. R. Eshleman. (TRANS. IRE,

vol. AP-3, pp. 32—39; January, 1955.) First-order approximations to the effects of size, shape, and density on the reflecting properties of electron-ion clouds are obtained. For low-density clouds the reflection coefficients are determined by summation of the wavelets from individual ions; high-density clouds are treated as total reflectors at the critical-density radius.

621.396.11:551.510.535   **1192**
Wave Solutions for Critical and Near-Critical Coupling Conditions in the Ionosphere—N. Davids and R. W. Parkinson. (*J. atmos. terr. Phys.*, vol. 7, pp. 173–202; October, 1955.) "Principal dielectric axis coordinates are used to put the coupled wave equations for ionospheric propagation into a form which is suitable for an analysis of critical coupling. This approach removes the singularity formerly associated with critical coupling. The analysis is carried out through the second order and compared with some recent data on polarization. The results compare favorably for several ionospheric models considered. A satisfactory analysis of split echoes at 150 kc is developed."

621.396.11:551.510.535   **1193**
Observations of the Effects of Ionospheric Storms over a North Atlantic Circuit—T. W. Bennington. (*J. atmos. terr. Phys.*, vol. 7, pp. 235–243; October, 1955.) The median muf (*i.e.*, the frequency up to which signals are propagated for 50 per cent of a given period) for normal and disturbed conditions has been deduced from regular observations of signals from WWV, Washington, received at Tatsfield, England, over the period July–December, 1953. The results show that disturbance of communications is most severe during the period 0700 to 1100 LT of any disturbed day. This agrees with the findings of Appleton and Piggott (2802 of 1952) from vertical-incidence data. The effect is also dependent on the normal value of muf for the time of day, being greater at night, particularly during winter when the normal muf is low.

621.396.11:551.510.535   **1194**
On the Variation of Ionospheric Absorption at Different Stations—Piggott. (See 1051.)

621.396.11:551.510.535   **1195**
Selective Annotated Bibliography on Ionospheric Propagation—M. Rigby and M. L. Rice. (*Met. Abstracts Bibliography*, vol. 6, pp. 489–547; April, 1955.) Includes some 300 references covering the period 1902–1955.

621.396.11:551.594.6   **1196**
An Atmospherics Analyzer—P. F. Smith. (TRANS. IRE, vol. AP-3, pp. 9–12; January, 1955.) A system is described which records the received atmospheric waveform and simultaneously derives a plot of the time intervals between peaks of the waveform/time curve, facilitating reduction of data relating to range and ionospheric layer height.

621.396.11:621.396.6   **1197**
Tests on Long-Range Decimetre-Wavelength Multiplex Links—R. Goublin. (*Bull. Soc. franç. Élect.*, vol. 5, pp. 700–709; October, 1955.) Transmissions on frequencies in the band 450–470 mc over distances from 50 to 100 km show ground losses varying from 6 to 36 db for angles of diffraction from 0 to 25×10^{-3} rad. Over paths of 215 and 250 km, one at grazing incidence to a forest terrain and the other over line of sight, fading is found to be worse in summer than in winter, especially over the forest, but communication is possible for practically all the time with a 20-w transmitter and parabolic antennas. Fm terminal equipment for permanent communication links is described.

621.396.11:621.396.67.012.12   **1198**
The Dependence of Metoric Forward-Scattering on Antenna Patterns and Orienta-

tions—C. O. Hines, P. A. Forsyth, E. L. Vogan, and R. E. Pugh. (*Canad. J. Phys.*, vol. 33, pp. 609–610; October, 1955.) Radio waves of frequencies above accepted muf may be propagated by scattering either from ionospheric irregularities [2581 of 1962 (Failey, *et al.*)] or from meteor trails [*e.g.*, 2117 of 1953 (Villard, *et al.*)]. In any given set of observations the predominant mechanism depends on the aerial radiation pattern; directing the radiation off the transmitter-receiver axis favors the meteor-trail-scattering mechanism.

621.396.11.029.53/.55   **1199**
A Theoretical Model for High-Frequency Backscatter from the Sea Surface via the Ionosphere—W. C. Hoffman. (*J. atmos. terr. Phys.*, vol. 7, pp. 278–284; October, 1955.) The average far-zone back-scattered power is computed for perfectly conducting doubly-trochoidal and doubly-sinusoidal surfaces. (See also TRANS. IRE, vol. AP-3, pp. 96–100; July, 1955.) Either assumption gives results of the correct order of magnitude; from the nature of the problem, this is the best that can be expected. The doubly-sinusoidal surface leads to much more convenient computations.

621.396.11.029.55   **1200**
Arrival Angle of H. F. Waves—A. F. Wilkins and C. M. Minnis. (*Wireless Engr.*, vol. 33, pp. 47–53; February, 1956.) "Apparatus is described for measuring the angle of elevation of hf waves arriving at the ground after transmission by way of the ionosphere. The system involves the comparison of the amplitudes of the signals received by two vertically-spaced horizontal loop antennas at heights above the ground of about 33 meters and 12.5 meters. The comparison is effected by amplifying the signal emfs in a twin-channel receiver and applying the IF voltages to the deflecting plates of a cathode-ray oscilloscope. It is shown that, if a single ray is incident on the system, the emfs produced in the two antennas are in phase irrespective of their height above ground, so that the corresponding oscilloscope pattern is a straight line, the slope of which is a simple function of the angle of elevation of the ray. Calibrations of the system over the band 10–20 mc have shown that its behavior is very close to that expected from the simple theory and that there is no noteworthy change in the calibration with azimuth. Methods of observation for the general case of the arriving consisting of more than one ray are considered."

621.396.11.029.55:551.510.535   **1201**
Azimuthal Fluctuations of the Direction of Arrival of Short Radio Waves—W. Kronjäger and K. Vogt. (*Nachrichtentech. Z.*, vol. 8, pp. 537–540; October, 1955.) The directions of arrival of signals from Tangiers, Rio de Janiero, Buenos Aires, Osaka, and Tokyo, were measured at Eschborn. The frequencies were between 13 and 21 mc and were in all cases below the muf. The distribution of deviations was Gaussian; maximum fluctuations were $\pm 3°$ for 80 per cent of the observations and $\pm 5°$ for 98 per cent. Median directions of arrival for the first three stations coincided with the great-circle directions, but those for Osaka and Tokyo deviated by 2° and 3° respectively, to the south. The antenna system comprised two rhombic antennas set at an angle of 9° to each other. Results are tabulated and presented graphically.

RECEPTION

621.396.82:551.594.6   **1202**
Atmospheric Noise Interference to Broadcasting in the 3-Mc/s Band at Poona—S. V. C. Aiya and K. R. Phadke. (*J. atmos. terr. Phys.*, vol. 7, pp. 254–277; October, 1955.) Using an objective method previously described [257 of of 1955 (Aiya)] systematic measurements were made daily from 1800 to 2300 I.S.T. throughout 1953; noise data required for the design of

broadcast services are deduced. The results are compared with estimates of noise taken from *National Bureau of Standards Circular* No. 462 and with experimental results given in *Radio Research Board Special Report* No. 26 [842 of 1954 (Horner)]; both of these tend to be low. An attempt is made to estimate noise levels from known thunderstorm data; reasonable agreement with measured values is obtained.

STATIONS AND COMMUNICATION SYSTEMS

621.376.5   **1203**
Calculation of the Spectra of Modulated Pulse Trains—M. Sánchez and F. Popert. (*Arch. elekt. Übertragung*, vol. 9, pp. 441–452; October, 1955.) The theory and method of representation developed by Bennett (see *Modulation Theory*, Black, p. 266, 1953) are applied to determine the spectra of pulse trains subjected to various types of modulation of practical importance.

621.39:621.376.5   **1204**
A Multichannel Pulse Communication System with Automatically Variable Number of Pulses—R. Filipowsky. (*Öst. Z. Telegr. Teleph. Funk Fernsehtech.*, vol. 9, pp. 113–129; September/October, and pp. 147–158; November/December, 1955.) The operation of a pcm system with asynchronous sampling is discussed in detail. In this system sampling is performed on the statistical basis of the amount of information in the different channels; this leads to improved use of over-all channel capacity. Circuits for selecting the information-carrying channels are described. See also 562 of 1956.

621.39:621.376.5:621.396.822   **1205**
Noise Characteristics of Pulse-Slope-Modulation—J. Das. (*Electronic Engng.*, vol. 28, pp. 16–21; January, 1956.) The calculated signal/noise ratio at the output of a psm audio amplifier is 27.4 db for an input peak ratio of 6 db with random noise only. This is confirmed experimentally. The ratio improves with increased bandwidth and for a signal containing impulse noise.

621.39.018.756   **1206**
A Type of Signal Practically Limited in Time and in Frequency—J. A. Ville and J. Bouzitat. (*Câbles and Transm.*, vol. 9, pp. 293–303; October, 1955.) The incompatibility of perfectly limited spectrum and finite duration in pulses is demonstrated; an expression is given for the spectrum of a finite-duration signal which can be considered limited for practical purposes. If as an approximation the spectrum of a nonlimited signal is represented by Shannon's series, the error introduced can be considered as a modulation; any signal can thus be represented as a sequence of modulated signals. This method is applied to various signal types, particularly the raised-cosine signal; the limited-spectrum signal is represented by a succession of raised-cosine signals.

621.396:621.376.5   **1207**
Pulse Multiplex Radiotelephone System in Greece—J. J. Muller. (*Onde élect.*, vol. 35, pp. 711–713; August/September, 1955.) An account of the network covering nearly 2,000 km, which was put into service in 1954. There are 34 stations, with separations ranging from 14 to 120 km, at altitudes ranging from 20 to 1,800 m. Some of the links handle telegraphy and radio-program transmission as well as telephony. Fading effects are reduced by using diversity reception. Carrier frequencies are between 1.7 and 2.3 kmc. Particular aspects of the system are dealt with in the following separate papers:
High-Quality Radio Links over Sea Paths in Greece—R. Cabessa (pp. 714–727).
Synchronization of the Greek Radio-Link System—G. X. Potier (pp. 728–732).
Operational Reliability of the Greek Radio-Link System—R. Basard (pp. 733–738).

621.396.41:621.396.65   **1208**
A 4-Channel Carrier Telephone System for the Argentine V.H.F. Radio Links—Y. Boers. (*Commun. News*, vol. 16, pp. 30–34; October, 1955.) Description of the Type-STR 128 system. Each channel has a width of 6 kc; the af band used is 300 cps—3.4 kc, while signaling is effected on 4.3 kc. The four bands are transmitted in the inverted position, so that the total modulation frequency range is transformed from 300 cps—22.3 kc to 1.7—23.7 kc; this reduces the modulation frequency spectrum by 2½ octaves, considerably reducing the risk of intermodulation distortion.

621.396.41:621.396.5:621.376.4   **1209**
V.H.F. Phase-Modulated Transmitter-Receiver for 4-Channel Telephony—J. M. M. Veldstra. (*Commun. News*, vol. 16, pp. 22–29; October, 1955.) Account of Type-SFR 329 radio equipment for use in conjunction with the channeling equipment described by Boers (1208 above).

621.396.44+621.397.242   **1210**
Distribution Systems—J. Kason. (*Wireless World*, vol. 62, pp. 88–90; February, 1956.) A system for relaying sound and television broadcasts, picked up on a central receiving antenna, to small blocks of flats, etc., is described. Signals are distributed at transmitted frequencies through channel amplifiers; suitable filter networks incorporated in mixing and splitter units enable subscribers to receive any program at will.

621.396.6:621.396.11   **1211**
Tests on Long-Range Decimetre-Wave-length Multiplex Links—Goublin. (See 1197.)

621.396.65.029.64:621.397.26   **1212**
New Microwave Repeater System using Traveling-Wave Tubes—N. Sawazaki and T. Honma. (Proc. IRE, vol. 44, pp. 19–24; January, 1956.) A system is described using traveling-wave tubes as wide-band amplifiers in a reflex arrangement permitting the same valve to serve at rf and IF. See also 2783 of 1954 (Nomura, *et al.*).

621.396.712:621.396.65   **1213**
F.M. for B.F.N—J. D. Parker. (*Wireless World*, vol. 62, pp. 81–84; February, 1956.) The British Forces broadcasting network in Germany brought into service in 1956 constitutes a radio relay system in which the intermediate stations function as broadcasting stations, reradiating the received program on different frequencies in the range 87.6–99.3 mc. FM is used and the stations are automatically operated.

621.396.721:621.396.6   **1214**
Two-Metre Transmitter-Convertor—G. P. Anderson. (*Wireless World*, vol. 62, pp. 60–66; February, 1956.) A portable 6-w crystal-controlled transmitter working in the band 144–146 mc and a receiver-converter are described for use with the equipment for 3.75 and 7.5 mc of which details were given earlier (530 of 1954).

SUBSIDIARY APPARATUS

621–526:621.3.016.35   **1215**
Stability Criteria for an Electrical or Mechanical System with Distributed Parameters—Gladwin. (See 992.)

621.311.62:621.314.5   **1216**
Advances in Vibratory-Power-Supply Techniques—L. W. D. Sharp. (*Brit. Commun. Electronics*, vol. 2, pp. 54–58; October, 1955.) A brief review of British commercial vibrators. A table of the comparative performance of three typical vibrator units is given.

621.314.63:546.289   **1217**
The EW54 Germanium Junction Rectifier—R. D. Knott and J. I. Missen. (*G.E.C. J.*,

vol. 22, pp. 197–208; October, 1955.) The junction is produced by alloying a controlled quantity of In with a Ge crystal about 6 mm square and 0.4 mm thick with resistivity about 10 Ω. cm. The manufacture, electrical characteristics, and methods of assessing the performance of the rectifier are described. Applications are grouped into (*a*) use with resistive load, (*b*) use with battery load, and (*c*) pulse and miscellaneous. By virtue of its high efficiency this rectifier can be used for high powers with comparatively simple cooling systems.

621.314.63:546.824–3   **1218**
High-Temperature Area-Type Titanium-Dioxide Rectifiers—H. C. Gorton, T. S. Shilliday, and F. K. Eggleston. (*Elect. Engng.*, *N. Y.*, vol. 74, pp. 904–907; October, 1955.) Modifications in the methods of production, including the deliberate introduction of impurities, have led to improvements over the performance reported previously [2755 of 1955 (Shilliday and Peet)] in respect of maximum operating temperature, reverse/forward resistance ratio, and reproducibility of characteristics. Satisfactory operation at temperatures above 250°C for hundreds of hours is reported.

621.352.32   **1219**
Behaviour of MnO_2 as Depolarizer [in Leclanché-type cells]—J. Brenet, A. Grund, and A. M. Moussard. (*Rev. gén. Élect.*, vol. 64, pp. 513–516; October, 1955.)

621.355:621.316.722.1   **1220**
Low-Voltage Stabilization—(*Wireless World*, vol. 62, p. 70; February, 1956.) A form of Ni-Cd secondary cell is described having applications to the cathode biasing of tubes. It provides a stable voltage of about 1.5 v which is practically independent of the current passed. The impedance is $<1\Omega$ and is independent of frequency.

TELEVISION AND PHOTOTELEGRAPHY

621.397.26:621.396.65.029.64   **1221**
New Microwave Repeater System using Traveling-Wave Tubes—Sawazaki and Honma. (See 1212.)

621.397.335   **1222**
→ Television Transmission without Synchronization Levels—H. J. Griese. (*Nachrichtentech. Z.*, vol. 8, pp. 552–555; October, 1955.) A system is described in which the picture brightness levels occupy the whole modulation range and synchronization depends on coincidence between a local pulse and a stepped pulse transmitted during the horizontal blanking interval. The principal advantages are the improved signal/noise ratio and the removal of difficulties connected with holding the various levels constant.

621.397.5   **1223**
Phonevision—an Effective Method for Subscription Television—A. L. C. Webb and A. Ellett. (*Proc. IRE, Aust.*, vol. 16, pp. 341–353; October, 1955.)

621.397.5:535.623   **1224**
Compatible Colour Television—J. Haantjes and K. Teer. (*Wireless Engr.*, vol. 33, pp. 3–9, January and pp. 39–46; February, 1956.) A system is described using two distinct subcarriers for the red and blue signals; the bandwidth for the red signal is 2 mc and that for the blue is 1 mc, and both lie within the normal-width luminance band. At the receiver the color signals are fed to separate demodulators which include appropriate band-pass filters, and an equivalent green signal is formed locally. Receivers for this system, in contrast to those for the NTSC system, do not require subcarrier generators or synchronization of the color-signal detectors. Important aspects of the two systems are tabulated for comparison.

621.397.61 1225

A 16-mm Projector for Operation with a Television Film Chain on a Partial-Storage Basis—E. C. Fritts. (*J. Soc. Mot. Pict. Telev. Engrs.*, vol. 64, pp. 576–577; October, 1955.) Apparatus described previously (268 of 1954) was modified for use with vidicon tubes. A 2–3 system separates the pull-down by the required integral number of television fields while maintaining the usual $2\frac{1}{2}$:1 ratio between television fields and motion-picture frames.

621.397.61 1226

The Development and Design of an Underwater Television Camera—D. R. Coleman, D. Allanson, and B. A. Horlock. (*J. Brit. Instn. Radio Engrs.*, vol. 15, pp. 625–636; December, 1955. Discussion, pp. 636–639.) The camera described uses an image orthicon operating at 625 lines 50 frames or 525 lines 60 frames. The mechanical design of the casing is discussed and the handling arrangements for both diver-controlled and deep-sea cameras are described. Problems of underwater illumination are examined and a new type of remotely focused lamp is mentioned.

621.397.611:778.5 1227

Critical Considerations on Optical Compensation by means Rotating Prisms in Television Film Scanners—H. Grabke. (*Tech. Hausmitt. NordwDtsch. Rdfunks*, vol. 7, pp. 166–170; 1955.) A prism with at least 24 sides and a built-in glass corrector is necessary to obtain satisfactory pictures. The coupling between film and prism is discussed.

621.397.611.2 1228

The "Scenioscope", a New Television Camera Tube—P. Schagen. (*Tijdschr. ned. Radiogenoot.*, vol. 20, pp. 291–305; September, 1955. In English.) Description of a tube in which the target is of slightly conducting glass, permitting charge to pass from the signal plate to the scanned surface. Very good picture quality can be achieved with an illumination of a few hundred lux; recognizable though "noisy" pictures have been obtained with illuminations as low as 15 lux. See also 3762 of 1955.

621.397.621.2:621.385.832:535.65 1229

Two Photoelectric Colorimeters for Television Picture Tubes—R. S. Hunter. (*J. electrochem. Soc.*, vol. 102, pp. 512–517; September, 1955.) The instruments described are intended primarily for measurements on monochrome picture tubes. One uses a single photocell and three filters on a disk, the other uses three photocells each with appropriate filter.

621.397.7 1230

A New N.W.D.R. Television [outside-broadcast] Transmission Van—H. Krause and H. Käding. (*Tech. Hausmitt. NordwDtsch. Rdfunks*, vol. 7, pp. 174–183; 1955.) The van is about 11 m long and weighs about 14 tons and carries complete equipment for three image-orthicon channels and 12 microphone channels. A detailed illustrated description is given.

621.397.7:535.623 1231

Integration of Color Equipment in a Television Station—P. B. Laeser. (*J. Soc. Mot. Pict. Telev. Engrs.*, vol. 64, pp. 537–541; October, 1955.) Problems involved in the installation at WTMJ-TV, Milwaukee, are discussed.

621.397.7:535.623 1232

CBS Television Color Studio 72—R. B. Monroe. (*J. Soc. Mot. Pict. Telev. Engrs.*, vol. 64, pp. 542–549; October, 1955.) Illustrated description of an installation in a converted theatre in New York.

621.397.8:535.8 1233

Influence of the Optical System on the Television Picture—F. Below and H. Grabke. (*Tech. Hausmitt. NordwDtsch. Rdfunks*, vol. 7,

pp. 171–173; 1955.) Results of preliminary measurements indicate that local variations of picture quality can be assessed with sufficient accuracy from observations of the reproduction of black-to-white steps.

621.397.8:621.396.822 1234

The Visibility of Noise in Television—(*B.B.C. Engng. Div. Monographs*, no. 3, pp. 1–22; October, 1955.) Comprises the following parts:—

Part 1—The Visibility of Noise over the Grey Scale—R. D. A. Maurice (pp. 5–12).

Part 2—The Visibility of Noise as a Function of Frequency—M. Gilbert (pp. 13–16).

Part 3—Photographic Records of the Effect of Random Noise on a Television Picture—G. F. Newell and J. G. Spencer (pp. 17–22).

TRANSMISSION

621.396.61:621.385:621.316.9 1235

Gas Tubes protect High-Power Transmitters—W. N. Parker and M. V. Hoover. (*Electronics*, vol. 29, pp. 144–147; January, 1956.) Fault-detection and protective devices for transmitter tubes are described.

TUBES AND THERMIONICS

621.314.63 1236

On the Transient Behavior of Semiconductor Rectifiers—B. R. Gossick. (*J. appl. Phys.*, vol. 26, pp. 1356–1365; November, 1955.) Theory and practical details of a pulse method of determining the characteristics of a *p-n* junction rectifier are discussed. See also 887 of 1954.

621.314.63.002.2:546.289 1237

Manufacture of Germanium Power Diodes—(*Elect. Commun.*, vol. 32, pp. 146–164; September, 1955.) Various stages in the production of diffused-junction diodes are illustrated by photographs.

621.314.632:546.289]+621.316.825 1238

The Turnover Phenomenon in Thermistors and in Point-Contact Germanium Rectifiers—Burgess. (See 994.)

621.314.7 1239

Transistor Characteristics for Circuit Designers—S. Schwartz. (*Electronics*, vol. 29, pp. 161–174; January, 1956.) Comprehensive tables giving the characteristics and operating parameters of 218 types of transistor made in the United States.

621.314.7 1240

The Field Effect Transistor—G. C. Dacey and I. M. Ross. (*Bell Syst. tech. J.*, vol. 34, pp. 1149–1189; November, 1955.) Theory presented previously (3445 of 1953) is recapitulated and extended. Considerations of the field dependence of cutoff frequency f and transconductance on the one hand, and power dissipation on the other, lead to the conclusion that the best operating point is the critical field E_c above which carrier mobility is proportional to $E^{-0.5}$. The performance for this case is discussed in detail and the results are summarized in design nomograms. f is found to be inversely proportional to the "pinch-off" voltage, but the latter cannot reasonably be reduced below 0.5 v, corresponding to a maximum value of 1 kmc for f. The manufacture and performance of various types, operating with field values in some cases below E_c and in others above, are described. Transistors can be designed for high-power operation at low frequencies and can be used to replace pentodes.

621.314.7 1241

Gain of Amplifying Transistors—R. Monelli. (*Alta Frequenza*, vol. 24, pp. 356–374; August/October, 1955.) Equivalent circuits are presented for point-contact and junction transistors. Expressions are derived for the gain, considering the transistor as an active

quadripole. Values of gain and input resistance are tabulated for various commercially available transistors with various connections.

621.314.7 1242

Accelerated Power Aging with Lithium-Doped Point-Contact Transistors—L. E. Miller and J. H. Forster. (*TRANS. IRE*, vol. ED-2, pp. 4–6; July, 1955.) Use of lithium-doped collector points facilitates observation of changes in transistor parameters during artificial aging tests; changes in the effective donor concentration in the formed region are responsible for the enhanced effects. The results indicate that changes associated with aging are not entirely due to changes in surface conduction.

621.314.7 1243

Negative-Resistance Regions in the Collector Characteristics of the Point-Contact Transistor—L. E. Miller. (*PROC. IRE*, vol. 44, pp. 65–72; January, 1956.) Anomalies of three different types have been observed in the V/I characteristics of various transistors. Typical curves are shown and the mechanisms responsible for the anomalies are discussed; the observed negative resistance is a property of the transistor itself and is attributable to a variation in the collection efficiency of the reverse-biased collector contact.

621.314.7 1244

The Dependence of Transistor Parameters on the Distribution of Base Layer Resistivity—J. L. Moll and I. M. Ross. (*PROC. IRE*, vol. 44, pp. 72–78; January, 1956.) Expressions are derived for the emitter efficiency, the transverse sheet resistance, the transit time and the cutoff frequency for uniform, linear, exponential, and complementary-error-function distributions of impurities in the base of a junction transistor. For equivalent parameters the non-uniform distributions permit the use of wider base layers, but require greater maximum impurity concentrations and higher current densities.

621.314.7:537.531.9 1245

Dependence of Barrier-Layer Photoeffect on X Radiation—J. Braunbeck and J. Zakovsky. (*Naturwissenschaften*, vol. 42, pp. 602–603; November, 1955.) Experiments on commercial junction transistors exposed to X rays are briefly reported; results are given for the Type-OC70 as typical. Curves show the variation of emitter and collector current (*a*) with wavelength and angle of irradiation and (*b*) with temperature.

621.314.7:621.396.822 1246

Shot Noise in *p-n-p* Transistors—G. H. Hanson. (*J. appl. Phys.*, vol. 26, pp. 1388–1389; November, 1955.) Measurements on several types of transistor at frequencies up to 800 kc are reported. The frequency dependence of noise at high frequencies is in accordance with a formula derived by van der Ziel (600 of 1956).

621.38:001.4 1247

Russian Vaccum-Tube Terminology—G. F. Schultz. (*PROC. IRE*, vol. 44, p. 112; January, 1956.) A short list of basic terms is given together with the English translations.

621.383.4:621.396.822 1248

Reduction of Noise in Photoconductive Cells—R. E. Burgess. (*Brit. J. appl. Phys.*, vol. 6, pp. 385–387; November, 1955.) "The factors determining the signal/noise ratio of photoconductive cells are briefly discussed and attention is drawn to the importance of the noise generated at the electrode contacts when current is flowing through the cell. Means are described for reducing or eliminating this component of noise by means of potential probes near the electrodes combined with suitable external circuits."

621.385+621.314.7+621.318.57 1249

Design of Electronic Devices for Production—J. Thomson. (*Nature, Lond.*, vol. 176, pp.

1059–1060; December 3, 1956.) Report of a summer school held at the Services Electronics Research Laboratories in September, 1955. Various aspects of tube design were discussed, with emphasis on uhf types; transistors and magnetic switching devices were also discussed.

621.385.029.6   **1250**
Thermal Motion of Electrons in a Two-Beam Amplifier—M. I. Rodak. (*Zh. tekh. Fiz.*, vol. 25, pp. 644–648; April, 1955.) The theory of a two-beam electron-wave tube is further developed by taking into account the effect of the thermal motion of electrons on amplification. The electron velocity distribution function is assumed to be Maxwellian. It is shown that this velocity distribution decreases the frequency range and the amplification. A sufficiently large velocity range makes amplification impossible.

621.385.029.6   **1251**
A Developmental Wide-Band, 100-Watt, 20 dB, S-Band Traveling-Wave Amplifier utilizing Periodic Permanent Magnets—W. W. Siekanowicz and F. Sterzer. (PROC. IRE, vol. 44, pp. 55–61; January, 1956.) Details are given of design, construction, and performance. A permanent-magnet focusing system weighing only 2.8 lbs. has been developed.

621.385.029.6   **1252**
Transverse-Field Traveling-Wave Tubes with Periodic Electrostatic Focusing—R. Adler, O. M. Kromhout, and P. A. Clavier. (PROC. IRE, vol. 44, pp. 82–89; January, 1956.) Tubes are described in which the wave-propagating structure constitutes a smooth balanced transmission line for rf signals and serves at the same time as a space-periodic focusing field. Experimental structures for the 500–900-mc band give wave-propagation velocities 1 per cent–2 per cent that of light, with characteristic impedances of about 500Ω. Analysis based on transverse electron waves indicates that in order to obtain gain the electron stream must travel faster than the circuit wave by a substantial margin; gain is proportional to the square root of beam current. Experimental results are in good agreement with predictions from theory; noise figures as low as 6 db have been obtained.

621.385.029.6   **1253**
Coupled Helices for Use in Travelling-Wave Tubes—G. Wade and N. Rynn. (TRANS. IRE, vol. ED-2, pp. 15–24; July, 1955.) Theory is presented for propagation along coaxial helices in the presence of an axial electron beam. Curves show the propagation constants as functions of coupling coefficient and beam velocity, the helix voltages as functions of the physical dimensions, and a parameter related to the frequency response for different input and output couplers. The optimum length for coupling between the helices is greater in the presence of the beam, and the frequency for maximum transmission is lower. Preliminary work on a coupled-helix attenuator is mentioned.

621.385.029.6:621.318.2   **1254**
Permanent Magnets for Microwave Electron Valves—M. de Bennetot. (*Onde élect.*, vol. 35, pp. 747–763; August/September, 1955.) Magnets are considered both for simple focusing, as in traveling-wave tubes and multi-

cavity klystrons, and for crossed-field systems, as in magnetrons. "Tubular" constructions are discussed for which the main flux is from regions other than the pole pieces; uniformity of magnet composition is particularly important in such cases. Weights of focusing magnets range from 1.5 to 4.5 kg. See also 2991 of 1954.

621.385.029.6:621.374.4   **1255**
Multi-beam Velocity-Type Frequency Multiplier—Y. Matsuo. (PROC. IRE, vol. 44, pp. 101–106; January, 1956.) Experiments on a klystron with two nearly parallel beams are described; owing to the reduction of mutual-electron-repulsion effects, much higher output is obtainable than with a single-beam klystron. The device is expected to be useful as a mm-λ generator.

621.385.029.6:621.396.822   **1256**
Spurious Modulation of Electron Beams—C. C. Cutler. (PROC. IRE. vol. 44, pp. 61–64; January, 1956.) Noise at frequencies up to about 5 mc in tubes with high-intensity beams is found to be due to positive ions and secondary electrons. Oscillograms of various types of resulting modulation are shown. The effects are eliminated by improving the outgassing and evacuating and if necessary by deflecting the secondary electrons out of the beam.

621.385.032.2   **1257**
A Design of Triode Electron Gun—K. C. Ho. (TRANS. IRE, vol. ED-2, pp. 10–14; July, 1955.) Analysis is given for a gun with two successive apertured-disk anodes, for producing a pencil beam. Focusing details for a 50-μA and a 250-μA beam are treated as examples.

621.385.032.216   **1258**
New Type of Diffusion Cathode—A. H. Beck, A. D. Brisbane, A. B. Cutting, and G. King. (*Elect. Commun.*, vol. 32, pp. 172–178; September, 1955.) Reprinted from *Le Vide*, vol. 9, pp. 302–309; November, 1954. See also 1841 of 1955.

621.385.032.216   **1259**
Theoretical Basis for measuring the Saturation Emission of Highly Emitting Cathodes under Space-Charge-Limited Conditions—C. R. Crowell. (*J. appl. Phys.*, vol. 26, pp. 1353–1356; November, 1955.) Analysis is presented confirming that the current at the inflection point of the I/V characteristic of a diode gives a sensitive indication of the saturation emission of an oxide cathode. See also 2787 of 1955 (Hopkins and Shrivastava).

621.385.032.216   **1260**
Measurements of Retarding Potential on the Hollow Cathode—A. W. Bright and J. S. Thorp. (*Nature Lond.*, vol. 176, pp. 1079–1080; December 3, 1955.) I/V characteristics of diodes with two different types of hollow cathode are compared with characteristics of planar diodes. The results appear to indicate that the electron temperature for the hollow cathode does not differ greatly from that for a normal oxide cathode at the same cathode temperature, thus supporting the hypothesis that the greater part of the emission comes from a region near the edge of the hole.

621.385.032.216:537.583   **1261**
Schottky Effect for SrO Films on Molybdenum—G. A. Haas and E. A. Coomes. (*Phys. Rev.*, vol. 100, pp. 640–641; October 15, 1955.)

Thermionic-emission measurements on Mo filaments with very thin films of SrO are discussed briefly in relation to the theory of the surface potential barrier.

621.385.832:681.142   **1262**
Digital Memory in Barrier-Grid Storage Tubes—M. E. Hines, M. Chruney, and J. A. McCarthy. (*Bell Syst. tech. J.*, vol. 34, pp. 1241–1264; November, 1955.) A description is given of the operation of a cr tube in which the same beam is used for writing and reading signals in the form of charges on a dielectric plate held between the barrier grid and a backplate; storage capacity and probability of error due to amplifier noise are particularly discussed. Experimental tubes have been produced with a capacity of 16,000 information bits, with reading and writing times of about 1 μs.

621.387   **1263**
Glow-Discharge Tubes—F. A. Benson and L. J. Bental. (*Wireless Engr.*, vol. 33, pp. 33–38; February, 1956.) Continuing the investigation reported previously [3422 of 1954 (Benson and Mayo)], an examination has been made of the influence of cathode material, gas filling, gas pressure and geometrical dimensions on the magnitude and duration of the initial drift, and on the running-voltage/temperature characteristics; specially made tubes were used. Results are shown graphically; they indicate that gas pressure and tube dimensions have little influence, while the cathode material and the nature of the gas filling do affect the characteristics.

621.387   **1264**
Improving Gas-Diode Voltage Characteristics—(*Tele-Tech & Electronic Ind.*, vol. 14, pp. 67, 123; October, 1955.) Note on a method developed at the National Bureau of Standards. By applying a pulsed voltage through a common resistor to a large number of cold-cathode gas diodes connected in parallel the individual operating characteristics are rapidly equalized and stabilized.

621.387:621.318.57   **1265**
Traveling-Glow-Discharge Counter Tube—E. W. Cowan. (*Rev. sci. Instrum.*, vol. 26, pp. 988–989; October, 1955.) Brief description of a tube using wire electrodes of special curved form.

MISCELLANEOUS

061.3:621.3   **1266**
Index to Convention Record of the IRE, vol. 3, 1955—(PROC. IRE, vol. 44, pp.149 *et seq.*; January, 1956.)

621.37/.39(083.74)   **1267**
Standard Functional Divisions for Electronic Equipment—R. S. Shultz and W. R. Waltz. (*Elect. Engng.*, *N. Y.*, vol. 74, pp. 896–900; October, 1955.) Preliminary report of a survey of existing U. S. Navy electronic equipment undertaken with a view to further standardization. Edge-punched cards used in the analysis are shown.

621.3   **1268**
Radio and Television Engineers' Reference Book [Book Review]—E. Molloy and W. E. Pannett. Publishers: Newnes, 1600 pp., (*J. Instn. elect. Engrs.*, vol. 1, pp. 717–718; November, 1955). " . . . well worthy of a place in the library of every radio engineer."